# Pliocene-Pleistocene evolution of Benguela upwelling and Agulhas Leakage in the SE Atlantic

By

Benjamin Fredericks Petrick

Submitted in Accordance with the Requirements for the Degree of Doctor of Philosophy

October 2014

School of Geography Politics and Sociology

Newcastle University

# Abstract

Understanding the impacts of the transition from the warmth of the middle Pliocene to the large amplitude, 100 ka glacial-interglacial cycles of the late Pleistocene helps us to better interpret both the local forcings and global impacts of possible future climate changes. In this thesis, changes in ocean circulation over the last 3.5 million years (Ma) are investigated using a marine sediment core recovered from the SE Atlantic Ocean, a region often described as an ocean gateway because it includes the transfer of heat and salt from the Indian to the Atlantic Ocean between Antarctica and South Africa (the "Agulhas Leakage"). However, the response of this region to Pliocene-Pleistocene climate evolution remains unclear. This thesis analyses the climate information recorded at Ocean Drilling Program (ODP) Site 1087 (31º28'S, 15º19'E, 1374m water depth) to investigate the history of Agulhas Leakage and associated ocean circulation changes including the Antarctic Circumpolar Current to the south, and the productive Benguela upwelling system to the north..

This thesis presents the results generated using several organic geochemistry proxies and foraminiferal analyses to reconstruct the climate history at ODP 1087. These include the $U^{K}_{37}{}'$ index (for sea surface temperatures, SSTs), the $TEX_{86}$ index (for ocean temperatures and an upwelling indicator), pigment analysis (for productivity changes), foraminifera assemblages (as water mass indicators), and dinoflagellate assemblages (for SSTs and water mass indicators).

During the Pliocene and early Pleistocene, ODP 1087 was dominated by the Benguela Upwelling system, which had shifted south relative to today, and three prominent cold periods punctuate the overall warmth (during the M2 and KM2 stages, and at 2.8 Ma). From 2.2 Ma a longer term cooling trend begins, and further cooling occurs at 1.6 Ma, both of which are interpreted to represent periods of intensification of the Benguela Upwelling. The start of modern Agulhas Leakage occurs at ~0.9 Ma, marked by the start of early warming at the site ahead of the terminations. Finally, from 0.6 Ma there is an intensification of Agulhas Leakage which has led to an overall warming of SSTs which span both glacial and interglacial stages. Overall, the ODP 1087 record shows that this region is more reactive to southern hemisphere and local forcings such as changes in the southern wind field and ice expansion around Antarctica, rather than to northern hemisphere forcing.

# Acknowledgements

# Table of Contents

# Table of Figures

# Chapter 1 Introduction

## 1.1 Introduction

Understanding how climate change affects the environment is crucial to understanding the impacts of future climate changes. The time from the Pliocene through the Pleistocene to the modern day (Figure 1.1) is of interest to climate researchers for a number of reasons. First, it is recent enough in geological time so that extensive records are preserved and they can be investigated using proxies developed for modern climates (Dowsett and Cronin, 1991; Salzmann *et al.*, 2009; Salzmann *et al.*, 2011). Second, there are multiple warm stages within this period that can be used as analogues for predicted future warming (Berger and Loutre, 2002; Loutre and Berger, 2003; Dickson *et al.*, 2009; Salzmann *et al.*, 2009). Climate transitions since the Pliocene can also help us to assess how global climate change occurs and what drives it. Finally, data can be obtained containing multiple lines of evidence, including evidence of the effects climate changes have on the biological primary producers. These are important in understanding current and future changes in the global climate. Finally recent studies have suggested that changes in the Agulhas leakage may play a role in mitigating or enhancing future warming that is expected (Turney and Jones 2010; Beal et al. 2011). therefore understanding changes in this system caused by climate change is important to understanding its role in future climate changes.
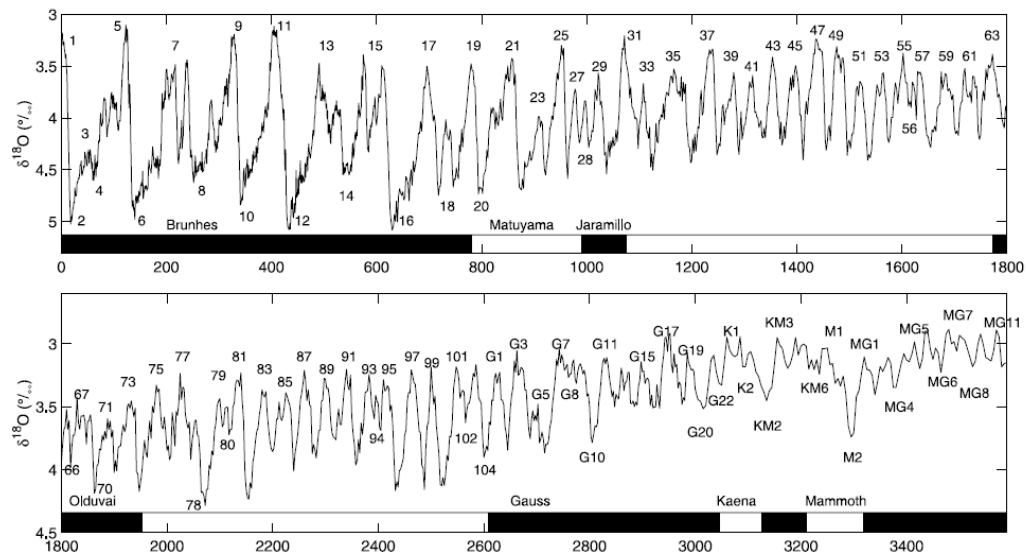
**Figure 1.1  The stack of 57 benthic ä18O records that is referred to as the LR04 record** (Lisiecki and Raymo, 2005)**.**  This represents an average benthic $\delta^{18}O$ signal which incorporates records from most ocean basins. It represents both global temperatures and global ice volume, and clearly demonstrates the glacial-interglacial cycles of the last 3.6 Ma.  The warm interglacials are represented by the odd numbers and the cold glacials by the even numbers.

In this thesis, the ocean circulation history of the Southeast Atlantic Ocean is investigated for the last 3.5 Ma (Figure 1.2). A marine sediment core from the Cape Basin region has been analysed. This region is an important link in one of the key systems that regulates global climate (Boebel *et al.*, 2003). The transfer of water from the Indian Ocean to the Atlantic Ocean, which represents an important heat transfer and a major input to the globally important *thermohaline circulation* (Broecker *et al.*, 1985), occurs in this region through the Agulhas Leakage (Chapter 2).  The Cape Basin is also one of the most important upwelling zones in the global ocean, with implications for biological production. Ocean circulation in the Cape Basin is closely associated with the Antarctic Circumpolar Current system, which is important for the production of cold Intermediate Water (AAIW) and Circumpolar deep water (CDW) as both a source and a sink for atmospheric $CO_2$ (Peterson and Stramma, 1991; Rintoul, 1991). However, a detailed understanding of the climate history of the Cape Basin over the last 3.5 Ma is lacking. This thesis will focus on reconstructing  the Pliocene and Pleistocene climate system, and will assess the causes and impacts of events identified in the Cape Basin region.
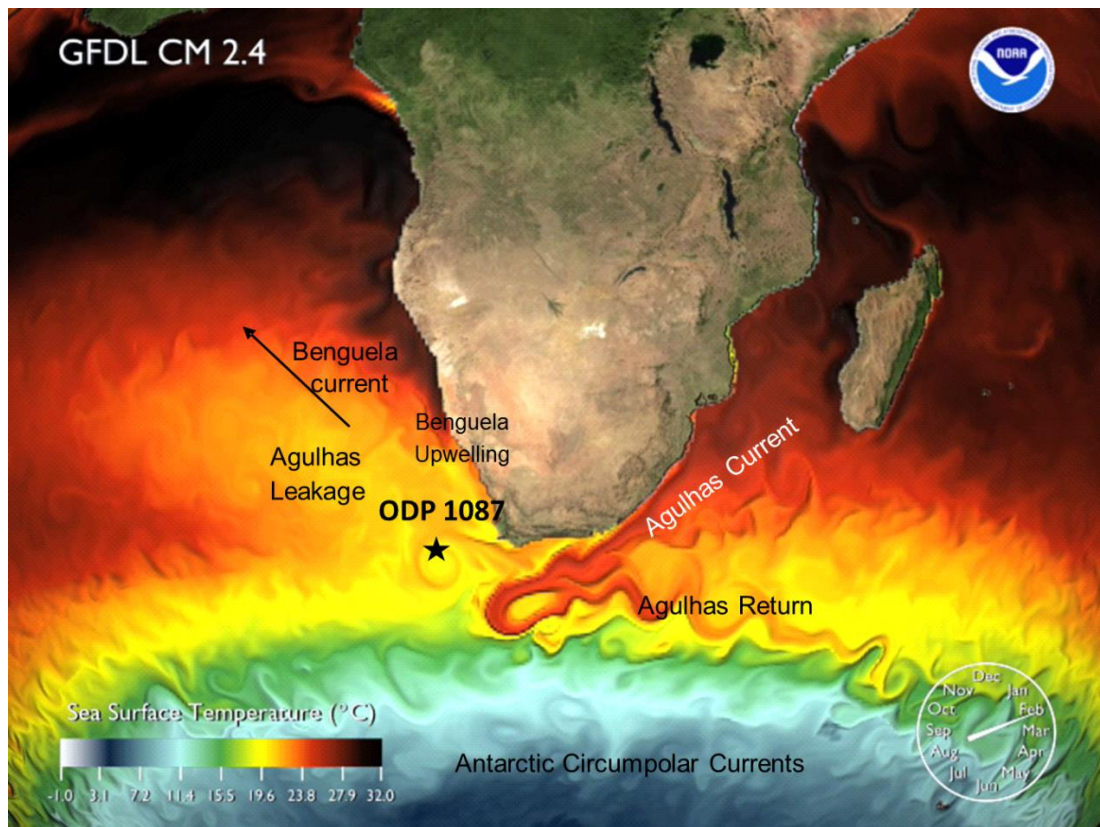
**Figure 1.2 The major currents affecting the southeast Atlantic ocean: the Agulhas Current, the Agulhas Leakage, the Antarctic Circumpolar Current, and the Benguela Upwelling.** The location of the ODP 1087 (this study) is marked. The base map represents a model of the southeast Atlantic during the austral summer at the time when the current is at its warmest, source: NOAA GFDL 2.4

## 1.2 Pliocene-Pleistocene climate change

### 1.2.1 Introduction

In order to understand climate change over the Pliocene and Pleistocene epochs, it is necessary to understand the timing of key events within this time window. One of the advantages of researching the time between the Pliocene and the Pleistocene (Lisiecki and Raymo, 2005) is that a well-established age model, can be used as a global template for stratigraphy for the time between 5.2 Ma and the present day. This stratigraphic model has been divided into marine isotope stages (MIS), defined by changes in the benthic $\delta^{18}O$ (Figure 1.1). MIS delineate high and low benthic $\delta^{18}O$, which have been tied to glacial/interglacial changes and tied to changes in isolation (Lisiecki and Raymo, 2005). Because they are assumed to be universal, at least over millennial time scales, it is assumed that changes in benthic $\delta^{18}O$ can be matched between the different sites in the oceans, providing a dating system for the entire ocean

(Lisiecki and Raymo, 2005). The current $\delta^{18}O_{benthic}$ stack was created using 57 $\delta^{18}O_{benthic}$ records (including ODP 1087) pattern matched and tuned to a simple ice model and tuned to insulation change (Lisiecki and Raymo, 2005).


### *1.2.2 Pliocene*

The late Pliocene (3.5-3.0 Ma) is considered to share some connections to current climate change (Haywood *et al.*, 2009b; Salzmann *et al.*, 2009; Dowsett *et al.*, 2012). This is because the late- Pliocene was warmer than present and in a comparable temperature range to what is predicted for future climate (Figure 1.3) (Dowsett *et al.*, 1996., 2009b, 2012). In addition, there have been reconstructions that atmospheric $CO_2$ levels in the Pliocene were similar to those predicted for the future (Pagani *et al.*, 2010; Bartoli *et al.*, 2011). In geological terms, the Pliocene occurred relatively recently, and as a result many modern techniques ("proxies") can still be used to assess climate conditions such as the sea surface temperatures and ocean currents (Dowsett *et al.*, 2009b., 2012). In order to understand the temperature of the Pliocene, the *Pliocene Research, Interpretation and Synoptic Mapping* (PRISM) project was started to collect temperature data including sea surface temperature (SST) from the period 3.0 to 3.4 Ma (Dowsett *et al.*, 1996., 2005., 2009a; Dowsett and Robinson, 2009; Dowsett *et al.*, 2009b, 2011, 2012). This is one of the most extensive reconstructions of past temperatures ever collected. Nevertheless, because there are gaps in the global extents of the records and most of the records are done at low resolution, many uncertainties remain in our understanding of the Pliocene (Figure 1.3).
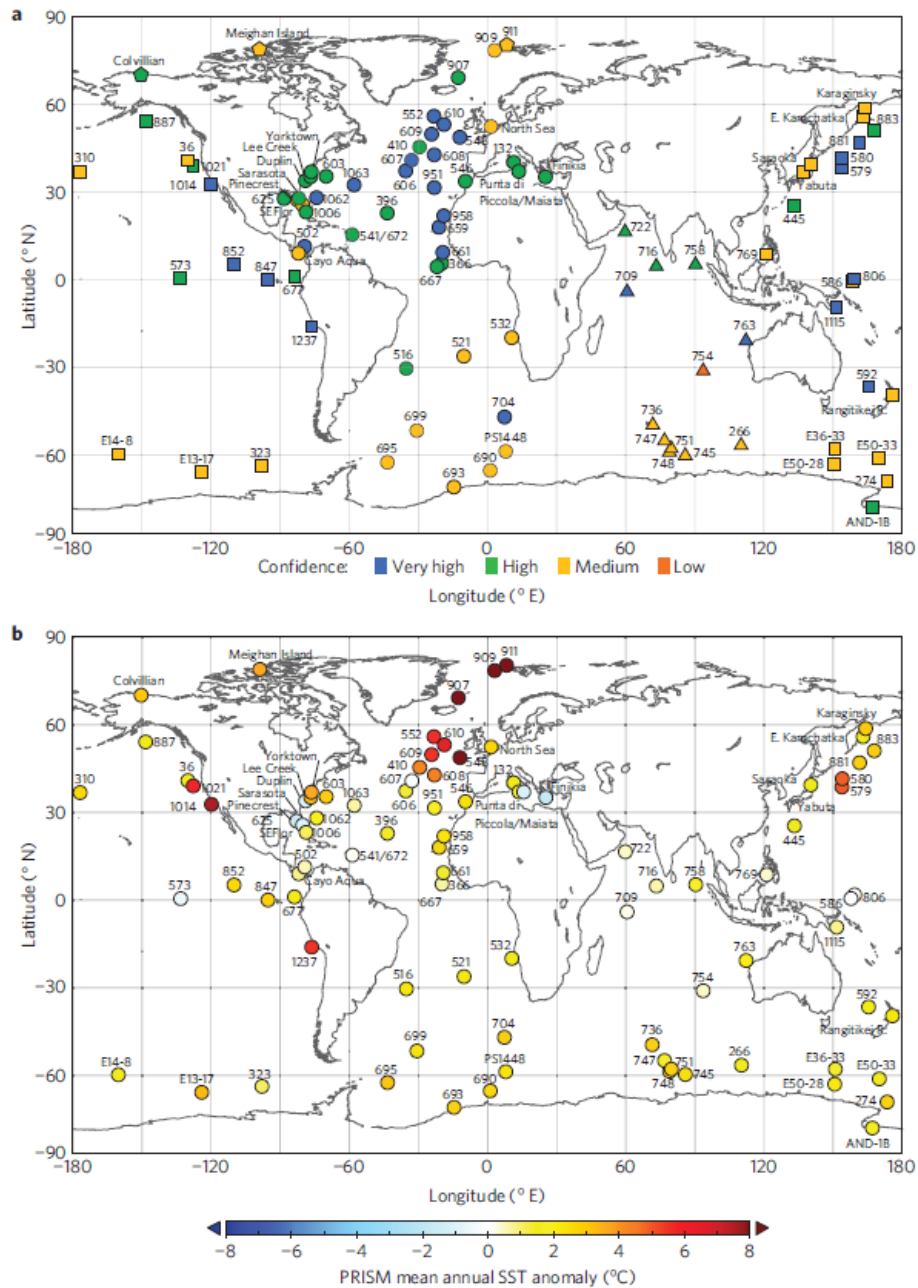
**Figure 1.3 Confidence estimates and sea surface temperature anomalies from the PRISM dataset.** A) Distribution of sites used by the PRISM data set, coloured according to the level of confidence in the accuracy and precision of the proxy it should be noticed that these confidences are primarily based on the accuracy of foraminifera reconstructions. B) Mean annual sea surface temperature SST anomalies at 95 confidence-assessed Pliocene localities, relative to the modern. Note that for most sites values are positive, indicating that Pliocene SSTs were warmer than present (Dowsett et al. 2012).

The Pliocene was a period of overall warmer temperatures (Figure 1.3) (Salzmann *et al.*, 2011). It also had a smaller temperature range across the long-term

6

climate cycles than the later Pleistocene (Draut *et al.*, 2003). There was however a reduced gradient in temperature from the polar regions to the tropics relative to the modern and late Pleistocene (Haywood *et al.*, 2000; Dowsett and Robinson, 2009; Robinson, 2009; Brierley and Fedorov, 2010; Martinez-Garcia *et al.*, 2010). The tropical warm pool in the ocean was expanded further poleward than during then it is currently (Haywood et al., 2000; Dowsett and Robinson, 2009; Robinson, 2009; Brierley and Fedorov, 2010; Martinez-Garcia et al., 2010). This has been suggested to lead to weak tropical upwelling, and weaker Hadley circulation cells in the atmosphere (Brierley *et al.*, 2009b; Etourneau *et al.*, 2010). Upwelling regions in the ocean, which are areas where cold water from the subsurface comes to the surface ocean, are usually caused by winds moving along the coast. These upwelling regions were warmer than they are today (Marlow *et al.*, 2000; Ravelo *et al.*, 2004; Dekens *et al.*, 2007a; Etourneau *et al.*, 2009; Lawrence *et al.*, 2009). It has been argued that this is related to warmer bottom waters and not a change in upwelling strength (Dekens *et al.*, 2007b). Others have speculated that some of the upwelling cells were absent during the Pliocene both in the Pacific and Atlantic Ocean (Fedorov *et al.*, 2006).

The Pliocene also saw important changes in the monsoon systems, including an intensification of the Asian monsoon although this is thought to be tied to the uplift of the Tibetan plateau (Zhang *et al.*, 2009). In Australia, there is evidence of large droughts occurring during the Pliocene (Dodson and Macphail, 2004). Ice sheets were located in East Antarctica and these had periods of instability (Naish *et al.*, 2009; Passchier, 2011). Weak cycles in temperature with a period of 41 ka have been identified (Martinez-Garcia *et al.*, 2010, Naish *et al.*, 2009; Pollard and DeConto, 2009a).

One of the most distinctive features of the late Pliocene is the possible presence of permanent El Niño-like conditions in the Pacific Ocean due to a lack of a temperature gradient between sites in the eastern pacific and western pacific (Fedorov *et al.*, 2006; Chiang, 2009; Dowsett and Robinson, 2009; Shukla *et al.*, 2009; Fedorov *et al.*, 2010). This could be a primary explanation for Pliocene warming, because some models find that the El Niño-like conditions are necessary to cause the temperature pattern seen in the Pliocene (Shukla *et al.*, 2009). There is some controversy over the idea of permanent El Niño in the Pacific. Some studies have suggested instead that permanent La Niña-like conditions were prevailing during this period (Rickaby and Halloran, 2005). Alternatively, climate model runs with a widened Indonesian seaway show an

opposite effect by allowing more water to flow though the Indian Ocean, leading to a weakened El Niño (Jochum *et al.*, 2009). Other studies suggest that, because of the time span over which reconstructions are performed, it is impossible to say whether the El Niño's were truly permanent or just that they were more frequent and had a shorter recurrence time (Wunsch, 2009).  Finally some researchers have expressed doubt that the temperature difference is real and not errors in the temperature reconstructions leading to an apparent lack of a temperature gradient.

As a key boundary condition for the climate system, through altering the radiative forcing of the planet, it is critical to understand: (a) whether $CO_2$ was higher in the Pliocene than present; (b) if so, by how much; and (c) whether elevated $CO_2$ could explain the temperature changes seen in the Late Pliocene.  Only a few studies have managed to reconstruct $CO_2$ during the Pliocene, but these indicate that $CO_2$ concentrations might have been 35% higher than preindustrial concentrations (Raymo *et al.*, 1996).  Pliocene reconstructions of 365 and 415 ppm of $CO_2$ are similar to current levels (Pagani *et al.*, 2010; Bartoli *et al.*, 2011, Seki et al. 2010, 2012)  and climate models, coupled with  our understanding of radiative forcing, show that this is likely to have accounted for some of the warmth (Haywood *et al.*, 2009a). An unresolved question is whether this increase in $CO_2$ was enough to account for all of the warming in the Pliocene and for the possible sustained El Niño conditions. A number of studies suggest this is not the case (Dowsett and Robinson, 2009). Instead, modeling studies suggest that increased greenhouse gas levels only account for 35% of the warming in the Pliocene (Dowsett and Robinson, 2009; Lunt *et al.*, 2009). They suggest that some other process such as meridional heat transport must have be influencing climate as well.

Extensive climate modeling work has been undertaken on the Pliocene (Haywood *et al.*, 2000).  The PRISM work has driven reconstructing climate during the Pliocene from proxy records (Haywood *et al.*, 2009a).  However, recently there is a number of higher resolution records developed, although their global coverage is much lower than the PRISM work.  The North Atlantic has continued to emerge as an area of data-model disagreement, with disagreement being as much as 8 °C (Dowsett *et al.*, 2012).  In order for the Pliocene to be used as an analogue for future climate change, it is crucial that the data for this period be better understood, in terms of climate processes and data-model disagreement.

Within the warmth of the Pliocene, a pronounced excursion in the benthic $\delta^{18}O$ record (Figure 1.1) marks the "M2 glaciation" at 3.3 Ma (Prell, 1984; De Schepper *et al.*, 2009). The M2 is marked by a pronounced cooling in several climate records (De Schepper *et al.*, 2009; McKay *et al.*, 2012). The M2 glacial stage also includes the first evidence of ice rafted debris (IRD) in the North Atlantic for widespread northern hemisphere glaciations (Kleiven *et al.*, 2002; Dwyer and Chandler, 2009), a fall in sea level (Lisiecki and Raymo, 2005), a weakening of the thermohaline circulation in the northern hemisphere (De Schepper *et al.*, 2009), and a major expansion of the ice sheet around Antarctica (Passchier, 2011; McKay *et al.*, 2012). However, despite arguments for this to be a global event, there is evidence that this cooling was a geographically restricted event, with the M2 not being found in a number of locations e.g. the Southeast Atlantic (Etourneau *et al.*, 2009). Another important outstanding question is whether the M2 marked the beginning of a more permanent "ice house" world (Kleiven *et al.*, 2002; McKay *et al.*, 2012), or whether the cooling and other changes in climate associated with M2 were just temporary (Ravelo *et al.*, 2004).

### *1.2.2 The Pliocene-Pleistocene Transition*

After the Pliocene warmth, it is assumed that there is a transition to the relatively colder climate of the Pleistocene (Filippelli and Flores, 2009). The traditional definition for the timing of this transition is when large-scale continental glaciations began in the northern hemisphere (Jansen and Sjoholm, 1991; Larsen *et al.*, 1994; Jansen *et al.*, 2000; Ravelo *et al.*, 2004; Haug *et al.*, 2005; Lawrence *et al.*, 2009, 2010). Defined as the "intensification of northern hemisphere glaciation" (INHG), this transition is dated to around 2.74 Ma, as shown by a decrease in both surface and deep ocean temperatures in the North Atlantic (Lawrence *et al.*, 2009; Sosdian and Rosenthal, 2009; Lawrence *et al.*, 2010) and evidence of increased continental glaciations as found in increased amounts of ice-rafted debris IRD (Jansen and Sjoholm, 1991; Larsen *et al.*, 1994; Raymo, 1994; Jansen *et al.*, 2000).

The INHG is associated with a transition from a relatively stable global climate to the larger amplitude glacial-interglacial cycles that define the Pleistocene (Figure 1.1) (Ravelo *et al.*, 2004; Raymo *et al.*, 2004; Bartoli *et al.*, 2006). The polar oceans in both hemispheres became permanently stratified, which could have led to increased $CO_2$ drawdown (Haug *et al.*, 1999; Sigman *et al.*, 2004; Nie *et al.*, 2008). In addition, the

Indian monsoon system weakened, which may have increased aridity in the African continent (deMenocal, 2004; Sinha and Singh, 2007; Zhang *et al.*, 2009).   This may be a very important change for human activity because this is the time when early human ancestors were evolving (deMenocal, 1995, 2004, 2011).   The transition in East Africa from a wetter to drier climate has been thought to play a role in the development of modern humans by allowing more grassland to develop in Africa while forests thinned, forcing early *homo sapiens* ancestors to adapt a more bipedal stance to deal with the new environment (deMenocal, 1995, 2004, 2011 Trauth *et al.*, 2009;).

The INHG is also marked by increased upwelling intensity in several regions (Marlow *et al.*, 2000; Dekens *et al.*, 2007a; Etourneau *et al.*, 2009). This includes the Benguela upwelling system, of importance to this thesis, given its proximity to the Cape Basin (Marlow *et al.*, 2000; Giraudeau *et al.*, 2002).  This change, which predates the INHG, is manifest within numerous upwelling zones as a diatom and biogenic opal maximum, referred to as the Matuyama Diatom Maximum (MDM) (Lange *et al.*, 1999; Berger *et al.*, 2002; Robinson and Meyers, 2002; Dupont *et al.*, 2005; Etourneau *et al.*, 2009), and is thought to caused by an increase in diatom production due to increased nutrient leakage from the deep ocean and a more efficient  delivery of nutrients to upwelling sites (Sigman *et al.*, 2004; Etourneau *et al.*, 2012; März *et al.*, 2013).  This increased productivity could have led to increased $CO_2$ drawdown, which might have been a reason for the transition to a globally cooler climate (Sigman *et al.*, 2004; Etourneau *et al.*, 2009).  The possible cause of the upwelling intensification at 2.2 Ma is an intensification of the Hadley and Walker cells, leading to more effective wind-driven upwelling (Etourneau *et al.*, 2010).

One of the most enduring explanations for why the Pliocene climate transitions occurred is the position and strength of ocean currents shifted in response to the changing positions of the continental land masses.  Although Pliocene continental configurations are similar to present (Haywood *et al.*, 2000; Haywood and Valdes, 2004), both the Isthmus of Panama and the Indonesia seaway are thought to have closed following the mid-Pliocene. The closing of the Isthmus of Panama is argued to have caused changes in the heat distribution of the Atlantic Ocean (Coates *et al.*, 1992; Burton *et al.*, 1997; Bartoli *et al.*, 2005; Haug *et al.*, 2005), whereas the closing of the straits around Indonesia may have restricted the movement of warm water from the Pacific to the Indian ocean warming the East Pacific warm pool and affected the exchange of fresh and salty water with the Atlantic Ocean (Cane and Molnar, 2001;

Molnar, 2008). Both of these processes could have restricted the amount of heat transfer across the globe, but especially to the region of major northern hemisphere ice sheet growth around the North Atlantic Ocean. Furthermore, both mechanisms would lead to changes in the surface salinity of the Pacific and Atlantic Oceans, which might also have had an impact on the Atlantic Meridional Overturning Circulation (AMOC) (Haug *et al.*, 2001; Nie *et al.*, 2008; Karas *et al.*, 2009). The AMOC describes the system of surface transport of warm water from the southern hemisphere to the northern hemisphere and then the return of cold water back to the south (Bradley, 1999). The AMOC is an important component of the thermohaline system.

There are problems with the theory that changes in tectonics are responsible for the INHG. Separating out the individual contributions of the Panama and Indonesian seaways is complicated by the range of other climate changes observed across the INHG. A problem is that the timing of both of these events is not well resolved and evidence for the timing of the final closure is debated (Molnar, 2008). Because the closure of both the Panama and Indonesian seaways have been estimated to occur in a broad range between 6 Ma and 2.7 Ma (Molnar, 2008), they may actually have occurred sometime before the INHG.

### 1.2.3  The Early Pleistocene

The early Pleistocene (3.0 and 1.5 Ma) is not as well documented as other climate periods. The benthic $\delta^{18}O$ stack (Figure 1.1), however, demonstrates that there is periodicity in the glacial-interglacial cycles of 41 ka, related to the obliquity cycle (Hays *et al.*, 1976). Sediment cores drilled from the West Antarctic ice sheet margin confirm that during the Pliocene there was a 41 ka cycle associated with the ice sheet retreats and advances (Naish *et al.*, 2009). These cycles suggests that an Early Pleistocene pattern of glacial and interglacial stages was a response to solar forcings similar to those which occurred during the Pliocene. Even during this period of increased cooler temperatures, however, there were warmer periods, the most prominent of which occurred during MIS 31 at 1.1 Ma. This very warm interglacial has been referred to as a "super interglacial" (DeConto *et al.*, 2007; Scherer *et al.*, 2008). This interglacial coincided with changes in the Southern Ocean (McKay *et al.*, 2012), and may have included a collapse of the Antarctic ice sheets (Figure 1.4) (Scherer *et al.*, 2008; Pollard and DeConto, 2009b). There were also shifts in the Antarctic

Circumpolar Current (ACC) currents, including a pronounced southward shift of the polar fronts (Flores and Sierro, 2007; Maiorano *et al.*, 2009).
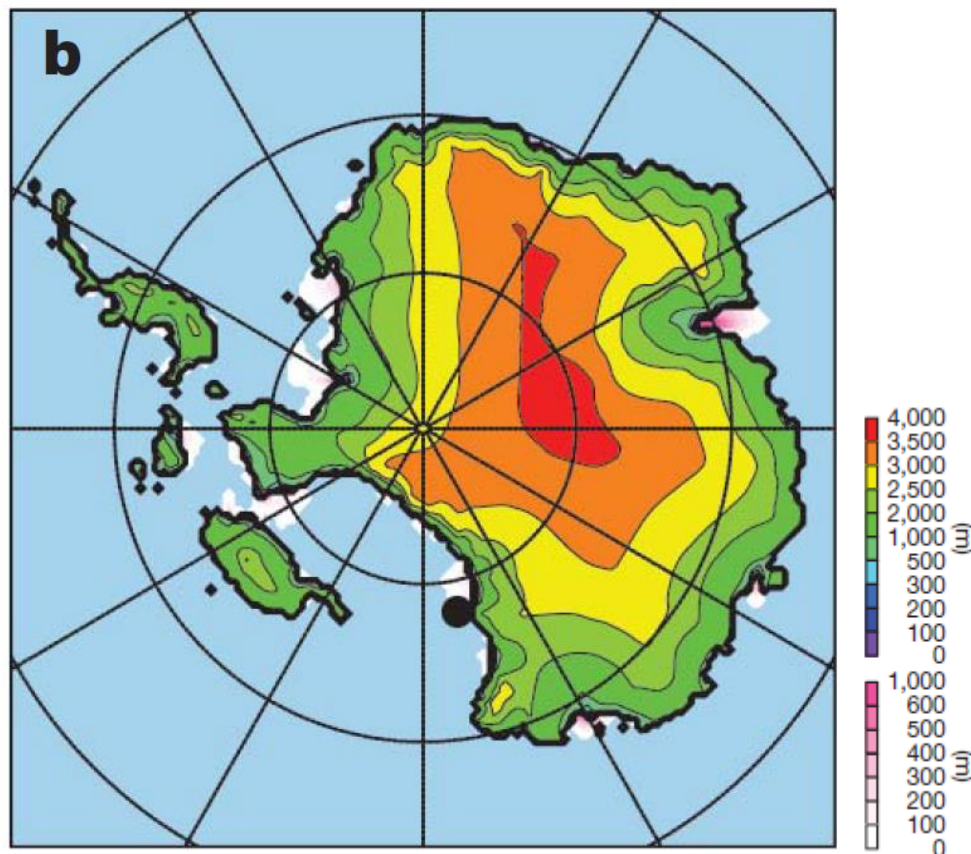
**Figure 1.4 the extent of ice in Antarctica during MIS 31.** Based on Ice sheet models, this figure shows an almost complete collapse of the West Antarctic ice sheet during the warm interglacial of MIS 31 (Pollard and DeConto, 2009b).


### *1.2.4 The Mid-Pleistocene transition (MPT)*

The mid Pleistocene transition (MPT) occurred ~ 1 Ma and marks a transition in the benthic $\delta^{18}O$ record from glacial-interglacial cycles with an obliquity-related period (41 ka), which dominated during the early Pleistocene, to the 100 ka cycles of the later Pleistocene (Figure 1.5). The exact timing of this event is debated, but the dominance of the 41 ka cycles ends around 900 ka. This change is linked to the 900 ka event (Clark *et al.*, 2006; McClymont *et al.*, 2013). Many of the changes associated with the MPT happen at 900 ka (Rodriguez-Sanz *et al.*, 2012; McClymont *et al.*, 2013) The extent of the continental ice sheets and sea ice increased during the MPT (Kitamura and Kawagoe, 2006; Sosdian and Rosenthal, 2009; Elderfield et al., 2012; Hernandez-Almeida et al., 2012, Sosdian and Rosenthal, 2009). There is evidence for northward shifts in the ACC (Becquey and Gersonde, 2002; McClymont *et al.*, 2005; Kemp *et al.*, 2010; Martinez-Garcia *et al.*, 2010), and the production of deep water in the Atlantic Ocean was reduced (Schmieder *et al.*, 2000; Marino *et al.*, 2009). The modern Walker

Circulation also began operating during this time (McClymont and Rosell-Mele, 2005). This has been suggested to explain enhanced moisture transport to northern hemisphere ice sheets (McClymont and Rosell-Mele, 2005) which could have been a major reason for their increase. There was increased aridity in Africa (deMenocal, 2004; Schefuss et al., 2004; Almogi-Labin, 2011). Based on a recent review of SST records which span the MPT, most regions show cooling at 1.2 Ma which is earlier than the expansion of continental ice (McClymont *et al.*, 2013).
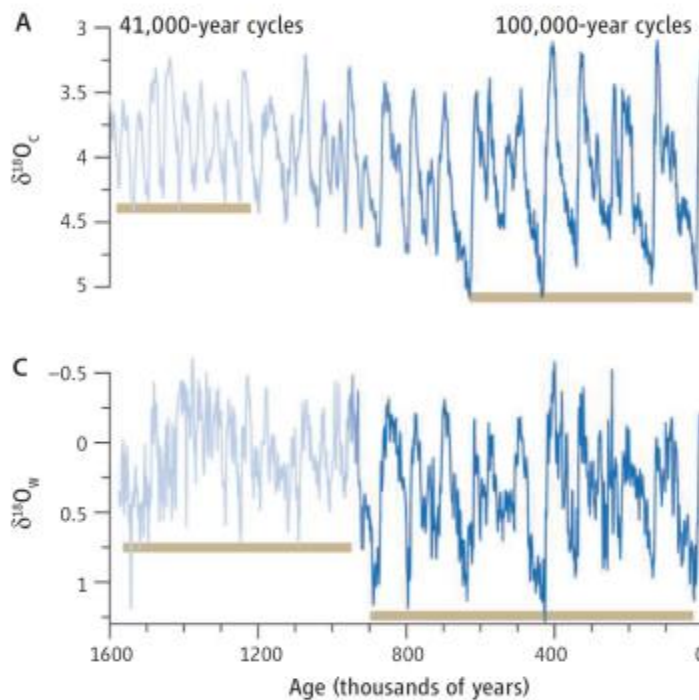


**Figure 1.5 evidence for the MPT.** (A) the LR04 record of the MPT with the bars indicating the period when clear cycles exist in the record. (B) The Elderfield et al. (2012) record of benthic $\delta^{18}O$ showing the sudden change that occurs at 900 ka (Clark, 2012).

The causes of the MPT are still being debated. There are three major theories. The first proposes that an increased drawdown of $CO_2$ cooled the climate (Marino *et al.*, 2009). This theory proposes that drawdown of $CO_2$ was sustained throughout the early Pleistocene, and that, over time, this caused the climate to become more sensitive to precession cycles. (Raymo *et al.*, 1997). The lack of ice core records for this perod means that there are only a few, low-resolution $CO_2$ reconstructions of the climate during this time making hard to test the assumptions of the theory (Luthi *et al.*, 2008; Honisch *et al.*, 2009; Seki *et al.*, 2010; Bartoli *et al.*, 2011). Furthermore, the data that

does exist for this time period does not necessarily show that $CO_2$ was changing, as both modelling and proxy reconstructions show $CO_2$ change over the MPT only occurred at that glacial-integlatial scales and there was no long term change in $CO_2$ levels (Hoogakker *et al.*, 2006; Honisch *et al.*, 2009).

A variant on this $CO_2$ drawdown theory is that the increased amount of crystalline bedrock exposed throughout the MPT could have led to more $CO_2$ drawdown through chemical reactions with the exposed bedrock (Clark and Pollard, 1998; Clark *et al.*, 2006; Clark, 2012). The theory became less spatially extensive because of the removal of regolith, allowing the ice sheets to build in thickness (Clark and Pollard, 1998; Clark *et al.*, 2006; Clark, 2012). This theory, suggests that the ice sheet could have grown without any need for a long term $CO_2$ drawdown.

Another theory by Huybers (2009) argues that the climate transition seen in the mid-Pleistocene transition a chaotic response. This chaotic response theory suggests that the switch from an interglacial to a glacial climate is a random chaotic switching between two steady states in the climate system (Huybers, 2009). In reality, while there is a great deal of controversy over the effect of different forcings, data has not yet reached the point where any one theory can be summarily rejected. Instead, Huyber's (2009) theory can only be credited when all other possible forcings have been eliminated.

Recently, new proposals have emerged which consider that changes in the Antarctic ice sheets and sea ice (rather than the traditional northern hemisphere focus) might have triggered the shift to the 100 ka world. This is based on growing evidence of an increase in Antarctic sea ice at the 900 ka event (Elderfield *et al.*, 2012) (Figure 1.5). This is shown by a drop in the $\delta^{13}C$ benthic data at this date which might represent an exposure of shelf carbon in addition to the $\delta^{18}O$ drop that is connected to changes in sea level (Elderfield *et al.*, 2012), which has been interpreted as a change in the productivity of the Southern Ocean at this time linked to expanded sea ice. This concurs with increasing evidence of building sea ice during the 900 ka event from data sources, (Elderfield *et al.*, 2012) ice sheet dynamics (Raymo *et al.*, 2006), and ice sheet models (DeConto *et al.*, 2007). A build-up of sea ice could lead to a shift in the ACC currents northward. In fact, there is evidence that there was indeed a shift northward of 7° of the ACC at the MPT (Diekmann and Kuhn, 2002; Marino *et al.*, 2009; Kemp *et al.*, 2010).

The MPT was a distinct period of climate and environmental change in many aspects of the climate system. This was a gradual transition, with different parts of the climate system evolving at different times (Liu *et al.*, 2008). The detailed structure of the MPT has recently been reviewed (McClymont *et al.*, 2013), and it is clear that initial cooling in the surface ocean began from 1.2 Ma, but at some sites this marked the end of a longer term cooling beginning as early as 1.8 Ma (McClymont *et al.*, 2013). This suggests that the MPT was a complex transition, involving multiple parts of the climate system, whose origins still remain unclear.

### *1.2.5. The Mid to Late-Pleistocene*

The mid- to late Pleistocene is the interval that has been the most extensively studied for climate reconstructions. It is the time of the largest amplitude and longest duration (100 ka) glacial-interglacial cycles (Figure 1.1), and includes evidence from ice core data of atmospheric chemistry (EPICA, 2004) to complement the sediment sequences. MIS 11 has been targeted for investigation because its orbital forcings are at have similar boundary conditions as the current Holocene interglacial (Loutre and Berger, 2003). The MIS 11 is also interesting because it was one of the warmest and longest interglacials of the mid- to late Pleistocene which may sugest that it is an analogue for today (Berger and Loutre, 2002). On the other hand there is evidence for major differences in the MIS 11 climate. For example, during MIS 11, Greenland had extensive forests and may have been ice-free (de Vernal and Hillaire-Marcel, 2008). Therefore because of the high temperature, length and conditions, MIS 11 is often used as an analogue for future warming (Berger and Loutre, 2002; Loutre and Berger, 2003). MIS 11 has also been investigated to understand how long an interglacial can be sustained and what controls the length of an interglacial (Ruddiman, 2003; Ruddiman, 2005; Ruddiman *et al.*, 2005; Dickson *et al.*, 2009; Dickson *et al.*, 2010a; Dickson *et al.*, 2010b). These are important questions when addressing whether the duration of the Holocene will be the result of natural conditions or human induced (anthropogenic) forcing (IPCC, 2007). However, some researchers have argued there are problems with relating the two interglacials and that, in MIS 11, the forcings were different from the current interglacial (Dickson *et al.*, 2009). It is also been suggested that there was a different water mass configuration in the southern hemisphere during this time (Kandiano and Bauch, 2007; Dickson *et al.*, 2009).

MIS 11 marks the start of a period of warmer interglacials that is referred to as the Mid-Brunhes Event (MBE) at 430 ka. Prior to the MBE, interglacials were less intense, with the change between glaciations and interglacials being around 1 °C (Lang and Wolff, 2011), whereas afterwards there were more intense interglacials, as shown by the increase in the average temperature change between glacials and interglacials in the record to 1.5 °C. (Candy *et al.*, 2010; Voelker *et al.*, 2010; Holden *et al.*, 2011). However, there is debate around whether the MBE was a global event e.g (Voelker *et al.*, 2010; Holden *et al.*, 2011; Lang and Wolff, 2011) or whether the observed interglacial changes were more regional (Candy *et al.*, 2010; Candy and McClymont, 2013). After the MBE, a number of recent interglacials have been identified as 'super-interglacials' during MIS 1, 5, and 11 (Pollard and DeConto, 2009b; Masson-Delmotte *et al.*, 2010; Turney and Jones, 2010). Super interglacials are warm and long interglacials, and therefore may help establish a context for the current warm and relatively long-lasting interglacial.

The Last Glacial maximum (LGM) is the most recent glacial period in the Earth's history. It dates from 23 ka to 18 ka. Because the LGM represents a period of time close to the present time, therefore high resolution data that allows the comparison of small scale changes in the Earth's climate to be produced (MARGO, 2009, Annan and Hargreaves 2013). One of the questions is whether $CO_2$ leads temperature changes or whether warming causes increases in $CO_2$ (MARGO, 2009). Understanding these questions will allow understanding of what the effect of $CO_2$, which is a "greenhouse gas", has on major climate changes (IPCC, 2007). Another key question is what changes in the AMOC occur and where do they occur. Many people have suggested that a collapse of the AMOC by fresh water from the northern hemisphere could collapse the AMOC (Carlson *et al.*, 2008; dos Santos *et al.*, 2010; Laurian and Drijfhout, 2011; Sepulcre *et al.*, 2011). Therefore, understanding the changes in the AMOC are also important reasons to reconstruct the LGM (MARGO, 2009).

### *1.2.7 Summary*

There are a number of major questions about the both the Pliocene and Pleistocene periods that require further study. These include:

- What are the changes caused by a warmer world and how these might relate to future climate changes? (Pliocene)

- What drove the changes to a cooler world and where and when did these changes occur? (Pliocene-Pleistocene transition)

- What drove changes in the cycles from the 100 ka world to the 41 ka world, and what did these changes mean for the global climate? (MPT)

- What is the exact timing of the glacial/interglacial changes and whether there has been super-interglacials?

The purpose of this thesis is to investigate, using data from a site in the Southeast Atlantic (Ocean Drilling Program, ODP, site 1087), Pliocene and Pleistocene climate changes, providing information that may contribute to answering these four questions.

## 1.3 The South East Atlantic

The ocean around the Cape of Good Hope is an important area for climate change because it is the meeting place of three major current systems (Boebel *et al.*, 1999), specifically where the Atlantic, Indian and Southern Oceans interact (Figure 1.2). The Southeast Atlantic is therefore considered to be an important gateway for ocean circulation and, in turn, global climate and onshore environmental change. The marine sediment core discussed in this project, ODP Site 1087A (31º28'S, 15º19'E, 1374 m water depth, Figure 1.2), is located at the intersection of these currents it is therefore ideally situated for the recovery of a core which could track changes over time. Also the sediment record at this site extends back to the early Oligocene (Shipboard Scientific Party, 1998) which means it is a good candidate for long climate reconstruction event further back then this current study.

### 1.3.1 The Benguela Current and Benguela Upwelling

The Benguela upwelling system is located along the margins of southern Africa, and is closely associated with the flow of the Benguela offshore current (BOC) and Benguela Coastal Current (BCC) (figure 1.6) (Andrews and Cram, 1969).  The Benguela upwelling comprises three major areas: the northern, central, and southern cells.  The northern and central cells currently experience perennial upwelling as a result of the year-round SE trade winds and longshore winds blowing seaward from the African continent (Hutchings *et al.*, 2009).  The northern and central upwelling cells are thus distinguished by higher productivity and unique cold water planktonic species (Ufkes *et al.*, 2000; Ufkes and Kroon, 2012).  The southern upwelling cell sees more seasonal upwelling since the trade winds which drive upwelling only affect this cell during the summer (Andrews and Hutchings, 1980; Burls and Reason, 2008). As a result, temperatures in the southern Benguela region are warmer, and the planktonic assemblage represents a lower nutrient and warmer environment (Jones, 1971; Andrews and Hutchings, 1980; Boebel et al., 2003; Hutchings et al., 2009, Boebel *et al.*, 1999).

The southern Benguela upwelling is also affected by interaction with the edge of the continental shelf, and the presence of warm water inputs from the Agulhas Leakage system (discussed in section 1.4.2). In combination, these also cause a reduction in upwelling in the southern Benguela region (Figure 1.6) (Andrews and Hutchings, 1980; Giraudeau et al., 2001; Blanke et al., 2009). The waters which form the Benguela upwelling system are sourced from Southern Component Water and Antarctic Intermediate Water (AAIW), and as a result have a connection to high latitude processes operating in the Southern Ocean (Lutjeharms, 1985; Lange *et al.*, 1999).
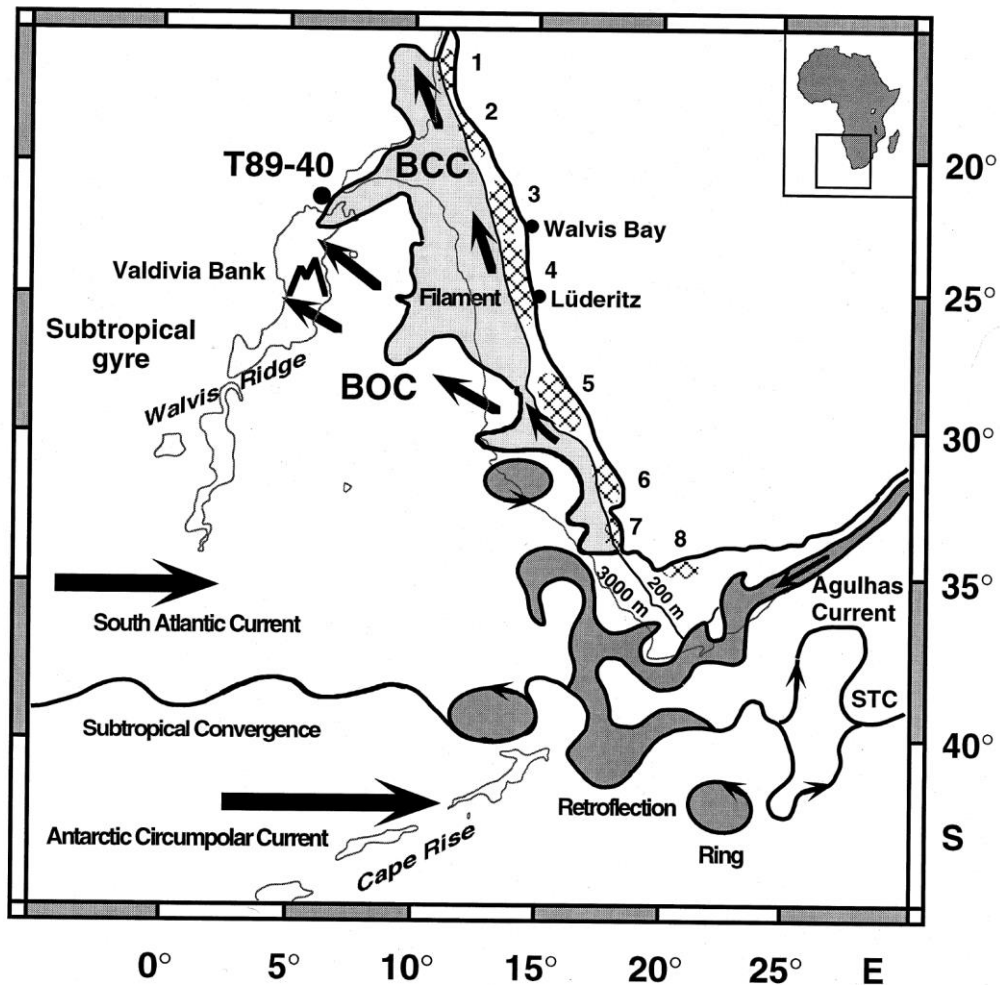
**Figure 1.6  The location of the Benguela upwelling showing the interaction with the Agulhas current** (Ufkes and Kroon, 2012).  The abbreviations represent BOC, Benguela Oceanic Current; BCC, Benguela Coastal Current.  The light grey area represents the temporary upwelling zone while the dark grey area represents the Agulhas Leakage.  The hatched area represents the central upwelling cells.

### *1.3.2 The Antarctic Circumpolar Current (ACC)*

The Antarctic Circumpolar Current (ACC) is a complex set of currents which circle Antarctica in the Southern Ocean, and which are marked by low SSTs and regions of high biological production  (Reid, 1989; Peterson and Stramma, 1991; Rintoul, 1991; Garzoli and Giulivi, 1994; Orsi *et al.*, 1995; Holliday and Read, 1998).  The currents are driven by changes in the westerly wind currents (Orsi *et al.*, 1995).  Both the Antarctic Bottom Water and Antarctic Intermediate Water (AAIW) are produced in this area (Rintoul, 1991) and it is an important draw down area for $CO_2$ (Diekmann *et al.*, 2003) as well as an upwelling site which causes $CO_2$ production (Sigman and Boyle, 2000; Sigman *et al.*, 2004). However recent research shows that during glacial periods

especially the last glacial maxim there was increased upwelling in the central ocean with the increase in the westerlies.  This change caused upwelling to decrease and the $CO_2$ input to decrease from the deep ocean to the atmosphere (Sigman and Boyle, 2000; Sigman *et al.*, 2004; Toggweiler and Russell, 2008).  This close connection between the ACC and the westerlies can be seen in the dust records from the southern ocean (Martinez-Garcia *et al.*, 2011).   The ACC system also prevents warm water from reaching the coast of Antarctica, resulting in Antarctica being even cooler than it would be otherwise  (Orsi *et al.*, 1995).  The formation of the ACC is thought to be related to the first evidence of glaciations on the continent (Mackensen, 2004). The ACC currents represent an important boundary current for the Southeast Atlantic systems

### 1.3.3 The Agulhas Current and Agulhas Leakage

The SE Atlantic is affected by the inputs of warm and salty water from the Agulhas Current and Agulhas Leakage systems (Ba and Duplessy, 1976; Harris and van Foreest, 1978; Gründlingh, 1980; Hutson, 1980; Lutjeharms, 1981; de Ruijter and Boudra, 1985; Boudra and De Ruijter, 1986; Olson and Evans, 1986; Gordon *et al.*, 1987; Fine *et al.*, 1988; Shannon and Hunter, 1988; Gordon and Haxby, 1990). The Agulhas Current moves warm water down the east coast of Africa from the latitude of the Red Sea to the southern tip of Africa (Lutjeharms, 2007; Roman and Lutjeharms, 2009).   It is a warm water and high salinity current (Lutjeharms, 2007).  The Agulhas Current does not enter the South Atlantic Ocean; instead, eddies formed by the current are spun off by a retroflection due to the zero-stress curl of the westerlies in this part of the ocean. The water moves through Ekman transport, which produces rings of water that move independently and constantly (Lutjeharms, 1981; Lutjeharms, 1985; Lutjeharms and Gordon, 1987; Lutjeharms, 1994; Lutjeharms *et al.*, 2001; Lutjeharms, 2007). These "Agulhas rings" are formed of warm water and are saltier than the surrounding Atlantic Ocean (Lutjeharms and Gordon, 1987; van Sebille and van Leeuwen, 2007).  After entering the Atlantic Ocean, the Agulhas rings then move in a north-westerly direction within the Benguela offshore current, joining with other ocean surface currents off the coast of Brazil (Figure 1.7).  This process, from the production of Agulhas rings and their northward transport, is known as "Agulhas Leakage" (Gordon, 1985; Lutjeharms, 1994; Reason *et al.*, 2003; Lutjeharms, 2007).  Agulhas Leakage has been shown to be an important component of the thermohaline circulation in  (Gordon, 1985; Weijer *et al.*, 1999; Reason *et al.*, 2003) moving heat out of the

Indian Ocean and into the Atlantic Ocean (van Sebille and van Leeuwen, 2007)(Figure 1.7). Second, it is an important method of transferring salt from the relatively salty Indian Ocean to the relatively fresh Atlantic Ocean (Weijer *et al.*, 1999). This salt and heat input contributes to the operation of the thermohaline system, which is one of the major transports of heat from the southern hemisphere to the northern hemisphere. It has, in turn, been argued that this process helps regulate global temperatures (Gordon, 1985; Weijer *et al.*, 1999; Reason *et al.*, 2003). Therefore the Agulhas current and the Agulhas Leakage form a crucial link in the modern climate system.
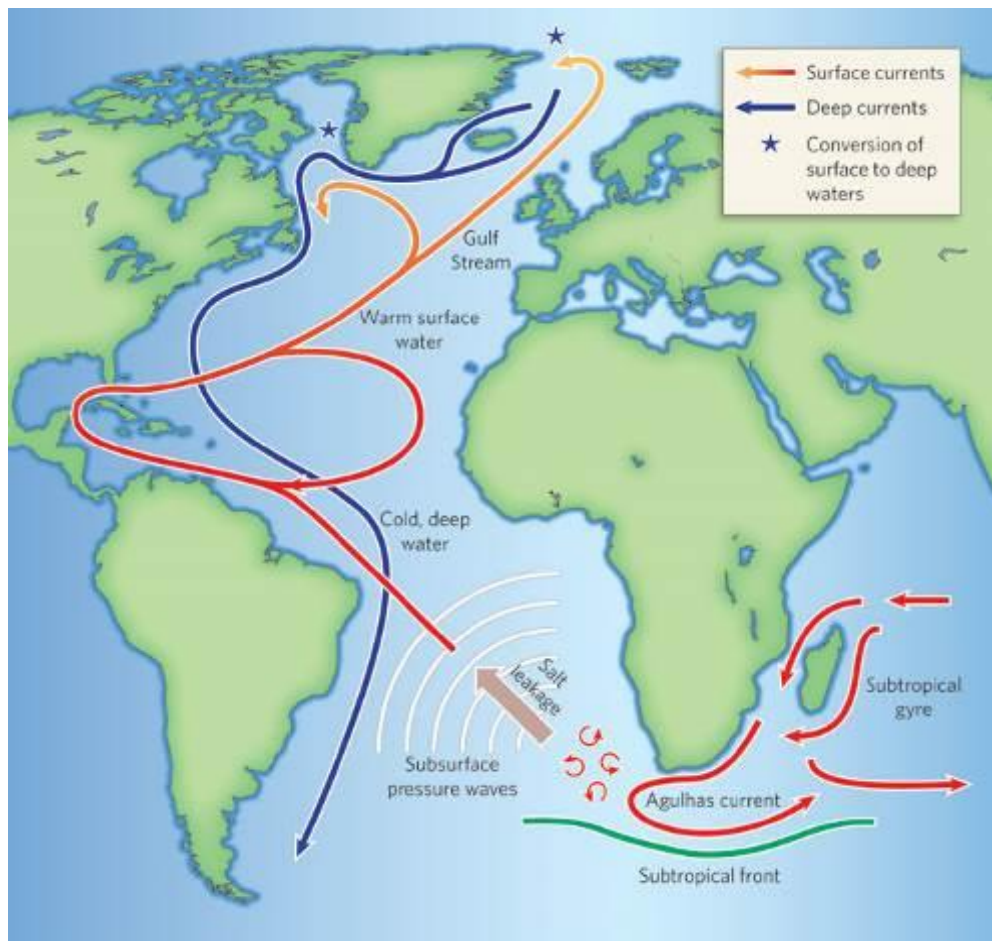
**Figure 1.7 The connection between the Agulhas Leakage and the thermohaline circulation. (Zahn, 2009)**. In the illustration warm surface currents are illustrated by red arrows while cold deep current are marked by blue arrows. Note the role the Agulhas current plays in linking the warm Indian Ocean currents to the warm Atlantic Ocean currents.

## 1.4 The Climate History of the South East Atlantic

The history of the southern Atlantic during the Pliocene and Pleistocene is not as well-known as some other parts of the ocean. A number of high quality reconstructions have been produced for the northern and central parts of the Benguela upwelling system (Marlow et al., 2000; Etourneau et al., 2009; Etourneau et al., 2012), but there are no reconstructions which are both high resolution (i.e less than 10 ka resolution) and which extend through both the Pliocene and Pleistocene available for the Agulhas Leakage, the Agulhas Current, or the southern part of the Benguela upwelling. However, to fully assess the mechanisms invoked to explain the Pliocene and Pleistocene climate events described above, it is important that new records for the SE Atlantic region be produced.

Existing data sets for the Benguela upwelling system suggest it was either not as active during the entire Pliocene and/or that it was upwelling warmer water (Marlow *et al.*, 2000; Dekens *et al.*, 2007b; Etourneau *et al.*, 2009). The ACC has been shown to have expanded towards the equator based on diatom mats and changes in the diatom assemblage during the Pliocene (Barron, 1996). It is thought that the surface leg of the AMOC was enhanced in the Pliocene, allowing more warm southern hemisphere water to move northward and increasing the amount of global warming during this time (Raymo *et al.*, 1996).

The amount and location of the focus of Agulhas Leakage remains unknown during the Pliocene. However, data studies suggest that the thermohaline circulation becomes weaker during times with warmer global temperatures (Lawrence *et al.*, 2009; Lawrence *et al.*, 2010). Others have suggested that the restriction of the Indian Ocean Throughflow might have restricted Agulhas Leakage based on decreasing tempeatures north of the Agulhas Leakage, although tectonic processes that have been slowly opening up the linkage between the two oceans have actually allowed more warm water from the Pacific warm pool to pass into the Indian ocean. This causes a warming of the Indian Ocean currents which are the source for the Agulhas Current. Therefore a warmer Agulhas Leakage is thought to be connected to more warm water input into the Indian Ocean (Karas *et al.*, 2009; Karas *et al.*, 2011a; Karas *et al.*, 2011b; Rommerskirchen *et al.*, 2011; Karas *et al.*, 2012). In contrast, because of the southward migration of the ACC during the Pliocene, the Agulhas Leakage should have had more space to operate and therefore should have been stronger (McKay *et al.*, 2012). Assessing the potential connection or interaction between the Indian and Atlantic Oceans during the Pliocene is further complicated by the presence of only one temperature reconstruction for the entire Indian Ocean during the Pliocene (Dowsett *et al.*, 2012)(Figure 1.2). Thus, the assessment of whether changes in Indian Ocean temperatures were translated into the Atlantic is not yet possible.

The transition from the Pliocene to the Pleistocene at 2.7 Ma was accompanied by the Matuyama Diatom Maximum (MDM), which occurred in the Benguela upwelling zone (Lange *et al.*, 1999; Berger *et al.*, 2002; Robinson and Meyers, 2002; Dupont *et al.*, 2005; Etourneau *et al.*, 2009). This was a time of increased diatom production in the surface ocean, argued to have been caused by increasing activity in the upwelling system, bringing more nutrients to the ocean surface. The MDM also saw an increase in the size of the Benguela upwelling area (Giraudeau *et al.*, 2002). It has been

argued that this is a result of more efficient silica leakage from the Antarctic ocean, brought in through AAIW, and a weak early upwelling (Etourneau *et al.*, 2012). Finally, around 2.4 to 2.0 Ma, it has been suggested that there was an intensification of the northern and central cells of the Benguela upwelling, shown in cooling SST trends of ~3.0 °C during this period (Etourneau *et al.*, 2009). In combination, the limited evidence available indicates that changes to the position of the ACC and intensity of Benguela upwelling were occurring across the Pliocene-Pleistocene transition, but the impact of these changes on the Agulhas Leakage is not yet known. As discussed in section 1.2, there are also changes in Benguela upwelling intensity and the position of the ACC associated with the MPT. Specifically there was a cooling in the Benguela Upwelling coupled with a 7° northward shift of the ACC (Becquey and Gersonde, 2002).

For the mid and late Pleistocene, a number of records focussed on Agulhas Leakage have been produced. Increased leakage has been identified to occur at the end of the glacial periods over the last 0.5 Ma, based on increases in distinctive Indian Ocean foraminifera species such as *G. menardii* (Kroon and Ganssen, 1989; Peeters *et al.*, 2004). In comparing the timing of the deglaciation in the Agulhas region, a number of temperature and foraminiferal records show Agulhas Leakage peaked between 10 and 5 ka before the onset of the global warming associated with the start of interglacials (Peeters *et al.*, 2004; Martínez-Méndez *et al.*, 2008; Dickson *et al.*, 2010b; Martínez-Méndez *et al.*, 2010; Turney and Jones, 2010). The reasons for this pattern are still not well understood but it is thought to be indicative of a strengthening of the Agulhas Current, causing more leakage to occur (Peeters *et al.*, 2004). It has been theorized this Agulhas Leakage has an important effect on global climate (Peeters *et al.*, 2004). In support of this theory, climate models show increased input from the Agulhas Leakage might have been effective in starting the Bölling warming event at the end of the Pleistocene, 11 ka (Chiessi *et al.*, 2008). During glacial periods, the early warming of the SE Atlantic driven by Agulhas Leakage might also be an important contributor to the "seesaw" pattern of climate warmings and coolings that takes place during the glacial period, whereby the North Atlantic (and Greenland) tend to cool during times of warming in the South Atlantic (and over Antarctica) (Barker et al., 2009; Wolff et al., 2009).

It is thought if there is northward movement of the subtropical front because of expanded sea ice, for example during glacial stages, this could result in the weakening

of the leakage or even cutting it off (Biastoch *et al.*, 2008c; Bard and Rickaby, 2009). Climate reconstructions from marine sediment cores within the zone of the ACC show northward movement occurred during the glacial stages over the last 1.15 Ma (Keany and Kennett, 1972; Hodell *et al.*, 2000; Becquey and Gersonde, 2002; Diekmann and Kuhn, 2002). However, from these reconstructions it is not possible to say how far north the ACC moved. A reconstruction of the southeast Atlantic for the mid-Pleistocene shows that there is a large cooling event at 1.1 Ma (MIS 32) just before the MPT (McClymont *et al.*, 2005). It is interpreted this could indicate a northward migration of the ACC and/or a failure of the Agulhas Leakage (McClymont *et al.*, 2005). Recently, using a sediment core recovered from the Agulhas Current (in the Indian Ocean), it has been suggested a complete shutdown of the Agulhas current by ACC might have contributed to two especially cold glacial periods seen in that record, MIS 12 and MIS 10 (Bard and Rickaby, 2009). However, there is little direct evidence for the Agulhas Leakage being cut off by the polar currents.

Studies of the temperature and volume of the leakage show that last few glacial periods shows the leakage was restricted and weakened during the glacial periods but was never cut off (Rau *et al.*, 2002; Franzese *et al.*, 2009). Although the pre-MPT cool glacial of MIS 32 in the SE Atlantic is argued to reflect reduced Agulhas Leakage (McClymont and Rosell-Mele, 2005), there is also evidence from changes in temperature for a southward shift of the ACC during the MIS 31 transition which could indicate that the circumpolar currents are more complex in their behaviour than just responding to global warming and cooling cycles (Flores and Sierro, 2007). Furthermore, the relationship between the position of the ACC and the Agulhas Leakage is not clear. Some have suggested a northward position of the ACC might weaken the Agulhas Current and even possibly cut off Agulhas Leakage (Bard and Rickaby, 2009). Other models suggest northward movement of the ACC could increase the amount of Agulhas Leakage (van Sebille *et al.*, 2009). Recent studies based on multiple cores along the boundary between the two currents trying to track of ACC and the history of the Agulhas Leakage using biological evidence propose the connection are more complex and that none of the models fully reflect that complexity (Franzese *et al.*, 2006; Franzese *et al.*, 2009).

Climate models have shown Agulhas Leakage is the most likely candidate for restarting the thermohaline circulation after it collapsed during the Younger Dryas event at 12 ka, during the last deglaciation (Knorr and Lohmann, 2003; Knorr and Lohmann,

2007; Zharkov and Nof, 2008). A warming of SSTs based on changes in radiolarian temperature during the late Pleistocene MIS 10 was found in cores throughout the Southern Ocean and in the air temperatures in the Vostok ice core, suggesting it was warmer in the Southern Ocean during the glacial (Cortese *et al.*, 2004). This may indicate a southward displacement of the Agulhas Leakage during certain glacial periods and further evidence of possible leakage continuing through the glaciations.

## 1.5 Summary

A number of major changes in climate during the last 3.5 Million years are shown to be related to ocean circulation changes in the southeast Atlantic. During the Pliocene, when the temperature and $CO_2$ levels were higher and within the range of predicted future changes with global warming, the southeast Atlantic Ocean indicates a lack of upwelling. The change from the warm Pliocene to the cold Pliocene is the most prominent climate shift over the last 3.5 million year. In the southeast Atlantic Ocean the main event is the strengthening of upwelling between 2.2 and 2.0 Ma. During the MPT there is a cooling in the SE Atlantic between 1.6-0.9 Ma. Finally in recent glacial and interglacial cycles there is evidence of Agulhas Leakage developing before the start of the interglacials, which is thought to have major impacts on the AMOC system. However, how long ago the Agulhas Leakage and these early deglacial warmings began is an open question. In this thesis the aim is to discover how the global climate changes of the last 3.5 Ma affected the Southeast Atlantic

## 1.6 Thesis Aims and Objectives

The overall aim of this thesis is to understand the connection between changes in ocean circulation in the southeast Atlantic Ocean and major climate transitions over the last 3.5 million years. An examination of the local/regional signatures of global climate transitions in the southeast Atlantic Ocean should help illuminate the mechanisms which drive global climate change. In order to achieve this aim the following research objectives are defined:

1. To reconstruct sea surface temperatures (SSTs) and other climatic variables in a key ocean gateway (the SE Atlantic), in order to determine local ocean circulation change over the last 3.5 Ma;

2. To understand the timing of the start and intensification of the Agulhas Leakage and whether or not this occurred during times of global climate transition;

3. To indicators of surface production and other oceanographic variables in order to assess the position and intensity of the Benguela Upwelling and to understand if the timing of these changes related to global climate change;

4. To compare the reconstructed changes in ocean circulation at ODP 1087 to the major coolings and warmings in the Earth's climate over the last 3.5 Ma in order to assess what role, if any, the Southeast Atlantic Ocean played in these changes.

The next section of the thesis will investigate the background of the methods used in the thesis. This is followed by an outline of the laboratory methods used in the project. Four discussion chapters then follow, Chapter 4 will reflect on the findings in the context of their implications for global climate changes over the last 3.5 Ma. This will be followed by three chapters outlining the local changes in the southeast Atlantic during the Pliocene (Chapter 5), across the Plio-Pleistocene transition (Chapter 6), and the Mid to late Pleistocene (Chapter 7). Finally, Chapter 9 will summarise the main conclusions of the thesis and offer some perspectives on limitations and future work.

# Chapter 2 Paleoclimate Proxies

## 2.1 Introduction

The overall aim of this thesis is to understand the interactions between major transitions between warm and cold climates over the last 3.5 ma and the Southeast Atlantic Ocean. In order to do this a *multi proxy* approach is necessary. Climate proxies are often a chemical or biological variable that can be directly related to a climate variable like temperature or salinity (Killops and Killops, 2005; Eglinton and Eglinton, 2008). The major proxies used in this thesis are biomarkers, microfossils and stable isotopes. These different proxies allow the reconstruction of SSTs, salinity, location of ocean currents, strength of upwelling, and terrestrial input at a given core site. In this chapter, each of the proxies to be applied in this thesis will be presented and evaluated.

## 2.2 Biomarkers

A biomarker is a molecular fossil related to changes in specific organisms (Eglinton and Eglinton, 2008; Rosell-Mele and McClymont, 2008). There are a number of advantages to using biomarkers in palaeoclimate research. As biomarkers are organic molecules, the identification of entire groups of organisms that often are not preserved or poorly preserved as hard fossils (e.g. carbonate shells) is possible (Eglinton and Eglinton, 2008; Rosell-Mele and McClymont, 2008). Perhaps the strongest support for using biomarker proxies in palaeoclimate research is the fact that certain biomarker signatures are closely associated with specific climate variables such as SST and sea ice cover (Brassell *et al.*, 1986; Powers *et al.*, 2005b; Schouten *et al.*, 2007; Kim *et al.*, 2010; Belt *et al.*, 2012).

To be a good biomarker a number of conditions must be met. First, the compound in question must be tied to either a specific group of organisms or even better a specific type of organism. Organic chemicals are found in a wide range of organisms are not as useful ( Eglinton and Eglinton, 2008; Rosell-Mele and McClymont, 2008). Second, the compounds must be well preserved and not degrade substantially over long periods of time (Rosell-Mele and McClymont, 2008). If degradation does occur, there must be preservation of the structure of the molecule well enough to identify its original source (Eglinton and Eglinton, 2008; Rosell-Mele and McClymont, 2008). The group of organic compounds that is most resistant to degradation is lipids. Thus, whilst some very specific organic molecules such as DNA could be useful for reconstructing past

environments, they are only preserved in unusual conditions and/or the technology does not exist yet to identify the compounds in complex organic samples (Coolen and Overmann, 2007).

A good understanding of how the biomarkers are delivered to the site in question is important. Some terrestrial biomarkers might be delivered within a year from initial production, whereas others can be trapped in soils for hundreds or thousands of years (Eglinton and Eglinton, 2008). Ocean currents at the surface and at depth, as well as the water depth at the site, might affect how quickly compounds are delivered to the seafloor sediment and also how much sediment mixing and resuspension might have taken place prior to deposition (Kim *et al.*, 2009; Kim *et al.*, 2012). To determine the source of the biomarkers to sediment thus requires a good understanding of wind systems, fluvial inputs, and ocean currents. As a result, the local, regional, and global controls over biomarker signals must be understood in order to interpret the data.

### *2.2.1 The $U^K_{37}$ and $U^K_{37}$' indices*

The $U^K_{37}$ index is a mathematical relationship between the surface temperature of ocean and the relative amount of various alkenone compounds (Volkman *et al.*, 1980a). Alkenones are long ($C_{36}$-$C_{39}$) unsaturated ethyl and methyl ketones (Figure 2.1). These compounds were identified first at Walvis Ridge (de Leeuw *et al.*, 1980), just to the north of the ODP 1087 site which is the focus of this thesis. The alkenones were soon identified in many major oceans sediments (Conte *et al.*, 1992). In the open ocean alkenones are produced by only a few species of organisms, largely members of the haptophyte algae group, and so are highly specific biomarkers. The most widespread of the haptophytes is the species *Emiliania huxleyi*, a coccolithophore (Volkman *et al.*, 1980a). *E. huxleyi* however has only been around for 200-300ka. Later, a second species of coccolithophore, *Gephyrocapsa oceanica,* was also found to produce alkenones (Volkman *et al.*, 1980a, 1980b; Marlowe *et al.*, 1984a, 1984b; Conte *et al.*, 1994). It was originally proposed that the alkenones are membrane lipids that help it regulate the rigidity of the organism at different temperatures (Prahl *et al.*, 1988) although this has not been definitively confirmed and is debated (Sikes *et al.*, 1997).

## Alkenones



C37:2Me  heptatriaconta-15E,22E-dien-2-one

C37:3Me  heptatriaconta-8E,15E,22E-trien-2-one

C37:4Me  heptatriaconta-8E,15E,22E,29E-tetraen-2-one

C38:2Me  octatriaconta-16E,23E-dien-2-one

C38:3Me  octatriaconta-9E,16E,23E-trien-2-one

C38:2Et  octatriaconta-16E,23E-dien-3-one

## Alkyl alkenoates

C36:2OMe  methyl hexatriaconta-14E,21E-dienoate

C36:2OMe  ethyl hexatriaconta-14E,21E-dienoate

**Figure 2.1 Examples of alkenones and associated compounds used in the UK37 and UK37'
indices for SST reconstructions.**   The first three ($C_{37:4}$, $C_{37:3}$, and $C_{37:2}$) are the ones used for
the indices (Killops and Killops, 2005).

The $U^K_{37}$ index was first published in 1986 (Brassell *et al.*, 1986).   The $U^K_{37}$
index is defined as a ratio of three different alkenones $C_{37:2}$ ,$C_{37:3}$ ,$C_{37:4}$, which are
straight chain ketones with 37 carbon atoms, and with minor differences in the number
of carbon-carbon double bonds present (2,3 and 4 double bonds) (Brassell *et al.*, 1986).
The differences is beween the cold water compound $C_{37:4}$ and the warm water
compound $C_{37:2}$ are averages by the total number of  $C_{37}$:

1  $U^K_{37} = [C_{37:2}-C_{37:4}] / [C_{37:2} + C_{37:3} + C_{37:4}]$

It was discovered that when the $U^K_{37}$ index was measured in a small scale laboratory cultures study, and compared to measured SST, a linear relationship was produced . This study was refined with extensive analysis of core top sediments through-out the ocean (Figure 2.2) (Müller et al., 1998).

In order to refine the index the $C_{37:4}$ molecule was removed because except for cold temperatures the peak is very often not present (Müller *et al.*, 1998; Bendle and Rosell-Mele, 2004; Ho *et al.*, 2012). In addition, studies show that $C_{37:4}$ can cause additional scatter in the $U^K_{37}$-SST calibration, (Sikes *et al.*, 1997). This led to the development of the $U^K_{37}$' index which works better in temperate sites (Müller *et al.*, 1997). :

2 $U^K_{37}$' = [$C_{37:2}$] / [$C_{37:2}$ + $C_{37:3}$]

Using a global suite of marine sediment core tops (Figure 2.2) and measured mean annual SSTs, Müller et al. (1998) created the following calibration equation:

3 $U^K_{37}$'= 0.033 SST + 0.044

This equation has a $r^2$ = 0.97 and an error of +/- 1.5 ℃. This calibration equation is almost identical to those produced in culture studies (Prahl and Wakeham, 1987):

4 $U^K_{37}$'= 0.033 SST + 0.043
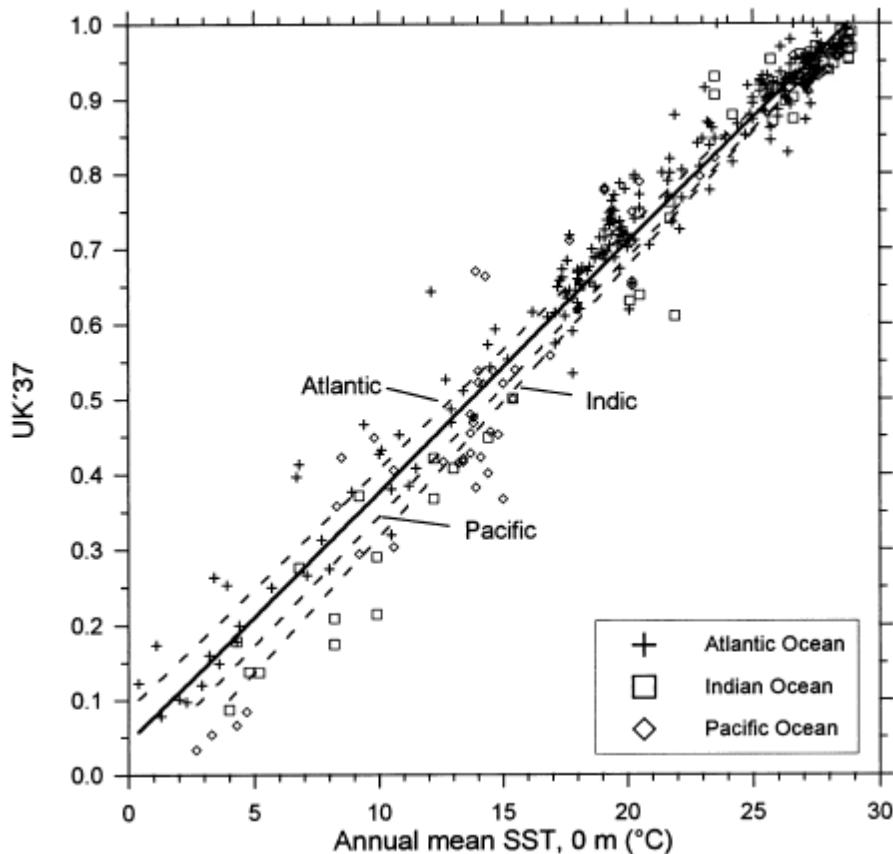
**Figure 2.2 The relationship between the UK37' index measured in marine sediment core tops and the measured mean annual SSTs of the overlying waters.** Note the lack of samples above 30º C and the weakening relationship below 15º C. Source: (Müller *et al.*, 1998)

However, there are some uncertainties associated with the $U^K_{37}$' at both ends of the temperature scale. At temperatures above 29 °C the $U^K_{37}$' index has a value of one (Figure 2.2) (Müller *et al.*, 1998). Therefore, there is an upper SST limit to the $U^K_{37}$' index. Also, the linear $U^K_{37}$' index-SST relationship has a greater amount of error at very cold polar temperatures (Figure 2.2) (Müller *et al.*, 1998). Finally, there is not much production of alkenones at the higher latitudes >45° N and S, which can lead to a greater amount of error due to the small sample of alkenones found in the sediments in these sites (Prahl *et al.*, 2010). Therefore there are parts of the world that the $U^K_{37}$' index cannot be used, or should be used with particular caution.

Studies have shown the depth in the water column of alkenone production is important to understanding the signal recorded by the $U^K_{37}$ or $U^K_{37}$' indices. Often the alkenones are produced at the sea surface but can also be produced below the surface in areas with high nutrient levels, although the temperatures produced by the indices seem

then be the same based on samples from the subsurface (Bentaleb *et al.*, 1999; Volkman, 2000). For example, in the Mediterranean Sea, the predicted temperature reflected by the $U^K_{37}$' index is the always the same as the temperature of the layer in the water column where the alkenones were being produced, which in this case was 30m below the sea surface (Bentaleb *et al.*, 2002). As a result, it is important to consider that in some locations the depth of alkenone production could lead to $U^K_{37}$' values under-estimating SSTs.

Although the $U^K_{37}$' calibration (Figure 2.2) demonstrates there is a close relationship between mean annual SST at a site and the temperature determined by the $U^K_{37}$ index (Müller *et al.*, 1998), it is known the cocolithphores produce the alkenones tend to bloom during specific times of the year (Sikes and Volkman, 1993; Volkman, 2000). For most of the ocean this either occurs during the spring and/or summer (Sikes and Volkman, 1993; Volkman, 2000). It has been argued (Rosell-Mele and McClymont, 2008) the excellent fit of the $U^K_{37}$ index to mean annual SSTs shows these differences seem to average out in the sediments.

Another major issue is differential degradation and whether it affects parts of the index, because different alkenones might degrade faster than others (Rontani *et al.*, 2013). If the relationship between the different compounds that make up the $U^K_{37}$' index changes due to differential degradation, this would change the SSTs reconstructed from sediments (Rontani *et al.*, 2013). A number of studies have tried to address this issue. It has been shown that alkenones are in fact labile, and may be more labile than other biomarkers (Grimalt *et al.*, 2000; Huguet *et al.*, 2009). However, the potential for any preferential decay of the different alkenones is not clear. Some evidence for an SST effect from differential degradation has been presented in both sediment samples investigating at the degradation occurring in subsurface, and in long-term degradation, in laboratory studies that replicate digenetic processes (Gong and Hollander, 1999; Rontani *et al.*, 2008; Kim *et al.*, 2009). The studies showed degradation may lead to SST variations of 1.8 °C-2.0 °C which is greater than the currently accepted error in the SST data of 1.0 °C (Kim *et al.*, 2009). In contrast, other studies have shown consistency in the $U^K_{37}$' index despite large losses of alkenones (as much as 90%) due to degradation (Prahl *et al.*, 1989; Prahl *et al.*, 2003; McClymont *et al.*, 2007). As a result, the impact of degradation on the $U^K_{37}$' index remains unclear, with inconsistent results, and many of the studies taking place on either small amounts of total alkenones, culture studies or studies in unusual environments (Grimalt *et al.*, 2000).

The alkenone temperature index has been used for a number of major studies. One of the recent uses of the $U^K_{37}$' index is in reconstructing past SSTs on a global scale for specific periods of time. This is because of the understanding of the strength and weaknesses of the index as mentioned above and the fact that $U^K_{37}$' can be used in many different parts of the ocean. Global compilations that have included alkenones include the MARGO project which has focused on the reconstructing the LGM (Kucera *et al.*, 2005; MARGO, 2009; Saher *et al.*, 2009; Hargreaves *et al.*, 2012) and the PRISM project reconstructing the temperatures in the Pliocene Warm Period (Haywood *et al.*, 2000; Haywood and Valdes, 2004; Dowsett *et al.*, 2009a, 2011). The mean annual SST recorded by the $U^K_{37}$' index also means it can be directly compared to ocean-atmosphere climate model outputs, which means the index is ideal for data model comparisons. There have been a number of studies based on large scale data model comparisons such as the PMIP and PMIP2 project (Haywood *et al.*, 2009a; Hargreaves *et al.*, 2012; Haywood *et al.*, 2013). Therefore, the $U^K_{37}$' index has been used to compare the timing of global change and leads and lags between different parts of the ocean (Bard, 2001; McClymont and Rosell-Mele, 2005; Lawrence *et al.*, 2009; Herbert *et al.*, 2010; Lawrence *et al.*, 2010).

### 2.2.2 The TEX$_{86}$ indices

The TEX$_{86}$ index (TetraEther index of tetraethers with 86 carbon atoms) is another major biomarker proxy used to reconstruct ocean temperatures. Recent studies show that the compounds are created by a type of Thaumarchaeota. This is an achaeota that is found universality in marine settings. The lipids which are used in the TEX$_{86}$ index are lipids called glycerol dialkyl glycerol tetraethers (GDGTs). These lipids contain up to 8 cyclopentane rings in their structure (figure 2.3). These are most likely used to rigidify the membrane based on their chemical structure. Studies have shown that these molecules are synthesised in different concentrations at different temperatures (Schouten *et al.*, 2002; Schouten *et al.*, 2003).

The TEX$_{86}$ temperature proxy was first proposed in 2000 (Schouten *et al.*, 2002; Schouten *et al.*, 2003), and records the relative distributions of 6 GDGTs with varying numbers of cyclopentane rings in the structure, according to the roman numerals from I-V'(Figure 2.3). Sediments from colder areas consist almost entirely of

GDGT-I while those from sediments in warmer areas have more of the other GDGTs (Killops and Killops, 2005).
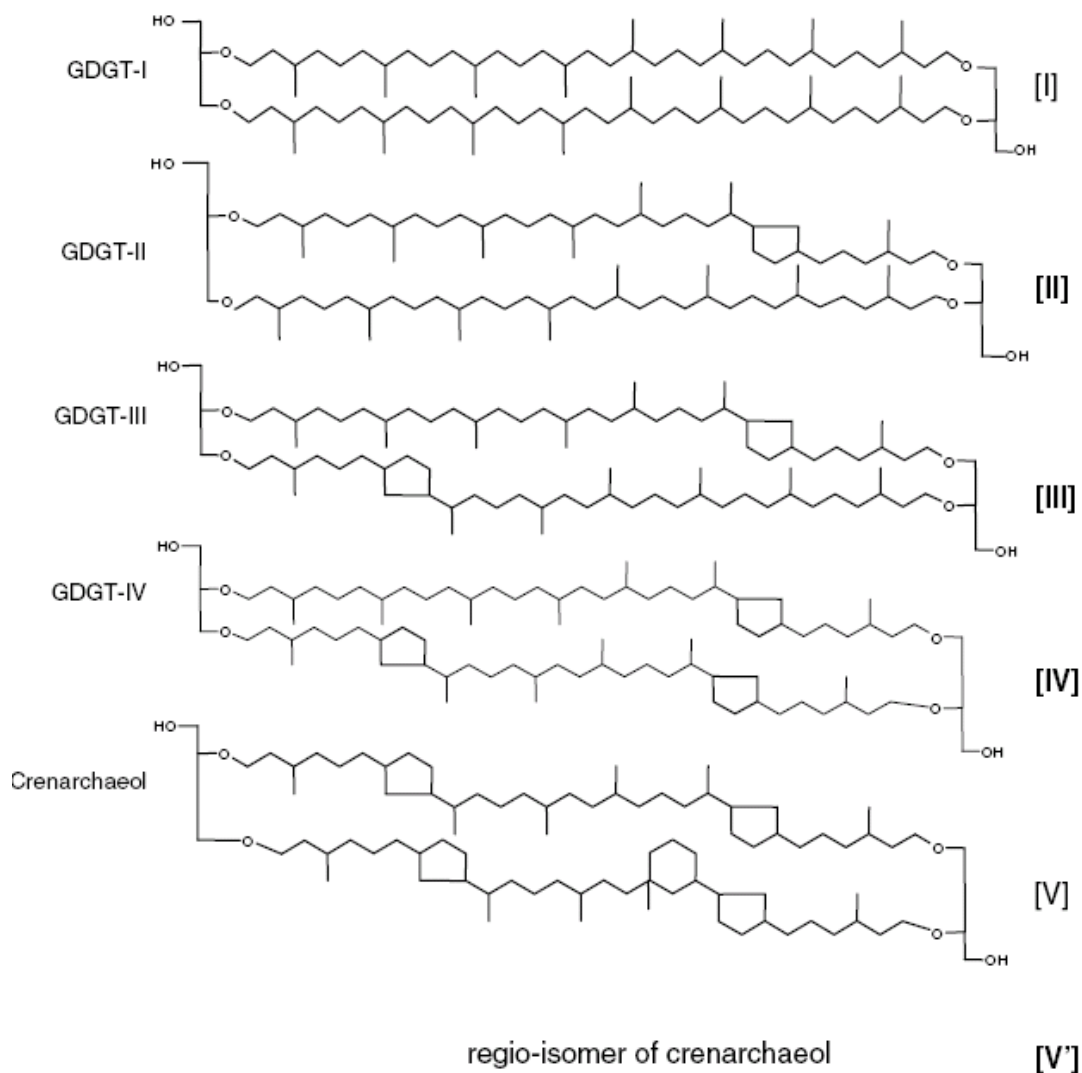


**Figure 2.3: The structures of the GDGT isomers** used to reconstruct the $TEX_{86}$ indices. From (Kim *et al.*, 2008)

There have been a number of changes to the $TEX_{86}$ index over the years to try and improve its accuracy (Figure 2.4). Originally (Schouten *et al.*, 2002; Schouten *et al.*, 2003), defined the $TEX_{86}$ index as:

5 $TEX_{86}=([III]+[IV]+[V'])/([II]+[III]+[IV]+[V'])$ (Figure 2.4).
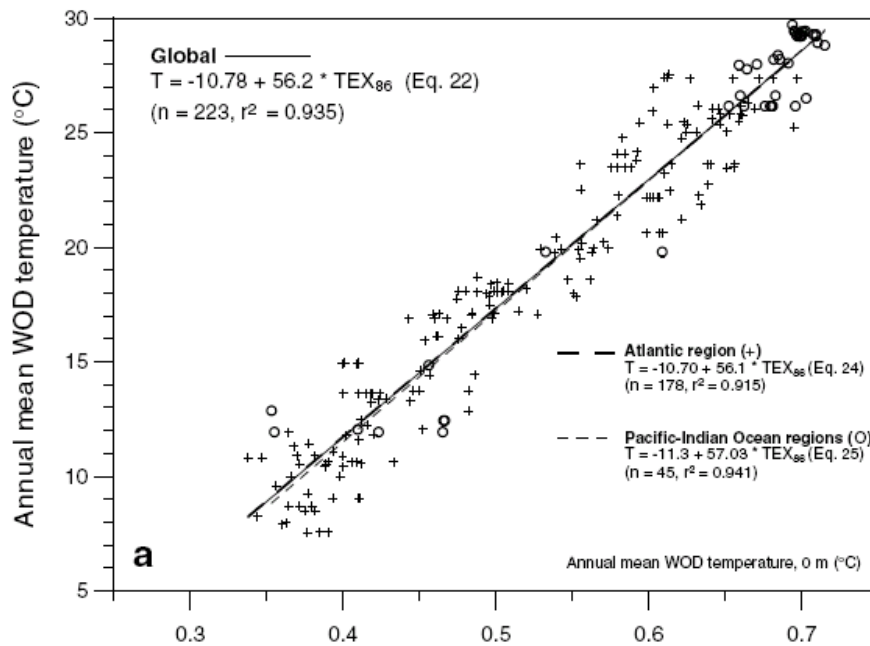
**Figure 2.4:  Original Calibration line determination for TEX86** (Kim *et al.*, 2008)

Using this calibration the original equation used to reconstruct SSTs using $TEX_{86}$ is:

6 $T = -10.78 + 56.2 * TEX_{86}$

This equation has an $r^2$ value of 0.935.  However it was found that the relationship described by this equation did not work as well for warmer or colder extremes.  Using a larger calibration data set, a new calibration was made (Kim *et al.*, 2010), which recognises that a single linear calibration does not capture the upper and lower temperature ranges  (Figure 2.5) (Kim *et al.*, 2010).  It was found that a non-liner relationship exists between the higher temperature sites and the resultant $TEX_{86}$ values.  It was also noted that there was a different liner relationship between the lower temperature values and the TEX86 values.  Therefore it was decided to split the proxy into two equations one for warmer waters and one for colder waters.   The new formula for warmer waters above 15°C is referred to as $TEX^{H}_{86}$  this is nonlinear relationship also prevents there from being a maxim temperature value at which temperatures cannot be reconstructed like the original equation.  The equation is as follows (Kim *et al.*, 2010):
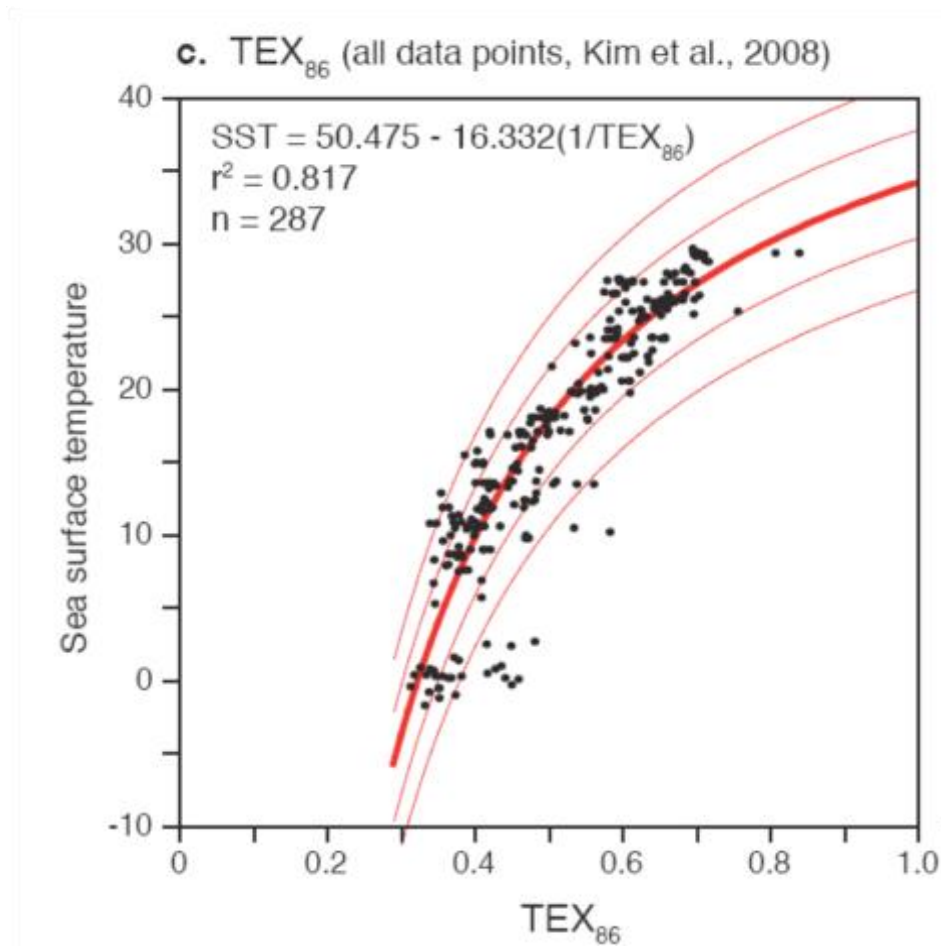
**Figure 2.5 the latest calibration for TEX86.** The upper parts of the calibration show a nonlinear trend (Kim *et al.*, 2010).

7 $SST = 68.54 * TEX^H_{86} + 38.6$

In addition a new formula was developed for temperatures below 15ºC.. The new proxy called $TEX^L_{86}$ is (Kim *et al.*, 2010):

8 $SST = 67.5 * TEX^L_{86} + 46.9$

There is a temperature sensitivity to the source organisms reflected by the lipids. It was initially noticed that for thermophilic Archaea, changes in temperature played a large role in determining the GDGT distributions (Schouten *et al.*, 2002; Killops and Killops, 2005). However when the $TEX_{86}$ index was first proposed it was unknown whether in nonthermophilic archaea changes in GDGTs reflected changes in temperature (Schouten *et al.*, 2002; Killops and Killops, 2005). Since then, laboratory cultures have shown that temperature is the main control over the production of different types of GDGTs (Wuchter *et al.*, 2004). Laboratory cultures have shown that

the temperature signal of $TEX_{86}$ is not affected by changes in nutrients or changes in salinity (Wuchter *et al.*, 2004).  This is part of the reason that $TEX_{86}$ can be used in lake environments (Powers *et al.*, 2004). Studies on ocean sediments also showed that the temperature reflected by the $TEX_{86}$ was that of the ocean water that was above 100 m (Wuchter *et al.*, 2005).   This suggested  that the temperatures reflected in the index are showing changes in surface water temperature not deep water, despite the presence of Archaea at all water depths and in sediments (Wuchter *et al.*, 2005).  However other studies suggest that is a subsurface signal recorded (Wuchter *et al.*, 2005; Huguet *et al.*, 2007; Lee *et al.*, 2008; McClymont *et al.*, 2012).  The depth of production of the proxy seems to be partialy contoled by primary prodcutivity and the depth of production in the water column.   This means that there often is a disconect bettween the TEX86 and $U^{K}_{37}$'.   Finaly recent studys have shown that even though golbaly the new formals do a better job explaning the golbal calibration this still leads to local offsets in the temperature calibration (Seki et al. 2014).  This has lead some reserchers to suggest that these offests may be related to local bilogic condtions.  Therefore they argue that calbrations should be done on the local scale (Seki et al. 2014).  Reserch is on going as to better explain the controls on the proxie but it is clear that the $TEX_{86}$ proxy is more complex then intill  studys suggested.

### 2.2.3 The n-*alkanes*

The *n*-alkanes are long straight chain normal (*n*-) hydrocarbons that typically have $C_{16}$–$C_{36}$ homologues with a dominance of an odd -over-even chain lengths (Eglinton *et al.*, 1962; Eglinton and Hamilton, 1963; Eglinton and Hamilton, 1967; Eglinton *et al.*, 1992).  The prominent homologues are $C_{23}$, $C_{25}$, $C_{27}$, $C_{29}$ and $C_{31}$ components.   Those above $C_{27}$ are primarily sourced from leaf waxes (Eglinton and Hamilton, 1963; Eglinton and Hamilton, 1967), and therefore are used to record the amount of terrestrial input into marine or lake sediment cores (Eglinton and Eglinton, 2008). Furthermore the length of the carbon chain can sometimes be related to plant families and groups meaning it is possible to identify individual plants based on the composition of the compounds found in the cores.  This is because the long-chain *n*-alkanes (number of carbon atoms above N= 29) are produced in the leaf waxes of higher plants but not in aquatic organisms (Pancost and Boot, 2004; Eglinton and Eglinton, 2008).  However, the transport of these *n*-alkanes to sediments could be from dust (wind driven) or river inputs (Simoneit *et al.*, 1991; Schefuss *et al.*, 2003a; Schefuss *et al.*,

2003b), and assessment of these contributions to sediments is required in order to understand where the sediment is coming from and the origin of the $n$-alkanes. However, there are a number of advantages with these proxies. First of all the compounds are very well preserved in the long term sedimentary record (Pancost and Boot, 2004). In addition to this the $n$-alkanes are identifiable even in sites with low terrestrial input and high marine input.

There are a number of additional ways $n$-alkanes have been used to analyse past climate change. $n$-alkanes are also used to interpret changes in the wind pattern in areas with a lot of dust input (Schefuss $et\ al.$, 2003a; Schefuss $et\ al.$, 2003b). By tracking changes in the marine sediments, $n$-alkane concentrations can track changes in wind patterns over long periods of time can be interpreted. For instance in the Southern Ocean, increasing $n$-alkane concentrations showed evidence of strengthening winds over the last 4 million years and helped to identify major wind shifts in the Southern Ocean and Antarctica (Martinez-Garcia $et\ al.$, 2011). An important application of $n$-alkane analysis has been to investigate the $\delta^{13}C$ signal of specific higher plant $n$-alkanes to assess the relative contributions of C4 or $C_3$ plant groups (Schefuss $et\ al.$, 2003b; Eglinton and Eglinton, 2008). Because it is known the $n$-alkanes come from the plants it makes it possible to directly measure the isotopic composition of the plants.

$\delta^{13}C$ is used to understand terrestrial vegetation changes. This is because there are two types of plants as mentioned in section (2.2.3) $C_4$ plants which live in dryer conditions than $C_3$ plants which make up the majority of the plants. $C_4$ plants (which are mainly grasses and grains) have an extra metabolic step involved in the generation of energy from $CO_2$ in order to prevent losing energy during the drier conditions when the plants need to prevent loss of water by evaporation (Barnes $et\ al.$, 1983; Ehleringer $et\ al.$, 1997; Still $et\ al.$, 2003). This leads to additional fractionation of the carbon isotopes in the plant and causes a distinctly different $\delta^{13}C$ signature for C4 plants than for C3 plants (Still $et\ al.$, 2003). Because C4 plants live in drier conditions then C3 plants the change in the isotope ratio has been used to investigate changes in the plant species in terrestrial environments (Barnes $et\ al.$, 1983). One example of this from a palaeocean study is changes in the African savannah (which is dominated by C4 plants) using cores off the coast of tropical Africa (Schefuss $et\ al.$, 2003a; Schefuss $et\ al.$, 2003b; Eglinton and Eglinton, 2008). Research has the movement northward in the last 1000 years in the African savannah showing that there have been changes in the extent of savannah and rainforests in Africa during this period of time. Therefore while there is

a lot of complexity to the $\delta^{13}C$ signals the $\delta^{13}C$ record remains a powerful climate proxy signal.

### 2.2.4 Pigments

The final biomarkers used in the thesis are photosynthetic pigment derivatives. Pigments are the molecules that produce the colour in living organisms (Eckardt *et al.*, 1991). Very few of them are specific to any one type of organism. The most common compound of pigment in the ocean is chlorophyll, which is produced by primary producers.   It is assumed changes in pigment are related to changes in primary production and this is confirmed by satellites which measure change pigments (Gordon *et al.*, 1980; Barale, 1987; Harris *et al.*, 1996; McClain, 2009; Szymczak-Zyla *et al.*, 2011).  The chlorophyll measured most by satellites is chlorophyll-*a* which is the most common pigment in the ocean(McClain, 2009).  However, pigments are complex molecules (Figure 2.6) and degrade rapidly in the water column and in sediments (Wright and Jeffrey, 2006).  Therefore instead of measuring pigments directly, analyse is done on derivatives of the pigments. In this case the primary derivative is chlorins produced by the different chlorophylls, these chlorins are better preserved in the sediment (Rosell-Melé and Maxwell, 1996; Rosell-Melé *et al.*, 1997; Kornilova and Rosell-Mele, 2003; Wright and Jeffrey, 2006; McClymont *et al.*, 2007; Szymczak-Zyla *et al.*, 2011).  However, chlorins are susceptible to degradation over time meaning that the record of pigment is more of a balance between production and degradation.  This needs to be taken into account when analysing millennial records of pigment (Wright and Jeffrey, 2006).  The other consideration is that peaks in pigment can be related to either peaks in primary productivity or they could also be a result of a greater sedimentation rate causing more chlorins to be preserved in the sediment which is referred to as the dilution effect (Wright and Jeffrey, 2006).  Therefore while chlorin records can be a powerful tool caution must be taken with the records produced (Kornilova and Rosell-Mele, 2003).
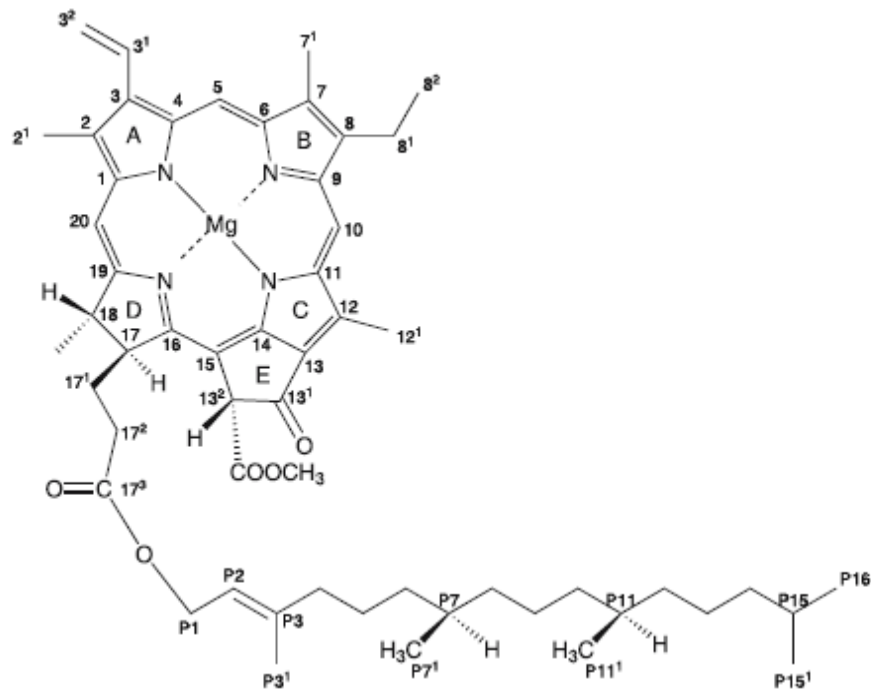
**Figure 2.6 structure of chlorophyll-a.** This is the primary pigment that is associated with primary production. Note the complex structure of the molecule which is why it breaks down easily. The chlorins measured in this thesis are a result of the breakdown of this molecule.

## 2.3 Micropaleontology

### 2.3.1 *Foraminifera*

Foraminifera have been an important part of palaeoceanography since the very beginning of palaeocean studies. The first oceanographic drilling expeditions realised that foraminifera represented one of the major paleontological groups found in ocean sediments (Bradley, 1999). This is because foraminifera make calcareous or silica grain tests which may be well preserved depending on the sediment properties. Their preparation and analysis by microscopy is also relatively straightforward (although assemblage analyses can be complex) (Pena *et al.*, 2005), and it has been demonstrated that the chemistry of the calcareous tests can record important information about seawater chemistry and other variables including temperature and salinity (e.g. Cronblad and Malmgren, 1981; Delaney *et al.*, 1985; Boyle, 1988; Nürnberg *et al.*, 1996; Lea *et al.*, 1999; Pena *et al.*, 2005)

Foraminifera are single-celled organisms and can be grouped into two types. Planktonic foraminifera which live in surface and subsurface waters, whereas benthic foraminifera live on (epifaunal) and within (infaunal) marine sediments, and so record conditions of the bottom waters affecting the seafloor. Thus, different palaeoclimate signals can be recorded depending on the foraminifera analysed, and the types of assemblage or chemical analyses performed.

### 3.3.1.1 *Planktonic Foraminifera*

Planktonic foraminifera live across a range of different temperatures and salinities, depending on the species (Jones, 1967; Be and Hutson, 1977; Deuser and Ross, 1989; Lee *et al.*, 2008), and can be found at different depths through the water column (Fairbanks *et al.*, 1980; Deuser and Ross, 1989; Lohmann, 1992). As a result, planktonic foraminifera can provide detailed information about surface ocean hydrography.

Planktonic foraminifera assemblages have been used to reconstruct sea surface temperatures (CLIMAP Project *et al.*, 1984; de Abreu *et al.*, 2005; Dowsett *et al.*, 2009a; Dowsett and Robinson, 2009). The assemblages are used to identify the presence, intensity and extent of upwelling given the close association of some species with the cool and productive waters of upwelling regimes (Kroon and Ganssen, 1989;

Ufkes *et al.*, 2000; Ufkes and Kroon, 2012). Using assemblage analysis changes in salinity (Be and Hutson, 1977; Ravelo *et al.*, 1990), contributions of specific water masses (e.g. Agulhas Leakage fauna) (Peeters *et al.*, 2004; Caley *et al.*, 2012), and changes in the stratification of the ocean (Mulitza *et al.*, 1997) have all been investigated. However, there can be issues with preservation that need to be considered when using planktonic foraminifera. The biggest issue is dissolution of carbonate begins in the deeper ocean, below the "lyscocline" or the carbon compensation depth (CCD), and thus some of the deepest ocean sediment cores may have poor or no preservation of calcite tests (Berger, 1970). As different species have different test thicknesses the dissolution process is not uniform, and could lead to a bias in the record (Berger, 1970; Bé, 1977). Past changes in the lysocline that have occurred with the rise and fall of sea level, fluctuations in ocean temperature and/or $CO_2$ which can also lead to changing impacts through time (Hoogakker *et al.*, 2006). Therefore understanding the history and deposition of sediments at the site is important to understanding the planktonic foraminifera history.

More recently, the Mg/Ca temperature proxy has been developed *(*Lea *et al.*, 1999; Elderfield and Ganssen, 2000; Dekens *et al.*, 2002; Dekens *et al.*, 2007a; Dekens *et al.*, 2008; Regenberg *et al.*, 2009; Groeneveld and Chiessi, 2011). It is known that the amount of Mg within the foraminifera changes with water temperature (Nürnberg *et al.*, 1996; Dekens *et al.*, 2002; Regenberg *et al.*, 2009). Since different species live at different depths, this technique has allowed reconstructions of water column structure in the upper regions of the ocean, down to 50 m water depth (Groeneveld and Chiessi, 2011). There are issues with alteration of Mg to Ca and digenesis that can affect the reconstructions because Mg can be removed and replaced by Ca altering the ratios (Johnstone *et al.*, 2011). Discussion of the importance of isotope analyses of planktonic foraminifera will be addressed in a separate section below (section 3.4).

### 3.3.1.2 Benthic Foraminifera

Benthic foraminifera live at the sediment-water interface (epifaunal) and immediately below (infaunal) the sediment surface. They scavenge on pelagic organic matter raining down from the overlying water column. Because different types of benthic foraminifera live at different depths it is necessary to understand the biology of the foraminifera being studied to understand the environmental signal it provides

(Corliss, 1983; Corliss, 1985; Linke and Lutze, 1993; Wollenburg and Mackensen, 1998). The epifaunal species are most often used in climatic reconstructions because they are thought to faithfully record the conditions of the bottom waters (Belanger *et al.*, 1981). This includes species such as *Cibicidoides wuellerstorfi* which has been used to analyse changes in bottom water masses (Hodell *et al.*, 1985; Lisiecki and Raymo, 2005; Molyneux *et al.*, 2007). However, there are times, due to changes in the bottom water chemistry (such as oxygen and salinity), when the epifaunal species are either not present, or are not well preserved in the sediment record (Murray, 2001; Gooday and Jorissen, 2012). In these cases, shallow infaunal species may alternatively be used because they live in the shallow sediments. They are considered to be an approximate proxy for bottom water properties, although the records may not be as reliable because the species are not living in contact with the bottom waters directly (Gooday *et al.*, 2001). Infaunal species living deeper in the sediment column record diffusion of chemicals into the sediments (Gooday *et al.*, 2001; Murray, 2001; Gooday and Jorissen, 2012).

It is important to understand changes in bottom water mass properties and circulation, because the bottom waters hold most of the $CO_2$ in the ocean (Flower *et al.*, 2000). Recent developments have also proposed that Mg/Ca in benthic foraminifera could be used to try and track bottom water temperatures, and they have to reconstruct Pliocene and Pleistocene deep water trends in the Atlantic and Pacific Oceans (Lea *et al.*, 1999; Dwyer and Chandler, 2009; Sosdian and Rosenthal, 2009; Sosdian and Rosenthal, 2010; Elderfield *et al.*, 2012). However, this work is still under development and there may be impacts of bottom water carbonate ion content on the temperature sensitivity of the Mg/Ca ratio (Elderfield and Ganssen, 2000; Elderfield *et al.*, 2012). Changes in the isotopes of benthic foraminifera are important to Palaeoceanography and will be discussed further below.

### 2.3.2 Dinoflagellates

Dinoflagellates are single celled microorganisms that are found throughout the marine environment (Evitt, 1963). They primarily feed on organic matter using their characteristic flagella to snag food in the ocean. Furthermore they are found in both salt water and fresh water environments (Mertens *et al.*, 2012) and can be used to understand a wide range of environments. Dinoflagellates have a complex life span with a number of periods of activity and a number of periods of non-motility (Dodge, 1985). Of interest to palaeoceanography is the fact that while they are non-mobile and living on the ocean floor, they form a "dinocyst" made of resistant organic material. This is referred to as a "resting cyst" and is deposited directly on the ocean floor, recording evidence of the species once living in the region but which were once present at the sea surface (Dodge, 1985). There are two types of dinocysts, organic and calcitic, although the organic dinocysts are more commonly used for climate reconstruction because they are preserved during pollen preparations (Heinrich *et al.*, 2011). Their cysts despite being made up of organic molecules, are resistant to degradation (de Vernal and Hillaire-Marcel, 2000; Versteegh and Zonneveld, 2002; Zonneveld *et al.*, 2010) and have been found in sediment which date back to at least 700 million years (Moldowan *et al.*, 1996). Therefore because of this preservation potential, dinocysts can be useful for developing a palaeoceanography record.

There are two major applications of dinocysts in the palaeoceanography record. First, assemblages can be used to identity environments and environmental change (Holzwarth *et al.*, 2007; De Schepper and Head, 2008), because certain dinoflagellates live in specific oceanographic environments (Marret and Zonneveld, 2003). For instance, some dinoflagellates are associated with upwelling conditions whilst others are associated with specific currents (Zonneveld *et al.*, 2001; Bockelmann *et al.*, 2007; De Schepper *et al.*, 2009). Since dinoflagellates are primary producers, changes in the total amount of dinoflagellates can indicate changes in primary productivity (Zegarra and Helenes, 2011).

However, the second and more common use of dinocysts is to reconstruct SST and sea surface salinity using transfer functions (de Vernal *et al.*, 2001; de Vernal *et al.*, 2005; Marret *et al.*, 2006). This uses the different tolerances and preferences of different species in the modern ocean to identify relationships to varying salinities and temperatures (Pflaumann *et al.*, 1996; De Vernal *et al.*, 1997; Marret *et al.*, 2008). By applying these modern transfer functions to the fossil record, variables such as SST,

salinity and sea ice can be reconstructed from a range of sites (de Vernal *et al.*, 2001; Guiot and de Vernal, 2007).

Several issues can affect transfer functions. First, evolutionary changes that might occur in dinoflagellates assemblages may alter the relationship between the organism and the environment it occupies used to drive the transfer functions (De Vernal *et al.*, 1997; de Vernal and Hillaire-Marcel, 2000). Secondly, selective preservation of certain cysts might also affect the reconstructions in that if the species that are preserved are from one environment there will be a bias towards that environment in the transfer functions. Finally, regional controls over dinoflagellate assemblages mean that reconstructions should not use transfer functions created in other parts of the ocean (De Vernal *et al.*, 1997; de Vernal and Hillaire-Marcel, 2000). Therefore it is useful to use the dinocyst reconstructions in tandem with other methods in order fully assess the accuracy of the different reconstructions (Peyron and Vernal, 2001).

## 2.4 $\delta^{18}O$

The $\delta^{18}O$ proxy was one of the first developed for understanding climate change. Harold Urey first realised the isotope fractionation of $^{18}O$ relative to $^{16}O$ in carbonate was related to changes in temperature (Figure 2.7) (Urey, 1948). They measured the carbonate $\delta^{18}O$ in the carbonate shells that were produced at different temperatures. They were testing the theoretical deposition of calcite changes with temperature. They found there was a linear relationship between $\delta^{18}O$ and temperature (McCrea, 1950).

9   $\delta^{18}O= 1.62_0 X 10^4/T\text{-}56.76,$

$\delta^{18}O$ is primarily measured in the calcite tests of foraminifera. There are three major controls on the $\delta^{18}O$ record in the palaeocean. One of the controls is the variation of the $\delta^{18}O$ of the water in which the calcite was formed. The major influences on this are temperature, in which increased temperature allows the increase uptake of $^{16}O$ (Urey, 1948; McCrea, 1950), salinity where higher salinities cause more uptake of $^{18}O$ (Epstein and Mayeda, 1953; Friedman *et al.*, 1961; Rohling, 2007), and global ice volume which removes $^{16}O$ in the formation of continental ice (Emiliani, 1955; Emiliani, 1966; Shackleton, 1967; Shackleton and Opdyke, 1973; Shackleton, 2000).

Under cold climates with higher ice volume, the $\delta^{18}O$ signal of sea water is higher due to the enriched water. Diagenesis and the associated alteration of calcite over time can also affect the $\delta^{18}O$ by lowering the $\delta^{18}O$ value through the preferred alteration of $^{18}O$ dominated compounds over those with 16O. Finally, there are further fractionations that happen when organisms build their calcite parts. These "vital effects" can vary since they are biologically controlled, and because different species utilize different amounts of fractionation therefore average $\delta^{18}O$ signal for different species is different. Some foraminifera have no vital effects allowing them to be correlated widely across the ocean (Prell, 1984). Other types of foraminifera and coccolithophores can have different offsets.
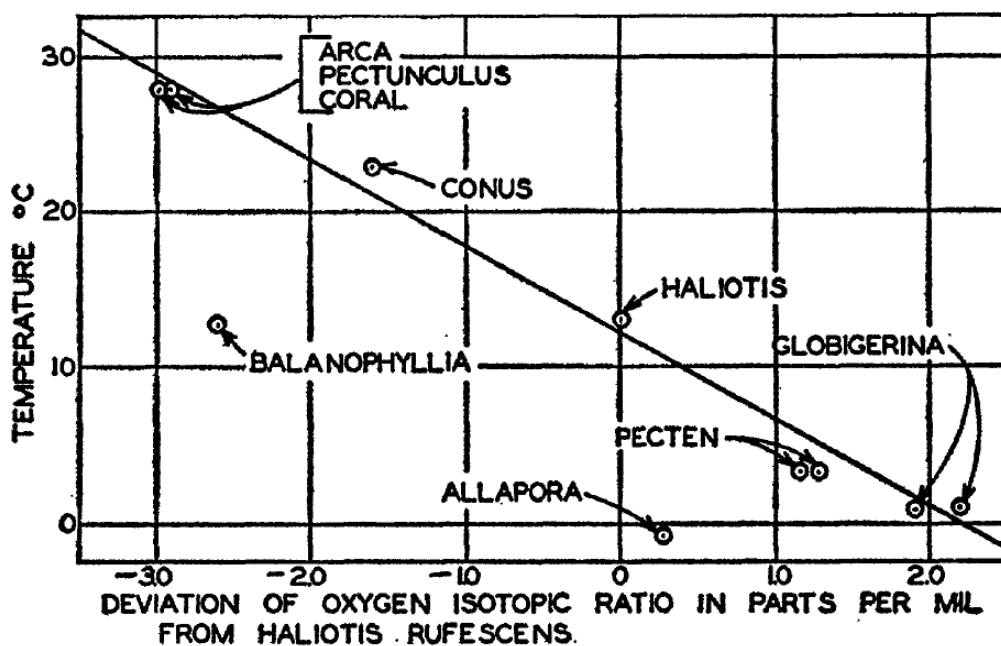


**Figure 2.7 The original δ18O-temperature calibration by Urey [1948].** This shows the relationship between the $\delta^{18}O$ of samples and the temperature at which they were produced.

There are two major recorders of $\delta^{18}O$: benthic, which describes changes in the bottom waters, and planktonic, which describes changes in the upper parts of the water column. Benthic $\delta^{18}O$ is primarily measured on the epifaunal benthic foraminifera. When *Cibicidoides wuellerstorfi* species are not present, infaunal species such as *Uvigerina peregrina* are used instead (Lisiecki and Raymo, 2005; Elderfield *et al.*, 2012). The change in temperature of the deep ocean is thought to be small on average, and salinity is assumed to be constant, therefore changes in the benthic $\delta^{18}O$ record have

traditionally been interpreted as a "global ice volume" record, at least for the last 4 Ma (Emiliani, 1955; Emiliani, 1966; Shackleton, 1967; Shackleton and Opdyke, 1973; Shackleton, 2000). This is because the isotope signature gets heavier when the more $^{16}$O isotope is incorporated into glacial ice more than $^{18}$O. Therefore when there are large scale continental glaciation the ocean becomes depleted in terms of $^{16}$O. This causes changes in the $\delta^{18}$O to be seen on the global scale which has allowed benthic stacks to be created that reflect the overall ice volume change (Figure 2.8) (Lisiecki and Raymo, 2005). The reason that benthic $\delta^{18}$O stacks are useful as an overall 'type section' is because the benthic $\delta^{18}$O has been shown to have a strong relationship to insulation which is the major driver of glacial and interglacial cycles (Lisiecki and Raymo, 2005). Therefore this means it is possible to correlate different benthic $\delta^{18}$O records from all over the world.
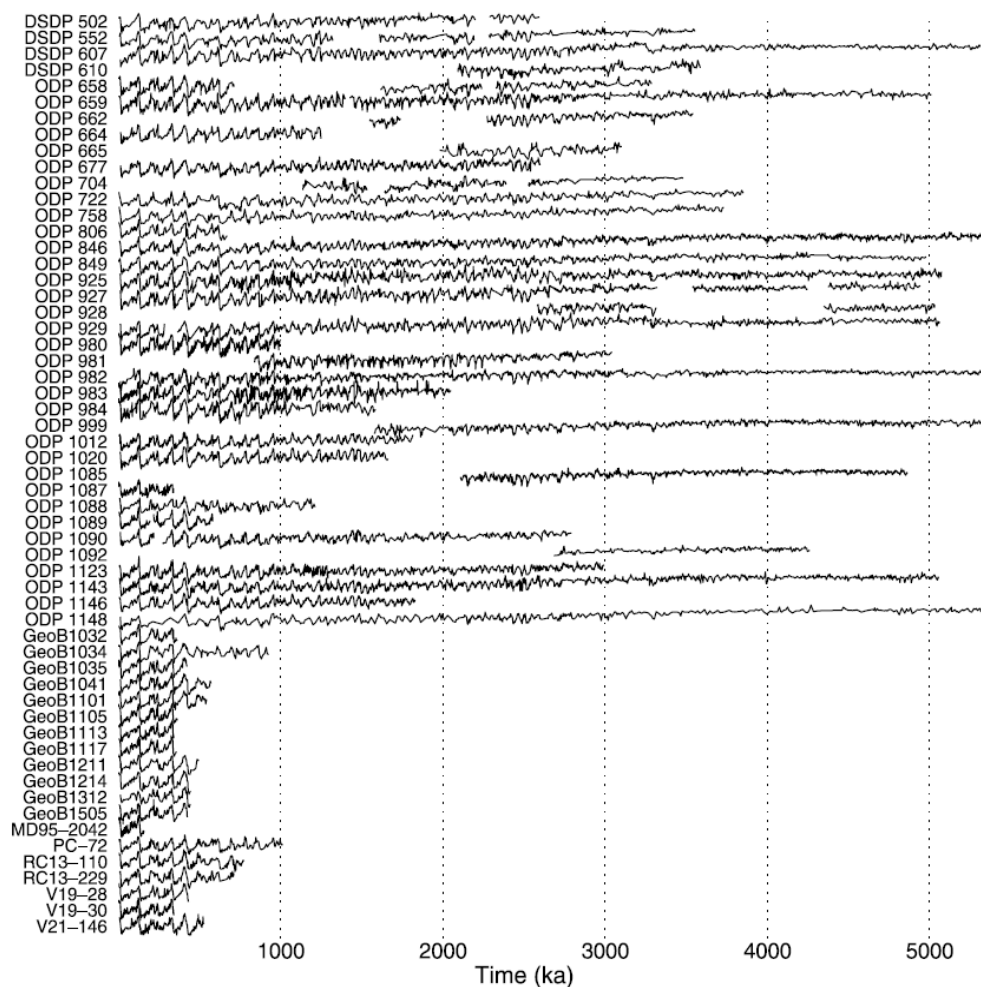


**Figure 2.8 the 57 benthic $\delta^{18}$O records to make the LR04 record (Lisiecki and Raymo, 2005).** The records come from all of the major oceanic basins and include ODP 1087.

The $\delta^{18}O$ signal recorded in planktonic foraminifera calcite is more complex than the benthic $\delta^{18}O$ signal, because the changes in temperature and salinity in the surface ocean are more variable than they are in the deep ocean. Understanding the life history of the planktonic foraminifera is also important because changes in environment while the tests are developing change the isotopic signature based on their migration in the water column depth. Initially planktonic $\delta^{18}O$ was primarily used for temperature reconstructions because this is the largest influence on $\delta^{18}O$ (McCrea, 1950).

One of the most recent uses of planktonic $\delta^{18}O$ is to combine it with temperature estimates to create a proxy for salinity (Rohling and Bigg, 1998; Rohling, 2007). Where the temperature of the site and where ice volume changes are known the salinity can be estimated using there the theoretical formula that Salinity= $\delta^{18}O_{planktonic}$ −((SST) factored to determine the contribution of temperature to $\delta^{18}O_{planktonic}$) − (water mass change) (Rohling and Bigg, 1998). There are some important considerations that need to be taken into account about $\delta^{18}O_{planktonic}$. There is not global fractionation curve for salinity based on $\delta^{18}O$ such as those that exist for other $\delta^{18}O$ proxies such as temperature (Figure 2.8). Instead individual curves exist for changes in $\delta^{18}O$ verses salinity for each part of the ocean (Rohling and Bigg, 1998; Rohling *et al.*, 2004; Rohling, 2007). Therefore in order to get the best interpretation with the greatest precision a local salinity curve needs to be used. Individual regional equations are also needed depending on what species the analysis is being performed on in order to account for vital effects (Rohling, 2007). Foraminifera are used the most often to reconstruct $\delta^{18}O$ salinity because the seawater temperature during calcite formation can be estimated using the Mg/Ca ratio in the same foraminifera as the $\delta^{18}O$ measurement, thus allowing the temperature impact on calcite $\delta^{18}O$ to be determined (Rohling, 2007). One of the most important examples of this is in the Red Sea where the relationship between $\delta^{18}O$ and salinity is linear because there are no significant sources of fresher water (Rohling, 1994; Rohling, 2007; Trommer *et al.*, 2012). This has allowed evidence of an almost 50% increase in salinity during glacial periods, which has been interpreted as a direct reflection of global sea level change because of the sill that protects the entrance to the Red sea and prevent interchange of the water from the rest of the ocean (Rohling, 1994; Rohling, 2007; Trommer *et al.*, 2012).

## 2.5 $\delta^{13}C$

The $\delta^{13}C$ record is the second most commonly used isotopic system because it is influenced by different climatic forcings to those that affect the $\delta^{18}O$ record. The two major isotopic components for $\delta^{13}C$ are $^{13}C$ and $^{12}C$. $\delta^{13}C$ is also complex because there are a large number of inputs from different sources that balance each other out in the carbon cycle which is made up of a number of different carbon sources such as $CO_2$ in the atmosphere or buried carbon in the earth. The $\delta^{13}C$ varies depending on the form the carbon is in. This is because $^{13}C$ is restricted in oxygenated compounds such as $CO_2$, organic molecules, and bicarbonate (Sharp, 2007). Because all three things can affect the $\delta^{13}C$ signal it results in a complex interaction of these different forms.

In the ocean there are two major sources of $\delta^{13}C$. First, erosion can cause an input of fresh carbon into the water column causing a shift in the $\delta^{13}C$. Second, changes in primary production increased draw down of $CO^2$ changing the $\delta^{13}C$ of the water column (Sharp, 2007). Therefore because there is a strong link between changes in nutrients in the water column and changes in primary productivity the $\delta^{13}C$ signal is often seen as a change in nutrients. These are then incorporated into either bicarbonate structures or complex organic molecules (Sharp, 2007). Therefore on a basic level changes in $\delta^{13}C$ are seen to reflect changes in the nutrients taken up by the organism.

There are complications in the $\delta^{13}C$ record that need to be considered. The most important of these are the "vital effects". Once again this is because most organisms prefer to incorporate $^{12}C$ are $^{13}C$ in their systems leading to different average ratios in different organisms (Zonneveld *et al.*, 2001). PH can play a role in the $\delta^{13}C$ single as well. This means that the $\delta^{13}C$ ratio is different for different species depending on how efficiently they take up one isotope over another. However, in this case differences in the species are greater than $\delta^{18}O$ because the fractionation effects are greater. Therefore understanding the organism that is being tested on is more important than with $\delta^{18}O$ analysis.

The $\delta^{13}C$ signal in the ocean is primarily considered to be a combination of three things; the long term changes in the background $\delta^{13}C$ , the changes in ocean circulation in the deep ocean, and changes in the nutrients in the upper ocean. The long term changes are related to long term changes in the earth's climate (Zachos *et al.*, 2001; Zachos *et al.*, 2006). Often $\delta^{13}C$ is used to track changes associated with extinction

events (Zachos *et al.*, 2001; Zachos *et al.*, 2006). Most importantly there have been numerous attempts to reconstruct changes in ocean currents using benthic and planktonic $\delta^{13}C$ (Curry and Lohmann, 1983; Hodell *et al.*, 1985; Curry and Crowley, 1987; Curry *et al.*, 1988; Oppo and Fairbanks, 1989; Oppo and Fairbanks, 1990; Raymo *et al.*, 1990; Oppo *et al.*, 1995; Raymo *et al.*, 1997; Billups *et al.*, 1998; Flower *et al.*, 2000; Hodell *et al.*, 2003; Raymo *et al.*, 2004; Ferretti *et al.*, 2005). The ocean circulation change proxies are supported by a negative correlation between oxygen in the bottom waters and the $\delta^{13}C$ value. Nutrient-rich waters have low oxygen and high $\delta^{13}C$ values because they incorporate $CO_2$ and remove oxygen from the system. For example, Antarctic Bottom Water (AABW), which is high in nutrients, has low $\delta^{13}C$ values, as compared to North Atlantic Deep Water which is lower in nutrients and therefore has a higher $\delta^{13}C$ value (Raymo *et al.*, 1990). In addition to this because oxygen is consumed in the bottom waters along with the dissolution of bicarbonate the older the water body is, this lowers the $\delta^{13}C$ values as well. Therefore the $\delta^{13}C$ proxy can be used to trace older water in the water column such as pacific deep water. Therefore different deep water masses have distinct isotopic signatures (Sharp, 2007). Caution should be taken because nutrient changes over time can affect the $\delta^{13}C$ signal (Raymo *et al.*, 2004).

Planktonic $\delta^{13}C$ is more complex because of the number of factors that can influence the carbonate-isotope fractionation in the surface waters. This means it is more susceptible to changes in nutrients, the $CO_2$ of the atmosphere, and erosion than the benthic $\delta^{13}C$ (Curry and Crowley, 1987; Pierre *et al.*, 2001). As a result planktonic $\delta^{13}C$ signals represent a mixture of both a local signal and a global one. Therefore it can be used to understand local changes in the system. One example of this is evidence of changes in upwelling using subsurface isotope gradients. Because $\delta^{13}C$ is depleted in the lower water column in upwelling areas, a lowering of $\delta^{13}C$ is evidence of more upwelling (Pierre *et al.*, 2001). This is done by doing using different species of foraminifera that live at different depths (Pierre *et al.*, 2001). By identifying times when the gradient is more uniform allows the tracking of changes in upwelling(Pierre *et al.*, 2001).

## 2.6 Summary

The multi proxy approach will allow objectives of this thesis to be addressed and contribute to our understanding of changes in currents over the last 3.5 Ma. Generation of the $U^{K}_{37}$' and $TEX_{86}$ indices will reconstruct changes in ocean temperature. Chlorin pigment analysis will assess changes in primary productivity. Assemblages of foraminifera and dinocysts will allow assessment of the dominant current and/or water mass affecting the core site. Finally, stable isotope analysis of calcite (benthic and planktonic) will be used for age control and to consider changes to water masses at the core site. Using the different proxies together will help offset the weakness associated with individual proxies. Combining different proxies together will allow a more complete picture of the climate history of the Southeast Atlantic Ocean to be generated.

# Chapter 3   Laboratory Methods

# 3.1 Introduction and Site Data

The samples used in this project are mainly from ODP 1087A (31º28'S, 15º19'E, 1374 m water depth) with a few samples from ODP 1087C to bridge a core gap. ODP 1087 core was originally taken on ODP Leg 175, whose expeditions goal was to investigate the history of the Benguela upwelling. ODP 1087 however was drilled outside of the upwelling with the aim of examining changes in the Agulhas leakage (Shipboard Scientific Party, 1998). ODP 1087 preserves a 492 m long composite record and extends back to the Oligocene (although with significant core gaps) (Shipboard Scientific Party, 1998). The core is primarily made up of light grey to green calcite ooze (Shipboard Scientific Party, 1998).

ADD MAP

## 3.2 Age Models and Sampling Strategy

The ideal age model would be to compare to the $\delta^{18}O$ stack of LR04 (Lisiecki and Raymo, 2005). This would mean that it shares the same age model as all other palaeocean records. However in order to do this a high resolution *C. wuellerstorfi* or other record that can be related to the $\delta^{18}O$ stack must be constructed. This was not always possible in ODP 1087.

### 3.2.1 Pliocene

A lack of tests *C. wuellerstorfi* in the depth range 151-149 mcd prevented confident tuning to LR04. To supplement the benthic $\delta^{18}O$ record, we followed the approach of Dickson et al. (2010) in a proximal core ODP 1085, which is to use $\delta^{18}O$ in fine fraction carbonate. The fine fraction carbonate $\delta^{18}O$ records changes in surface ocean temperature and salinity (Section 3.4). However, Dickson et al. (2010) showed that at site 1085 changes in the fine fraction $\delta^{18}O$ correlate to the benthic $\delta^{18}O$ and that they both recorded changes in temperature. Therefore, in both Dickson and this study the fine fraction $\delta^{18}O$ record to be used in addition to the fragmentary benthic $\delta^{18}O$ record

The fine fraction carbonate $\delta^{18}O$ record from ODP 1087 was tuned to LR04 visually using the two major cold periods of the period as tie. As shown in figure 3.1 the new model does not differ from the original depth model or from the existing benthic $\delta^{18}O$ data. The age uncertainty in the model is ~ 10 ka based on the various differences in the models based on comparing the $\delta^{18}O_{FF}$ to a model based on the benthic $\delta^{18}O$. The accuracy of the fine fraction model is based on the fact that the fine fraction is primarily made up of coccoliths (Dickson *et al.*, 2009; Dickson *et al.*, 2010a). Studies from this

region have shown that the vital effect between the different species is ~0.25‰ (Dickson *et al.*, 2009; Dickson *et al.*, 2010a). Finally, comparison between the fine fraction and benthic $\delta^{18}O$ in the Pliocene data show that the offset between the two records (where enough data existed to compare them) is 4 ka at most. The timing of a large positive excursion in $\delta^{18}O$ marking the "M2 glaciation" is close to the timing of the magnetic excursion (Shipboard Scientific Party, 1998). The new age model produced using fine fraction and benthic $\delta^{18}O$ in this thesis indicates that the 4 cm sample spacing across the mid- and late Pliocene corresponds to an average temporal resolution of 3 ka.
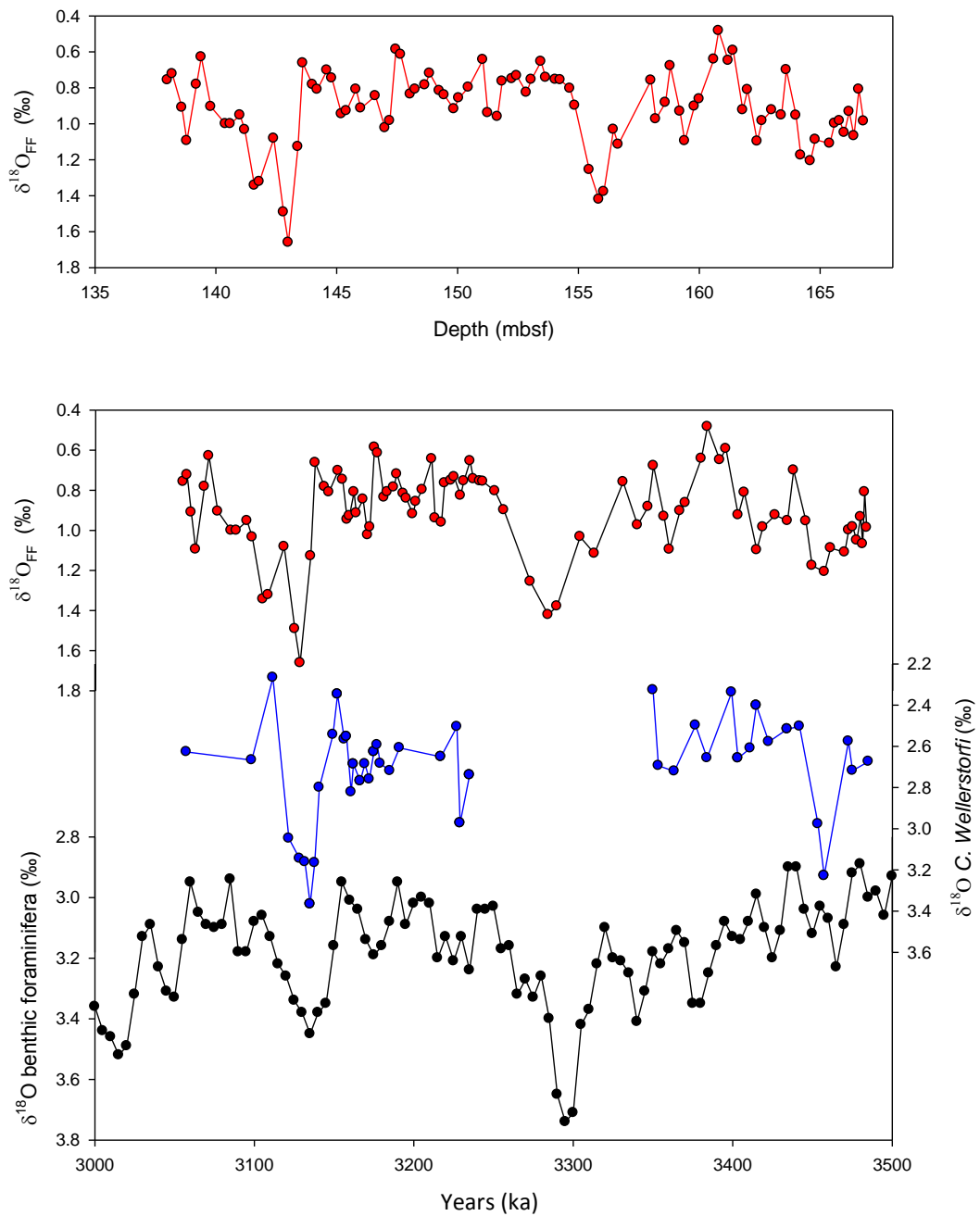
**Figure 3.1 Records used in the construction the age model for the mid-Pliocene.** Top: $\delta^{18}O_{FF}$ Record against original depth in core (mbsf). Bottom $\delta^{18}O_{FF}$ (red) benthic $\delta^{18}O$ (blue) and LRO4 stack (black). The age model was originally constructed using the $\delta^{18}O_{FF}$ and then confirmed with the benthic $\delta^{18}O$. .

### 3.2.2 Early Pleistocene

The age model used here was originally developed by Clarkson (2010), who used the Shipboard biological stratigraphy. This uses the known age disappearance or first appearance of distinctive species to create a relative age model based calcareous

nannofossil datums. In ODP 1087 there are 4 tie points used to create the age model. The error associated with this dating method was originally 100 ka (Figure 3.2) but this is lowered to 10 ka by comparing it to the Paleomagnetic age model (Figure 3.2). This is based on the timing of magnetic reversals in the core. In ODP 1087 there are two tie points used to construct the model.

Previous work by Clarkson (2010) had analysed 45 samples to produce a sampling resolution of 125 ka between 149-60 mbsf. For this thesis, the sampling resolution was increased to ~12 ka between 50 and 138 mbsf.
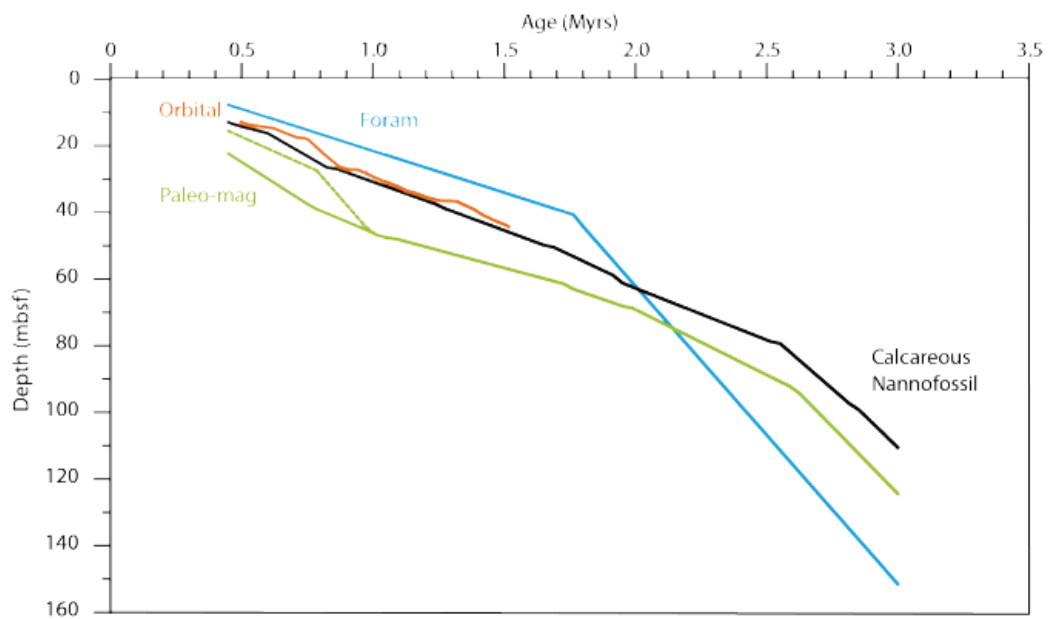


**Figure 3.2 The different age models from ODP 1087 between 1.5 and 3.0 Ma by** (Clarkson, 2010).

### 3.2.3 Mid to late Pleistocene

The late Pleistocene was sampled every 4 cm down to 14 mbsf from the top to give a temporal resolution of about 4 ka across the last 1.5 Ma. The original age model for 0 – 1.5 Ma (McClymont *et al.*, 2005) tuned a combined benthic and planktonic $\delta^{18}O$ stratigraphy (*Cibicidoides wuellerstorfi* and *Globorotalia inflata*) to the cyclostratigraphy of Lourens et al. (1994) (Figure 3.3). For this thesis, the benthic $\delta^{18}O$ record was re-tuned to the LR04 benthic $\delta^{18}O$ stack (Lisiecki and Raymo, 2005) between 0-0.6 Ma using matching of significant peaks as tie points to achieve the best $r^2 = 0.8$ using the computer program Analyseries (Paillard *et al.*, 1996) (Figure 3.3). In order to fill a core gap in ODP 1087A across MIS 10, samples were taken from ODP 1087C to form a spliced record. The ODP 1087C samples were selected based on the original shipboard spliced age model

developed from the shipboard age model. This was then adjusted visually so the temperatures in the parts of the core that overlapped temperature data for ODP 1087A (Figure 3.4).
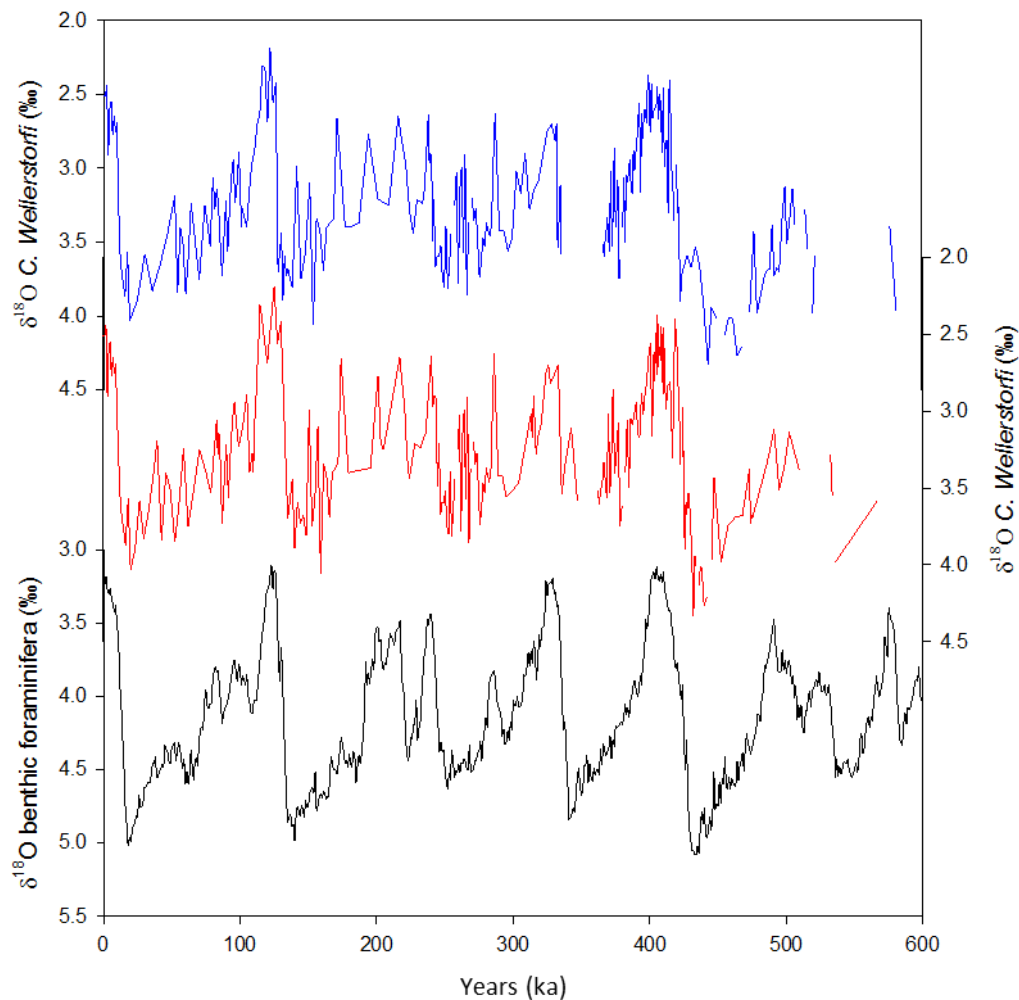


**Figure 3.3 Showing the adjusted age model for ODP 1087 between 0 and 0.6 Ma** The original age model from McClymont *et al* (2005) (blue) the new adjusted age model (This study) (red) and LR04 black.

## 3.3  Biomarker analysis

The reagents and the solvents used during the extraction process include the following chemicals shown in the following table (4.1).  Before being used all glassware was treated in the following way.  The glass was washed and scrubbed before being put into a decontaminate bath which was made up of water with 10%  Decon 90® soap solution (Decon Laboratories Ltd. Hove U.K.).  The glassware was then left in the bath at least overnight.  The glassware was then removed from the bath and rinsed three times

in tap water before having an additional rinse in DI water. The samples were then left to dry or put into a drying oven. The samples were then rinsed three times with dichloromethane (DCM) immediately before being used. All disposable glass (pipets) was fired at 450 °C for at least 5 hours before use then discarded after use. Reagents were activated using 10% deionized water.

Table 4.1 **Solvents and reagents used in this thesis.** With scientific abbreviations and analytical grade. All supplied by Fisher Chemicals, U.K.

| Notation | Name | Grade |
|----------|------|-------|
| *Solvents.* | | |
| DCM | Dichloromethane(Mythylene Cloride) | Residue Analysis |
| MeOH | Methanol | Residue Analysis |
| | Hexane | Residue Analysis |
| | Acetone | Residue Analysis |
| *Regents* | | |
| BSTFA | Bis(trimethlsiyl)trifluoroacetamide | 98% |
| | Anhydrous sodium Sulfate | Ceritfied |

### 3.3.1 Lipid Extraction

Freeze-dried and homogenised samples were solvent-extracted using a CEM MARS 5 microwave system and the methodology of Kornilova and Rosell-Melé (2003). Around 3.5 g of sediment was extracted with 10 ml of HPLC grade dichloromethane: methanol (3:1) in Teflon vessels by heating to 70°C over 5 min, holding at 70°C for 5 min, and allowing the sample to cool for at least 30 min or until temperatures dropped below 40 °C. Known weights of three standards (5α-cholestane, hexatriacontane ($C_{36}$) and Tetracontane ($C4_0$) were dissolved in 20ml hexane, of which 40 μl was added to each sample before microwaving. The sediment-solvent mixture was then transferred to 7ml glass test-tubes, and centrifuged for at least 3 min. The supernatants (solvent and extracted lipids) were decanted into round bottom flasks, and dried using a rotary evaporator. Each round bottomed flask was rinsed with DCM and the extract transferred to a 3.5 ml vial. At least five washes were used to transfer the sample from the flask to the vial. Rinsing continued until there was no more colour present in the sample. The solvent extracts were then dried under a stream of nitrogen and stored in a freezer until required.

### 3.3.2 Pigment analysis

Two different instruments were used to record the total abundance of the chlorophyll pigment degradation products, chlorins (section 3.2.4). Initially, total chlorin concentrations were calculated using a WPA Lightwave UV-vis spectrophotometer. The entire solvent extract was dissolved in 2ml of acetone and

transferred to a quartz cuvette. The spectrophotometer was programmed to scan at 2 wavelengths: 410 nm and 665 nm, since these reflect the key wavelengths to identify chlorins (Rosell-Melé *et al.*, 1997). Measurements were taken in triplicate for all samples, and a sample average was calculated. Variability in the analysis of samples was 0.05 abs (absorbance), and in the analysis of a "standard" sample (one analysed repeatedly and across batches) was 0.1 abs.

The majority of samples in this thesis were analysed for chlorins using an High-performance liquid chromatography (HPLC) system coupled to a photo-diode array spectrophotometer. Solvent extracts were divided in two, and the ½ aliquot was dissolved again in 2ml of acetone. Three injections of 40 µl per sample were made, with the PDA scanning across 350 – 800 nm. From the scans, absorbance at the wavelengths 410 and 665 nm could be achieved, and sample means were quantified across the three injections(Figure 3.4). Analytical variability was monitored using repeat measurements of a standard, and was determined at 0.07 abs. Finally, for all samples, the absorbance at 410 nm or 665 nm was divided by the original weight of the total sample to get a value of absorbance/g.
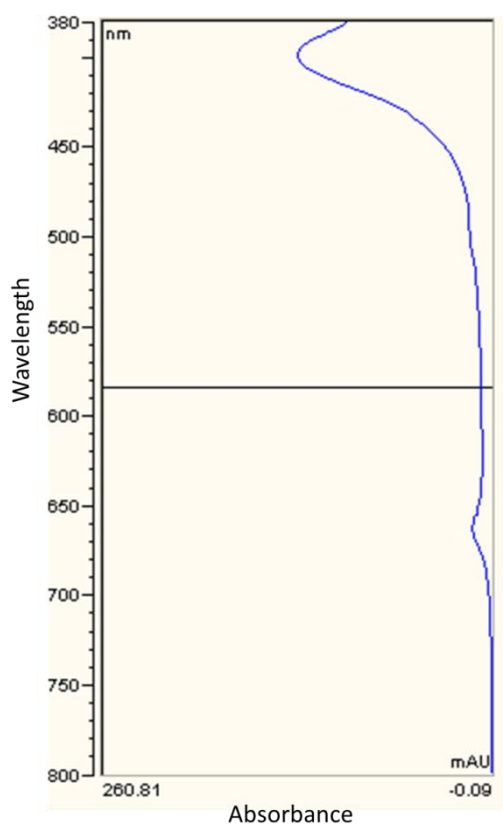


**Figure 3.4 showing the scanning procedure used by the HPLC**. Two peaks represent 410 nm and 665 nm.

To ensure that the results were compatible between the two sets of analyses, a comparison test was undertaken. The same samples were measured between the two instruments. This showed a strong linear trend with a $R^2$ value of 0.96 and a Y intercept of 0.01 indicating a good fit (Figure 3.5).



Graph with x-axis labelled "HPLC Abs/g" (0 to 9) and y-axis labelled "UV/Vis Abs/g" (0 to 0.6), showing scatter points with a linear trendline. Equation shown: $y = 0.0632x + 0.0065$, $R^2 = 0.9633$.
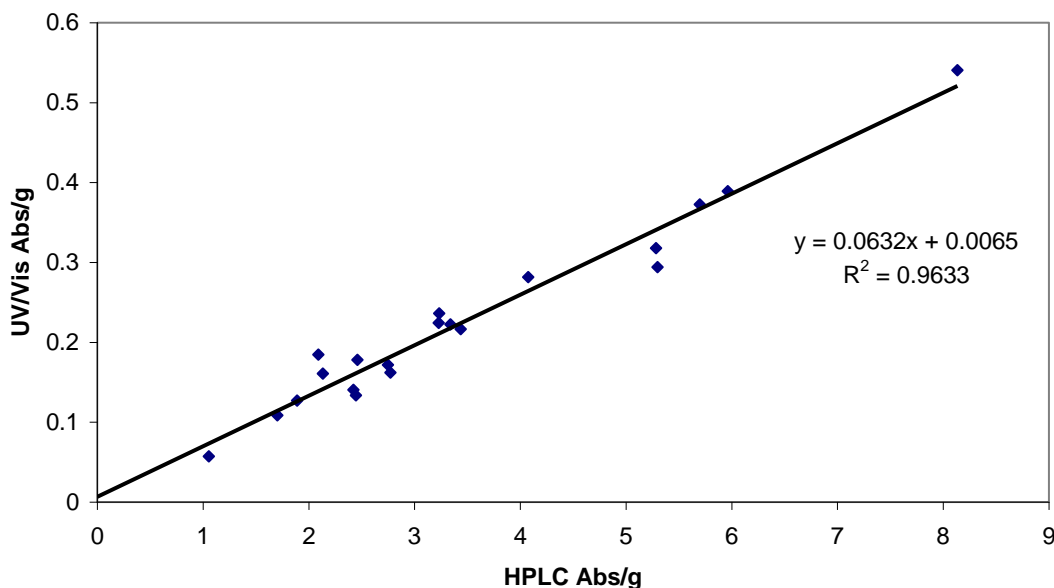
**Figure 3.5 showing the relationship between the two instruments used to collect chlorin data.** Note that these also show that despite some differences the relationship between the two data sets is strong. However there is an uncertainty of 0.5 Abs/g

### 3.3.3 Gas Chromatography (GC)

Samples to be analysed by gas chromatography (GC) were derivatised prior to analysis, to ensure that the compounds in the samples would not stick on the GC column. The samples were then derivatised using 20 µl of N,O- Bis(trimethlsiyl)trifluoroacetamide with trimethylchorosilane and 20 µl of DCM, heated to 70ºC for 1 hour. Samples were then dried under a stream of nitrogen, and redissolved in 200 µl of ethyl acetate HPLC grade.

To quantify the alkenones present in the ODP 1087 samples, the solvent extracts were analysed using a GC fitted with a flame-ionisation detector (GC-FID) and a 30m HP1-MS capillary column. Hydrogen was the carrier gas (3 ml min^{-1}, column head pressure 18 psi). The injector temperature was held at 300 ºC, and the detector at 310º C. After injection, the oven temperature was held at 60ºC for 1 min, then increased at 20º C to 120º C, to 310º C at 6º C, and held at 310ºC for 30 min. Alkenone identification was confirmed through analysis by GC mass spectrometry (GCMS). The peak areas of the $C_{37}$ alkenones with two and three unsaturations were used to calculate the $U^K_{37}$' index, and converted into SST values using the sediment core top calibration of Muller et al. (1998)

as described in section 2.2.1 (Figure 3.6).  The alkenones and n-alkanes were quantified using the internal standards by the following equation

9   (unknown sample) = ((Known weight of standard)*(area of unknown sample))/(area of standard)

   Variability in the analysis was determined by repeat injections of selected samples and standards, and was quantified at 0.09 $U^{K}_{37}$' units, equivalent to 1.5 °C.
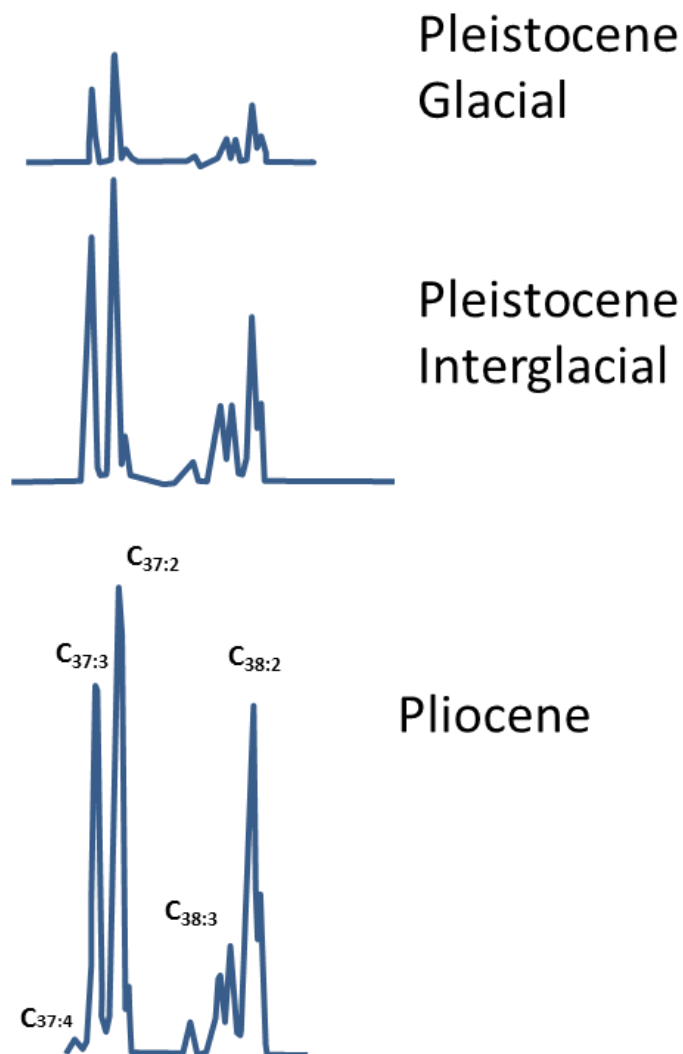
**4.6 Chromatograms of alkenones for Pleistocene and Pliocene.** Notice the difference between the Pliocene and Pleistocene and glacial and interglacial.

### 4.3.4 Silica column chromatography

Based on the results from the $U^K_{37}$' analysis, a subset of 42 samples was selected for further investigation for the $TEX_{86}$ index and n-alkane concentrations. The samples were divided into two equal aliquots before being derivatised. The underivatised samples were run through silica columns and fractionated into different compound classes. The silica columns were created by plugging the bottom of a pipette with extracted cotton wool, then ~4 cm of silica with 5% $H_2O$ was added. The samples were dissolved in hexane which was then filtered through the silica column. This "fraction 1" was collected into a vial, and contained the *n*-alkanes. Fraction 2 was recovered by adding DCM to the column (alkenones eluted here), then methanol was used to recover fraction 3 (polars, including GDGTs for TEX86). All solvents used were HPLC grade (Fisher). All fractions were dried under a stream of $N^2$.

Fraction 1 was dissolved in 100 μl and injected into the GC to identify the *n*-alkanes using the GC-FID programme outlined above. The *n*-alkanes were quantified using the internal standard (section 4.3.3). The methanol fraction was dried down and prepared for GDGT analysis.

## 4.3.5 High Performance Liquid Chromatography Atmospheric Pressure Chemical Ionization Mass Spectrometry (HPLC-APCI-MS)

Fraction 3 (methanol) was re-dissolved in 200 μl of hexane:n-propanol (98.5:1.5, v/v) and an internal standard was added and then filtered through a 0.5 μm PTFE filter. The samples were automatically then injected in to an LCMS and the individual GDGT peaks were characterised by a program created by Gemma Rueda and Antoni Rosell-Mele at UAB in Barcelona to isolate the peaks used in the $TEX_{86}$ reconstruction. A Dionex P680 HPLC coupled to a Thermo Finnigan TSQ Quantum Discovery Max quadrupole mass spectrometer with an atmospheric pressure chemical ionization (APCI) interface set in positive mode was used to analyse the sample. The extracts were then eluted through a Tracer Excel CN column (Teknokroma) with a length of 20 cm, a diameter of 0.4 cm and a particle size of 3 μm. The samples were filtered before entering the column and there was a guard column on the other end of the set up. The mobile phase was initially hexane:n-propanol (98.5:1.5) at a flow of 0.6 mL min$^{-1}$. The proportion of n-propanol was kept constant at 1.5% for 4 minutes, after it increased gradually to 5% during 11 minutes, then it increased to 10% for 1 minute and it remained at this proportion for 4 minutes. Finally, it decreased back to 1.5% during 1 minute and was held at these conditions for 9 more minutes until the end of the run. The parameters of the APCI interface were set as follows to generate positive ion spectra: corona discharge 3 μA, vaporizer temperature 400 ℃, sheath gas pressure 49 mTorr, auxiliary gas ($N_2$) pressure 5 mTorr and capillary temperature 200 ℃. GDGTs were detected in selected ion monitoring (SIM) mode at the following mass to charge ratio (*m/z*): 1302, 1300, 1298, 1296, 1292, 1050, 1048, 1046, 1036, 1034, 1032, 1022, 1020, 1018 and the internal standard GR at 1208 *m/z* Figure(3.7).
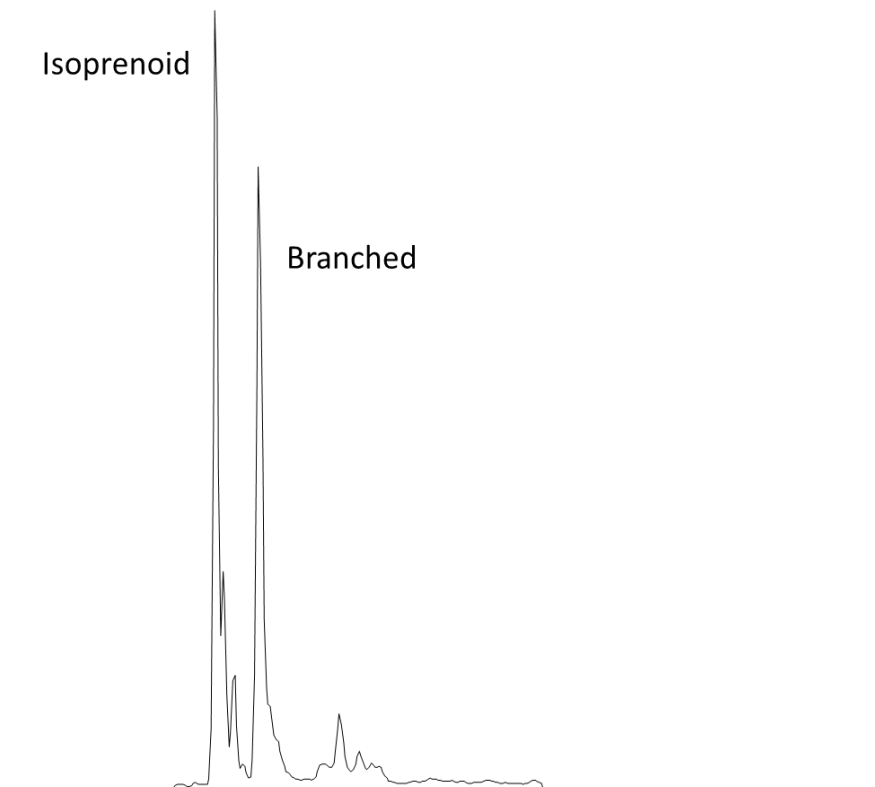
**Figure 3.7 Total ion content for sample from ODP 1087 showing isoprenoid and Branched forms from the HPLC-APCI-MS.**

## 3.4 Microfossils

### 3.4.1 Dinoflagellates

A sub-set of seven freeze-dried samples were analysed for dinoflagellate cyst assemblages, following the method in Marret *et al.* (2008) and in collaboration with Fabienne Marret at the University of Liverpool. Sediments were weighed and their volume estimated. Prior to the treatment of samples, a tablet of exotic markers (*Lycopodium clavatum*) was added to each sample to assess the concentrations of palynomorphs (Mertens *et al.*, 2009). The sediments were digested using repeated additions of cold 10% Hydrochloric acid to decalcify the samples. This preparation was followed by adding cold 40% Hydrofluoric acid to remove the siliceous fraction. Finally, a third rinse of cold 10% Hydrochloric acid removed any remaining calcite. The digested samples were passed through a 10 µm sieve to remove fine fraction sediments. The residue was mounted on glass slides and then investigated under a microscope. A minimum of 100 specimens were counted per sample by the author to give a statistically significant sample (Marret *et al.*, 2008).

### 3.4.2 Stable isotope analyses in carbonates

In the Pliocene section of the core (section 4.3.3), approximately 5cc of 80 samples were sieved though a 150 μm sieve. The sample that passed through the sieve was then saved for fine fraction analysis. 3-8 tests of *C. wuellerstorfi* were picked using a thin paintbrush and viewing the sample using a binocular microscope. The picked foraminifera were then crushed and homogenized in a mortar and pestle. The samples were then dissolved in phosphate acid and injected into a mass spectrometer (MS) at the Natural Environment Research Council (NERC) Isotope Geochemistry Laboratory (NIGL) in Keyworth, Nottingham, in collaboration with Melanie Leng. For the isotope analysis, approximately 30-100 microgrammes of carbonate (fine fraction (FF) or benthic foraminifera (BF)) were analysed for isotope ratios using an IsoPrime dual inlet mass spectrometer plus Multiprep device. Isotope values ($\delta^{13}C$, $\delta^{18}O$) are reported as per mille (‰) deviations of the isotopic ratios ($^{13}C/^{12}C$, $^{18}O/^{16}O$) calculated to the VPDB scale using a within-run laboratory standard calibrated against NBS-19 standards. Analytical reproducibility of the standard calcite (KCM) is < 0.1‰ for $\delta^{13}C$ and $\delta^{18}O$.

### 3.4.3 Planktonic Foraminifera

Planktonic foraminifera analysis was performed by Sonja Felder (Newcastle University) in order to assess evidence for changing water masses reaching ODP 1087 in the Pliocene. Fourteen planktonic foraminifera samples were selected for assemblage analysis between 138 mbsf and 167 mbsf, based on $U^{K}_{37}$' and chlorin concentration to cover a range of both different SSTs and productivity signals. The samples were sieved initially at 150 μm to recover the benthic foraminifera. The samples were then further sieved though a 125 μm sieve to remove fine fraction carbonate, broken and juvenile tests. Using a binocular microscope, more than 300 planktonic foraminifera were selected from the >125 μm fraction of each of the selected samples in order to reflect the total planktonic foraminifera assemblage., The amount of each species is noted as dominant (meaning this species makes up >30% of the 300 isolated individuals in that sample), abundant ($30 - 10\%$), few ($10 - 5\%$), rare ($5 - 1\%$), and rare (<1%).

# Chapter 4: Assessing the global significance of the climate transitions identified in ODP 1087

## 4.1 Introduction

In this chapter, the entire 3.5 Ma record will be examined to identify and understand the major climate changes present in the ODP 1087 record which will then be described in more detail in the following chapters and compare it to other global records of oceanic change (Figure 4.1). The major questions to be answered is what are the teleoconnections between ODP site 1087 and other parts of the ocean and what do the long term changes in the record relate to global changes. To understand the causes of these changes, the interaction of the Benguela Upwelling and Agulhas Leakage systems will be discussed further, and the implications of these interpretations for understanding the role of the SE Atlantic in global climate events will be considered.
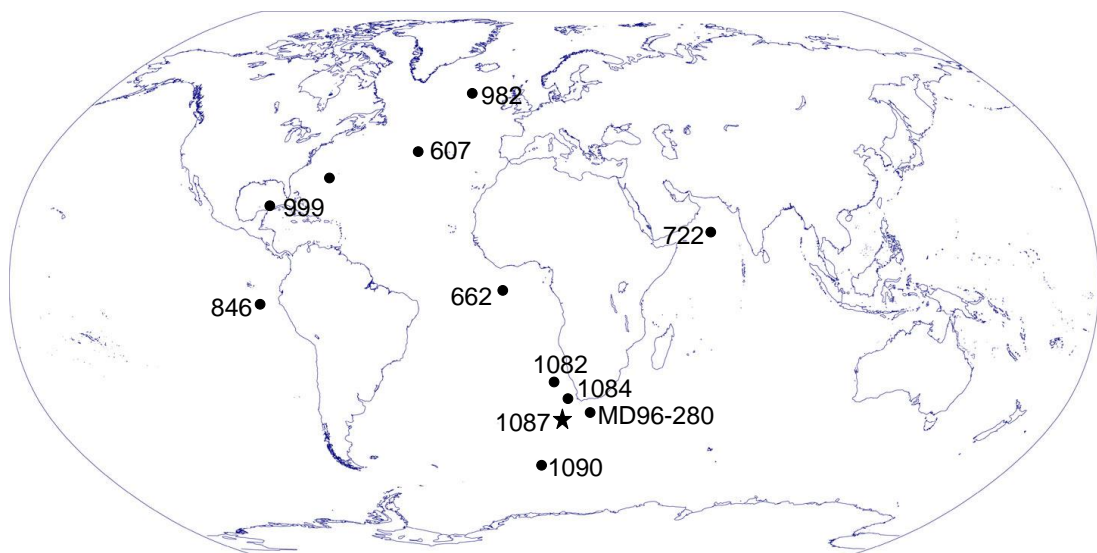


**Figure 4.1 showing the location of cores mentioned in this chapter.**

## 4.2. The 0-3.5 Ma SST Record

Figure 4.2 shows the combined 3.5 Ma record of ocean temperatures (from $U^K_{37}$' and $TEX_{86}$ ) and chlorin concentrations from site 1087. The changes in the various proxies will be discussed in more detail in the following chapters however an overview of the major trends will be discussed in this section. Pliocene ocean temperatures were warmer than the late Pleistocene, although this is not seen in $TEX_{86}$ which is offset from the $U^K_{37}$' SST reconstruction (Figure 4.2).
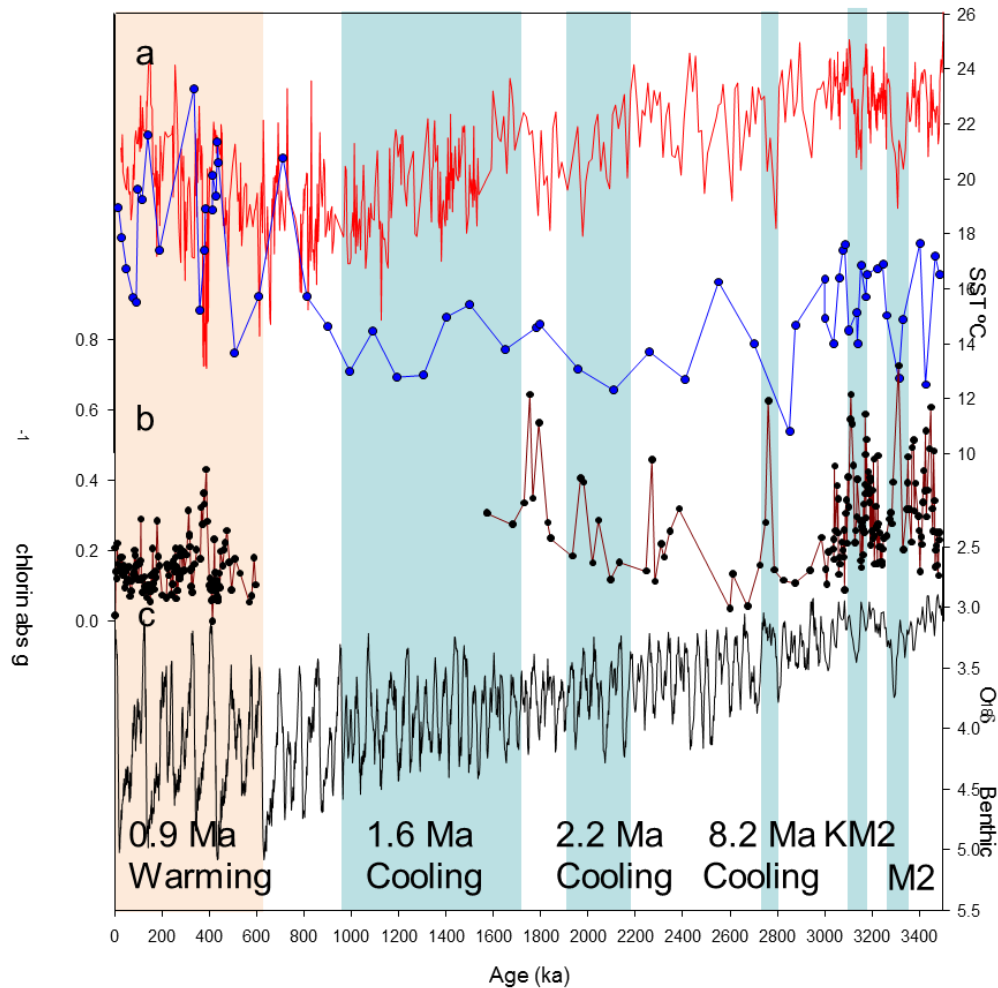
**Figure 4.2. The complete 3.5 Ma record of selected climate variables from ODP 1087.** a. $U^K_{37}$' SST record, from this study and from McClymont et al. [2005]; $TEX_{86}$ reconstruction (blue circles) b. Chlorin concentrations (dark red). c. LR04 benthic stack (black). Some of the major events discussed in the chapter are marked by coloured bars with blue bars indicating periods of cooling and red bars periods of warming.

The only exceptions to this period of relatively stable temperatures are the three cold MIS (M2, KM2 and '8.2 Ma') which were characterised by short-lived cooling events where temperatures reached late Pleistocene levels and high chlorin values. This was matched by a cooling in the $TEX_{86}$ record at all three points. While there had been slight cooling from 3.0 to 2.2 Ma (<1°C), 2.2 Ma marks the beginning of the first instance of a cooling trend leading to a long-term cooler period, which continues to 1.75 Ma, along with higher chlorin values. This cooling in the record occurs at the same time as cooling in the other Benguela Upwelling sites and indicates an overall cooling of the Benguela Upwelling area (Figure 4.3). This was followed at 1.75 Ma by a short-term warming that lasted until 1.65 Ma (Figure 4.2). Then the longest sustained cooling

seen in ODP 1087 between 1.50 to 0.95 Ma occurs. This cooling is seen throughout the southeast Atlantic and in the Subantarctic Atlantic ODP 1090 record as well (Figure 4.3).
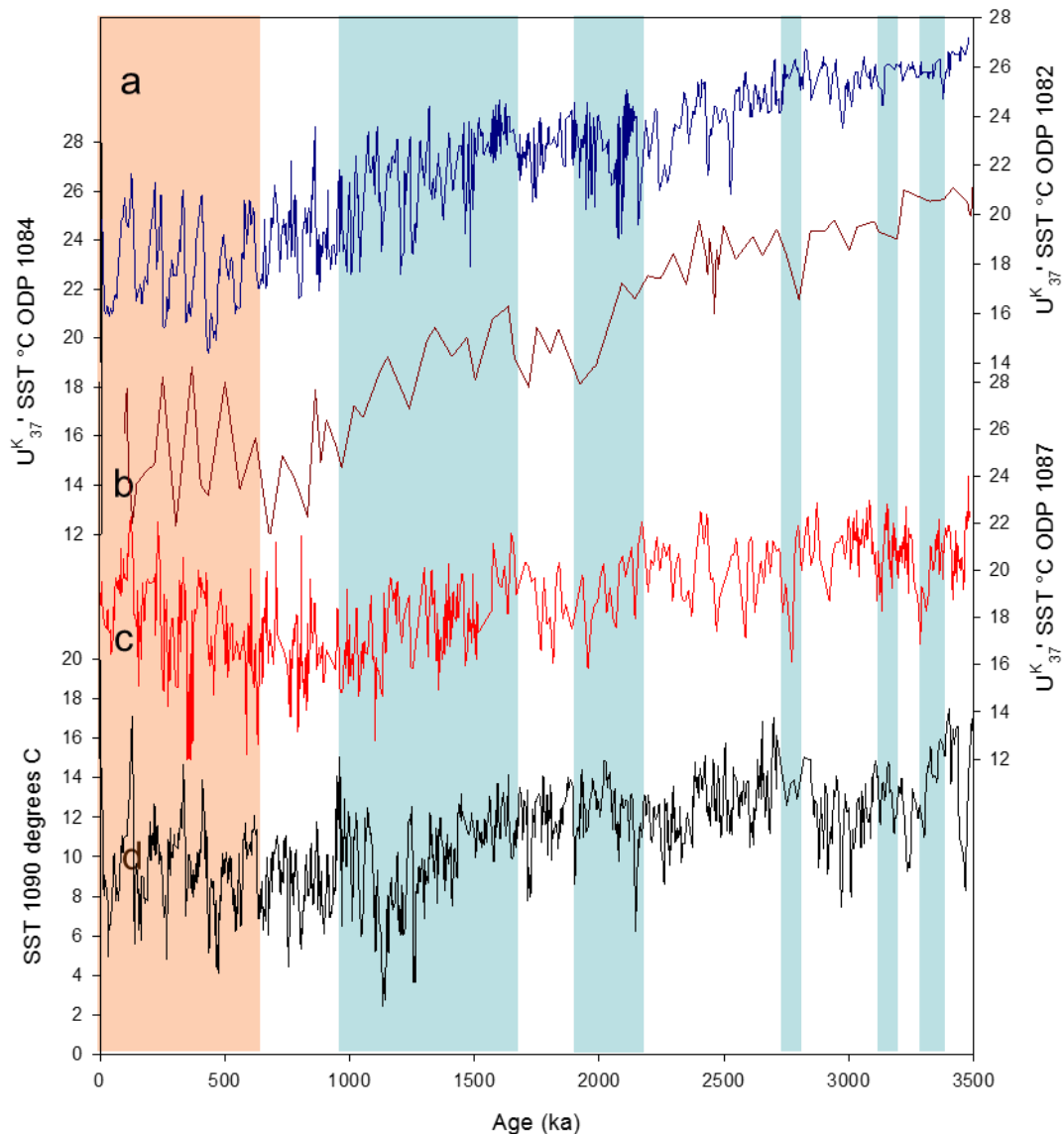


**Figure 4.3 Southeast Atlantic records** a) ODP 1084 $U^K_{37}$' SST record (dark blue) (Marlow *et al.*, 2000). b) ODP 1082 $U^K_{37}$' SST records (brown) (Etourneau *et al.*, 2009) c) ODP 1087 $U^K_{37}$' SST record (red) d) $U^K_{37}$' ODP 1090 SST (blue) (Martinez-Garcia *et al.*, 2010). Major events are marked by blue bars for cool periods and red bar for the warming.

Between 0.95 and 0.6 Ma the cooling trend ends. From 0.6 Ma to the present, both average and maximum temperatures during interglacials have increased at ODP 1087. Changing temperature trends from cooling to either warming or neutral seen in a

number of SE Atlantic records indicate a body of warm water affected this region. The focus of this Chapter is to evaluate the proposed causes of these changes and to consider what impact or implications these mechanisms might have for understanding global climate change since the Pliocene.

There are a number of climate theories that can be tested from the data gathered at ODP 1087, particularly for some of the major climate transitions. First, the onset of northern hemisphere glaciation (INHG) is a major event in the climate record, but its impact on the global climate is still being debated (Bradley, 1999). Second, at the Pliocene-Pleistocene transition questions remain about both the cause of the transition and when the transition occurred (Raymo, 1994; Bradley, 1999; Bartoli *et al.*, 2005). Third, the mid-Pleistocene transition (MPT) marks a major shift in the earth's climate dynamics, but its causes are still poorly understood (McClymont *et al.*, 2013). Fourth, there is the effect of the Agulhas Leakage into the Southeast Atlantic on the thermohaline circulation and Atlantic meridional overturning circulation (AMOC) and whether this plays a major role in driving these systems (Peeters *et al.*, 2004; Biastoch *et al.*, 2008b). To begin with a look at how changes in the record may be influenced by changes in the Indian Ocean

## 4.3 Indian Ocean teleconnections

There are no continuous SST reconstructions in the Indian Ocean that span the last 3.5 Ma at the resolution of our new ODP 1087 record (Figure 4.1). Indeed there are few long-term records that exist in the Indian Ocean at all. Therefore it is important to evaluate the few cores that do exist to understand possible teleconnections between the Indian Ocean and Southeast Atlantic.

The Indonesian Throughflow is a gateway that allows Pacific Ocean water to flow into the Indian Ocean. Ultimately, these waters contribute to the source region of the Agulhas current in the tropical Indian Ocean. It has been proposed that the Indonesian Throughflow may have evolved since the Pliocene, which could, in turn, have influenced SSTs in the West Pacific Warm Pool and thus the Agulhas current (Karas *et al.*, 2011). Using Mg/Ca and $\delta^{18}O$ analysis of surface and subsurface dwelling foraminifera, Karas et al. (2011) reconstructed SSTs and salinity at ODP 709 and ODP 763 at the heart of the Indonesian Throughflow for the Pliocene (3.0-3.5 Ma). Decreasing temperatures from 3.5 Ma during the mid-Pliocene were proposed to reflect

the restriction of the Indonesian Throughflow.  In turn, Karas et al. (2011) proposes that a teleconnection existed between the strength of the Throughflow and the Benguela upwelling system, based on the fact that records from both regions showed cooling trends throughout the MPWP. Karas et al. (2011) argued that the teleconnection might come from the Agulhas Leakage into the Southeast Atlantic, or alternatively though the Antarctic Intermediate Water (AAIW).  This would have been because these systems move Indian Ocean water into the Atlantic Ocean through the Southeast Atlantic Ocean.

However, the new SST data from ODP 1087 shows no decreasing temperature trend at the time of the cooling observed by Karas et al. [2011] in the Indonesian Throughflow.  In Chapter 5, a strong influence of Benguela upwelling at ODP 1087 was suggested on the basis of higher chlorin values, lower than predicted $U^K_{37}$' temperatures and foraminiferal evidence, making it impossible to say if the observed trends fit the signal of reduced Agulhas Leakage predicted by Karas et al [2011].  The ODP 1087 record does, however, show the predicted temperature changes did not occur in the upwelling.  If change in the Indonesian Throughflow is affecting the ODP 1082 record, then changes in the Indonesian Throughflow would also be expected at ODP 1087 given the much more vigorous (and therefore better reflecting subsurface temperatures) upwelling that was occurring at ODP 1087.   The ODP 1087 records do not, therefore, appear to react to changes in the Indonesian Throughflow as expected.
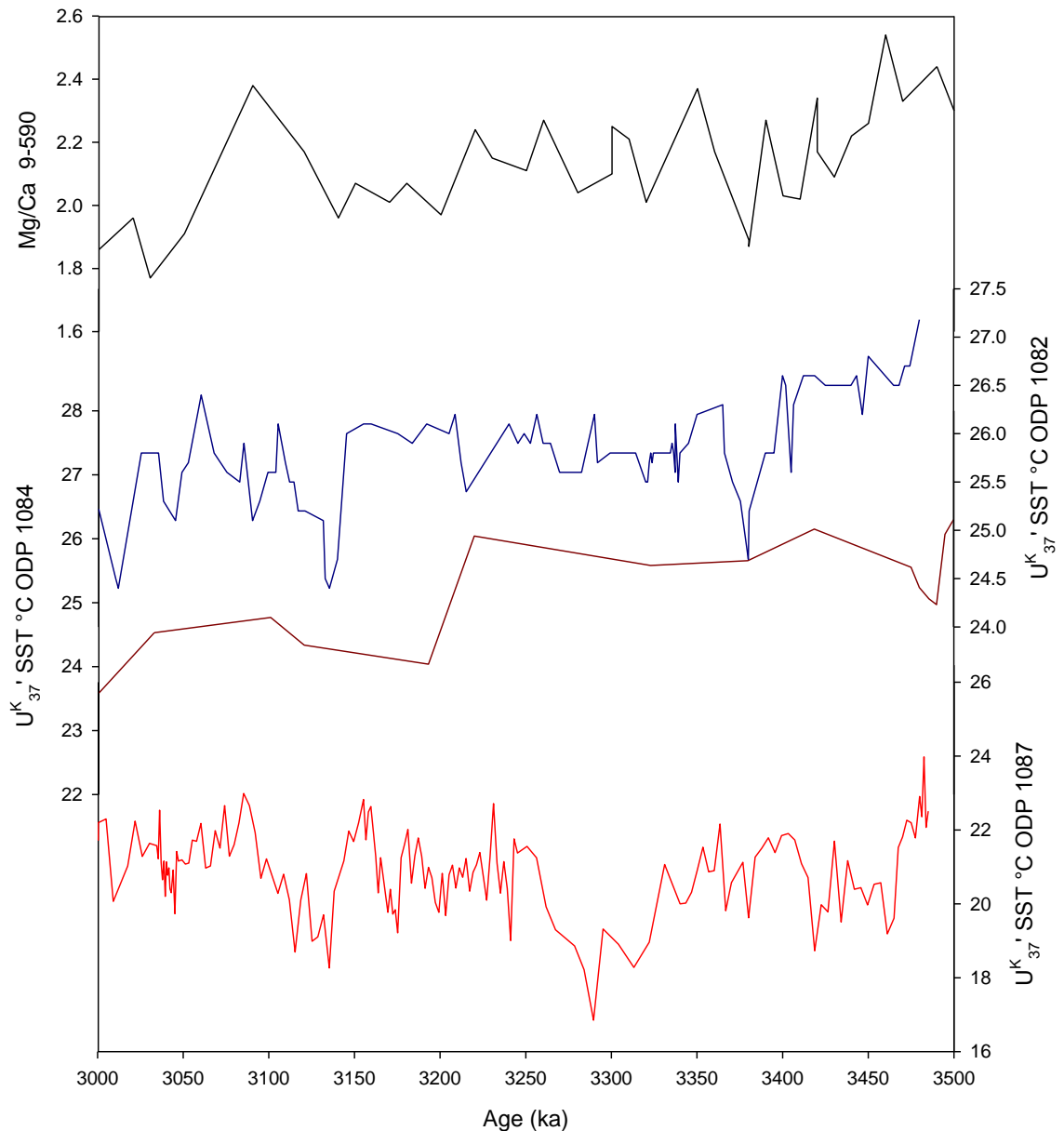
**Figure 4.4. Karas et al [2011] record compared to other Southeast Atlantic records.** a. Mg/Ca record of the Indonesian Throughflow (black) (Karas *et al.*, 2009; Karas *et al.*, 2011) $U^{K}_{37}$' SST records from the Benguela upwelling. b. ODP 1082 (Etourneau *et al.*, 2009) (blue) c. 1081 (Marlow *et al.*, 2000) (dark red) d. ODP 1087 (red).

## 4.4 Major climate transitions 3.0-1.5 Ma

It has long been assumed global climate reacts to changes in the Northern Hemisphere (Shackleton and Opdyke, 1973; Ruddiman *et al.*, 1989; Raymo, 1994; Clark *et al.*, 2006; Crowley and Hyde, 2008) and to changes at the high latitudes (Bartoli *et al.*, 2011). However, some recent researchers have suggested the southern hemisphere and changes at low and mid-latitudes may play a key role in major climatic

changes (Ravelo *et al.*, 2004; Martinez-Garcia *et al.*, 2010).  Furthermore, some researchers have suggested changes in the southern hemisphere might even force changes in the tropics (Martinez-Garcia *et al.*, 2010).   The different proxy records of ODP 1087 can help evaluate the theories and help to understand what southern hemisphere and mid- latitude temperature changes occurred since the Pliocene.
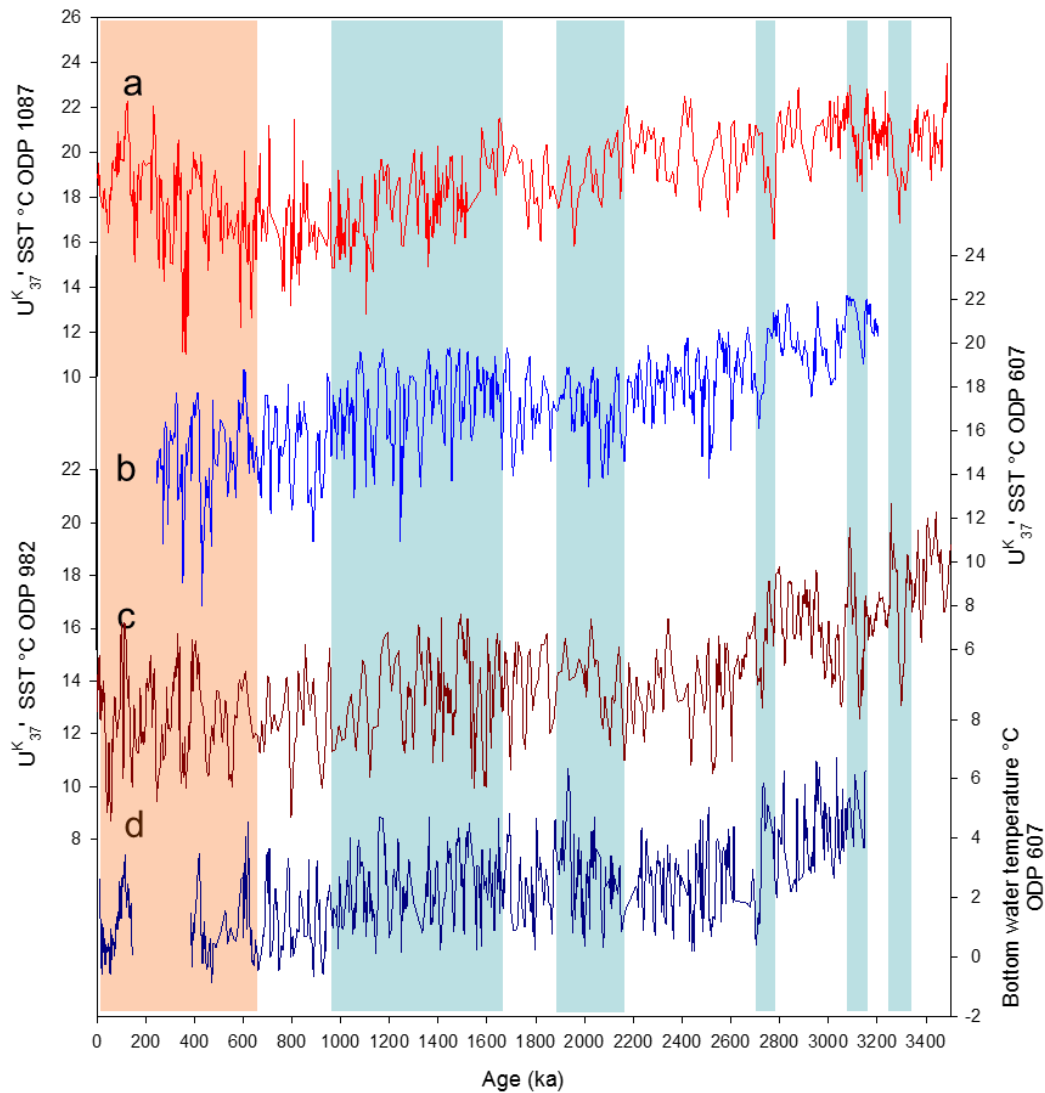
**Figure 4.5 North Atlantic records compared to ODP 1087.** a. The ODP 1087 $U^{K}_{37}$' SST record (red). b. $U^{K}_{37}$' SST record ODP 607 (Lawrence *et al.*, 2010). c. SST $U^{K}_{37}$' record for ODP 982 (brown) (Lawrence *et al.*, 2009). d. Bottom water temperatures from ODP 607 based on Mg/Ca (dark blue) (Sosdian and Rosenthal, 2009). Blue bars represent timing of major cooling events in the ODP 1087 core and the red bar represents the warming as shown in figure 4.2.

### *4.4.1 INHG*

The change from the warm climate of the Pliocene to the colder glacial interglacial record of the Pleistocene is a major climate switch in the 3.5 Ma climate record (Emiliani, 1955; deMenocal, 1995; Lisiecki and Raymo, 2005). The original explanation for these changes was that they were triggered by the onset of the Northern Hemisphere glaciation (INHG) at 2.7 Ma (Ruddiman *et al.*, 1989; Raymo, 1994). Although a number of alternative theories about the cause and timing of the change

(which will be discussed below) have been put forward, the INHG is still considered by some to mark the start of the transition to colder climates (Flesche Kleiven *et al.*, 2002; Haug *et al.*, 2005; Lawrence *et al.*, 2009; Sosdian and Rosenthal, 2009; Herbert *et al.*, 2010; Lawrence *et al.*, 2010).   This is because it is a prominent feature marking the start of the long-term cooling trend in a number of Northern Hemisphere records i.e. (Lawrence *et al.*, 2009; Sosdian and Rosenthal, 2009; Lawrence *et al.*, 2010).   Figure 4.5 shows a comparison of the ODP 1087 SST record with those from the Northern Hemisphere.   Unlike the Northern Hemisphere records, the cooling at ODP 1087 does not start at 2.7 Ma: instead there is an initial decrease in temperatures starting at 3.0 Ma, which then culminates in the 2.8 Ma cooling. SSTs then stabilise and slightly increase from 2.7-2.2 Ma, before cooling again (Figure 4.2).   Therefore 2.7 Ma does not mark the start of cooling in the ODP 1087 record and does not represent a permanent shift to colder conditions.   However, there is a prominent cooling that is associated with this period at ~2.8 Ma (Figure 4.2).   It is therefore necessary to understand if this cold period is linked to the INHG.

The 2.8 Ma cooling most likely corresponds to the cold stages of MIS G10 or MIS G5 in the LR04 record.   Because this part of the record has not been tuned with LR04, however, the dating is somewhat uncertain, so such a correlation is tentative (Figure 4.2).   MIS G10 does represent the highest $\delta^{18}O$ isotope excursion since the earlier M2 (3.3 Ma) event. This fits with the temperature changes seen in the ODP 1087 record. In fact, comparing the 2.8 Ma cooling to the M2 event shows a number of similarities. At ODP 1087 there is a peak in chlorins with the first cooling, which is consistent with what is seen in M2.

Understanding the relationship of the 2.8 Ma cooling to the global record is difficult because it has not previously been identified as a key event.   There are some exceptions – e.g., at ODP 1084 a temperature excursion was seen at 2.8 Ma cooling and described as a signal related to expansion of ice in Antarctica (Marlow *et al.*, 2000), and 2.8 Ma represents the beginning of the MDM in ODP 1082 (Etourneau *et al.*, 2009). Investigating other records shows a 2.8 Ma cooling event (defined as a clear temperature or other proxy excursion around 2.8 Ma)   [ODP 1084, ODP 846, LR04] and possibly at [ODP 607, ODP 1082 and  ODP 662] (Marlow *et al.*, 2000; Etourneau *et al.*, 2009; Herbert *et al.*, 2010; Lawrence *et al.*, 2010) (Figure 4.4, 4.5, 4.6). Therefore it seems to have been an event with a global expression, but it was not a *universal* event in that it is not seen everywhere in the record.

In the northern hemisphere, the 2.8 Ma cooling events tends to be part of the start of cooling linked to the INHG (Lawrence *et al.*, 2010). However, in other places, the cooling is a short-lived event and is not tied to the start of any major cooling – i.e. Etourneau *et al.* (2009). While there is no permanent decrease in temperature at ODP 1087, evidence from other Benguela Upwelling sites and other global upwelling sites shows that 2.8 Ma marks the shift in diatom production associated with the MDM (Lange *et al.*, 1999; Berger *et al.*, 2002; Etourneau *et al.*, 2009; März *et al.*, 2013). It is not clear if the changes linked to the MDM are in any way linked to the INHG. Because the MDM did not represent a permanent shift in the environment of the upwelling sites, it is hard to argue that it represents a permanent climate shift as would be expected from a Plio-Pleistocene transition. Therefore, it appears that the INHG marks more of a temperature change in the local environment in the Southeast Atlantic than the beginning of a long term cooling trend, as it does in the Northern Hemisphere.

There is a possibility that changes which occurred at 2.8 Ma might have been the final cooling, representing a "tipping point" in the northern hemisphere that, when combined with long term global cooling and changes in greenhouse gasses, led to the INHG (Ravelo *et al.*, 2004). Therefore, understanding what causes the cooling at 2.8 may be useful in understanding how signals seen in the ODP 1087 relate to climate changes further upstream. From the new data presented at ODP 1087, one cause of the cooling at 2.8 Ma could be (using M2 and KM2 as an analogy) an expansion of Antarctic sea ice (Marlow *et al.*, 2000). For other cold periods especially M2, cooling of the AAIW and AABW is thought to have impacted the North Atlantic subsurface currents leading to a general cooling of the currents and by changing strength of the global thermohaline circulation (De Schepper *et al.*, 2009; McKay *et al.*, 2012). Unfortunately, because, for this period, there are few records of bottom water temperatures and the record of Antarctic glaciation is also incomplete, it is hard to confirm that this could explain INHG. Likely it is a combination of these two forcings that drove the unusually strong 2.8 Ma cooling at ODP 1087.

Therefore, whether there is evidence of the INHG at ODP 1087 is a simple question with a complex answer. The most likely answer is that the 2.8 Ma cooling is probably related to a cooling that is, in turn, related to the INHG. Furthermore, there is a possibility that at ODP 1087 the 2.8 Ma cooling is linked to a cooling of bottom and intermediate waters that might have had a role in causing an intensification of glaciation in the Northern Hemisphere. However the 2.8 Ma is a temporary cooling and there is

no evidence of a long-term, sustained, and permanent cooling at ODP 1087 that would be associated with the expected shift from the warm Pliocene to the colder Pleistocene. In fact, the only major changes associated the INHG is the start of the MDM elsewhere in the Benguela Upwelling which, although it may be linked to INHG, does not represent a permanent change in the environment a major climate shift is expected to have.
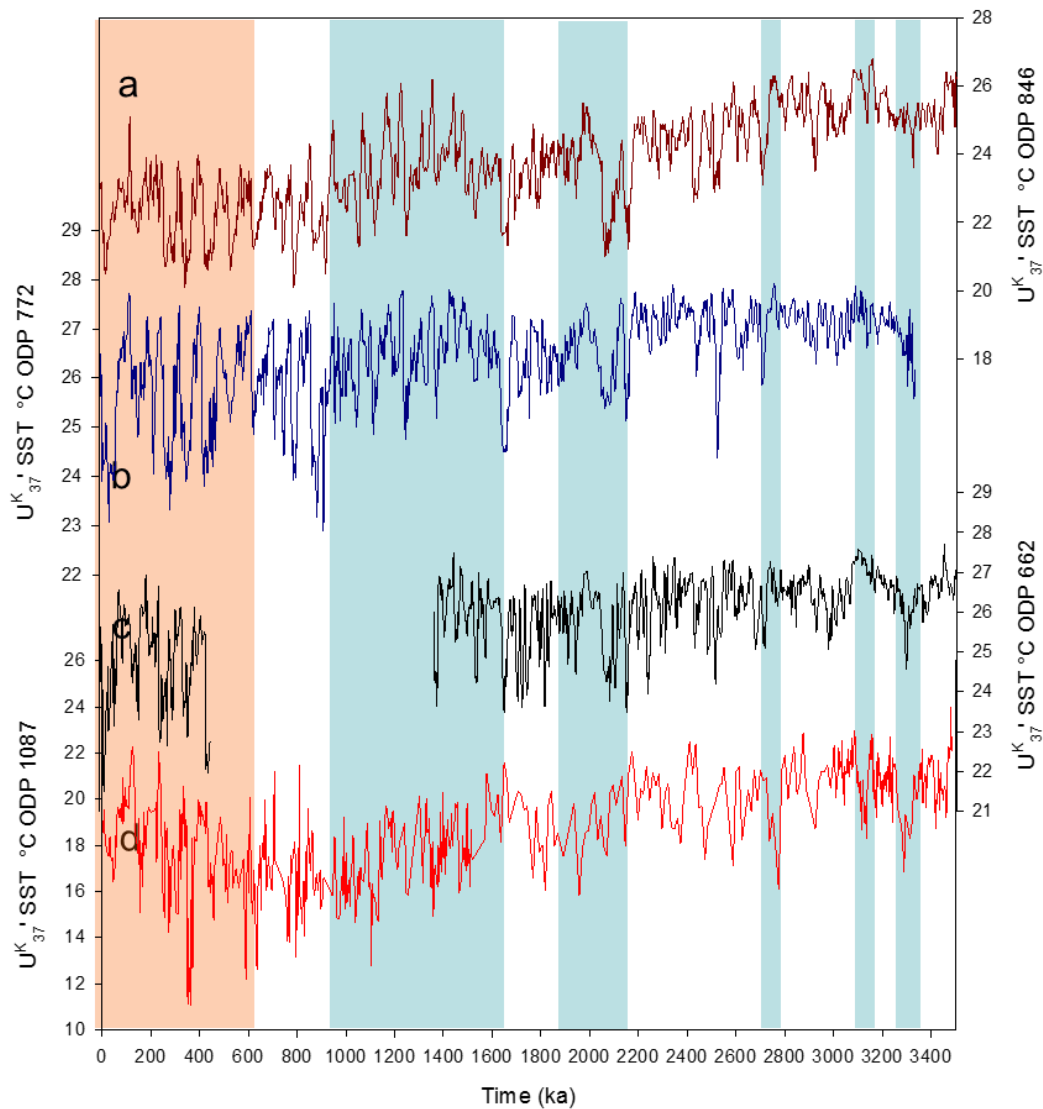
**Figure 4.6 records of tropical temperatures compared to the ODP 1087 UK37' SST record** (red). a. ODP 846 (Dark red), b. ODP 772 (Dark blue), c. ODP 662 (Black) (Herbert *et al.*, 2010) and d. ODP 1087. Major coolings in the ODP 1087 are marked by blue bars and the warming after .6 Ma is marked by a red bar. Blue bars represent timing of major cooling events in the ODP 1087 core and the red bar represents the warming as shown in figure 4.2.

### 4.4.2 Pliocene-Pleistocene Transition

The timing of the Pliocene-Pleistocene transition is the shift from the warmer Pliocene world to the colder Pleistocene dominated by interglacial glacial cycles (Bradley, 1999). Understanding the causes of a climatic shift from a warmer world to a colder has been the focus of a number of studies. The causes of the shift are debated

but usually focus on either tectonic change (Raymo, 1994; Burton *et al.*, 1997; Bartoli *et al.*, 2005), or a change in the level of $CO_2$ (Haug *et al.*, 1999). These studies have found that between 3.0 and 1.5 Ma there was a shift in the global climate of about 1°C (although individual areas have shown a greater amount of temperature shift) (Lisiecki and Raymo, 2005). However, there is a disparity in the timing of the start of the shift and the time span over which it occurs, depending on the global location of the record (Ravelo *et al.*, 2004). For example, in the global benthic stack, a long permanent cooling begins at 2.7 Ma and this is also true of the North Atlantic Ocean records, all of which have been timed to link with the INHG, as mentioned above (Lisiecki and Raymo, 2007). However, as more records have been produced, the timing of this event has been questioned. It has been suggested the timing of the coolings in the tropical and subtropical regions was a result of the establishment of the modern upwelling cells at 2.0 Ma based on evidence from the Benguela Upwelling and Peruvian Margin (Ravelo *et al.*, 2004). Martinez-Garcia et al. (2010) sees teleconnections between cycles in the Tropical Ocean and the Polar Regions, but the major cooling in ODP 1090 he links with the establishment of the pacific cold tongue at 1.8 Ma, which he suggests is the major driver of cooling in the Sub-Polar Regions. Finally, Etourneau *et al.* (2010) argues that the intensification of the Hadley and Walker cells between 2.2 and 2.0 led to changes in the ocean circulation, which may have caused cooling by shifting the major wind patterns and by confining the warm tropical body of water to a much smaller area, and which in turn led to an expansion of the cold water bodies in the ocean. Therefore the ODP 1087 record can help answer a number of questions about the Pliocene-Pleistocene transition, namely:

1) What was the timing of the cooling in the Southeast Atlantic?

2) What is the duration of the cooling and whether it was sudden or gradual?

3) What is the degree of cooling?

4) Whether the cooling was permanent?

5) Whether the changes seen in ODP 1087 relate to changes seen elsewhere in the world?

Answering these questions is not as simple as it seems. The ODP 1087 record reveals not one major cooling event but instead three cooling events between 3.0 and 0.9 Ma (figure 4.2). The first, which was discussed above, is from 3.0 Ma to 2.8 Ma

and might be related to the INHG. The second cooling in the ODP 1087 record occurs around 2.2 Ma and 2.0 Ma and will be discussed in the next few paragraphs. As discussed in Chapter 6, this marks a major cooling of the Benguela Upwelling in a number of local records. This cooling started at different times in different parts of the Benguela Upwelling, namely at 2.2 Ma in the ODP 1087, at 2.4 Ma in the ODP 1082 and at 2.1 Ma in the ODP 1084 (Figure 4.3) (Marlow *et al.*, 2000; Etourneau *et al.*, 2009). The increases in the various proxies measuring upwelling, both in the ODP 1087 and elsewhere in the Benguela Upwelling, suggest the upwelling was expanded compared to its modern extent. It has been suggested the cooling seen in the tropical and subtropical regions was a result of the establishment of the modern upwelling cells at 2.0 Ma (Ravelo *et al.*, 2004). The timing of the 2.2 Ma cooling in the ODP 1087 record fits this model in that the expansion and intensification of the Benguela Upwelling started at 2.2 Ma and lasted until 2.0 Ma. Furthermore, the timing of the 2.2 Ma cooling matches major cooling events seen in a number of tropical records (Herbert *et al.*, 2010) (figure 4.6). The tropical records also show the same approximate 1°C warming as ODP 1087, reflecting the short term warming seen between 1.7 and 1.5 Ma (Herbert *et al.*, 2010) (Figure 4.6). This suggests there might have been a strong teleconnection between changes in the tropics and changes in the Benguela Upwelling.

There are a number of explanations for the link between what is seen in ODP 1087 and the tropical records. One explanation is related to a shift in the Hadley cells that drive the Benguela upwelling (Brierley *et al.*, 2009; Etourneau *et al.*, 2010). In chapters 5, 6, and 7, changes in the wind systems were interpreted as the cause of the shift of the major oceanic systems between 3.5 and 0.9 Ma. The ODP 1087 core is located near the boundary of the Hadley cells, and therefore small changes in the Hadley Cells should influence the location of the Southeast Atlantic oceanic systems because of the influence on the winds in driving these systems (Etourneau *et al.*, 2010). This has been seen elsewhere in the Benguela Upwelling (Etourneau *et al.*, 2010). It has been shown previously even small scale changes in global temperature can have influence on the location and strength of the Hadley cells (Brierley *et al.*, 2009). However the Hadley cells also affect changes in the tropical oceans. This is because changes in the Hadley Cells would lead to an expansion or constriction of the global warm water pool. Therefore, changes in the Hadley cells would be expected to affect records both in the southeast Atlantic Ocean and in the tropical ocean. The connection

between the intensification of the Hadley cells and changes in the tropical ocean should cause a reduction in the extent of tropical waters in the ocean (Etourneau *et al.*, 2010).

Alternatively, there is also evidence there was cooling of the bottom waters during between 2.2 and 1.7 as well (Ravelo *et al.*, 2004).  It has been hypothesised more cold water upwelling in intermediate and tropical upwelling area started at 2.0 Ma and led to a cooling of the thermohaline circulation and therefore drove the cooling in the tropics by cooling the temperature of the waters throughout the ocean (Ravelo *et al.*, 2004).  In previous chapters, changes in the ODP 1087 have been traced to changes in the AAIW; therefore, it is possible that the changes in ODP 1087 might be tied to cooling of the subsurface temperatures.  However, the evidence from the ODP 1087 proxies for this period, and previous cool periods suggests that the record at ODP 1087 reflects a combination between an expansion of the Benguela Upwelling due to changes in the dominant wind cells and a cooling of the temperature of the AAIW.  Therefore the evidence shows that the cooling between 2.2 Ma and 2.0 Ma, and the cool period between 2.0 and 1.7 Ma, had possible teleconnections with tropical temperature changes.

The final event occurs between 1.6 and 0.9 Ma, when both ODP 1087 and the rest of the Southeast Atlantic experienced cooling.  This cooling of 1.5 ºC at ODP 1087 precedes a global cooling event starting at 1.2 Ma  (McClymont *et al.*, 2013).   ODP 1087 cools in synchrony with many other eastern boundary upwelling systems.  It is also known there is a major freshwater expansion in the pacific cold tongue during this time, which is thought to have caused the cooling of the ACC currents (Martinez-Garcia *et al.*, 2010).  While originally thought to affect the Agulhas Leakage at site 1087 and cause a permanent cooling at ODP 1087 (McClymont *et al.*, 2005), the recent work in this thesis disproves the theory there was a permanent cooling of ODP 1087.   Here, it is argued that prior to 0.9 Ma the ODP 1087 record is reflecting changes in upwelling.  Cooling from 1.6 Ma, and again at 1.2 Ma, might therefore reflect increasing upwelling intensity, perhaps in response to an increasing strength of the atmospheric circulation (Dekens *et al.*, 2007; Martinez-Garcia *et al.*, 2011) or a more efficient delivery of colder waters to the upwelling sites (Fedorov *et al.*, 2007).   Unfortunately, the proxies do not exist for this part of the record to evaluate which of these is more likely for ODP 1087.  However other sites show changes and cooling in the temperature of bottom water currents, some of which are very close to ODP 1087 (Becquey and Gersonde, 2002; Elderfield *et al.*, 2012).  Those bottom water temperature records show cooling

temperatures occurring at the same time as the cooling seen in the surface waters (Sosdian and Rosenthal, 2009; Elderfield *et al.*, 2012).   All of this is evidence of cooling of the intermediate waters during this time. Therefore, the signal is a combination of an increase in wind driven upwelling and a cooling of the bottom waters.   Then, starting at 1.2 Ma, a global cooling is seen that may be responsible for the MPT, which is discussed further in the next section (McClymont *et al.*, 2013).

### *4.4.3 The Timing of the Pliocene-Pleistocene Transition*

The ODP 1087 record provides new insight into the transition to a cooler world that dominated the Pleistocene.  Many researchers have tried to assign specific triggers to explain the transition from a warmer world to a colder glacial interglacial world. Others have suggested that it was a gradual, more natural long-term cooling. The ODP 1087 record suggests the changes are more complex at least locally than either of these models. The ODP 1087 record shows long term cooling between 3.0 and 0.9 Ma, punctuated by a number of rapid more pronounced cooling events.  These cooling events are related to and may influence changes seen elsewhere such as the INHG, intensification of the Benguela Upwelling, and the MPT.  However, none of these could be described as '*the*' cooling event that marks the transition from the Pliocene to the Pleistocene.  Furthermore none of the coolings seen in the core represent a permanent cooling in the record.  All of them are followed after different periods of time by warming in the core.  Often these warming events result in temperatures reaching levels similar to what they were before the onset of cooling.  Therefore, the record is better described as a record of long term cooling punctuated by short term cooling and warming events.   This suggests there was not one event that drove the local climate change from the Pliocene to the Pleistocene but instead it was a combination of a number of different events. Over all the ODP 1087 record shows a cooling that starts latter in the record and cools in a number steps.

However there a similarity in the possible driving forces between all three of the major cooling events in ODP 1087 that might provide an explanation for why the events seem different than in other records. All of the major cooling events seen in the record could be explained by a global cooling of the intermediate and deep water temperatures combined with an expansion of wind driven upwelling.  While there is not much direct evidence for changes in the deep water temperatures, there is circumstantial evidence

for changes in the intermediate temperature throughout the ODP 1087 record. Coupled with evidence from the ODP 1087 record for changes in the winds around the Southeast Atlantic, shifts in the wind driven upwelling and changes in the temperature of the upwelling could have combined to produce the temperature changes seen in the ODP 1087 record. Furthermore the changes seen in the system relate too many of the major climate changes between 3.5 and 0.9 Ma.

**4.5 MPT**

After 0.9 Ma, a change in the dominant trend is seen in the ODP 1087 record. Average temperatures increase by 2 °C between 0.9 and the present day, with most of that change occurring since 0.6 Ma. As demonstrated in chapter 7, this reflects strengthening of the Agulhas current coupled with weakening of the Benguela Upwelling. Furthermore, this change occurs at the same time as the MPT and the 900 ka event. This suggests that changes happened to the strength and organisation of the Agulhas Leakage. It suggests that at 0.9 Ma there was a wholesale reorganisation of the entire Southeast Atlantic ocean. While some of the implications for this connection are discussed in chapter 7, in this section the global nature of these changes will be described. There are questions about what caused the MPT. There are two major theories. The MPT was either the result of gradual change in a climate parameter i.e. (temperature, $CO_2$ ) (Mudelsee and Schulz, 1997; Schmieder *et al.*, 2000; Clark *et al.*, 2006; Sosdian and Rosenthal, 2009; Lawrence *et al.*, 2010) or was due to a much more sudden change, such as changes in the regolith, or changes in Bottom Water temperatures due to changes in Antarctica (Kitamura and Kawagoe, 2006; Elderfield *et al.*, 2012). The ODP 1087 record might help resolve this question based on the major changes that happened in ODP 1087 at the MPT.

A recent survey of changes during the MPT found in 27 separate records showed that only 6 records had evidence of an increase in temperature during the post MPT period (McClymont *et al.*, 2013). Furthermore, the ODP 1087 record is the only one that showed warming that exceeded the error for the temperature proxy (McClymont *et al.*, 2013). This suggests that the changes seen in the Southeast Atlantic are in some ways unique. It also suggests there might be a connection between a stronger Agulhas Leakage in the Southeast Atlantic and the onset of the 100 ka cycles. It has been hypothesised that the early warming caused by the Agulhas Leakage should

prevent an early return to glacial conditions in the record. This has been confirmed by computer models (Flores *et al.*, 1999; Knorr and Lohmann, 2003; Turney and Jones, 2010). Therefore, there appears to be a strong connection between the beginnings of interglacials and greater amounts of Agulhas Leakage (Peeters *et al.*, 2004; Caley *et al.*, 2012). Coupled with the evidence from the ODP 1087 of increasing Agulhas Leakage, this suggests a connection between the increased strength of the Agulhas Leakage and the longer and warmer interglacials. It could mean that the increased salt input is increasing the strength of the AMOC. This continues at 0.6 Ma, where the increased leakage is connected to the 'super-interglacials' which will be discussed in Chapter 7. Therefore there are possible significant connections between the changes seen in ODP 1087 and the global climate.

**4.6 South Atlantic influence on changes in the Thermohaline Circulation**

One of the impacts of the Agulhas Leakage is the hypothesised control over the thermohaline circulation by changes in the leakage input.   As mentioned in chapter 1, increased Agulhas Leakage is thought to be responsible for restarting the thermohaline circulation after the Younger Dryas (Gordon *et al.*, 1992; Knorr and Lohmann, 2003; Laurian and Drijfhout, 2011). It does this by supplying salty water, which restarts the Thermohaline circulation after it collapses (Gordon *et al.*, 1992; Laurian and Drijfhout, 2011). The Southeast Atlantic Ocean is thought to be a gateway in the global circulation system (Knorr and Lohmann, 2003); therefore it is necessary to understand how the changes that have been seen in the ODP1087 record relate to changes in the overturning circulation.   However, this is challenging because there are no good proxies for the thermohaline circulation that can be applied for the Pliocene and Pleistocene, and the proxies that do exist are sparse in their coverage. The most common proxy used is the benthic $\delta^{13}C$ proxy. This is because it is thought that the proxy reflects the amount of changes in the nutrients and age of the water masses (Bradley, 1999; Sharp, 2007). Higher amounts of $\delta^{13}C$ are thought to indicate water masses that have higher amounts of nutrients and/or are younger in age (Bradley, 1999).  Therefore, high $\delta^{13}C$ values are often interpreted as indicating a greater amount of southern ocean deep-water input because the water is high in nutrients and relatively young (Bradley, 1999).  Thus, while ODP 1087 is not the ideal record to understand the interactions between the Agulhas

Leakage and changes in the Thermohaline circulation, there are still important reasons for doing so.

.
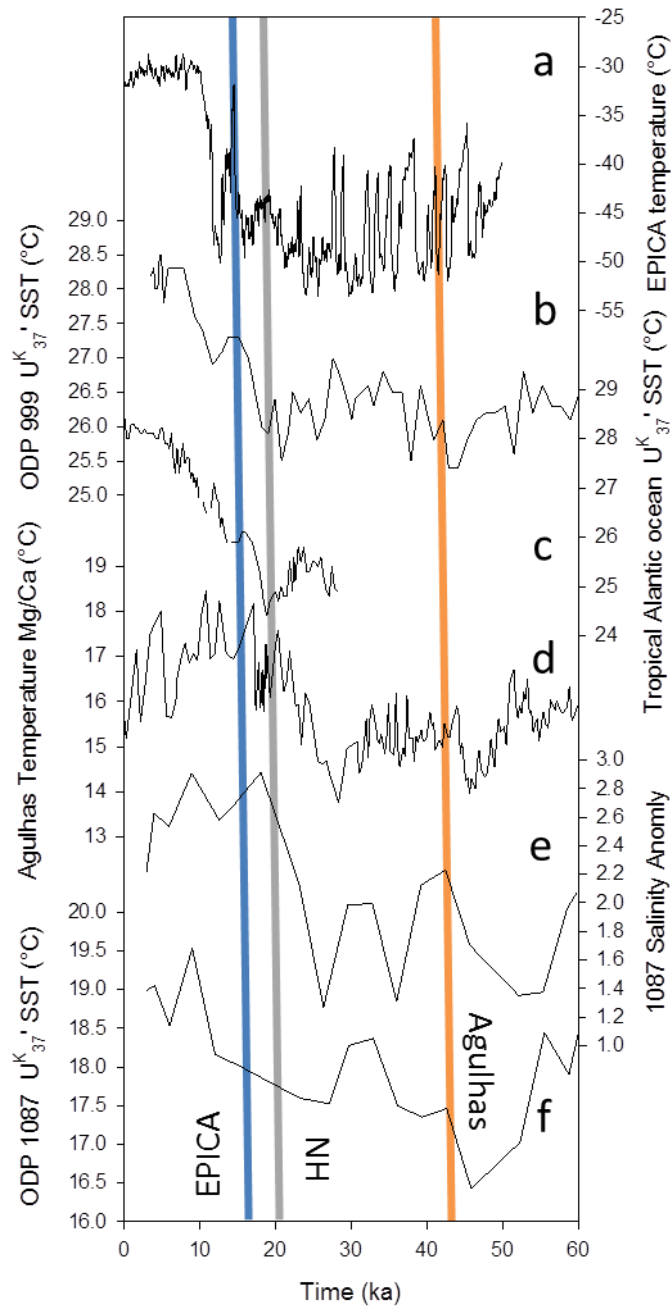


**Figure 4.7 A comparison of the records of Agulhas Leakage from the southeast Atlantic to records of the northern hemisphere for the last deglaciation.** a. The EPICA core temperatures (Alley, 2000) b. ODP 999 from Caribbean Sea (Schmidt *et al.*, 2004) c. $U^{K}_{37}$' SST's Tropical Atlantic (Ruhlemann *et al.*, 1999) d. the Agulhas Leakage record from the cape (Martínez-Méndez *et al.*, 2008) e. the 1087 Salinity anomaly $U^{K}_{37}$' f. SST ODP 1087. Bars mark the beginnings of Agulhas Leakage (Agulhas) and initial warming of the Northern Hemisphere (NH) and Greenland Ice cap (EPICA).

The last glacial to interglacial transition is shown in Figure 4.7, and compares SST data from a number of cores from the Agulhas Leakage region (Martínez-Méndez *et al.*, 2008), records showing thermohaline circulation in the north Atlantic (Ruhlemann *et al.*, 1999; Schmidt *et al.*, 2004) and changes in temperature in the GISP2 ice record (Alley, 2000) in order to show the pattern of warming in the thermohaline circulation and the effect of the Agulhas Leakage (Figure 4.7).  Given the low resolution of the ODP 1087 record, the impact of changing Agulhas Leakage on millennial timescales is challenging. However, the expected pattern of early warming in the southeast Atlantic Ocean during deglaciation is observed.  This is then followed by warming of the Northern Hemisphere ocean temperatures.  Finally, the Greenland record warms.  This pattern is what would be expected if the Agulhas Leakage were causing a strengthening of the thermohaline circulation, which was then causing northern hemisphere warming.  It also matches the pattern of warming seen for MIS 6-5 transition and the pattern seen in between MIS 12-11 (Dickson *et al.*, 2010b; Turney and Jones, 2011).   Furthermore, the Southeast Atlantic temperature continues rising through the Younger Dryas, which also fits with the predicted pattern of continuing leakage keeping the temperatures from returning into glacial conditions during the Younger Dryas (Knorr and Lohmann, 2003; Biastoch *et al.*, 2008a; Biastoch *et al.*, 2008b).

However, the relationships are more complex when examined over multiple glacial to interglacial transitions. For example, issues arise when comparing the timing of the Agulhas Leakage as recorded in the ODP 1087 to the proxy based on Atlantic and Pacific benthic $\delta^{13}$C records developed by Bard and Rickaby (2009), to reconstruct the strength of the overturning circulation (Figure 4.9).   It has been argued that there were connections between the changes seen in Agulhas Leakage and this gradient, with periods of increased Agulhas Leakage connected to stronger overturning by the current (Bard and Rickaby, 2009; Caley *et al.*, 2012).  However, the ODP 1087 record does not show this linkage. First, the MIS 11 leakage peak shows that the peak of early warming temperatures and salinity, which are interpreted to represent an Agulhas Leakage maximum, precedes the proposed intensification of the overturning circulation by 30 ka. This is too long to argue a connection.  Furthermore, the relationship between peaks in Agulhas Leakage and peaks in the overturning circulation proxy continues to change until the most recent intensification of the overturning circulation, which occurs 5ka before the onset of warming in the ODP 1087 core.   Therefore, periods of increased

Agulhas Leakage do not relate to changes in the strength of the overturning current over short time scale as would be expected between the ODP 1087 record and the Bard and Rickaby reconstruction.
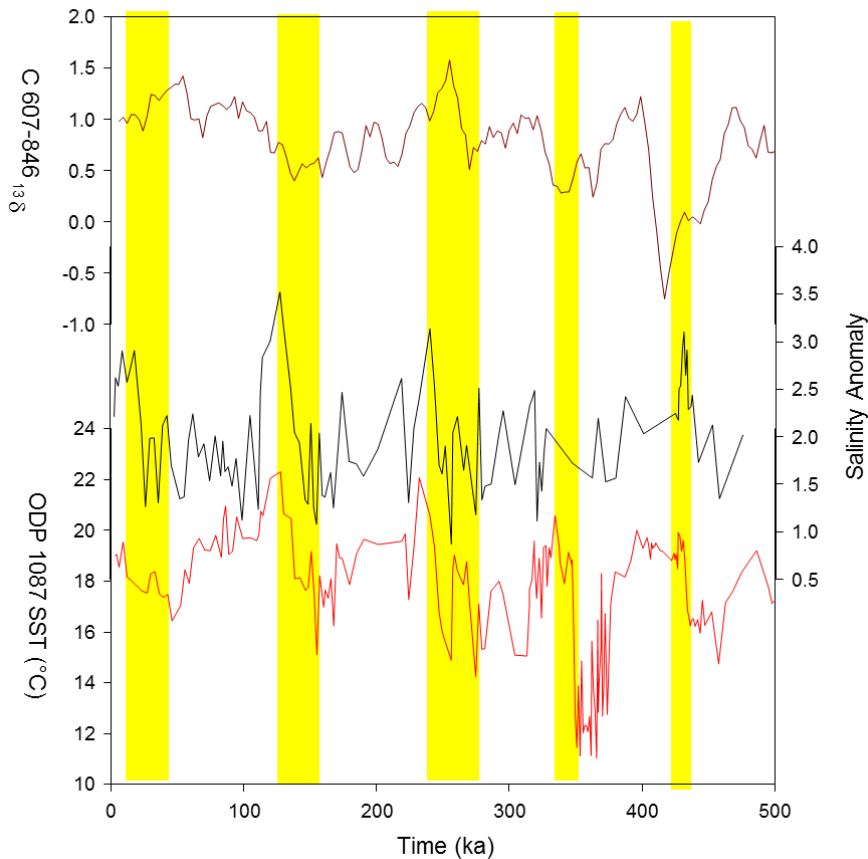


**Figure 4.9 A comparison of the ODP 1087 leakage records showing the timing of the leakage events verses the overturning proxies**. ODP 1087 $U^K_{37}$' SST (red) and the Salinity Anomaly from ODP 1087 (black) compared to the Bard and Rickaby [2009] overturning model (dark red). Yellow bars represent the timing of leakage events based on the change in temperatures before the onset of warming in the global record. Best fit lines created using polynomial regression.

Over longer timescales (>glacial-interglacial cycles), the ODP 1087 record reveals a possible long term connection between changes over the last 1.5 Ma and changes in global circulation (Figure 4.10) (Raymo *et al.*, 1997; Bard and Rickaby, 2009; Elderfield *et al.*, 2012). As mentioned above, at 0.9 Ma and especially after 0.6 Ma, there are changes in ODP 1087 from a decreasing temperature trend to a warming trend. Also there is the establishment of the Agulhas Leakage at this time with the beginning of early warming events. This therefore marks the establishment of the modern ocean circulation at 0.9 Ma. It also represents the establishment of what has

been hypothesised as a major link in the transfer of water from the southern hemisphere to the northern hemisphere and a driver of the modern thermohaline circulation. In addition, the warming after 0.6 Ma, is seen in only a few other records besides ODP 1087 and the magnitude of the change is unique. Therefore there are major changes in the Southeast Atlantic Gateway at both 0.9 Ma and 0.6 Ma.

At the same time, a number of benthic $\delta^{13}$C records shown in figure 4.10, also show increasing isotope values after 0.6 Ma. In addition, most of these records show that the initial change from decreasing to increasing $\delta^{13}$C values occurs at 0.9 Ma and the beginning of the exponential increase in all the records occurs at 0.6 Ma (Figure 4.10). These changes occur at the same time in the ODP 1087 SST record. They all show a reversal of both decreasing temperatures and decreasing $\delta^{13}$C ‰ around 0.9 Ma. Even more interesting, both the $\delta^{13}$C records and the ODP 1087 temperatures show increases around 0.6 Ma (Figure 4.10).

The data suggests an intensification of the global circulation over the last 0.6 Ma based on the increasing $\delta^{13}$C values, which indicate either younger or more nutrient rich southern ocean water is moving through the system. Either explanation would indicate a more active circulation. The data also suggest that the establishment and intensification of the Agulhas Current might have played a role in causing this intensification of the overturning circulation. This makes sense, because evidence from the ODP 1087 shows a strengthening of Agulhas Leakage between 0.9 Ma and the present, which would have increased the amount of water being transferred from the Indian Ocean through this important oceanic gateway. This increase in the volume of input of Indian Ocean water to the Atlantic Ocean also would have increased the total volume of water being moved throughout the global conveyer belt. It is possible that all of these relationships are just a consequence of global background changes in the $\delta^{13}$C curve, as mentioned in chapter 3. The $\delta^{13}$C records are complex and there have been warnings about using these to infer circulation changes (Raymo *et al.*, 2004). However, the similarity in the timing of these events in two different proxies suggests a connection between the $\delta^{13}$C trends, the intensification of the thermohaline circulation and the establishment of the modern Agulhas Leakage.
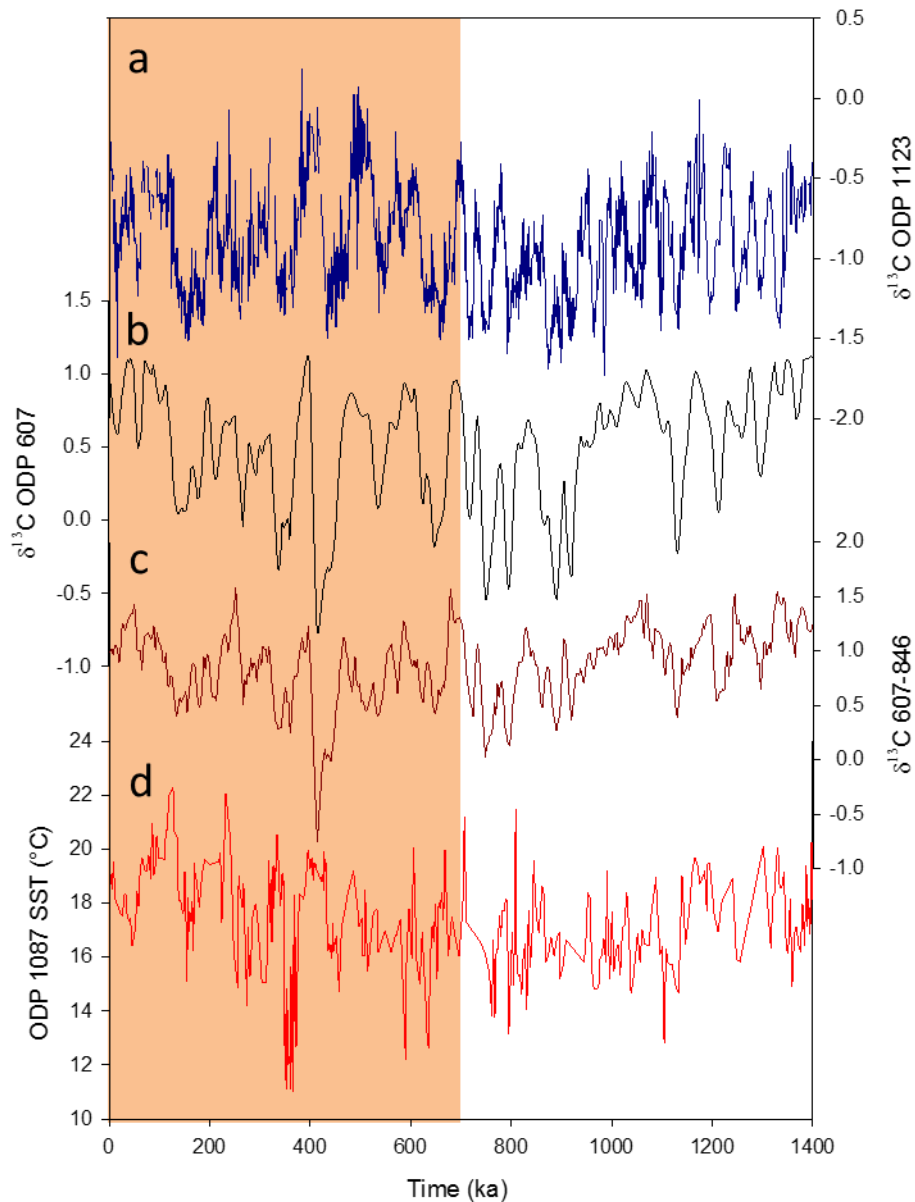
**Figure 4.10 $\delta^{13}$C records compared to the SST record from ODP 1087** d. (red). a.
Overturning circulation estimate $\delta^{13}$C from 607-846 (dark red) (Bard and Rickaby, 2009), b.
$\delta^{13}$C from ODP 607 (black)(Raymo *et al.*, 2004), and c. $\delta^{13}$C from ODP 1123 (blue)
(Elderfield *et al.*, 2012). Red bar represents warming period in the ODP 1087 d. (red) record.

**4.7 Influence of Southeast Atlantic on global climate over the last 3.5 Ma**

The major aim of this thesis was to understand the interaction between major
climate changes over the last 3.5 Ma and the ODP 1087 record. This thesis has
demonstrated there are connections between changes seen in the ODP 1087 record and
major climate changes over the last 3.5 Ma. The final question to be posed is whether
global climate change is driving the changes at ODP 1087 or whether changes in the

southeast Atlantic drive global climate change. The answer to this question is complex, but it appears that there are processes revealed in the ODP 1087 record that shed light on major climate transitions and suggest connections.

Before 0.9 Ma, the data shows that the Southeast Atlantic is sensitive to changes in Antarctica. In a number of time periods, the changes seen in the ODP 1087 record have links to changes in Antarctica, as a result of expansion of ice causing changes in the temperature of the deep water currents (McKay *et al.*, 2012) or changes in the southern hemisphere winds, which can be driven by changes in the ice mass in Antarctica (DeConto *et al.*, 2007). Unfortunately, the history of the glaciation of Antarctica and its affects over the last 3.5 Ma are not well understood. However, the ODP 1087 record suggests that changes in Antarctica play a crucial role in changes in the Southeast Atlantic. Furthermore, the ODP 1087 record also suggests that during major cooling events in the global climate record such as the M2 and KM2 stages, the intensification of upwelling at 2.0 Ma, and even the INHG might have been driven by changes in the water masses around Antarctica. This is important because it suggests that changes in Antarctica may play a role in changing global climate than has been previously hypothesised. Moreover, because ODP 1087 is located near the edges of the Upwelling system, it responds more sensitively to changes in the location and strength of the upwelling. The ODP 1087 record suggests that it is necessary to develop a better understanding of the role that changes in Antarctica play on the global climate record.

The other major finding in the ODP 1087 record, which occurs after 0.9 Ma, is the temperature increases match the timing of the MPT. As mentioned above, the strengthening Agulhas Leakage fits with the start of the 100 ka cycles, increasing deep water circulation and the intensification of the interglacials at 0.6 Ma. The intensification of the Agulhas Leakage emphasises this point. The timing of the intensification suggests that changes in the Agulhas Leakage played a role in the climate shifts at the MPT and the establishment of the modern ocean circulation and climate regime. Therefore, this represents a local change with global impacts. The ODP 1087 record argues that understanding how localized changes affect the global climate is as important as understanding large scale climate changes themselves.

**4.8 Conclusions**

ODP 1087 is significant because it is at a unique location in an important ocean gateway and at the intersection of two major oceanic systems. Two intervals characterise the new records presented here, in the broadest sense: the early record from 3.5 to 0.9 Ma is dominated by Benguela Upwelling; the later record from 0.9 to 0.0 Ma is dominated by Agulhas Leakage. In this chapter, comparisons to other evidence of Plio-Pleistocene climate change were examined. It was noted there is no evidence of changes in the ODP 1087 records that could be linked to changes in the Indonesian Throughflow during the Pliocene. There is a prominent cooling of the record at 2.8 Ma that might be related to the onset of northern hemisphere glaciation, although this does not mark the start of long term cooling in the record. The major cooling at ODP 1087 starts at 2.2 Ma with evidence of strengthening upwelling and teleconnections with tropical ocean changes. Furthermore, there is a cooling between 1.6 and 0.9 Ma which precedes a global cooling that intensifies around 1.2 Ma (McClymont *et al.*, 2013). Then there is an unusual warming in the record from 0.6 Ma which might have impacts on the efficiency of the Thermohaline Circulation. Overall the ODP 1087 record is very sensitive to changes in the global climate and therefore is an excellent proxy for examining the effect of changes in a number of important oceanic surface and subsurface systems and the operation of a major oceanic gateway. Over the next three chapters the impacts of the ODP 1087 record will be investigated on shorter time scales to better investigate the smaller scale changes in the record.

# Chapter 5: Shifts in the Benguela Upwelling and Agulhas Leakage During the Mid Pliocene Warm Period.

## 5.1. Introduction

The geological record provides opportunities to understand climate feedbacks under a warmer global climate state. The mid-Pliocene warm period (MPWP), or the late Piacanzian, from 3.0-3.3 Ma (Crowley, 1996), has been studied extensively as a possible analogue for future warming (Dowsett *et al.*, 1996; Raymo *et al.*, 1996; Haywood *et al.*, 2009b) because it is the most recent 'greenhouse world' (Haywood *et al.*, 2009b) and $CO_2$ was the same as now and temperatures are were similar to those predicted for the end of this century (IPCC, 2007). Atmospheric $CO_2$ concentrations have been reconstructed to between 300 and 400 ppmv, and thus lie close to those of modern climate (Henderiks and Pagani, 2007; Dowsett *et al.*, 2009a; Seki *et al.*, 2010). Numerical climate models give estimations for palaeoclimate that can be tested or verified by Pliocene data (Haywood *et al.*, 2000; Haywood *et al.*, 2009a). As outlined in Chapter 1 (1.2.2). the Pliocene Research, Interpretation and Synoptic Mapping (PRISM) project was developed to collect data that could be used to evaluate model reconstructions of the mid Pliocene (Dowsett and Robinson, 2009; Dowsett *et al.*, 2009b; Dowsett *et al.*, 2012). PRISM sea surface temperature (SST) data has been gathered between 3.025 and 3.260 Ma (Dowsett *et al.*, 2012). PRISM SST maps are produced by identifying the three temperature maxima during the 3.0-3.3 Ma time period for each core site, and then averaging them in order to avoid the influence of Pliocene cold periods and to target the warmest signal of Pliocene climate (Figure 5.1) (Dowsett *et al.*, 2012). The current PRISM dataset includes 95 individual sites from both the terrestrial and oceanic environments (Figure 1.2) (Dowsett *et al.*, 2012). Despite the size of the data set, there are still critical areas of the Earth that have yet to be added to the PRISM data set.
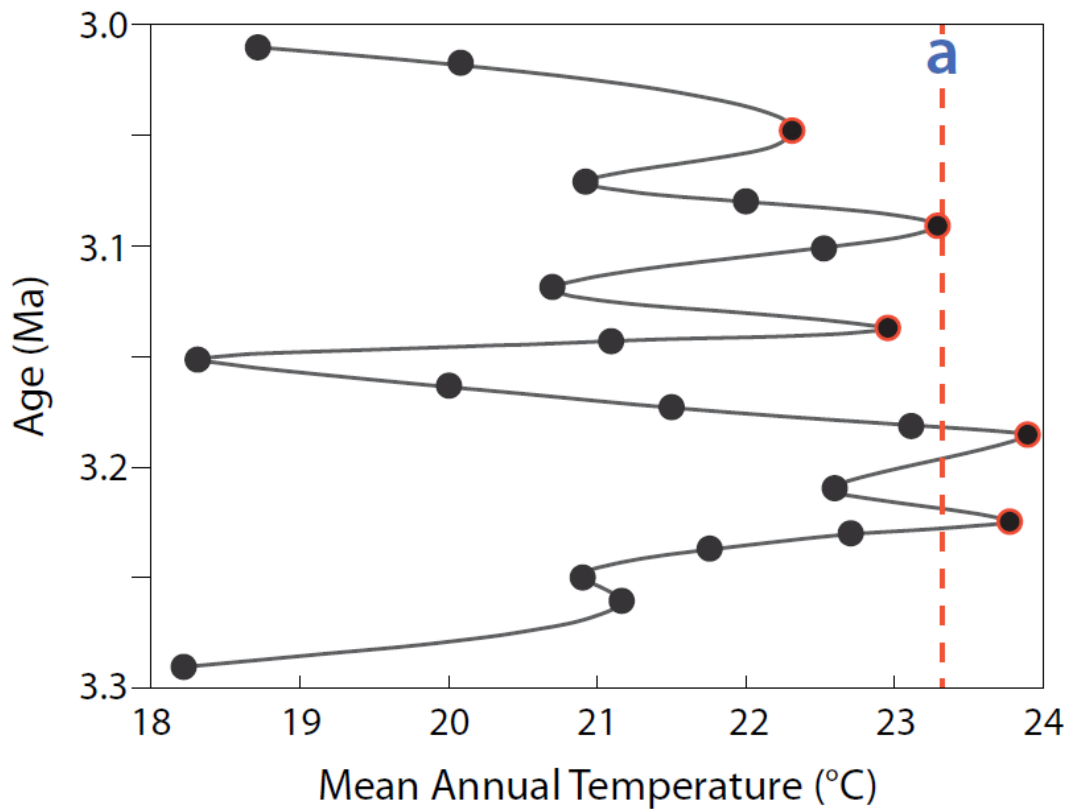
**Figure 5.1. PRISM warm-peak average SST example**. An idealised time series of mean annual temperature estimates is plotted and warm peaks are identified. Peaks are averaged to develop a warm peak average (WPA) temperature estimate (a). The WPA temperature thus represents the warm phase of climate at a single locality, within the PRISM time slab. (Dowsett *et al.*, 2012)

The aim of this Chapter is to describe the MPWP record from ODP 1087A to understand how the important southeast Atlantic gateway region operated during the globally warmer Pliocene climate (Figure 5.2). It is not yet understood how the major oceanic systems of the SE Atlantic, such as the southern part of Benguela upwelling, the Agulhas Leakage and the Antarctic Intermediate Water, behaved during the warmer conditions.
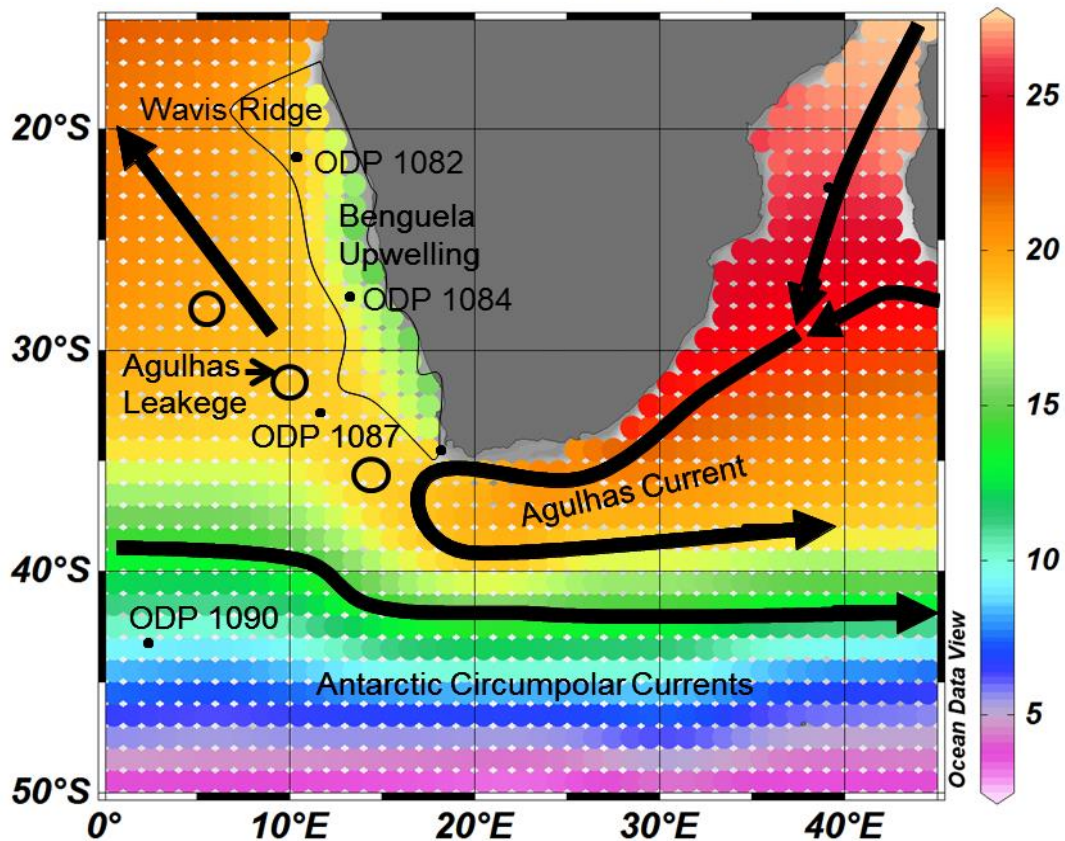
**Figure 5.2 Location map.** Showing the location of the core site (ODP 1087) on a SST map (World Ocean Atlas 2001, Ocean Data View mapping program). The location of local Pliocene records and the location of major oceanic systems in their modern day positions are shown.

Fine fraction carbonate $\delta^{18}O$ ($\delta^{18}O_{FF}$) records the temperature of the water and salinity, and has previously been used in the southeast Atlantic to create a high-resolution age model record of a single glacial-interglacial transition (Dickson *et al.*, 2010b). The $\delta^{18}O_{FF}$ signal primarily reflects coccolithophore carbonate and therefore can be related to the alkenones because they are formed by the same source. The benthic $\delta^{18}O$ records incorporate changes in global ice volume and water temperature. Changes in the planktonic $\delta^{13}C$ have been interpreted to be related to changes in the nutrients in the upper water levels and benthic $\delta^{13}C$ is reflected as changes in $CO_2$ and oxygen in the intermediate water bodies (Pierre et al. 2001). As a result, $\delta^{13}C$ data sets can be related to the relative influence of different water bodies, which have different amounts of $CO_2$ which effect the $\delta^{13}C$ affecting the core site(Pierre et al. 2001). Additionally the Benguela upwelling is thought to have high levels of nutrients and

lower $\delta^{13}C$ values (Pierre *et al.*, 2001).   For a more detailed explanation of methods and methodology see chapter 3 and 4.

## 5.2. Results

Results are presented for the interval between 3.0 to 3.5 Ma. As discussed in Chapter 4 (section 4.2.1), samples were taken between 137 to 169 mbsf at approximately 20 cm spaces. Given the age model which has a uncertainty of 4 ka (section 4.2.1), the average temporal resolution of the samples is 4 ka for alkenones and pigments, and 12 ka for foraminifera stable isotopes.

### *5.2.1 Temperature*

The $U^{K}_{37}$' values between 3.0 and 3.5 Ma range between 0.59 and 0.83, converted to an SST range of 17 to 22.5 °C (mean SSTs at 21 °C)  using the Müller, *et al* (1998) calibration (Figure 5.3). There are two prominent cold periods in the record. The first occurs between 3.32 and 3.26 Ma, when SSTs are between 16.5 and 19 °C. This temperature drop occurs during the M2 stage one of the most prominent stadials (Figure 5.3).   The second major period with lower temperature occurs between 3.15 and 3.10 Ma, with SSTs ranging between 18 and 21 °C.  The timing of this period is associated with the KM2 MIS.

Two variations of the $TEX_{86}$ proxy ($TEX_{86}$ and $TEX^{H}_{86}$) were used to calculate temperatures. $TEX^{L}_{86}$ was not used because the predicted lowest temperatures did not fall within the rage recommended for using the $TEX^{L}_{86}$ Between 3.0 and 3.5 ma values range between 0.45 to 0.49 and the temperature range for $TEX_{86}$ from 13 to 17 °C with a mean of  15 °C while $TEX^{H}_{86}$  ranged from 14 to 17.5 °C with a mean of 15 °C.  The record shows two cold periods at 3.4 and 3.3 (during M2 stage).  The difference between the two formulas is usually less than 1 °C therefore for the rest of the thesis the original $TEX_{86}$ index is used unless there is a significant difference of more than 1 °C between temperatures.
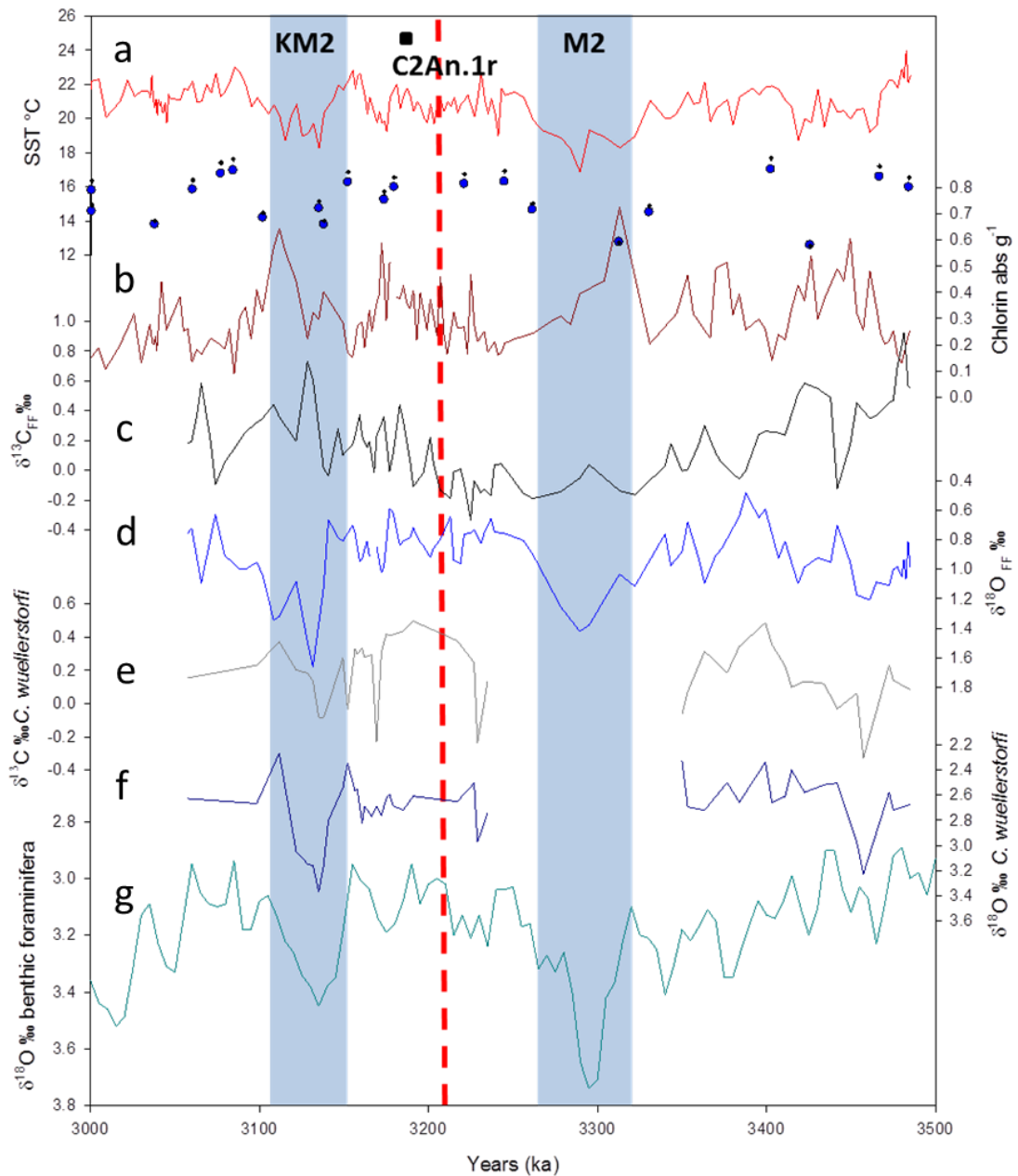
**Figure 5.3 Mid Pliocene SST, pigments and isotopes from ODP 1087 plotted against the new benthic δ18O stratigraphy.** The two major cold periods are marked in the records by blue bars. a) $U^K_{37}$' SSTs, calculated using the calibration of Muller *et al.* (1998); $TEX_{86}$ (blue diamonds) and $TEX^H_{86}$ (blue crosses) determined using calibration of Kim *et al.* (2010) b) Chlorin pigment concentrations are defined by the amount of absorbance per gram of original sample weight. ; c) $δ^{18}O_{FF}$; d) $δ^{13}C_{FF}$. e) benthic $δ^{13}C$ from *C. wuellerstorfi* ; f) record of benthic $δ^{18}O$ from *C. wuellerstorfi*, re-tuned to the LR04 global benthic $δ^{18}O$ stack (Lisiecki and Raymo, 2005). g) LR04 global benthic δ18O stack. At the bottom the location of the 3.3 Ma C2An. 1r magnetic reversal is marked in the record.

### 5.2.2 Chlorins

Total chlorin concentrations range between 0.1 and 0.75 absorbance units $g^{-1}$ (Figure 5.3). The lowest pigment values are 0.088 abs $g^{-1}$ at 3.85 Ma. The highest pigment values are 0.73 abs $g^{-1}$ and occur at 3.3 Ma during the M2 MIS. A second strong pigment peak occurred at 3.11 Ma. There are short-lived intervals of high pigment concentration, at 3.47-3.41 Ma, 3.39-3.27 Ma, 3.23-3.16 Ma, 3.15-3.09 Ma and 3.060-3.017 Ma. These peaks in chlorin concentration often correspond with colder periods in the temperature record.

### 5.2.3 Stable isotope records: fine fraction and benthic foraminifera carbonate

The $\delta^{18}O_{FF}$ ranges between 1.66 and 0.5 ‰ (Figure 5.3). The mean $\delta^{18}O_{FF}$ is 1.0 ‰ with a maximum of 1.6 ‰ and a minimum of 0.48 ‰. There are two increases in $\delta^{18}O_{FF}$ centred on 3.3 and 3.1 Ma, where $\delta^{18}O$ exceeds 1.4 ‰. The mean $\delta^{13}C_{FF}$ is 0.15 ‰ and the maximum is 0.93 ‰ and minimum -0.33 ‰. The $\delta^{13}C_{FF}$ shows a long-term decrease by 1 ‰ from 3.5 to 3.3 Ma. The $\delta^{13}C_{FF}$ values then increase by about 0.7 ‰ from 3.3 to 3.0 Ma.

The benthic $\delta^{18}O$ shows broadly similar trends (Figure 5.3). There is a major positive isotope excursion centred on 3.1 ma of 1 ‰. There is also another positive excursion at 3.45 Ma of 0.6 ‰. The lack of *C. wuellerstorfi* preserved in the benthic record around 3.3 Ma causes a lack of data for 115 ka.

### 5.2.4 Planktonic foraminifera assemblages

The planktonic foraminifera record can be divided into two parts, before and after 3.241 Ma (Figure 5.4). In the first part (3.47 to 3.24 Ma), the majority of the identified planktonic foraminifera are *Globigerinoides bulloides*, which is always either "abundant" or "dominant", and *Globigerina inflata*, which is mainly classified as "abundant". The only time when these two species do not dominate the planktonic foraminifera assemblage is in the sample dated 3.25 Ma; here, *G. inflata* is classified as "rare" although *G. bulloides* is still abundant. In contrast to the other samples, *Neogloboquadrina pachyderma (sinistral)* is abundant in this sample, although it is usually less than 10% of the assemblage (few or rare abundance) for the Pliocene samples analysed here.
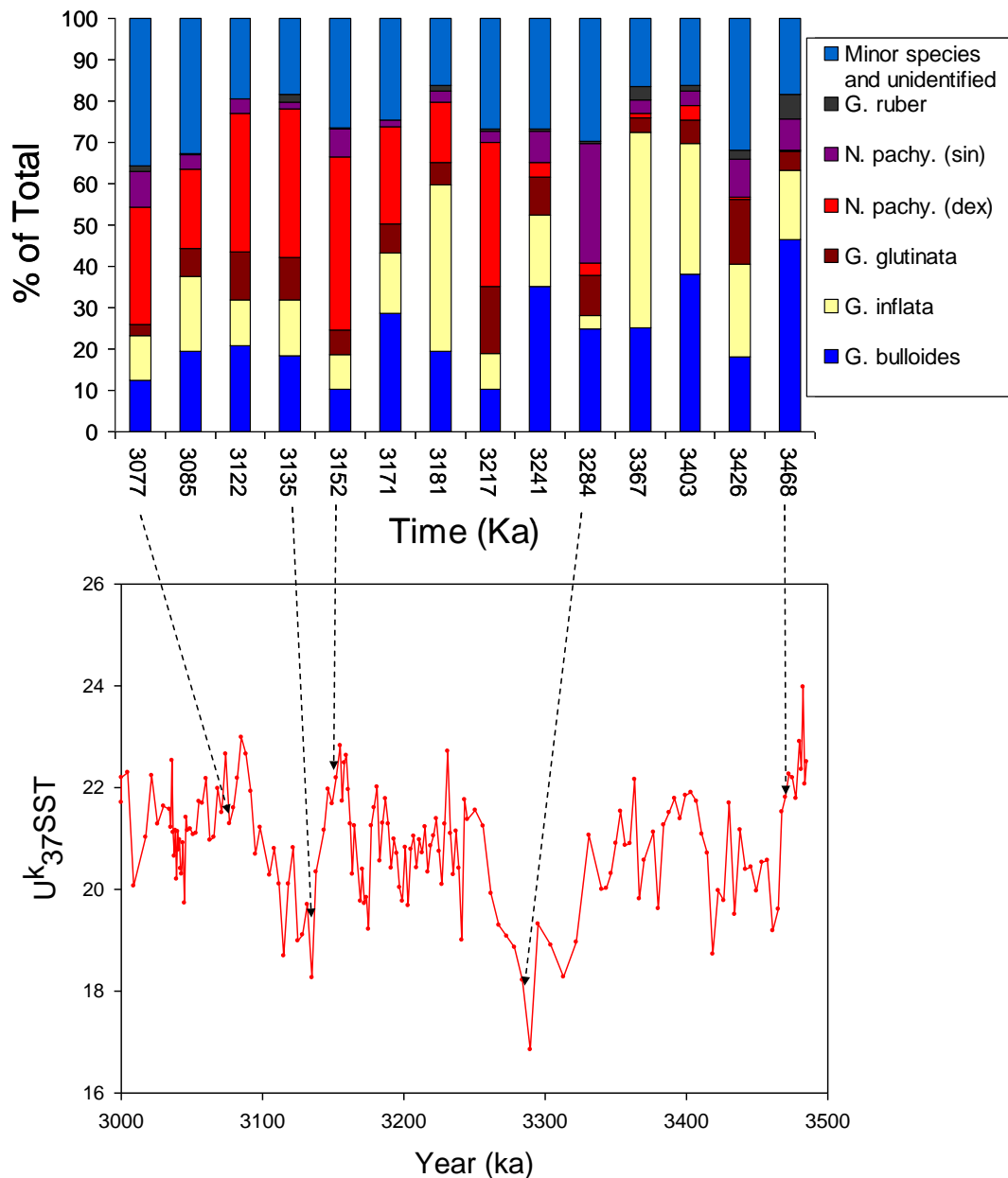
**Figure 5.4 Planktonic foraminifera record of the Pliocene**. Top: the major foraminifera species, presented as percentages of the total number of tests counted in sample. The arrows indicate where the samples are taken on the $U^K_{37'}$ temperature record (bottom).

After 3.22 Ma, the majority of foraminifera are comprised of *G. bulloides*, *G. inflata,* and *N. pachyderma (dex)*. The abundant or dominant classification of *N. pachyderma (dex)* contrasts with its much lower inputs to the assemblage prior to 3.241 Ma. Minor contributions from several other species are noted throughout the Pliocene. *Globigerinoides ruber* comprises of less than 5% of the Pliocene assemblage except in the earliest sample. A small number of warm water, Indian Ocean, species (Peeters *et al.*, 2004) occur in the Pliocene record from ODP 1087: *Globigerina falconensis* is

present throughout, but is usually categorised as few (<5%). There are 7 samples where *Globorotalia menardii* are identified, although there are never more than 4 individuals per sample. *G. menardii* is another important Indian Ocean warm water species, and has been identified in ODP site 1087 and other SE Atlantic sediment cores during the late Pleistocene (Peeters *et al.*, 2004; Sexton and Norris, 2011; Caley *et al.*, 2012).

## 5.3. Discussion

### 5.3.1 Pliocene conditions at stie  ODP 1087

At ODP 1087, the mid-Pliocene is marked by an overall absence of any long term trends in SST, surface and bottom water $\delta^{18}O$, $TEX_{86}$ or chlorin concentrations. Only the $\delta^{13}C_{FF}$ shows a long-term decrease to a minimum at 3.3 Ma before gradually increasing to 3.0 Ma. All other proxy indicators are composed of a series of oscillations about a stable mean. In general, the relationships between the records shown in Figure 5.2 are as follows: higher SST ($U^{K}_{37}$' and $TEX_{86}$) is usually associated with low chlorin concentrations, and lower $\delta^{18}O_{FF}$ and benthic $\delta^{18}O$ . Periods of lower SST ($U^{K}_{37}$' and $TEX_{86}$) are associated with higher chlorin concentrations and lower $\delta^{18}O$ in surface waters and in the benthic $\delta^{18}O$. This suggests connections between the different proxies but not necessary a 1:1 relationship.

### 5.3.2 Evaluating the PRISM interval

The potential ocean circulation processes responsible for the observed changes in site ODP 1087 during the Pliocene are discussed below. First, the resolution of the SST data sets presented here enables a comparison of Pliocene SST anomalies with those predicted and constructed as part of the PRISM programme. The overall average $U^{K}_{37}$' SST temperature during the Pliocene is 1 °C warmer than the present day using the warm peak averaging approach definition given by the PRISM project. A Pliocene warm anomaly of 1 °C is consistent with the extrapolated data given by the PRISM reconstruction for the southeast Atlantic, as well as with the PRISM modelling experiments, both of which indicate a Pliocene SST anomaly of 1 ºC for the region of ODP 1087 (Dowsett *et al.*, 2012). A closer examination of the ODP 1087 record shows some problems with using the PRISM method to define Pliocene SSTs. The PRISM

method uses the highest three temperatures during the 260 ka PRISM time slab and then averages them to determine the average warm temperature of the site (Dowsett *et al.*, 2012). However, the new data presented here for ODP 1087 show that the three warmest periods of the PRISM interval are often short lived, the shortest of which lasted only 8 ka. These three SST maxima are at least 1.5 °C warmer than the average temperature of the Pliocene, not including the two cold periods of the M2 and KM2. Applying the PRISM methodology thus gives a misleading over-estimation of overall Pliocene warmth at ODP 1087, because the three-point average does not reflect the amount of variability in this higher resolution record.

As a result, with the emergence of higher resolution reconstructions for the Pliocene, such as that presented here, the PRISM approach may no longer be valid because it causes a bias towards warm extremes, which may not be representative of overall climate state and climate variability. Furthermore, the time-averaging approach for PRISM data sets has recently been challenged (Haywood et al., 2013). This is because it is becoming clear that both the models and the emerging higher resolution data sets are increasingly showing evidence for orbital scale variability in Pliocene climate, which isn't taken into account in the time-averaging approach of creating the PRISM data sets. Haywood et al. (2013) argue that higher resolution analyses are required to pinpoint a more focussed time window for analysis (a "time slice"), which can be compared to better constrained climate model simulations. They have suggested using a time slice centred on 3.205 Ma BP (3.204 to 3.207 Ma BP). The new data presented here for site 1087 marks one of the few high resolution data sets available which can immediately contribute to this new approach.  Using the time slice approach to analyse the record yields a temperature of 20.7°C.  Given the average temperatures of the Pliocene are ~21°C, this represents a better estimate of temperature in this high resolution record than the old PRISM model.


### 5.3.3 Benguela Upwelling vs. Agulhas Leakage at Site 1087

ODP Site 1087 is located offshore of the southern Benguela upwelling cells at the present day. This location, in combination with the influence of Agulhas Leakage, keeps the site warmer and less productive than the main Benguela upwelling cells to the north.  In the Pliocene, SSTs at site 1087 are warmer than present (as discussed above), which could imply increased Agulhas Leakage of warm waters into the SE Atlantic

during the Pliocene. However, in comparing the SST record at ODP 1087 to those from the northern and central part of the Benguela upwelling (Marlow *et al.*, 2000; Etourneau *et al.*, 2009) between 3.0 and 3.5 Ma, shows that Mid-Pliocene SSTs at ODP 1087 are colder than both ODP 1082 and ODP 1084, which lie beneath the northern edge and central cells of the upwelling at the present day (Figure 5.5) (Marlow *et al.*, 2000; Etourneau *et al.*, 2009). This is the reverse of the modern situation, and is an unexpected scenario if the Agulhas Current and its leakage were more vigorous during the mid-Pliocene, as has been predicted under globally warmer conditions accompanied by a southward movement of the circumpolar currents (Bard and Rickaby, 2009), and a less vigorous Benguela upwelling (Etourneau *et al.*, 2009). The relatively cool SSTs observed at ODP 1087 indicate that there was not a contribution of warmer water affecting the site as is the case during periods of increased Agulhas Leakage (Figure 5.5) (Peeters *et al.*, 2004). Furthermore, two species of primarily Indian Ocean foraminifera also occur in low abundances during the mid-Pliocene: *G. falconensis* (rare/present) (used to identify Agulhas Leakage by (Peeters *et al.*, 2004)) and *G. menardii* (rare/present) (Figure 5.4). The latter species is particularly important because it is considered to be indicative of Agulhas Leakage during the late Pleistocene for ODP 1087 (Caley et al. 2012). *G. menardii* is present (but rare) during the Pliocene at ODP 1087 during times of lower pigment concentrations and inferred lower primary productivity. The mid-Pliocene data from ODP 1087 thus suggests a reduced influence of Agulhas Leakage to the SE Atlantic. One possible explanation is that Agulhas Leakage occurred but is not recorded at ODP 1087 because it was located further to the south overall. This might explain, for example, the rapid fluctuations in SST and chlorin concentrations which occur over tens of thousands of years (Figure 5.3) and which could represent sensitivity to short lived migrations north or pulses of enhanced Agulhas Leakage over ODP 1087. On the other hand there is a number of other explanations including changes in the assemblage, On the evidence presented here, however, weaker Agulhas Leakage during the mid-Pliocene suggests that the theory that the vigour and scope of the Agulhas current has increased gradually since the Miocene to the Pleistocene might be valid (Diekmann *et al.*, 2003).
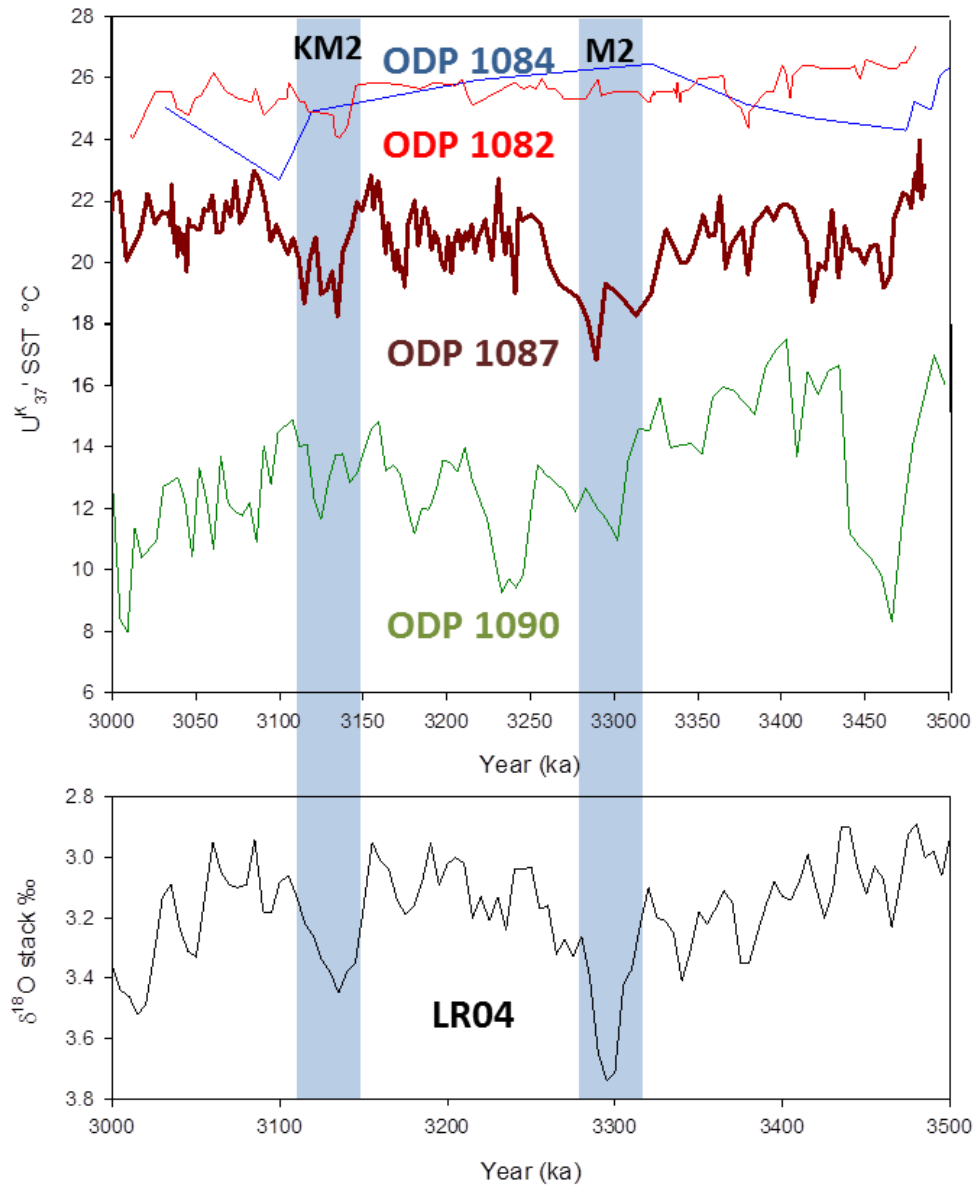
**Figure 5.5. Mid Pliocene SSTs in SE Atlantic.** Top: U$^K_{37}$' SST records from the Benguela Upwelling (Red), 1082 (Etourneau *et al.*, 2009) (blue), 1081 (Marlow *et al.*, 2000) and dark red) 1087 (This study) 1090 (Dark green) (Martinez-Garcia *et al.*, 2011) Lower: (Black) LR04 Benthic stack (Lisiecki and Raymo, 2005). Blue bars represent cold MIS.

The absence or weak influence of Agulhas Leakage at site 1087 during the Pliocene means that the oceanographic regime in the southeast Atlantic then was different from the modern one.  In particular, the position and intensity of the Benguela upwelling system might have been different, as reflected in the presence of relatively cold SSTs at site 1087 (compared to sites 1084 and 1082) (Figure 5.5).  These patterns indicate the entire southern Benguela region shared surface ocean properties in the Pliocene warm period.

Additionally, there is the offset of the $TEX_{86}$ temperatures with the $U^K_{37}$ temperatures.  Studies have shown there is an offset of $TEX_{86}$ with $U^K_{37}$ when there is upwelling occurring in the Benguela Upwelling (Lee *et al.*, 2008).  In the upwelling cells, the $TEX_{86}$ is being produced lower in the water column than the $U^K_{37}$' SST because there are nutrients available for the production of $TEX_{86}$.  The pigments are higher during the cold SST periods and lower during the warmer SST, suggesting a connection between colder waters (more intense upwelling) and higher primary productivity (another indication of upwelling).

The micro-paleontological evidence also supports the interpretation the Benguela upwelling was more vigorous in the southern Benguela region during the mid-Pliocene.  The dominant foraminifera species are *G. inflata* and *N. pachyderma (dex),* which are prominent in the modern Benguela upwelling system (Lee *et al.*, 2008).  *G. inflata* is indicative of the outer edges of the upwelling (Groeneveld and Chiessi, 2011), while *N. pachyderma (dex)* is found in the filaments produced by seasonal upwelling around the permanent upwelling cells (Figure 5.4) (Ufkes *et al.*, 2000; Ufkes and Kroon, 2012). In combination, the temperature, pigment and foraminifera assemblage data sets indicate that, during the Pliocene, the Benguela upwelling was more vigorous at ODP 1087 than in either the late Pleistocene or in the modern era.


### 5.3.4 Changes in the Southeast Atlantic during the Pliocene

Based on all of these proxies, a reconstruction of the southeast Atlantic is possible, drawing on the patterns of SST and chlorin concentration changes, as well as the planktonic foraminifera assemblages present in selected time intervals. The evidence from ODP 1087 is also compared to data from sites that are considered to be under the main central and northern upwelling cells at the present day, ODP 1082 and 1084.   It has been argued by other authors the northern and central upwelling cells developed at

the time of the Pleistocene-Pliocene transition, around 2.0 Ma (Etourneau *et al.*, 2009; Etourneau *et al.*, 2010), because there is an increase in both temperature and productivity at this point.

In contrast, the new data presented here for ODP 1087 suggests that the southern part of the Benguela Upwelling was already in place before 3.5 Ma (Figure 5.5). The evolution of the Benguela Upwelling saw the development of more complex seasonal upwelling filaments based on the increase in *N. pachyderma (dex)* which is characteristic of this part of the upwelling system in addition to the more permanent cells that existed before this that have continued to be an important component of the southern upwelling cell today. Finally, the SSTs at ODP 1087 for the Pliocene and early Pleistocene are consistently below those of the Benguela sites to the north; this is interpreted to indicate either a weaker or absent Agulhas Leakage to this site and/or a shift southwards of the Agulhas Leakage, away from our study site, during the MPWP. The evidence presented here for an influence of Benguela upwelling at ODP 1087 during the Pliocene is in contrast to earlier studies that have assumed there was little to no Benguela upwelling occurring before 3 Ma (Fedorov *et al.*, 2006; Fedorov *et al.*, 2010).

Given both Benguela Upwelling and the Agulhas Leakage are wind driven systems (Boudra and De Ruijter, 1986; Hutchings *et al.*, 2009), the differences in circulation identified here for the Pliocene suggest a change in the wind patterns in the Southern Hemisphere might be responsible. Today, the trade winds only affect the southern part of the Benguela upwelling during the summer, whereas perennial upwelling dominates the central and northern Benguela regions (Andrews and Hutchings, 1980). This means that that the central upwelling cells are much bigger than the southern cells and extend further out where as the southern cells are smaller so do not effect as far out as Site ODP 1087. However, during the mid-Pliocene, it has been argued that, based on temperature gradients across important boundaries in the Pacific Ocean, the Hadley cells were expanded 3-4 degrees of latitude southward and also strengthened (Brierley *et al.*, 2009a; Etourneau *et al.*, 2010). An expansion southward of 4-5 degrees latitude could have shifted the seasonal trade winds so they were effectively permanently over the southern Benguela region. One impact of a southward displacement of the trade winds may therefore have been a southward shift of the point of the Agulhas Leakage retroflection, as well as an influence of the Benguela upwelling to ODP 1087. However, to fully test this hypothesis requires the identification and

analysis of sediments situated to the south of ODP 1087, which may capture any evidence of Agulhas Leakage during the Pliocene.

### *5.3.5 Cold MIS (M2 and KM2) in the Pliocene*

The M2 stage contains two minima in SSTs and maxima in fine fraction $\delta^{18}O$. After the initial cooling at 3.31 Ma, where temperatures lower from 21.0 ℃ to 18.3 ℃+/- 1 ℃ , and which was associated with very high pigment concentrations, there was a short-lived (8 ka) warming (19.3 ℃) at the core site, followed by a second cooling at 3.29 Ma (16.0 ℃) but no corresponding increase in pigments. As a result, the early and late parts of the M2 glacial stage have different properties in the surface ocean at ODP 1087 (Figure 5.5). This two-phase structure of the M2 glacial has been identified previously in benthic $\delta^{18}O$ records but not many temperature records (Lisiecki and Raymo, 2005). One cause of the isolated evidence for this two-phase structure of the M2 glacial stage could be a scarcity of records with the temporal resolution needed to record oscillations within the overall duration of the cold stage (~40 ka) (Figure 5.5).

At ODP 1087, the M2 glacial stage is unusual compared to isotopic excursions during the Pliocene because it is marked by a major increase in the amount of *N. pachyderma (sin)* in the planktonic foraminifera assemblage (Figure 5.4). *N. pachyderma (sin)* has been found in the heart of the permanent upwelling cells as opposed to *N. pachyderma (dex)* which is found on the outer edge of the upwelling cells (Ufkes *et al.*, 2000; Lee *et al.*, 2008; Ufkes and Kroon, 2012). It has been used as an indicator of small scale cold events in the northern Benguela Upwelling during the late Pleistocene (Little *et al.*, 1997). Contributions to the planktonic assemblage exceeding 10% of *N. pachyderma (sin)* have only been seen in ODP 1087 once during the late Pleistocene (Giraudeau *et al.*, 2001). As *N. pachyderma (sin)* is associated with very cold/polar waters, its increased dominance suggests that there was a major expansion or shift in the position of the Benguela upwelling cells during the M2 glacial stage. Furthermore, the M2 glacial stage marks a shift in presence of *N. pachyderma (dex)* at ODP 1087: it was a minor component of the planktonic foraminifera assemblage before M2, after the M2 (and during the late Pleistocene) this species dominates the assemblage (Giraudeau *et al.,* 2001). This is likely a signal of the expansion of seasonal upwelling filaments in the southern Benguela region (Lee *et al.*, 2008). As a result, the MPWP is marked by an increase in the complexity of the southern Benguela

upwelling system, from a potentially smaller but more permanent upwelling system initially to one with a stronger seasonal component after the M2 glacial stage.

Finally, the M2 glacial stage is unusual because this cooling seen at ODP 1087 is not seen at other southeast Atlantic records. The records [ODP 1082 and 1084] from the southeast Atlantic show no cooling event and temperatures between 25 and 26 ºC (Marlow *et al.*, 2000; Etourneau *et al.*, 2009) (Figure 5.5). This could be for a number of reasons. First, it could be a lack of a high enough resolution to see the M2 event at other cores in the area, although this doesn't seem to be the case for ODP 1082 which has a record with a similar resolution to ODP 1087 for this specific time window. It could also be the records are not aligned properly because of errors in the age model of the other records. There is a cooling event in the ODP 1090 SST record at ~3.4 Ma that has a pattern that could be interpreted as an M2-like event although there is no evidence for changes at the 3.3 Ma date (Figure 5.5). However, the lack of a similar cooling seen in any other local sites suggests that most of the rest of the southeast Atlantic Ocean and Southern Ocean do not experience an M2 event of similar magnitude as in the ODP 1087 record.

Given the local nature of the cooling seen at ODP 1087, there are a number of hypotheses for the cause of the localised cooling. It could be evidence of a southward shift of the trade winds changing the locus of upwelling, a shift in the local winds causing the water from the central part of the upwelling to expand over the site (both of which involve a shift in the winds altering the upwelling system) or a cooling of the intermediate waters in the upwelling. There is good evidence of a shift in the winds at the M2 stage. The planktonic foraminiferal evidence shows that during the M2 there is good evidence for perennial upwelling waters reaching the site. Finally there is a rise in pigment values to their highest values during the Pliocene M2 which also display evidence of the expansion of the upwelling cells at this time. This matches an increase in TOC seen at the same time. Therefore it means that it is likely that the cooling seen was partially a result of a shift in the local wind systems, forcing central upwelling waters over the ODP 1087 site. However, given the magnitude of cooling seen in the ODP 1087 it is impossible to completely discount the idea there was no cooling of the subsurface upwelling waters as well as a shift in the winds systems. This is especially true of the second cooling within M2 which sees temperatures cool with a much lower chlorin peak suggesting that changing winds were not increasing productivity as much

during this period although there is some evidence from other areas that changes in the upwelling can be decoupled from temperature and wind changes (Dekens *et al.*, 2007a).

The second cold interval marked in the record is KM2 at 3.13 Ma (Figure 5.5). The SST record for KM2 has a number of warming and cooling events similar to the M2 records. The chlorin data also shows one of the drops in temperature is associated with higher chlorins like M2. However the other proxy records do not show the same response to the KM2 glaciation. $\delta^{13}C_{FF}$ shows however instead continues increasing. Further, the planktonic foraminifera assemblage does not react at all to the cooler temperatures like they did during the M2 where they saw major changes in the species found. Lastly, there is a more structure to this glacial than the M2 stage in that it contains a number of warming events. One of these at 3.21 Ma sees a short-lived (8 ka), nearly complete recovery of the temperature after the end of the KM2 stage. These patterns suggest that the KM2 stage was a multistage cooling event much like the M2 stage. At the same time the degree of cooling was similar to the M2 glaciation even without the same level of change in the proxies for the winds and nutrients. It suggests that for the KM2 stage there is a decoupling between changes in the wind patterns, changes in nutrients and changes in temperature.

When comparing the KM2 signal at ODP 1087 to other local records, there is a lack of evidence of a prominent KM2 cooling event in the rest of the Southeast Atlantic Ocean, as was also observed for M2 (Figure 5.5). In addition the benthic $\delta^{18}O$, which has a small gap at 3.1 Ma, shows a strong isotope excursion at KM2 stage. Furthermore, when comparing to the excursion seen in ODP 1087, LR04 shows the excursion is greater in ODP 1087 with negative excursion of 0.4 ‰ in LR04 compared to an excursion of 1 ‰ in ODP 1087. It is thought the major driver of changes in the benthic $\delta^{18}O$ is temperature so it is likely there was a cooling in the bottom waters at ODP 1087 that exceeds the cooling seen in the global records. A cooling of the upwelling waters also might explain the disappearance of *C wuellerstorfi* during M2 and (briefly) at KM2. If the bottom waters are cooling, they would carry less oxygen. C. *wuellerstorfi* has been shown to be susceptible to reduction in oxygen (Boltovskoy, 1983). However this may also be dissolution due to changes in carbonate content. Therefore, there is some suggestion a cooling of the upwelling occurred at ODP 1087 during the KM2 stage.

It has been speculated, based on changes seen in the terrestrial Antarctic records (McKay *et al.*, 2012) and records from benthic $\delta^{13}$C (Billups *et al.*, 1998) and dust and opal concentrations (Martinez-Garcia *et al.*, 2011) there was an expansion of Antarctic sea ice at 3.3 Ma during the M2 MIS. This is based on reductions of biogenetic opal and a hypothesized slowdown of AMOC because of the decrease in Southern Ocean $\delta^{13}$C (Billups *et al.*, 1998). Based on this, McKay proposes there should be a strengthening and cooling of Antarctic Intermediate Water (AAIW), which upwells at the ODP 1087 around 3.3 Ma (McKay *et al.*, 2012). Therefore there is some evidence for change in the deep water that may be related to AAIW based on the evidence of changes seen in the intermediate waters that upwell at the site. The problem is there is no temperature data available for the Antarctic Intermediate waters (AAIW) are upwelling at ODP 1087. In order to understand these changes better future work needs to concentrate on developing bottom water temperature reconstructions. This would allow a direct measurement of the AAIW which bathes the site and see whether it is cooling during the M2 stage. While this cannot be proven there is strong evidence that the cooling of AAIW in during both M2 and KM2.

## 5.4 Conclusions

The aim of this chapter was understand how the ocean circulation of the southeast Atlantic Ocean changed under warmer conditions that are thought to be similar to those of future climate change. This was assessed using proxies for SST reconstruction ($U^{K}_{37}$'), primary productivity (surface isotopes, foraminifera, TEX$_{86}$ and chlorins), and bottom water conditions (Benthic isotopes). The data shows that SSTs remained stable and were higher than modern. Finally, $U^{K}_{37}$' SST's were lower by 5-6°C than other records from the modern Benguela upwelling. The data at 1087 thus suggests that the pattern of ocean circulation in the southeast Atlantic was different from the modern, with Benguela upwelling having shifted southward and a weaker Agulhas Leakage that does not affect the site at all. Finally, there is possible cooling of intermediate waters during both the M2 and KM2 stages which could suggest intensification and cooling of AAIW at the site during the Pliocene. The implications of these findings for understanding Pliocene climates will be discussed further in Chapter 7.

# Chapter 6:  The Pliocene-Pleistocene transition in the Southeast Atlantic Ocean

## 6.1 Introduction

In Chapter 5, the ocean circulation patterns of the southeast Atlantic Ocean during the mid-Pliocene warm period (MPWP) were discussed. After the MPWP, a series of major climate transitions occurred as the Earth shifted towards a climate state dominated by the large amplitude glacial-interglacial cycles of the last 0.9 Ma of the Pleistocene (Chapter 1). Although it is known that there was an overall shift from warmer to cooler global climates after 3 Ma (Jansen *et al.*, 2000; Bartoli *et al.*, 2005; Sosdian and Rosenthal, 2009; Etourneau *et al.*, 2010), there is still a debate as to why the Pliocene-Pleistocene shift occurred. Different theories include a gradual drawdown of atmospheric $CO_2$ (Lawrence *et al.*, 2010), a response to increased chemical erosion of the lithosphere (Raymo, 1994), more vigorous upwelling (Ravelo *et al.*, 2004), closing of the straits of Panama (Bartoli *et al.*, 2005) or/and the onset of northern hemisphere glaciation (Lawrence *et al.*, 2009).

The aim of this Chapter is to understand whether the shift to a colder climate affected the Southeast Atlantic Ocean, and if so, when?  In Chapter 4, a number of lines of evidence indicated that during the Pliocene there had been a southward shift of the Benguela upwelling cells relative to the modern, and there was evidence for reduced inputs of warm and saline waters via the Agulhas Leakage to the SE Atlantic. This chapter will assess when the transition(s) to the modern pattern of ocean circulation occurred. Two temperature proxies ($U^K_{37}$', $TEX_{86}$) were used to determine the change in the ocean temperatures at ODP 1087. Chlorins were used to understand changes in primary productivity.  Finally, higher plant leaf waxes (*n*-alkane) proxies were used determine  changes in the amount of terrestrial sediment input into the Southeast Atlantic Ocean and  to understand changes in the origin of sediment input and what this means for changes in the winds around the southeast Atlantic.

ODP 1087 can help answer key questions about the timing and location of the initial cooling at the mid-latitudes.  Some researchers have suggested the initial cooling is linked to the initial glaciation of the northern hemisphere, which has been timed at 2.7 Ma (Ruddiman *et al.*, 1989; Flesche Kleiven *et al.*, 2002; Kleiven *et al.*, 2002; Raymo *et al.*, 2004; Haug *et al.*, 2005; Mudelsee and Raymo, 2005; Lawrence *et al.*, 2009; Meyers and Hinnov, 2010; Bartoli *et al.*, 2011).  It has also been suggested the higher latitudes only show increased sensitivity to insolation forcing after the establishment of upwelling at 2.0 Ma at the lower and mid-latitudes and overall the transition was gradual with no one forcing (Ravelo *et al.*, 2004).  Recently, an analysis of the ODP

1090 $U^K_{37}$' record has suggested changes in the southeast sub-Antarctic region during the Plio-Pleistocene shift happened synchronously with the emergence of the Pacific cold tongue, which occurred around 1.8 Ma (Martinez-Garcia *et al.*, 2010). ODP 1087 is located at a mid-latitude site and affected by changes in the trade winds; it has the potential to shed light on major questions about the timing and the mechanisms behind the transition from the Pliocene to the Pleistocene both globally and localy.

## 6.2. Results

### 6.2.1 $U^K_{37}$'-SSTs

A low resolution record of $U^K_{37}$'-SSTs was initially produced by Mathew Clarkson (unpublished Masters Thesis, 2010, University College London) (Clarkson, 2010). Here, the resolution of this record was enhanced through the addition of an average of 2 samples between each of Clarkson's (Figure 6.1). The maximum $U^K_{37}$'-SST between 3.0 and 1.5 Ma is 22.8 ℃ at 2.88 Ma, and the minimum is 15.8 ℃ at 1.96 Ma (Figure 6.2). The mean SST decreases through time, from 21.0 ℃ at 3.0 Ma to 18.0 ℃ at 1.5 Ma.
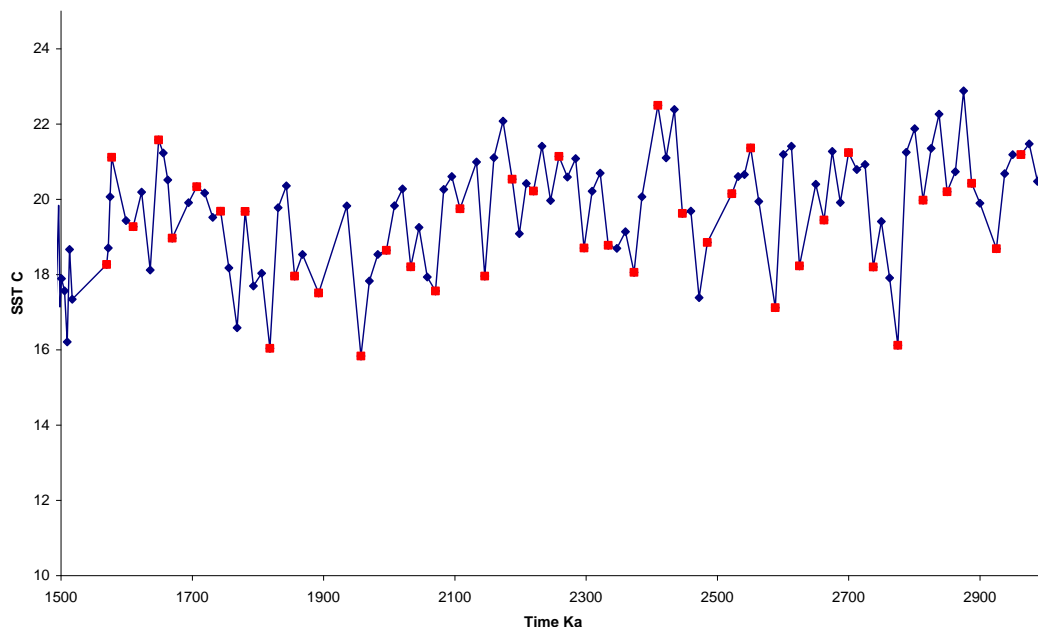


**Figure 6.1 SST Record showing samples taken by Clarkson.** $U^K_{37}$' Samples taken by Mathew Clarkson at the University college of London for his masters project are indicated by red squares and additional samples collected for this thesis indicated by blue diamonds.
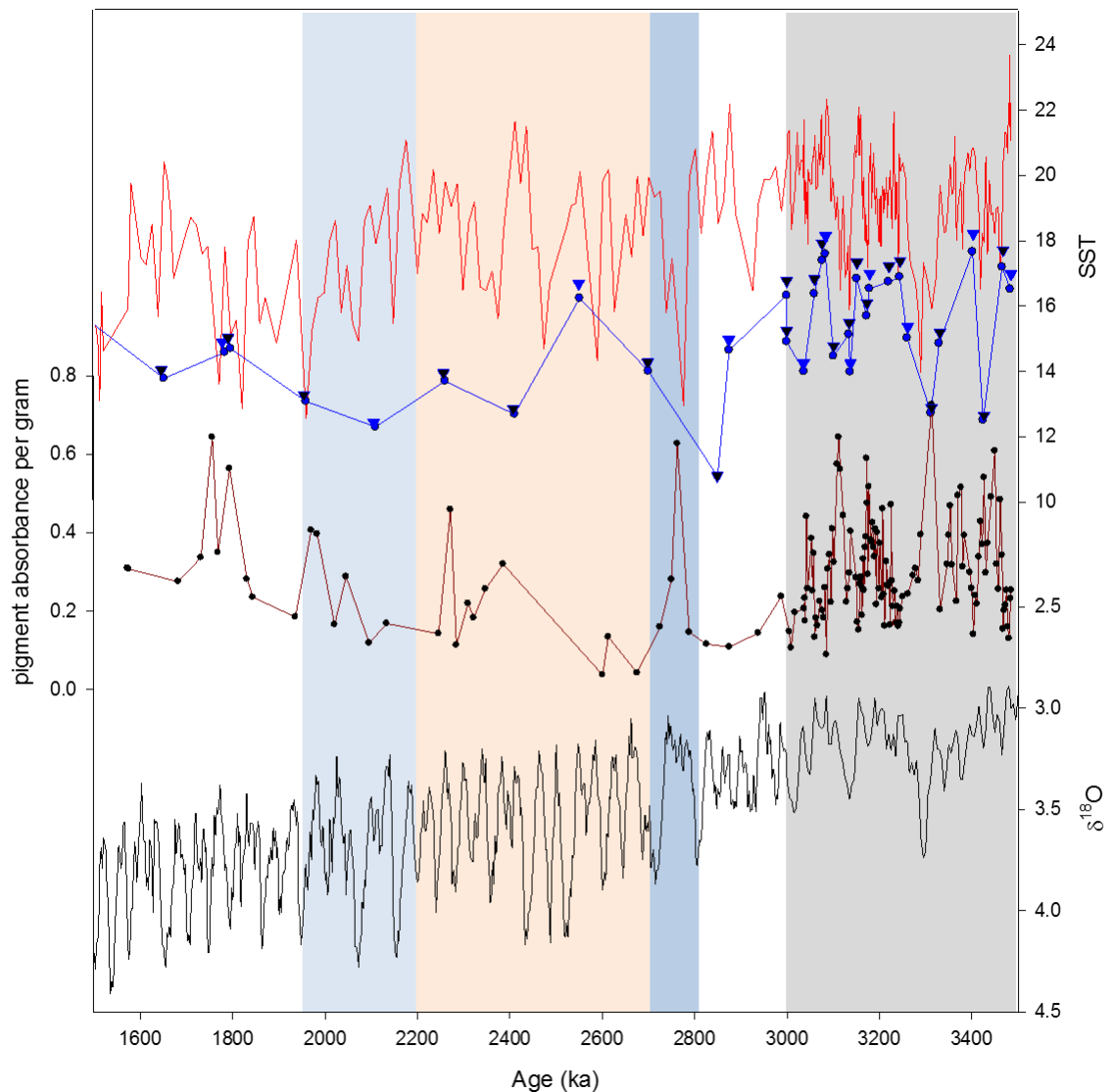
**Figure 6.2 Proxy records between 3.0 and 1.5 Ma** a) $U^K_{37}$' SST record (red) SSTs are calculated using the calibration of Muller et al. (1998); $TEX_{86}$ reconstruction (blue) and $TEX^H_{86}$ (Blue triangles) SST are calculated using Kim et al [2010] c) Concentrations of chlorins as absorbance per gram. d) LR04 stack of benthic $\delta^{18}O$ ‰ measurements (Lisiecki and Raymo, 2005). Best fit line represent polynomial best fit regression lines. Major events in the core indicated by coloured boxes.

The long term cooling trend (highlighted by the polynomial best-fit regression) is marked by an initial decrease in the average SST between 2.9 and 2.5 Ma from 21ºC to 19ºC, followed by an increase in SSTs beginning at 2.17 Ma, where average SSTs increase to a maximum of 22.0 ºC. The temperature then decreases starting at about 2.17 Ma down to 18ºC at 1.95 Ma. SSTs remain low until 1.77 Ma, when there is a

short-lived increase in temperatures up to a maximum of 21.6ºC (Figure 6.2). SSTs then decrease to 18ºC starting at 1.58 Ma. Finally, there are a number of points in the record where temperature drops below the previous minima seen during the M2 glaciation, where minimum temperatures were 17ºC. These points occur at 2.78, 1.96, 1.82 and 1.77 Ma with most occurring between 2.0 and 1.70 Ma. These troughs last about 0.26 Ma and represent the coolest temperatures seen during the period between 3.0 and 1.5 Ma.

### 6.2.2 TEX$_{86}$

All of the TEX$_{86}$ records between 3.0 and 0.9 Ma of the ODP1087 were produced by Mathew Clarkson (unpublished– see above). In contrast to the U$^K_{37}$' the TEX$_{86}$ and TEX$^H_{86}$ temperature records show no long term trend between 3.0 and 1.5 Ma (Figure 6.2). The highest values for TEX$_{86}$ and TEX$^H_{86}$ are 15.8ºC and 16.2 ºC, respectively, which occur at 3.0 Ma, while the lowest values in the TEX$_{86}$ and TEX$^H_{86}$ records are 11.2 ºC and 10.8 ºC, respectively, which occur at 2.85 Ma. The average temperature during the period 1.5-3.0 Ma is about 13ºC. The one exception is around 2.85 Ma when there is a drop in TEX$_{86}$ SSTs to 10.8ºC. However, this lack of variability is likely due partially to the low resolution at which the data was produced for this part of the record.

### 6.2.3 Chlorin concentrations

Overall, there is a long-term increase in chlorin concentrations between 3.0 and 1.5 Ma, from an average of 0.10 amt g$^{-1}$ at 3.0 Ma to 0.30 amt g$^{-1}$ at 1.5 Ma (Figure 6.2). Superimposed on this long-term increase are a number of short-lived and large increases, which occur at 2.76, 2.27, 1.97, 1.79, and 1.76 Ma. These chlorin peaks range between 0.40 and 0.63 abs g$^{-1}$ and are associated with lower temperatures in the U$^K_{37}$' record.

### 6.2.4 n-alkane

The total *n*-alkane range from 3.50 concentration per g at 2.8 Ma to 0.25 concentration per g at 0.16 Ma (Figure 6.3). The n-alkane proxy [C$_{27}$-C$_{35}$] n-alkanes are the homologues tied to terrestrial and higher plants (Eglinton and Eglinton, 2008). The highest total n-alkane value 1.8 concentration per g occurs at 0.05 Ma while the lowest

value 0.183 concentration per g occurs at 0.35 Ma. *n*-alkane values start increasing from 0.48 μg at 3.3 Ma and continue to increase to 1.57 concentration per g until at least 2.8 Ma.
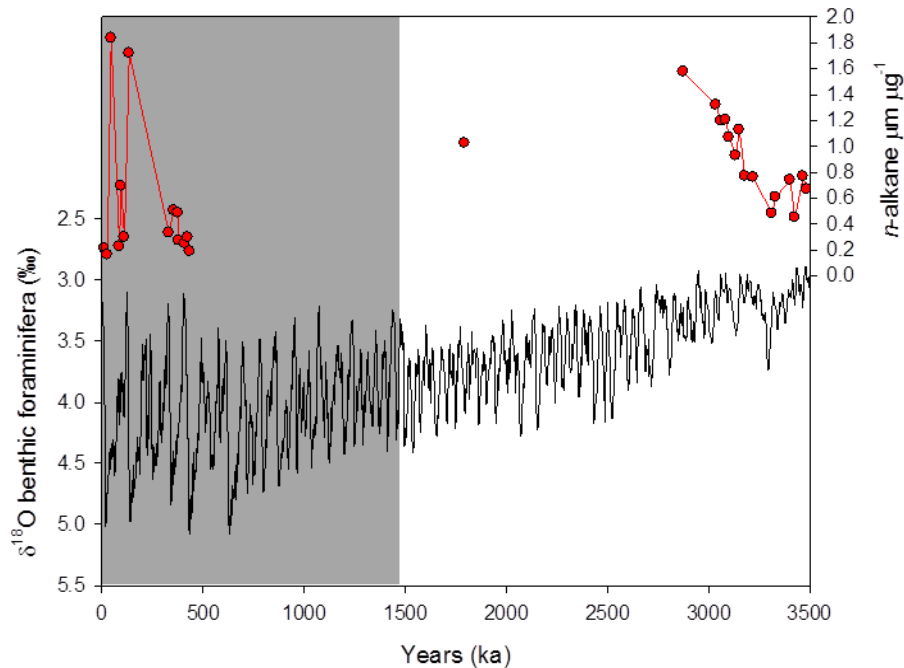


**Figure 6.3 n-alkanes (red) compared to LR04 record (black).** The white area represents the record discussed in this chapter.

## 6.3 Discussion

### *6.3.1 Evidence for circulation change*

There are a number of trends and relationships between 3.0 and 1.5 Ma of the ODP 1087 record that suggest connections between the different proxies. While overall there is a cooling trend in the $U^K_{37}$' SST, there are periods of pronounced cooling. The first occurs from 2.2 Ma to 1.7 Ma. Chlorin concentrations increase at the same time as the initial cooling in the $U^K_{37}$' temperature records, as well as to short term coolings in SSTs. In fact, the highest peak in the early part of the chlorin record is associated with the short term cooling event seen in the both the SST and in the $TEX_{86}$ at 2.8 Ma. This suggests the event at 2.8 Ma and especially the SST cooling at 2.2 Ma are important events in the ODP 1087 record that might have had impact on a further climate.

In contrast, the $TEX_{86}$ record does not experience much change over this period. Temperatures remain around 13 °C and continue to be offset from the $U^K_{37}$'

temperature.  The one exception is the cooling at 2.8 Ma where a $TEX_{86}$ cools before the main cooling ($U^{K}_{37}$') and chlorin concentration increase.

### *6.3.2 Evolution of the Benguela Upwelling*

In the modern ocean the permanent Benguela Upwelling is located mostly north of the ODP 1087 and is mostly influenced by the Agulhas rings from the Agulhas Leakage system (Figure 6.2).  In the previous chapter, the Pliocene proxy records all showed a strong permanent and seasonal upwelling signal.   It is important to understand when the modern system of leakage dominated water started affecting the Southeast Atlantic Ocean.   Comparing the new Site 1087 data presented here to the other Benguela Upwelling site data (Marlow *et al.*, 2000; Etourneau *et al.*, 2009) allows an assessment of the relative contributions of Benguela upwelling and Agulhas Leakage to the site over the last 3.5 Ma (Figure 6.4).  In Chapter 4 the evidence that site 1087 was affected directly by Benguela upwelling during the Pliocene was outlined. Figure 6.3 confirms that, between 3.0 and 2.2 Ma $U^{K}_{37}$' sea surface temperatures at site ODP 1087 continued to be lower than sites in the northern upwelling cells (1081, 1082) (Marlow *et al.*, 2000; Etourneau *et al.*, 2009) (figure 6.4).  This suggests the temperature imbalance which was associated with upwelling in the Pliocene has continued between 3.0 and 2.2 Ma.
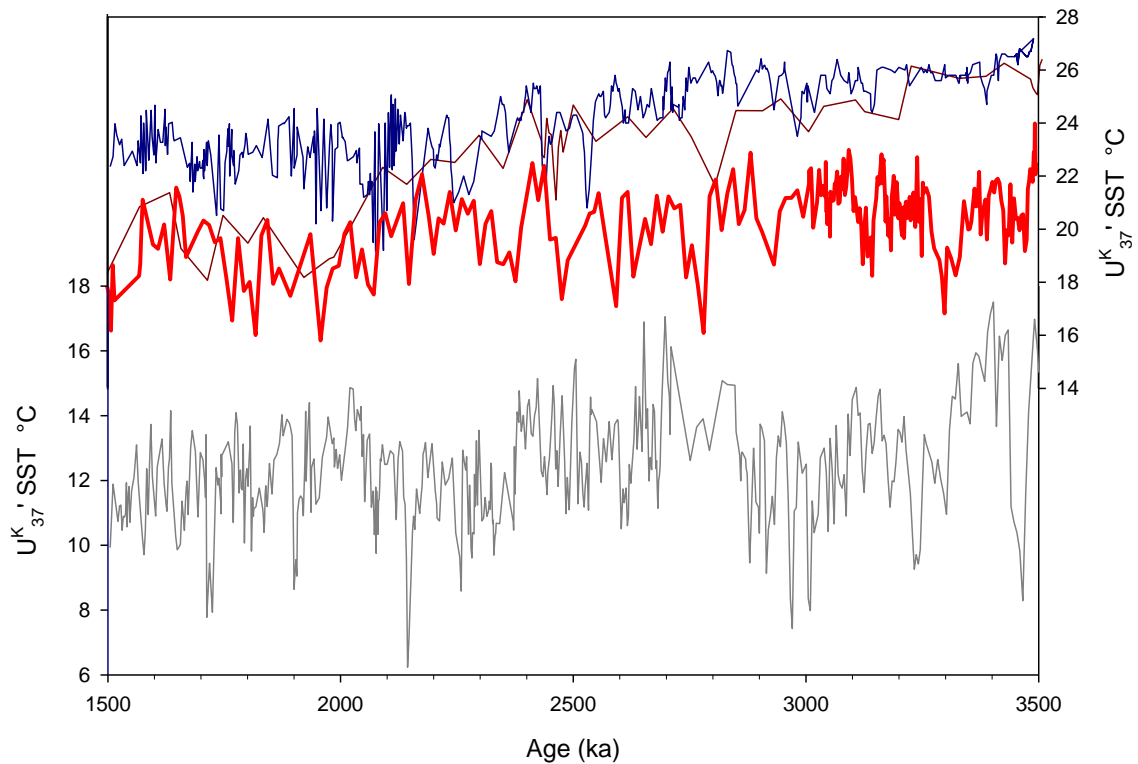
**Figure 6.4 Southeast Atlantic records of temperature change.** ODP 1084 $U^K_{37}$' SST record (dark blue) (Marlow *et al.*, 2000). ODP 1082 $U^K_{37}$' SST records (brown) (Etourneau *et al.*, 2009). ODP 1087 $U^K_{37}$' SST record (red). $U^K_{37}$' ODP 1090 SST (blue) (Martinez-Garcia *et al.*, 2010).

Higher chlorin concentrations at ODP 1087 accompanied by an offset between the $U^K_{37}$' values and $TEX_{86}$ are also interpreted as signs of upwelling. The $U^K_{37}$' index reflects surface temperatures because the source organisms, coccolithophores, are phytoplankton (Conte *et al.*, 1994). From the analysis of surface ocean and sediment trap samples in the Benguela upwelling, Lee *et al.* (2008) identified $TEX_{86}$ always reflected temperatures recorded below the surface ocean at around 70 m water depth (Lee *et al.*, 2008). Under upwelling regimes, it appears the $TEX_{86}$ signal is being produced below the mixed layer rather than at the surface. Such a pattern has been observed in a number of other upwelling areas during the late Pleistocene (Huguet *et al.*, 2007; Lee *et al.*, 2008; McClymont *et al.*, 2012). Therefore it is suggested the offset between $U^K_{37}$' and $TEX_{86}$ temperatures at ODP 1087 reflects the persistence of upwelling from the Benguela system between 3.0 and 1.5 Ma.

Between 3.0 and 2.2 Ma, the temperature difference between the $U^K_{37}$' record at ODP 1087 and sites 1081, 1082, and 1084 decreases, although ODP 1087 remains

cooler than the other sites (Figure 6.3). A number of patterns indicate, however, that although upwelling likely continued to influence ODP 1087, the location of the main upwelling cells started to migrate northward.  First, there is some cooling of the northern and central Benguela sites between 3.0 and 2.2 Ma, which could be inferred to represent more intense upwelling and the increased presence of cooler waters at the ocean surface. Second, chlorin concentrations are relatively low at site 1087 between 3.0 and 2.2 Ma, although still higher than average Pleistocene pigment values (Figure 6.2). This pattern could reflect a reduction in primary productivity, which might also be indicative of a weaker upwelling cell during this time.

However, the evidence for a northward migration and/or intensification of Benguela upwelling appears to be isolated to the central Benguela site (1084).  In contrast, the northern site (1082) has been interpreted as showing weak upwelling based on many different proxies for upwelling such at nitrogen isotopes which show reduced nutrient cycle, diatom mats which showed less vigorous upwelling and higher temperature all have been cited as evidence of reduced upwelling at this time (Etourneau *et al.*, 2012).  All this evidence suggests reduced or lack of upwelling at the northern most upwelling cells between 3.0 Ma and 2.2 Ma.

Between 2.2 to 1.6 Ma there is a cooling trend in the $U^K_{37}$' record at ODP 1082, of 8 ºC in mean SSTs over 2.0 Ma.  Although the northern Benguela site continues to be warmer than site 1087, site 1084 SSTs also cool at 2.3 Ma (Figure 6.3) (Marlow *et al.*, 2000). As a result, by 2.0 Ma, the SSTs at sites 1084 and 1087 converge. After 2.0 Ma, the two SST records cools in synchrony until 1.6 Ma, including sharing a short-lived warming centred on 1.63 Ma. This synchrony is interpreted here to suggest the two sites are reflecting the same oceanic processes in their SST records, and specifically the Benguela upwelling cells had expanded northward but were still affecting the southern Benguela region. This interpretation is supported by the continued offset between $TEX_{86}$ and $U^K_{37}$' temperatures at ODP 1087 and by the maximum chlorin concentrations observed at the site for the last 3.5 Ma which occur at 3.8 Ma.  The timing of these events aligns with an increase in the diatom production in ODP 1084 that occurs between 2.2 and 1.7 Ma (Marlow *et al.*, 2000). The chlorin concentrations at ODP 1087 suggest that 2.2 Ma might have been one of the most productive periods at this site.  Furthermore, the period which follows the cooling from 2.0 until 1.7 Ma was punctuated by a number of cold events throughout. These events were also associated with high chorine events.  Therefore this was not just an establishment of the modern

upwelling but a greatly expanded and more active Benguela Upwelling. In combination, these data sets imply that, between 2.2 and 1.6 Ma, there was an overall intensification of the Benguela upwelling system, which was particularly focussed in the southern and central Benguela region.

### *6.3.3 The Matuyama Diatom Maximum*

The Matuyama Diatom Maximum (MDM) (Lange *et al.*, 1999; Berger *et al.*, 2002) in the southeast Atlantic Ocean is the local reflection of an event that has a global expanse (März *et al.*, 2013). The MDM is marked by an increase in diatom production between 2.8 and 2.2 Ma (Figure 6.5), initially described as the beginning of upwelling at sites ODP 1082 and 1084 (Berger *et al.*, 2002). However, recent research has led to a theory that the MDM is increased nutrient leakage of elements such as silica and nitrogen to the site which was caused by stored nutrients being realised by increased deep-water circulation (Etourneau *et al.*, 2012; März *et al.*, 2013). The MDM is important because the increased diatom production might have caused a drawdown of $CO_2$, at the same time as the onset of Northern hemisphere Glaciation (INHG) (Etourneau *et al.*, 2012). Studies have speculated as to what the MDM signal means for the history of the southern part of the Benguela upwelling and even the Agulhas current. From these theories, a number of testable assumptions have been made about the ODP 1087 area and the Benguela upwelling. These are:

- The MDM shows an initial upwelling signal but the Benguela Upwelling remained weak until the end of the MDM, which represents the first intensification of the Benguela upwelling (Etourneau *et al.*, 2009; Etourneau *et al.*, 2012).

- There was more active upwelling in the southern cells of the Benguela upwelling because of the southward shift of the wind systems (Lange *et al.*, 1999; Etourneau *et al.*, 2009; Etourneau *et al.*, 2010).

- The Agulhas Leakage was weaker from the southward displacement of the wind systems (Lange *et al.*, 1999).
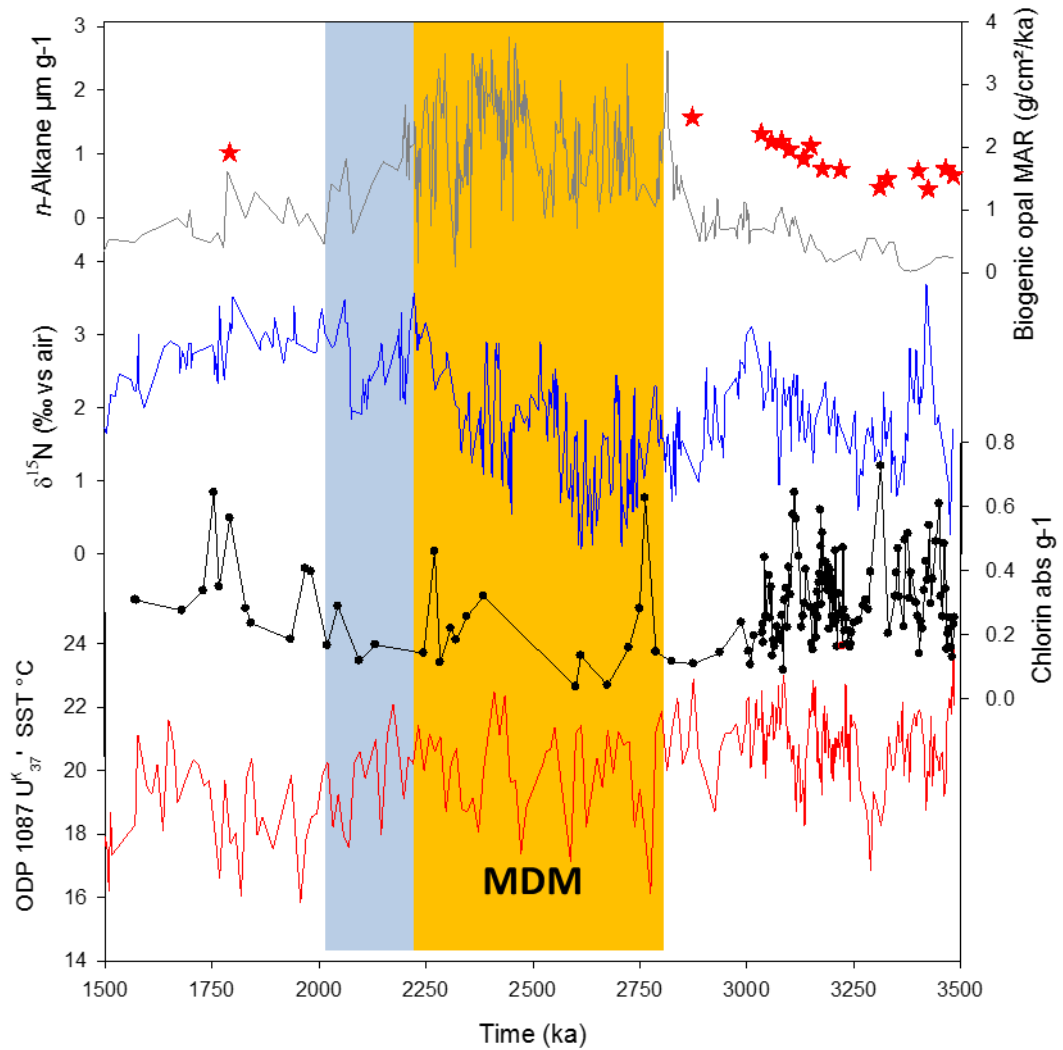
**Figure 6.5 records spanning the MDM.** ODP 1087 $U^{K}_{37}$' SST reconstructions (red), chlorin records (abs $g^{-1}$) (black), and *n*-alkanes μm $g^{-1}$ (Red stars). ODP 1082 $\delta^{15}N$ a measure of the amounts of nutrients in the Benguela upwelling (blue) and biogenic opal MAR (grey) (Etourneau *et al.*, 2009).

The new data presented here from ODP 1087 provides an opportunity to evaluate the evidence for the MDM in the southern cells of the Benguela Upwelling and thus to test these theories. However there is a limit to the ability to reconstruct the MDM signal at ODP 1087 because no proxy for diatoms or diatom productivity was produced for this thesis. Despite this, some of the assumptions about the MDM are supported by the data at ODP 1087. There is evidence of increased upwelling in the southern cells based on the TEX$_{86}$ data showing lower temperatures than the $U^{K}_{37}$' during the MDM and the fact that temperatures at ODP 1087 are colder than the other Benguela Upwelling sites. This fits with the first two hypotheses the Southern

Benguela upwelling should be more intense and that there was a weaker Agulhas Leakage.

However, some of the hypotheses about the MDM are not supported or at least questioned by the data from ODP 1087.  To begin with as mentioned in chapter 5 there is evidence for upwelling preceding the MDM at ODP 1087.  Additionally there is a decrease in chlorin concentrations at the time of the MDM (Figure 6.5). This suggests that, instead of a slight increase or at least sustained upwelling, there may have been a weakening of upwelling starting at 3.0 Ma that continued, with the exception of the 2.8 Ma cooling, until the end of the MDM at 2.2 Ma.   Along with this there are no significant changes in the ODP 1087 SSTs, which remain level with the exception of a few cooling events.  This suggests there is not a change in the upwelling temperature structure during this period.  This might mean there was a general weakening of the entire upwelling system instead of weak upwelling being only constrained in the northern part of the upwelling.  This would fit well with the theories about weaker upwelling and more nutrient leakage providing more stimuli to diatom production at this time which is the recent theory about the cause of the MDM  (Etourneau *et al.*, 2012; März *et al.*, 2013).  However it could indicate a change in the nutrient input into the southern hemisphere.  There is a possibility it could mean the increased nutrients were only affecting the northern and central parts of the upwelling and the southern part of the upwelling was not affected directly by the MDM.  Without a more specific dataset to target the effects of the MDM (i.e. diatoms) this question cannot be fully answered.   Therefore, while not showing data to specifically address the effects of the MDM, the ODP 1087 record does produce the necessary background conditions, namely weak upwelling and more southerly focused upwelling have been hypothesised to cause it.  More importantly it shows that the theories about stronger upwelling was focused in the southern upwelling cells is suggested by the Site ODP 1087 data.

### 6.3.4 Terrestrial changes

The *n*-alkane proxy is related to how much terrestrial material is reaching the core site (Killops and Killops, 2005).  In the record there is an increase of *n*-alkanes found in the core from 3.3 Ma until at least 2.7 Ma.  Because of missing data it is not known when this trend ends although by 1.6 Ma the levels of *n*-alkanes in the core have

dropped back to the original levels (Figure 6.4). There are three theories to explain the source of the terrestrial material in ODP 1087:

- It is being carried in on a strengthened Agulhas Current which contains a increased amount of sediment off the southern part of the African content (Biastoch *et al.*, 2008b).

- It is a result of wetter conditions on the African continent leading to a greater delivery of fluvial material to the site (Diekmann *et al.*, 2003) .

- It is a result of a change in the wind patterns over ODP 1087 allowing more dust input to the site (Darwin, 1846; Huang *et al.*, 2000; Krueger *et al.*, 2008).

It is unlikely to be an indication of an Agulhas Leakage because, as mentioned above, there is no evidence of Agulhas Leakage effecting ODP 1087 and certainly no evidence of intensification. The a change to wetter conditions in Africa is more likely as the Pliocene has been shown to be wetter although the evidence is that by the end of the Pliocene conditions were getting drier (Diekmann *et al.*, 2003). However there are no large river systems in this part of Africa to provide input into the ODP 1087 site. It is possible that there existed these river systems during the Pliocene. The third is somewhat more likely because there is good evidence of shifting winds as has been discussed both in this chapter and the previous chapter. However given the distance offshore and the location of the wind patterns around the ODP 1087 they should not carry a lot of dust to this region because the prevailing winds are blowing in from across the ocean not Africa (Krueger *et al.*, 2008). Therefore the source of the terrestrial material into ODP 1087 is currently unknown. Attempts to do compound specific isotopes to investigate the source were hampered by the small sample size. Given the options and evidence for shifting winds at the end of the Pliocene means that changes in the wind patterns is most likely responsible for the trends in the data. This could be a result of the northward movement of the Benguela upwelling cell or it could be just a reduction in upwelling at the end of the Pliocene. The most likely linkage between the increasing terrestrial input during the Pliocene-Pleistocene is a shift in the wind pattern associated possibly with the transition from the Pliocene. It will be necessary in the future to produce more samples to try and understand the changes seen in this part of the core. Therefore the *n*-alkane record preserves a significant trend which needs to be studied in more detail.

## 6.4 Conclusions

Between 3.0 and 1.5 Ma the global climate system climate shifted from the warmth of the Pliocene to a time of large scale glacial/interglacial cycles of the cooler Pleistocene. This chapter examined the evidence for changes in ocean circulation from the SE Atlantic across this time window. Using proxies for sea surface and subsurface temperatures as well as primary productivity in the surface ocean, the evolving influence of Benguela upwelling over the core site was examined. The data show that, overall, ocean temperatures decreased, but did so through an intensification of cooling and upwelling between 2.2 and 1.6 Ma. SSTs at ODP 1087 were always either cooler than, or equal to, SSTs recorded at a central site of the Benguela upwelling system. In combination with evidence for subsurface recording of temperatures by $TEX_{86}$ and high chlorin concentrations at ODP 1087, we interpret these patterns to reflect an influence of Benguela Upwelling at this site, as was also the case in the Pliocene. However, there is some indication of the beginning of northward movement of the Benguela Upwelling cells, especially towards 2.2 Ma when SSTs in ODP 1087 and SSTs in ODP 1084 are the same, starting with the cooling beginning at 2.2 Ma. This is also the same time as the cooling seen in the ODP 1082 record meaning that the entire Benguela upwelling experienced an intensification in upwelling at this time or that the core site was responding to global cooling. Finally, the new data from ODP 1087 supports the weaker and southward focussed upwelling of the MDM, as predicted by the diatoms from elsewhere in the Benguela Upwelling. Furthermore, trends in the terrestrial data indicate changes occurred during the transition. Although the source of these changes remains unknown, a shift in the wind fields remains the most likely explanation. The implications of these results and processes will be discussed in chapter 8.

# Chapter 7 Interaction between the Agulhas Leakage and the Benguela upwelling system over the last 1.5 Ma

## 7.1 Introduction

In this Chapter the record of Agulhas Leakage to the SE Atlantic over the last 1.5 Ma is investigated. The previous two chapters have established that ODP 1087 is primarily a record of the Benguela Upwelling before 1.5 Ma. However, at the present day the dominant influence over SSTs and primary productivity above this site is the input of warm and salty waters of Indian Ocean origin, introduced to the Atlantic Ocean by the Agulhas Leakage (Chapter 1)(Figure 7.1). The aim of this chapter is to identify whether there is evidence for Agulhas Leakage at ODP 1087, and to identify when it started to affect this site and what this means for changes in the southeast Atlantic Ocean.
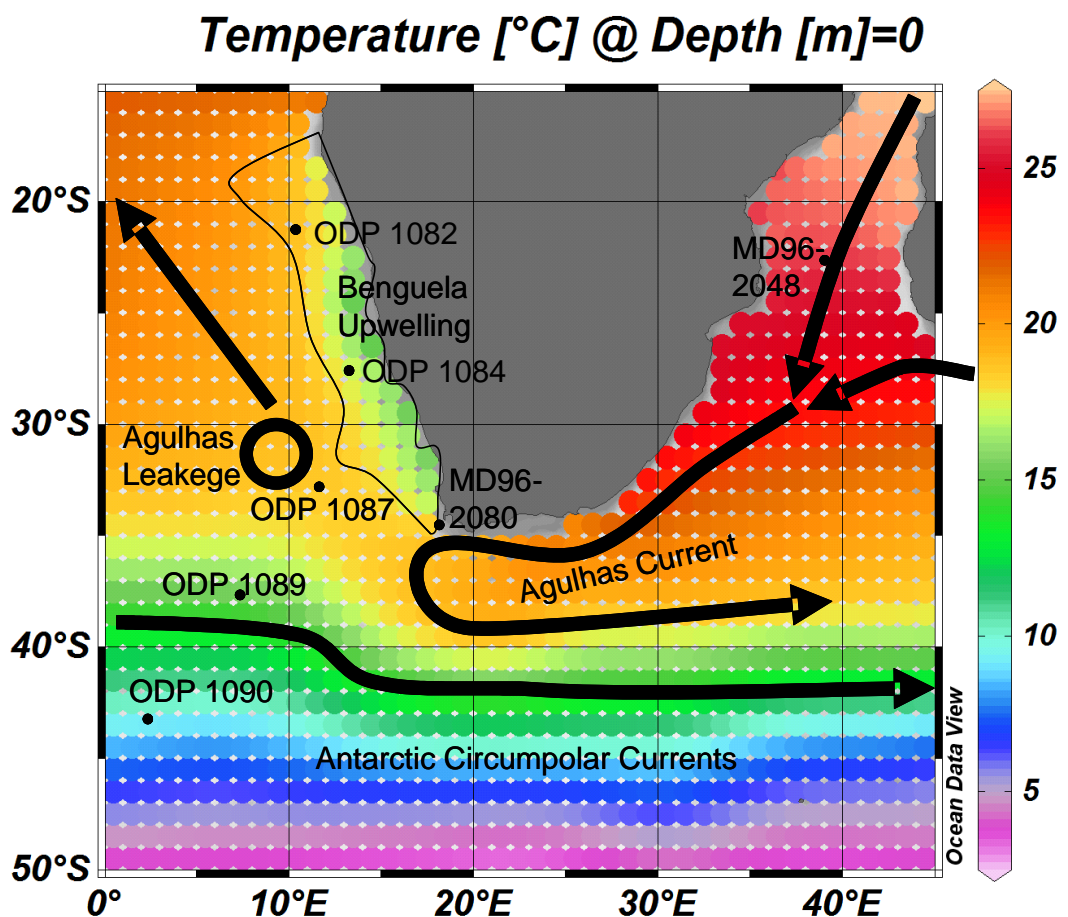


**Figure 7.1 Site Map for the Mid to late Pleistocene.** Showing the location of the core site (ODP 1087) on a SST map (World Ocean Atlas 2001, Ocean Data View mapping program). The location of local Pliocene records and the location of major oceanic systems in there modern day positions are shown.

The last 1.5 Ma of Earth's history contains several so-called 'super-interglacials', during MIS 1, 5, 7, and 11 (Figure 7.2) (Pollard and DeConto, 2009b; Masson-Delmotte *et al.*, 2010; Turney and Jones, 2010). 'Super-interglacials' are warm and long interglacials, and have gained interest recently as potential ways of understanding the effect of the long-term warming conditions of the current interglacial. One mechanism proposed to explain these super interglacials focuses on the potential role played by the Agulhas Leakage into the SE Atlantic during deglaciations (Figure 7.2) (Turney and Jones, 2010; Turney and Jones, 2011). As discussed in Chapter 1, these authors argue early warming in the southeast Atlantic allowed more salt to be transferred through the southern Atlantic over to southern Brazil. This saline water which is lighter than the surrounding water, causes a strengthening of the transport of the AMOC which in turn carries more warm water from the southern hemisphere to the northern hemisphere. However, there is still some controversy about the existence of 'super-interglacials' in terms of their global expression, and also whether or not enhanced Agulhas Leakage could be responsible. Here, new data from the SE Atlantic covers the last 500 ka,.
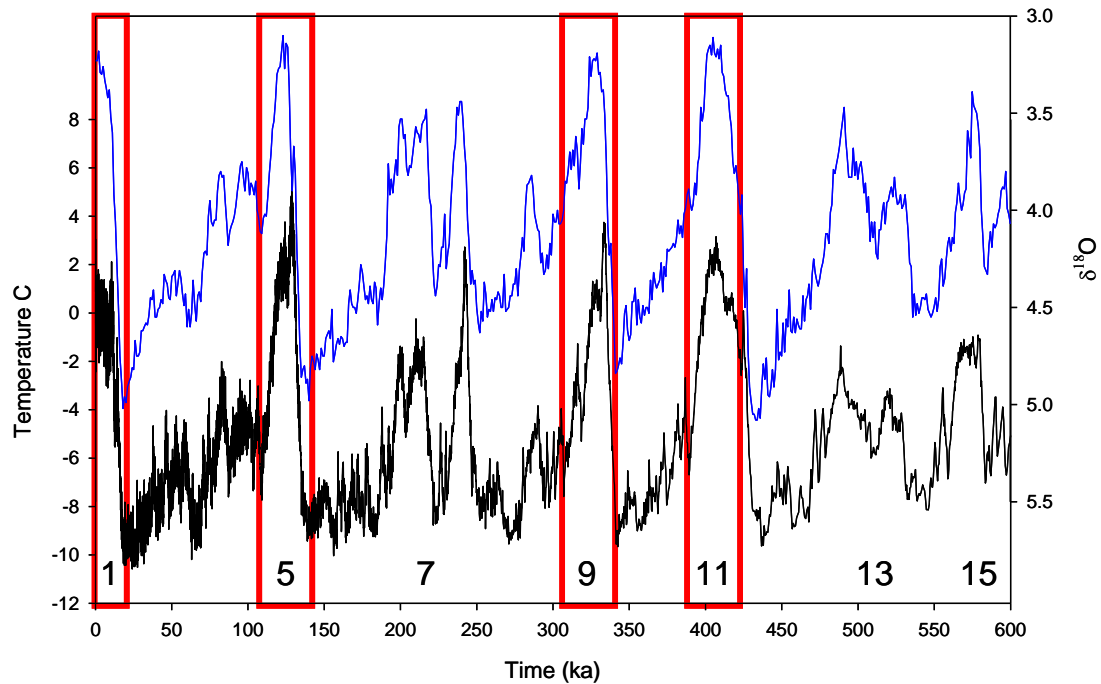
**Figure 7.2 Super-interglacials over last 0.6 Ma.** The records shown are LR04 global benthic $\delta^{18}O$ stack (blue) (Lisiecki and Raymo, 2005) and EPICA Antarctic ice core (black) (EPICA, 2004). The interglacials are marked by the MIS numbers, and the stages described as super-interglacials are marked with red boxes.

Over the last 1.5 Ma there has also been a shift in the periodicity of glacial cycles from 41 to 100 ka at ~1 Ma, known as the mid-Pleistocene transition or MPT (Imbrie *et al.*, 1993). The cause of the MPT is still debated, but might include changes in Antarctic ice sheet configurations, sea-ice distribution changes, ocean circulation or $CO_2$ draw down (Schmieder *et al.*, 2000; Liu *et al.*, 2008; Sosdian and Rosenthal, 2009; Zhang *et al.*, 2009; Rae *et al.*, 2011). Whether changes in Agulhas Leakage drove the 100 ka cycle deglaciations as hypothesised will be tested in this chapter (Peeters *et al.*, 2004; Caley *et al.*, 2012).

To determine the relative importance of Agulhas Leakage to the SE Atlantic over the last 500 ka, a multi-proxy approach is applied here to reconstruct key oceanographic variables at ODP 1087. The focus is on reconstructing SSTs, salinity and primary productivity, which can be used in the modern ocean to identify the positions and contributions of Agulhas Leakage, Benguela upwelling, and the ACC, to the core site. SSTs are reconstructed using the $U^{K}_{37}{}'$ index and $TEX_{86}$ Index (Brassell *et al.*, 1986; Müller *et al.*, 1997; Schouten *et al.*, 2002; Conte *et al.*, 2006). Primary

production is reconstructed using the concentrations of the chlorin pigments and assemblages of dinoflagellates. Finally, a salinity record was developed following the method described by Cortese *et al.* (2004). This subtracts the temperature and ice volume components of planktonic carbonate $\delta^{18}O$ using the $U^K_{37}$' SST proxy and the benthic $\delta^{18}O$ pattern, respectively, to quantify the contribution of salinity to planktonic $\delta^{18}O$.

## 7.2 Results: the 0-0.5 Ma record

The new data produced in this thesis, focussing on the 0-0.5 Ma interval, will be presented here.

### *7.2.1 $U^K_{37}$' SSTs*

For the period 0 to 0.5 Ma, the $U^K_{37}$' index ranges from values of 0.4 to 0.8, corresponding to an SST range from 15 to 21 ºC over glacial-interglacial cycles (Figure 7.3). The sample resolution varies but is about 3ka. The SST record is marked by an unusually cool glacial stage at 0.373 to 0.349 Ma (MIS 10), with SSTs at 12 ºC (glacial stages are usually recorded with SSTs of 14 to 16 ºC). The SST maxima are recorded around 0.243 to 0.228 Ma (MIS 7) and 0.135 to 0.112 Ma (MIS 5). Rapid warming is evident on every glacial-interglacial transition for the last 0.5 Ma. The warming in $U^K_{37}$' precedes all interglacial onsets since 0.5 Ma. On average, SST warming leads $\delta^{18}O$ decreases by 10-30 ka. The earliest deglacial warming is identified at ~30 ka before the onset of MIS 1. During the transition to MIS 11, SSTs peak at 20 ºC but this occurs 5 ka before the onset of the interglacial. In contrast, the interglacial maximum (as recorded in benthic $\delta^{18}O$) has lower SSTs (18.5 ºC at ~.403 MA). The wavelet analysis shown in figure 7.4 of the $U^K_{37}$' temperature data shows no evidence of 41 ka cycles.

Wavelet analysis compares the data to a pre created waveform to determine the dominate cycles that change throughout the record (Grinstead *et al.* 2004). Therefore it provides an illustration of changes in the dominance of cycles over a period of time. The significance of these cycles is determined by comparing the record to random generated red noise. The waveforms and analysis here was one that had been previously set up by Grinstead *et al.* (2004). It should be noted that there are assumptions regarding the waveform used and the age model that can introduce drastic

errors into the wavelet analysis.   Therefore caution should be taken in interpreting the presence of cycles in the wavelet analysis. There is evidence of 100 ka cycles in two parts of the record.  There are strong but not significant 100 ka cycles between 1.5 and 0.9 Ma.   Then between 0.6 and 0.0 Ma there are strong and significant cycles in the record (Figure 7.4)
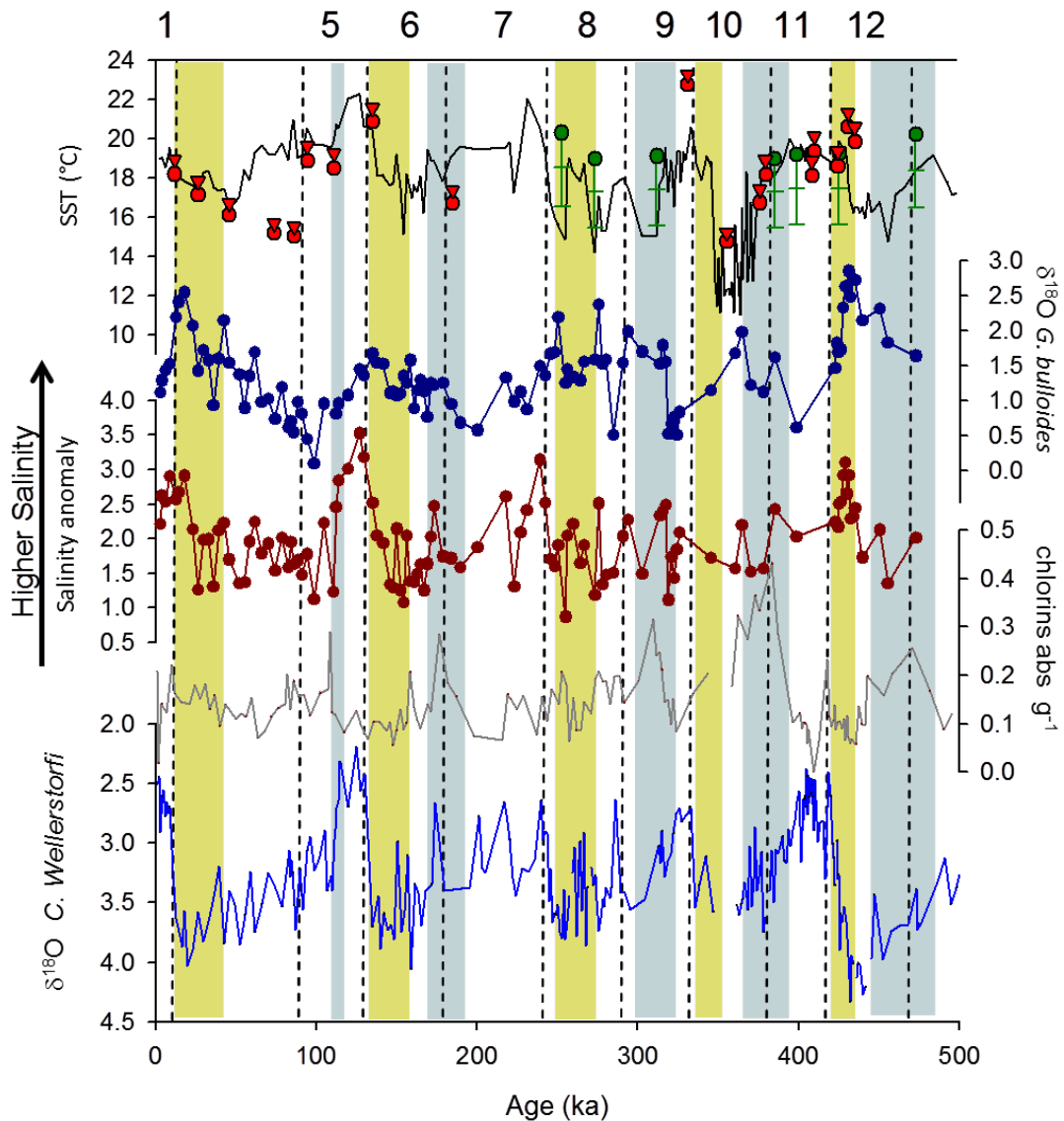
**Figure 7.3. New late Pleistocene records of SST, salinity and pigments from ODP 1087** plotted against previously published benthic $\delta^{18}O$ stratigraphy (McClymont *et al.*, 2005). Pre-interglacial warmings are indicated by the yellow bars, and identified as the time when d18O is at its minima (full glacial conditions) but warming is observed in the SST data; late-interglacial pigment peaks are indicated by blue bars. The vertical dashed lines represent the transitions from glacial maxima to interglacials. a) $U^{K}_{37}$' SST record (black) $TEX_{86}$ (red circles), $TEX^{H}_{86}$ (Red Triangles) and SST range calculated using dinoflagellate assemblages (green) (Marret *et al.*, 2008). $U^{K}_{37}$' SSTs are calculated using the calibration of Muller *et al.* [1998].; $TEX_{86}$ and $TEX^{H}_{86}$ temperature calculated using the calibration of Kim *et al.* [2010] b) published $\delta^{18}O$ record of *G. bulloides (Pierre et al., 2001)* ; c) Salinity anomaly reconstructed using previously published $\delta^{18}O$ record of *G. bulloides* (b) *(Pierre et al., 2001)* and corrected for temperature using the $U^{K}_{37}$' record shown in; d) Changes in chlorin concentration reflecting changes in the Pigment record. e) record of benthic $\delta^{18}O$ from *C. wuellerstorfi* (Pierre *et al.*, 2001), re-tuned to the LR04 global benthic $\delta^{18}O$ stack (Lisiecki and Raymo, 2005) and previously published (McClymont *et al.*, 2005).
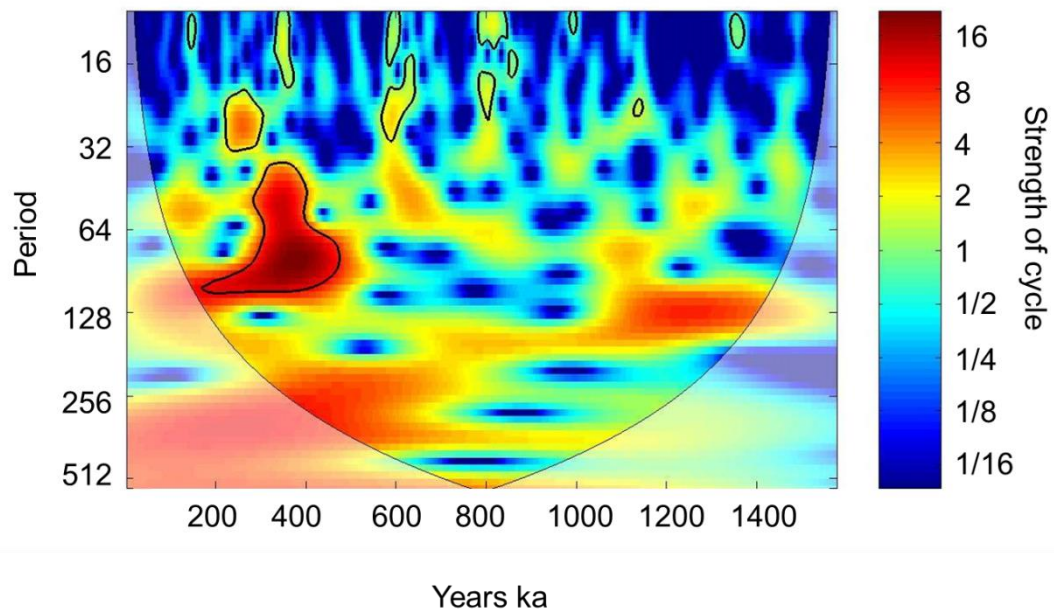
**Figure 7.4 The wavelet analysis of the ODP 1087 UK37' SST** using the Matlab code originally developed by Grinstead et al. [2004]. Black lines and the shaded cone of influence indicate parts of the record that are statistically significant using phase angle statistics.

### 7.2.2 TEX$_{86}$

The TEX$_{86}$ and TEX$^H_{86}$ were reconstructed for the last 0.5 Ma for this thesis. The TEX$_{86}$ and TEX$^H_{86}$ data between 1.5 Ma and 0.5 Ma was produced by Mathew Clarkson as part of his masters project. The minimum value TEX$_{86}$ for the last 0.5 Ma is TEX$_{86}$ 14.9 and for TEX$^H_{86}$ is 15.2ºC and occurs at 0.345 Ma. The maximum value is 22.8 ºC for TEX$_{86}$ and 23.5 ºC for TEX$^H_{86}$ and occurs at 0.331 Ma. The average values from 1.5 Ma and 0 Ma for the TEX$_{86}$ is 18 ºC and for TEX$^H_{86}$ it is 18.8 ºC (Figure 7.5). The low value for TEX$_{86}$ is 12.8 for both indices which occurs at 1.19 Ma. From 0.82 Ma the temperatures calculated by the TEX$_{86}$ and U$^K_{37}$' indexes converge (Figure 7.5), although during deglacial warmings the TEX$_{86}$ temperatures exceed those of UK37' by as much as 3°C. During colder times in the U$^K_{37}$' record, TEX$_{86}$ temperatures are cooler than the U$^K_{37}$' SSTs. However, the magnitude of this difference (3.5 to 1 ºC) is much smaller than the offset observed through the Pliocene and early Pleistocene (5-8 ºC, and Chapters 5 and 6). Because of the minor difference between the different indexes TEX$_{86}$ is used to describe the temperatures in this thesis.
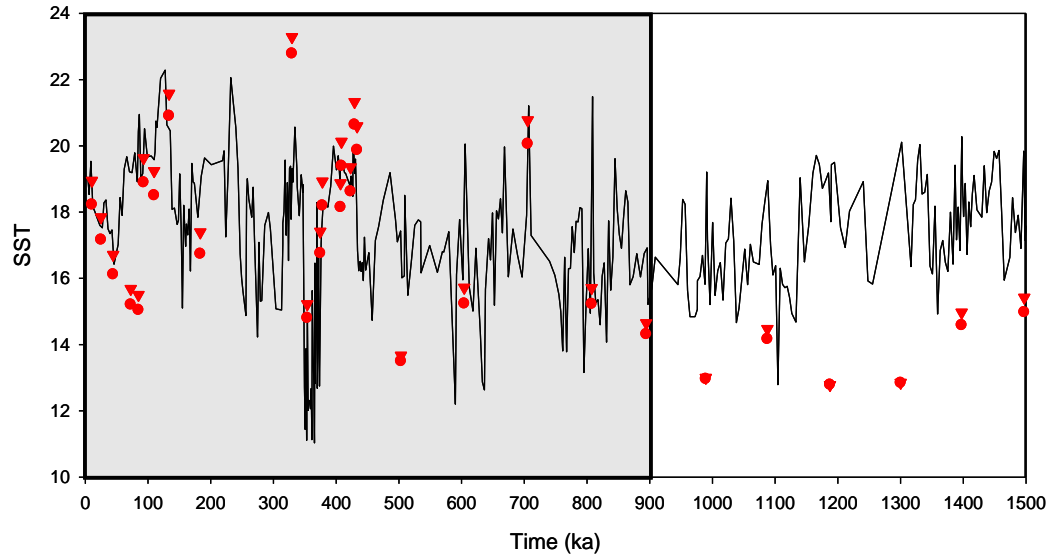
**Figure 7.5 comparing SST proxies over the last 1.5 Ma.** The proxies compared are $U^{K}_{37}$' (black), $TEX_{86}$ (red circles), and TEX86H (red triangles). The grey box indicates the period of time when the average different in the proxies is closer to 0. $TEX_{86}$ Data before 600 was gathered by Mathew Clarkson (UCL)

### 7.2.3 Sea surface salinity

Figure 7.3 shows the reconstructed "salinity anomaly" record which was generated using the published *G. bulloides* planktonic $\delta^{18}O$ data (Pierre *et al.*, 2001) and corrected for $U^{K}_{37}$'-SSTs and benthic $\delta^{18}O$. *G. bulloides* was chosen because there were existing studies for this area that produced a local relationship for how *G. bulloides* was affected by salinity (Labeyrie *et al.*, 1996; Cortese *et al.*, 2004). Studies show that there is evidence that the salinity changes caused by the thermohaline circulation can be seen at subsurface locations (~10m) which is where *G. bulloides* is commonly found (Labeyrie *et al.*, 1996; Cortese *et al.*, 2004). The salinity record is of lower resolution than for $U^{K}_{37}$'-SSTs due to gaps in the record of *G. bulloides* (Pierre *et al.*, 2001), but most of the major glacial-interglacial transitions can be observed. Therefore it is important to only analyse the large magnitude events as these are more likely to represent changes in salinity. Figure 7.3 shows that at glacial terminations, the salinity anomaly ($\Delta^{18}O‰$) increases 5-10 ka after the early rise in SST but before the fall in benthic $\delta^{18}O$. Furthermore, the highest salinity values always occur before or at the beginning of interglacials: $\Delta^{18}O‰$ exceeding 2.5 ‰ occurs 4-20 ka before the $\delta^{18}O$ minima which mark the start of the interglacial. The exception to this pattern is for the transition between MIS 10 to 9, where no change in salinity is observed. However, this is likely an artefact of the low resolution data set for *G. bulloides* $\delta^{18}O$ in this time window.

136

### 7.2.4 Chlorin concentrations

Chlorin concentrations range from 0.05 to 0.48 abs g$^{-1}$ (Figure 7.3d). There was no relationship seen between changes in sedimentation and changes in chlorin concentrations. There is no long-term trend in overall chlorin concentration. However, chlorin maxima seem to occur at times of increasing benthic $\delta^{18}O$, but decrease in intensity before the glacial maxima are reached. The amplitude of the chlorin peaks diminishes in concentration and duration from a maximum at MIS 10 to a minimum during MIS 3. The most prominent chlorin concentrations (by both amplitude and duration) occur during MIS 10, when concentrations are sustained at 0.3-0.4 abs g$^{-1}$ for 50 ka (Figure 7.3 a).

### 7.2.5 Dinoflagellate cyst assemblages

Seven samples were selected for dinocyst analysis in order to reflect different SSTs for specific time intervals. Overall, the dinoflagellate diversity is relatively low, with only 13 species identified. The assemblages are mostly dominated by *Operculodinium centrocarpum* (between 74-3% of dinocysts) and *Nematosphaeropsis labyrinthus* (between 41-5% of dinocysts) and have significant percentages of *Spiniferites ramosus*. *O. centrocarpum* is a cosmopolitan species, whereas *N. labyrinthus* is more restricted to open oceanic conditions. *S ramosus* is a sub-polar to sub-tropical species and is often abundant in upwelling regions (Marret and Zonneveld, 2003; Marret *et al.*, 2008). SSTs were estimated using established transfer functions (Section 3.3.2) and show values between 17 and 18.5ºC (figure 7.3) (Marret and Zonneveld, 2003; Marret *et al.*, 2008).

## 7.3 Discussion

### 7.3.1 Early deglacial warmings over the last 0.5 Ma

The Pleistocene $U^{K'}_{37}$-SST record from ODP 1087 is marked by a series of warming events which precede the glacial-interglacial transitions as recorded by the benthic $\delta^{18}O$ record from the same core. This warming is also represented in the reconstructions using dinoflagellates and in the $TEX_{86}$ record after 0.5 Ma. The new data from ODP 1087 confirms the early warming signal seen in another core from the southeast Atlantic (MD96-2080) (Figure 7.6). In contrast, rapid warming which is closely coupled to the onset of deglaciation, can be observed in other records from the southern hemisphere, including ODP 1089 and 1090 (Figure 7.5). Increases in salinity are also recorded at ODP 1087 before and at the start of interglacials. However, salinity increases can lag those observed in the SSTs by as much as 5 ka. Two possible mechanisms could explain the early deglacial warming at ODP 1087: changes to the strength of the bipolar seesaw and/or Agulhas Leakage.
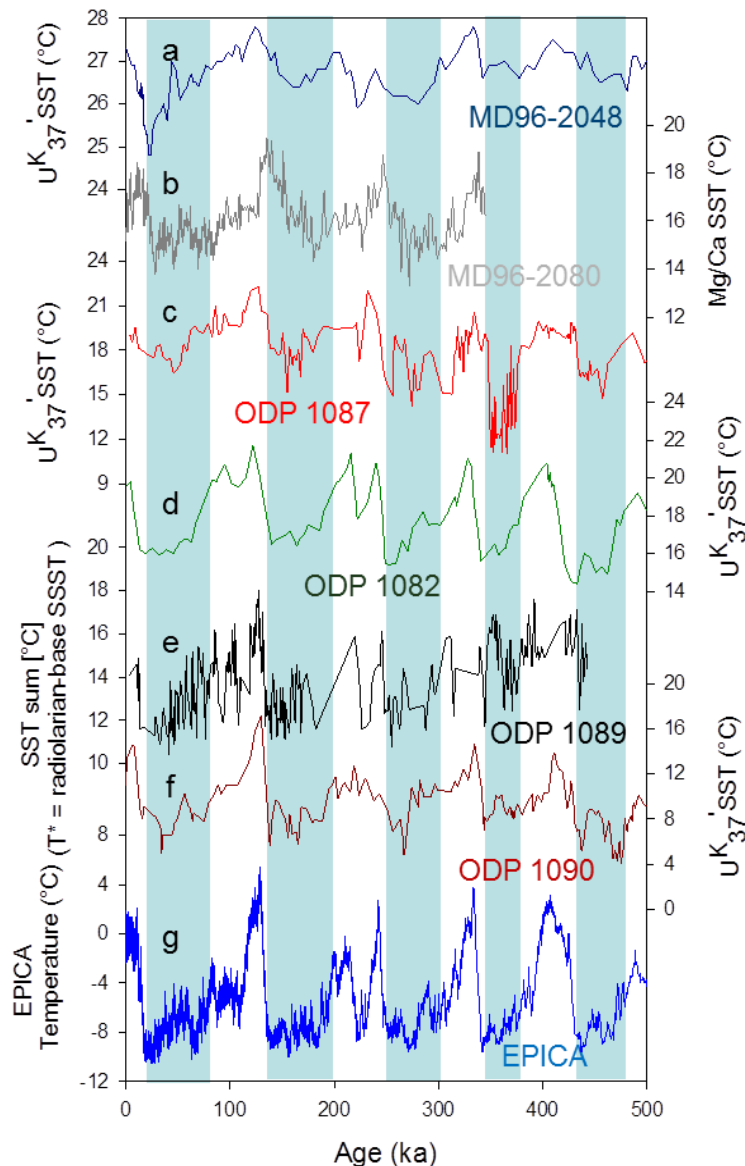
**Figure 7.6 SST records from the Agulhas Current and Agulhas Leakage region.** a) M96-2048 U$^K_{37}$' SST Indian Ocean upstream in the Agulhas current (Caley *et al.*, 2011). b) Agulhas bank Splice Mg/Ca SST from the terminus of the Agulhas current (Martínez-Méndez *et al.*, 2008). c) Record from the Benguela Upwelling U$^K_{37}$' SST ODP 1082 (Etourneau *et al.*, 2009). d) ODP 1087 record U$^K_{37}$' SST (this study). e) ODP 1089 from just north of the ACC based on radiolarian temperature (Cortese and Abelmann, 2002). f) ODP 1090 U$^K_{37}$' SST from the ACC area (Martinez-Garcia *et al.*, 2010). g) Antarctic δD record of temperature (EPICA, 2004). Blue bars represent glacial periods identified using the age model developed by Peirre *et al* [2001].

One hypothesis to account for early warming in the SE Atlantic region during deglaciations is to invoke the operation of the "bipolar seesaw" (Barker *et al.*, 2009; Dickson *et al.*, 2009; Barker *et al.*, 2011). The bipolar seesaw theory suggests during

cold periods in the northern hemisphere (such as glacial maxima), the weakening of Atlantic meridional overturning circulation (MOC) reduces heat piracy by the North Atlantic and leads to warmer climates in the southern hemisphere (Broecker, 1998; Seidov and Maslin, 2001). The warming trend that occurs during deglaciation at ODP 1087 might therefore reflect the impact of the bipolar seesaw on SSTs in the SE Atlantic (Barker *et al.*, 2009; Barker *et al.*, 2011). However, the timing of the early warmings at ODP 1087 does not fully support this theory. Although SSTs warm in tandem with other Agulhas sites (Figure 7.6), they precede the warming which occurs in Antarctic temperatures and which is used as a demonstration of the bipolar seesaw in operation (Figure 7.6); (EPICA, 2004; Barker *et al.*, 2009). For example, during the last deglaciation, southern hemisphere records with a bipolar signature show warming beginning around 18ka (Barker *et al.*, 2009). In contrast, the ODP 1087 SST record warms from 45 ka, and shows increased salinity from 23 ka (Figure 7.5). Thus, the events which drive the deglacial warming at ODP 1087 must reflect a more local influence, such as Agulhas Leakage.

In the modern ocean, the signature of Agulhas Leakage into the Atlantic Ocean is increased temperature and salinity relative to the Atlantic or Benguela upwelling waters, given the warmth of the source Agulhas Current. Rising SSTs ($U^K_{37'}$) and increased salinity ($\Delta^{18}O‰$) identified at ODP 1087 for every termination of the last 500 ka is therefore consistent with enhanced Agulhas Leakage to the SE Atlantic. Furthermore, at the same site, Caley et al. (2012) observed enhanced accumulation of the subtropical planktonic foraminifera species *G. menardii* for every termination of the last 1.35 Ma (Figure 7.7). This foraminifera species is specific to warm waters and during the glacial periods is restricted to the Indian Ocean (Caley *et al.*, 2012); its presence in ODP 1087 is argued to reflect early "re-seeding" events during terminations as a result of Agulhas Leakage (Rau *et al.*, 2002; Caley *et al.*, 2012). A number of other studies have identified early localised warming and/or increased Agulhas Leakage faunal inputs preceding interglacials in the SE Atlantic during the Pleistocene (Peeters *et al.*, 2004; Martínez-Méndez *et al.*, 2008; Dickson *et al.*, 2010a). Figure 7.5 shows the early warmings identified in the SE Atlantic occur in synchrony with warmer SSTs in the Agulhas Leakage zone (e.g. MD96-2080) over the last 450 ka (Martínez-Méndez *et al.*, 2010). This correlation indicates that this 500 ka record of SSTs likely reflects changing Agulhas Leakage to the SE Atlantic.
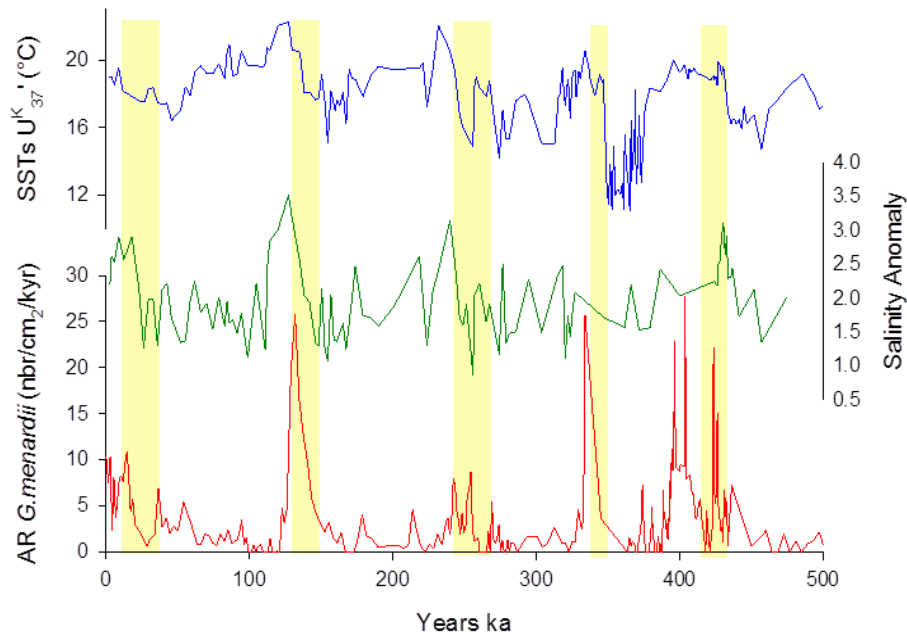
**Figure 7.7  A comparison of the G. menardii record to proxies of Agulhas Leakage**  (Caley *et al.*, 2012) (red) to the SST record (blue) and Salinity (green) records produced in this study. Yellow bars indicate the periods where early warming occurs in the core.  All analyses were performed at ODP 1087.  This indicates that the 0.5 Ma record of SSTs likely reflects changing Agulhas Leakage to the SE Atlantic.

### 7.3.4 'Super-Interglacials'

There are a number of previously identified 'super-interglacials' that occur during the time covered by the 500 ka record.  While there is no current consensus on what a 'super-interglacial' is, the MISs 11, 9, 5, and 1 have all been described as 'super-interglacials' (Loutre and Berger, 2003; de Abreu *et al.*, 2005; DeConto *et al.*, 2007; Turney and Jones, 2010; Turney and Jones, 2011). These are defined by having "higher than average" temperatures during the height of the interglacial and/or "longer than normal" duration (Turney and Jones, 2010).  Turney and Jones (2010) have also argued the onset of Agulhas Leakage into the SE Atlantic early in the deglaciations might play a role in driving the amplitude or duration of the super interglacials. This hypothesis is tested here using our new data from ODP 1087. Figures 7.3 and 7.8 confirm that the 'super-interglacials' of MIS 1, 5, 9 and 11 are marked by the strongest indication of early deglacial warming in the timing of the start of the Agulhas Leakage at ODP 1087 which is not only seen in the temperature record but in the wavelet analysis as well, which shows a start of strong 100 ka cycles at 0.6 Ma (Figure 7.4).  In contrast, MIS 7 is the only interglacial of the last 0.5 Ma that has not been identified as a 'super-

interglacial' (DeConto *et al.*, 2007), and is also the only stage without any clear evidence of pre-stage warming (this study) nor large inputs of *G. menardii* (Caley *et al.*, 2012), both of which are indicators of enhanced or early Agulhas Leakage to site 1087. These relationships suggest there may be some connection between the strength of Agulhas Leakage and the 'super-interglacial' era.
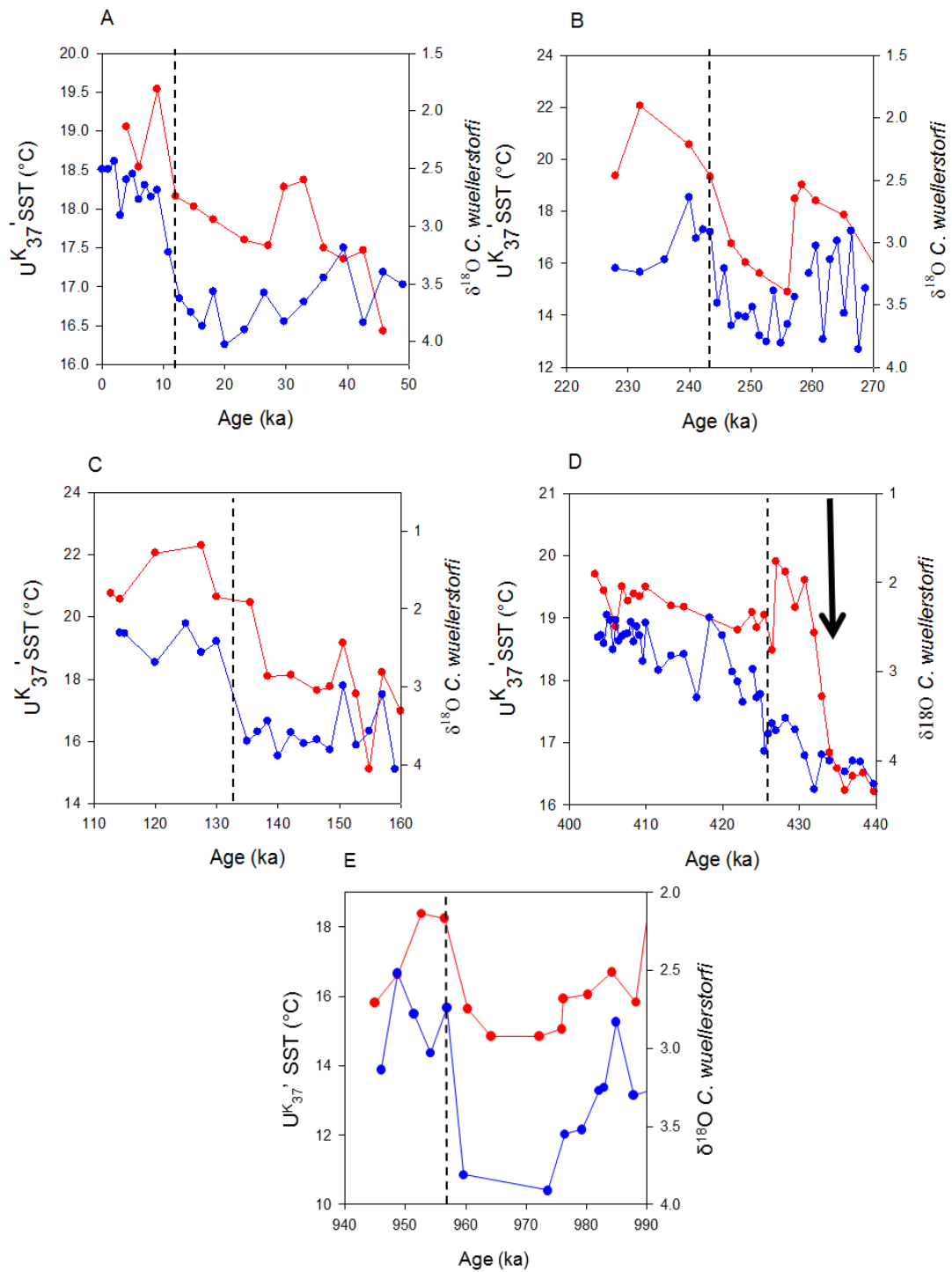
**Figure 7.8 Records showing 4 of the transitions to interglacials the δ18O benthic (blue) and UK37' (red) data comes from ODP 1087.** Dotted lines indicate the start of the interglacial based on the reconnection done by Perrier (2001). A) MIS1 B) MIS 7 C) MIS 5 D) MIS 11. E) MIS 24 which is before the 900 ka event.

However other parts of the ODP 1087 record raise questions about the 'super-interglacial' theory. For example, although never considered to be a 'super-interglacial', MIS 7 has some of the warmest SSTs in the last 0.5 Ma. This pattern is repeated in a number of the Southern Ocean records (ODP 1082, MD96-2080, ODP 1089) and the EPICA ice core deuterium isotope record (Figure 7.6). Furthermore, MIS 11 is arguably one of the most prominent and warm interglacials globally (Loutre and Berger, 2003; de Abreu *et al.*, 2005; Dickson *et al.*, 2010b), yet at ODP 1087 the SSTs are cooler during MIS 11 than all of the other interglacials over the last 0.5 Ma. Despite the pre-warming peak seen in the SST data, where temperature reaches the same temperatures as the other later Pleistocene maxima, the timing of the warming occurring in the ODP 1087 record before the interglacial onset is only 5 ka, which is one of the shortest periods of warming seen in the record. The patterns in SSTs shown at ODP 1087 raise questions about the definition of individual stages as 'super-interglacials' because in the Southeast Atlantic ocean it appears that the non-super interglacials are often warmer than the 'super-interglacials'.

### 7.3.3 Evidence for Benguela upwelling influences

In Chapters 5 and 6, the data from ODP 1087 was interpreted a reduced influence of Agulhas Leakage at this site in the Pliocene and early Pleistocene, and instead showed a stronger signal of upwelling which is presumed to represent an expansion and/or intensification of upwelling in the southern Benguela region. The Benguela upwelling, which lies to the north of ODP 1087, is marked by high primary production, which reflects the presence of high nutrient upwelled waters. It is hypothesized here the peaks in chlorin concentration at ODP 1087 during the Pleistocene might be accounted for by an expanded Benguela upwelling system during the transitions to glacial stages.

MIS 10 is an unusual stage in the Pleistocene record from ODP 1087, as it is marked by sustained low SSTs and high chlorin abundance (Figure 7.3). MIS 10 was identified as a particularly cold stage in the Agulhas Current (Bard and Rickaby, 2009), and thus SSTs at ODP 1087 might reflect cooling upstream of the retroflection and/or restricted Agulhas Leakage to the SE Atlantic. However, MIS 10 is also unusual at site ODP 1089 (to the south of ODP 1087) due to its relatively warm glacial-stage SSTs (Figure 7.6) (Cortese *et al.*, 2004; Cortese *et al.*, 2007). Since ODP 1089 lies just

outside of the modern path of Agulhas Leakage, the warmth of MIS 10 has been interpreted to reflect an increase in the intensity of Agulhas Leakage during the glacial (Cortese *et al.*, 2004). These patterns suggest that the location and/or intensity of Agulhas Leakage were different during MIS 10 compared to other glacial stages. Therefore MIS 10 may represent a southward shift of the Benguela Upwelling that was similar to earlier periods in the Early Pleistocene. It also provides evidence for the location of the Agulhas Leakage at these earlier times. This interpretation is supported by the change in the dominant species in the dinoflagellates during MIS 10 from *Operculodinium centrocarpum* to *Nematosphaeropsis labyrinthea*. At ODP 1087 *O. centrocarpum* is well known to be dominant in the waters at the edge of the Benguela upwelling in the Benguela current (Marret and Zonneveld, 2003). *N. labyrinthea* has been found to dominate on the shelf break at the edge of the Benguela upwelling cells (Zonneveld *et al.*, 2001). The presence of these species during times of high chlorins during MIS 10 therefore supports the theory there was Benguela upwelling waters at ODP 1087.

Evidence for shorter-term influences of Benguela upwelling over ODP 1087 can also be identified during the last 0.5 Ma. The transitions from interglacials to glacials at ODP 1087, as recorded by increases in benthic $\delta^{18}O$, are marked by falling SSTs but not salinity change, and by peaks in pigment concentration. This pattern suggests a local influence of high productivity waters during the transitions to glacial stages.

Times of more expansive Benguela upwelling cells have also been suggested in sites close to ODP 1087 during the late Pleistocene. Site T89-40 from the Walvis Ridge indicated an increase in *N. pachyderma (dex)* foraminifera associated with upwelling over a similar time window of transitions to glacial conditions, where there is increase in *N. pachyderma (dex)* foraminifera which is argued to reflect expansion of the Benguela upwelling cells during transitions to glacials, especially at 401 and 326 ka, which is similar in timing to the chlorin increase in ODP 1087 (Ufkes *et al.*, 2000; Ufkes and Kroon, 2012). In the new analyses of ODP 1087, potential evidence for Benguela upwelling expanding to the site during the transitions to glacial stages has been identified. This shows that even sites relatively distal to the upwelling cells in the modern ocean may have been affected more strongly by upwelling in the past.

## 7.4 Conclusions

This chapter has used records of SSTs, surface salinity, primary production and dinoflagellate assemblages at ODP 1087 to investigate changes to the Agulhas Leakage and Benguela upwelling over the last 0.5 Ma. The data show that around 0.9 Ma the record changes from one dominated by Benguela Upwelling to one dominated by Agulhas Leakage. Our results show that over the last 0.5 Ma there is a consistent pattern observed in the timing of SST and salinity changes, whereby both variables increase in advance of the deglaciations as recorded by benthic $\delta^{18}$O. The evidence for Agulhas warming includes the early SST warming preceding the end of the interglacial in the $\delta^{18}$O record, as well as increased salinity and warming in the TEX$_{86}$ record

In contrast, the chlorin and dinoflagellate records highlighted changes towards the end of interglacials which might be associated with more expansive upwelling cells. Elevated chlorin concentrations, and low resolution dinoflagellate assemblage data sets, suggest that the Benguela upwelling system may have had short-lived influences over the site during the transitions to glacial conditions.

Given the interaction between atmospheric circulation and both upwelling and Agulhas Leakage in controlling the surface ocean circulation in the SE Atlantic, the data presented here suggest that the transitions into and out of glaciations seem likely to have been influenced by shifting wind systems in the SE Atlantic region. The long-term decline in pigment peak intensity suggests a lessening influence of the Benguela upwelling over time at ODP 1087. However there still remain questions about what the possible impacts of this major reorganization of the southeast Atlantic Ocean are on the global climate system both over the long timescale and the glacial-interglacial timescales. These will be explored in the next chapter.

# Chapter 8 Conclusions

## 8.1 Conclusions

The aim of this thesis was to understand how the Southeast Atlantic Ocean interacted with major climate changes over the last 3.5 Million years of Earth history. This is important because a number of oceanic systems come together in the southeast Atlantic Ocean (ACC, Agulhas Current, Agulhas Leakage, AAIW, and Benguela Upwelling). Through their interactions, they are thought to have major influences on the global ocean circulation and therefore the global climate. Even small changes in this part of the ocean may have an inordinate impact downstream, it is important to understand how these currents change in response to major climate transitions.

The first objective was to reconstruct sea surface temperatures (SSTs), and other climatic variables in a key gateway of the ocean (the SE Atlantic) in order to determine ocean circulation change over the last 3.5 Ma. To meet the thesis aim, a marine sediment core, ODP 1087, was analysed. ODP 1087 is located in the Southeast Atlantic at the confluence of these currents. A full 3.5 million year sea surface temperature record was produced using the $U^K_{37}$' index. Additional temperature and biomarker proxies (TEX$_{86}$, chlorins, and *n*-alkane,) were gathered to understand terrestrial input, changes in primary productivity and benthic temperature change. Stable isotopes were used to understand both changes in the surface ocean and bottom water conditions. Finally, analyses of microfossil assemblages were used to understand changes in the water masses affecting the core site. Together, all of these proxies allowed a full picture of the hydrography that occurred at the ODP 1087 site to be reconstructed between 0-3.5 Ma. Therefore the first objective was achieved.

The second objective was to understand the timing of the start and intensification of the Agulhas Leakage and whether or not this occurred during times of global climate transition. During the Pliocene and early Pleistocene there is no evidence of Agulhas Leakage. Instead all of the proxies indicate a weaker Agulhas Leakage during this time. An exponential increase of temperature at ODP 1087 started at 0.9 Ma. This is interpreted as a reflection of the onset of Agulhas Leakage affecting ODP 1087, and a beginning to the characteristic early deglacial warming pattern starting at 0.9 Ma. These dates are close to what has been seen in studies of the MPT and indicate that there is a link between changes in the dominant global cycles and the strengthening of the Agulhas Leakage. Finally, since 0.6 Ma the increasing maximum interglacial temperatures suggest there has been an intensification of Agulhas Leakage during this period. This may be connected with the start of the so called 'superinterglacials' although the ODP 1087 record raises questions about this characterisation. Finally no

evidence to support the idea (Bard and Rickaby, 2009) that the Agulhas Leakage was "cut off" by the ACC was observed. Therefore by achieving the second objective it has been shown that the modern Agulhas Leakage was only established around 0.9 Ma.

The third objective was to reconstruct SSTs and indicators of surface production and other oceanographic variables in order to assess the position and intensity of the Benguela Upwelling and to understand if the timing of these changes were related to global climate change. The record shows that before the 0.9 Ma the site was dominated by the higher productivity waters of the Benguela Upwelling. Surprisingly, this includes the Pliocene where previous research suggested that there was no upwelling present (Dekens *et al.*, 2007a; Etourneau *et al.*, 2009). Rather, the data from ODP 1087 strongly implies that there was upwelling but the locus of upwelling has shifted southward. Then, between 3.0 and 2.2 Ma the upwelling started migrating northward. There is also evidence of cooling of the upwelling and expansion of the Upwelling system during global cold periods such as the M2, KM2, 2.8 Ma and between 2.0 and 17 Ma. During the last of these there is evidence that the upwelling reached its greatest extend. Finally, in the last 0.5 Ma the upwelling is argued to have expanded at the end of interglacial periods. Therefore objective two was achieved as well showing a much longer existence of the Benguela Upwelling then has previously been thought.

The final objective was to compare the reconstructed changes in ocean circulation at ODP 1087 to the major coolings in the Earth's climate over the last 3.5 Ma in order to assess what role, if any, the Southeast Atlantic Ocean played in these changes. Understanding how the local patterns and trends at ODP 1087 might be linked to the global climate changes has shed some interesting light on the assumptions about global climate change over the last 3.5 Ma. As stated above, ODP 1087 did not respond to major northern hemisphere changes such as the onset of northern hemisphere glaciation. In fact, the only response to this event seems to be a short-lived cooling at ~ 2.8 Ma, which is evidence for short-term expansion of the Benguela upwelling as observed during the earlier M2 and KM2 stages. These three events seem to be reflecting upwelling expansion due to changes in the local wind forcings, and cooling of the AAIW that provides water to the upwelling system. The fact that this cooling occurs at the same time as beginning of northern hemisphere glaciation suggests a possible link to the cooling of intermediate waters and changes in the global ocean currents at this time though theorised links between changes in bottom water temperatures and the AMOC. In fact all of the major climate transitions between 3.5 and 0.9 Ma seem to be related to times of changes in the extent and temperature of

upwelling at ODP 1087. This suggests that these changes are related to global climate changes during this period.

Then, after 0.9 Ma, the ODP 1087 record the average SST starts warming and interglacial SST increase as well after 0.6 Ma (excluding MIS 10), whereas most other globally distributed SST records either cool or remain stable during this period (McClymont *et al.*, 2013). The organization of the modern Southeast Atlantic oceanic system that occurs around 0.9 Ma occurs alongside an important shift in the global climate (the MPT), and Chapter 8 discussed the potential for changes in southeast Atlantic to have had global impacts via the thermohaline circulation system. The establishment and strengthening of the modern Agulhas leakage is linked to changes in the thermohaline circulation and the change to 100 ka cycles. It suggests that there could be a link between the establishment and continued changes of the modern Southeastern Atlantic Ocean and the establishment of the modern climate regime.

There are three major findings from the ODP 1087 record. First, changes in Antarctica play a role in controlling changes in the Southeast Atlantic. This means that changes in Antarctic ice may play a more important role in affecting the global climate than has previously been suggested. Second, the core shows a more complex record of cooling then has previously been seen. Significantly it suggests a combination of gradual change punctuated by major cooling events. This perhaps implies that, while the record seen in the ODP 1087 is a reflection of local changes, those changes might have global impacts. Finally, there are strong indicates of a connection between the establishment of the modern Agulhas leakage system and the 100ka cycles and establishment of a more efficient AMOC. Therefore by achieving the final objective sheds light on major climate transition and suggests that changes in the southeast Atlantic might have influenced changes in the global climate regime. Therefore all together this thesis has gone a long way towards achieving the aim set out at the beginning.

## 8.2 Future Work

There is more work that could be done to try to improve the record presented here. First, there are a number of data sets that could be improved with additional data. Most importantly would be to improvements to the age model between 3.0 and 1.5 Ma are required. Right now the age model is based on the original shipboard age model, while the rest of the record has been tuned to the benthic $\delta^{18}O$ record. Other problems

include the lack of *n*-alkane data for this period, which means that it cannot be determined if the trend in increasing *n*-alkane is coupled to the MDM. Additional data sets would help improve some of these gaps in the record.

There are additional data sets that would help illuminate the changes seen in the core. The importance of changes in the bottom water means that it would be useful to have some estimation of the bottom water temperatures, especially in light of some of the recent studies on benthic temperature estimates. Preliminary work shows a potential for these reconstructions to be possible. Also, because there are currently no direct proxies for the MDM, a study of diatoms in the ODP 1087 record would be useful. Also a record of biological silica might be useful. Although the initial reports suggested that there was not evidence of increasing biologic silica at site ODP 1087 the work here suggests that there might be change in the diatom component of the site. Therefore it would be good to do a more detailed study of biogenic to confirm the initial findings or reject them. It would also help understand the dynamics of the southern Bengula upwelling which in this study has been shown to be complex.

There are a number of recent proxy developments that might help better identify changes in the system. First of all recent work has been done in identifying new salinity proxies. While for this core has a salinity record developed for it this has only been done for the Pleistocene. It also is not done using Mg/Ca which is the ideal temperature proxy to use to do the reconstruction. There are also some questions about the accuracy of the proxy. One of the best of these new salinity proxies is the Dδ of Alkenones which has been shown to respond to changes in salinity. This would be especially useful for this site because it is dominated by high amounts of alkenones. Therefore it may be useful to use these to reconstruct salinity at the site. Finally given the high amount of alkenones in this core it also may be an excellent site to test other alkenone proxies such as those for the $CO^2$

There is also a number of new proxies that might help our understanding of ocean current changes. Understanding how currents change and shift is one of the biggest questions currently in climate change research. While this thesis has used a number of lines of evidence to infer current changes in the southeast Atlantic. Also some attempt was used to tie these changes to changes in the thermohaline circulation. The issue is there is a lack of information about past changes in currents and very little work has been done on the longer time scales discussed in this thesis. However there are a number of new methodologies to do this. First of all at short time scales there is d14C radio carbon dating. This can be used to track the distance particles move latterly

and help identify changes in the strength of various currents.  However given the sedimentation rate for the core this might not be the ideal proxies for ODP 1087.  A better option might be neodymium isotopes.  Neodymium isotopes have shown to vary depending on the oceanic source of the isotopes.  Therefore they have begun to be used to track currents changes in the ocean.  The advantage is that they do not decay over time and have been shown to be stable over long periods of time.  Therefore they could help define change in the thermohaline circulation and how the Agulhas leakage chanes effect the global current.

There are a number of additional projects that would help with the understanding of the ODP 1087 record.  One of these would be to extend the record back to about 5 Ma.  This timeframe marks the establishment of the circumpolar current and theoretically the Agulhas Leakage.  Understanding when the salt imbalance and Agulhas Leakage began might help understand when the modern circulation system emerged.  It would also be helpful to do more small scale modelling to understand how the wind field develops around the Southeast Atlantic.  This would also provide more accurate evidence for the shifting currents during this time.  Additionally, it would be useful to have additional cores across the Agulhas Leakage path.  Right now all of the records from the Atlantic Ocean come from the edges of the leakage zone.  Given the hypothesized shifts that happened in the last 3.5 Ma, it would be useful to track the changes more directly.  Therefore, while the ODP 1087 record provides good evidence for climate change over the last 3.5 Ma, there is still more work that could supplement the data in the core and further test the arguments made in this paper.

Finally it would be useful to study other areas of the ocean to confirm some of the findings of this study.  First it would be useful to see if the other major oceanic upwelling zones behave the same way as the Bengula upwelling.  It is important to understand if changes seen in these systems is a result of shifts in the local wind fields like in the Bengula current or an actual change in in the intensity of upwelling.  Finally it would be useful to track changes upstream where the Agulhas leakage merges with the thermohaline circulation.  This is especially true of the Brazil margin which is a relatively unknown system especially over the time periods over which this study was done.  Therefore a similar biomarker study of this region might be valuable in linking changes in Agulhas leakage and the thermohaline circulation.  Finally given the role changes in Antarctica have on this core more work needs be done understanding changes in sea ice and changes in the circumpolar currents.  While the biomarkers and proxies don't really exist for this at the current time a lot of work is being done in trying

to better understand changes in sea ice around Antarctica. All of these will help extend the work done in this study

# Appendix: Data sets

A1: U$^{K}_{37}$' temperatures from ODP 1087A.  Nomenclature is as follows Core- section (archive (a) or working (w)- depth from top of section

| Name | Age (ka) | U$^{K}_{37}$' | Temperature (°C) |
|---|---|---|---|
| 01-01a-015 | 3.00 | 0.6666 | 18.99 |
| 01-01a-020 | 4.00 | 0.6686 | 19.05 |
| 01-01a-030 | 6.00 | 0.6516 | 18.53 |
| 01-01a-045 | 9.00 | 0.6846 | 19.53 |
| 01-01a-055 | 12.00 | 0.6392 | 18.16 |
| 01-01a-060 | 15.00 | 0.6348 | 18.02 |
| 01-01a-070 | 18.17 | 0.6293 | 17.86 |
| 01-01a-080 | 23.23 | 0.6206 | 17.60 |
| 01-01-085 | 27.10 | 0.6183 | 17.52 |
| 01-01a-090 | 29.69 | 0.6431 | 18.28 |
| 01-01a-095 | 32.92 | 0.6461 | 18.37 |
| 01-01a-100 | 36.15 | 0.6173 | 17.49 |
| 01-01a-105 | 39.38 | 0.6126 | 17.35 |
| 01-01a-110 | 42.61 | 0.6162 | 17.46 |
| 01-01a-116 | 45.85 | 0.5821 | 16.43 |
| 01-01a-125 | 52.31 | 0.6018 | 17.03 |
| 01-01a-130 | 55.54 | 0.6485 | 18.44 |
| 01-01a-135 | 58.77 | 0.6308 | 17.90 |
| 01-02a-000 | 62.00 | 0.6769 | 19.30 |
| 01-02a-005 | 66.20 | 0.6891 | 19.67 |
| 01-02a-010 | 70.40 | 0.6741 | 19.22 |
| 01-02a-015 | 74.60 | 0.6732 | 19.19 |
| 01-02a-020 | 78.80 | 0.6931 | 19.79 |
| 01-02a-025 | 83.00 | 0.6642 | 18.92 |
| 01-02a-035 | 84.60 | 0.7141 | 20.43 |
| 01-02-045 | 86.20 | 0.7312 | 20.95 |
| 01-02a-055 | 88.50 | 0.6683 | 19.04 |
| 01-02a-065 | 91.50 | 0.6723 | 19.16 |
| 01-02a-075 | 94.50 | 0.7170 | 20.52 |
| 01-02a-085 | 99.00 | 0.6892 | 19.67 |
| 01-02a-095 | 105.00 | 0.6899 | 19.69 |
| 01-02A-110 | 109.75 | 0.6861 | 19.58 |
| 01-02-120 | 111.25 | 0.6940 | 19.82 |
| 01-02a-130 | 112.75 | 0.7246 | 20.75 |
| 01-02a-140 | 114.25 | 0.7184 | 20.56 |
| 01-03a-000 | 120.00 | 0.7673 | 22.04 |
| 01-03a-010 | 127.50 | 0.7755 | 22.29 |
| 01-03a-015 | 130.00 | 0.7209 | 20.63 |
| 01-03a-020 | 135.50 | 0.7150 | 20.45 |
| 01-03A-030 | 138.33 | 0.6368 | 18.08 |
| 01-03A-040 | 142.13 | 0.6380 | 18.12 |
| 01-03a-050 | 146.38 | 0.6217 | 17.63 |
| 01-03A-055 | 148.50 | 0.6258 | 17.75 |
| 01-03a-060 | 150.63 | 0.6720 | 19.15 |
| 01-03a-065 | 152.75 | 0.6183 | 17.52 |
| 01-03A-070 | 154.88 | 0.5384 | 15.10 |
| 01-03a-075 | 157.00 | 0.6408 | 18.21 |
| 01-03a-080 | 160.00 | 0.5999 | 16.97 |
| 01-03a-085 | 161.25 | 0.6221 | 17.64 |

| | | | |
|---|---|---|---|
| 01-03a-090 | 163.38 | 0.6113 | 17.31 |
| 01-03a-095 | 165.50 | 0.6369 | 18.09 |
| 01-03a-100 | 167.63 | 0.5753 | 16.22 |
| 01-03A-105 | 169.75 | 0.6825 | 19.47 |
| 01-03a-110 | 171.88 | 0.6640 | 18.91 |
| 01-03a-115 | 174.00 | 0.6628 | 18.87 |
| 01-03a-120 | 179.40 | 0.6289 | 17.85 |
| 01-03a-125 | 184.80 | 0.6697 | 19.08 |
| 01-03a-130 | 190.20 | 0.6879 | 19.63 |
| 01-04a-000 | 201.00 | 0.6812 | 19.43 |
| 01-04a-020 | 218.75 | 0.6852 | 19.55 |
| 01-04a-025 | 221.38 | 0.6951 | 19.85 |
| 01-04a-035 | 224.00 | 0.6094 | 17.25 |
| 01-04a-040 | 228.00 | 0.6791 | 19.37 |
| 01-04a-047 | 232.00 | 0.7680 | 22.06 |
| 01-04a-055 | 240.00 | 0.7184 | 20.56 |
| 01-04a-070 | 243.45 | 0.6777 | 19.32 |
| 01-04a-085 | 246.90 | 0.5924 | 16.74 |
| 01-04a-095 | 249.20 | 0.5685 | 16.02 |
| 01-04a-105 | 251.50 | 0.5549 | 15.60 |
| 01-04a-126 | 256.10 | 0.5310 | 14.88 |
| 01-04a-130 | 257.25 | 0.6497 | 18.48 |
| 01-04a-135 | 258.40 | 0.6672 | 19.01 |
| 01-04a-145 | 260.70 | 0.6471 | 18.40 |
| 01-05a-015 | 265.30 | 0.6290 | 17.85 |
| 01-05a-026 | 267.60 | 0.6588 | 18.75 |
| 01-05a-035 | 269.90 | 0.6054 | 17.13 |
| 01-05a-056 | 274.50 | 0.5096 | 14.23 |
| 01-05a-066 | 276.80 | 0.6039 | 17.09 |
| 01-05a-076 | 279.10 | 0.5452 | 15.31 |
| 01-05a-086 | 281.40 | 0.5459 | 15.33 |
| 01-05a-106 | 286.00 | 0.6207 | 17.60 |
| 01-05a-116 | 292.00 | 0.6336 | 17.99 |
| 01-05a-121 | 295.00 | 0.6174 | 17.50 |
| 01-05a-126 | 304.00 | 0.5376 | 15.08 |
| 01-05a-131 | 313.00 | 0.5364 | 15.04 |
| 01-05a-141 | 315.00 | 0.6230 | 17.67 |
| 01-05a-146 | 316.80 | 0.6346 | 18.02 |
| 01-06a-001 | 318.60 | 0.6679 | 19.03 |
| 01-06a-006 | 320.40 | 0.6110 | 17.30 |
| 01-06a-011 | 322.20 | 0.6634 | 18.89 |
| 01-06a-016 | 324.00 | 0.5858 | 16.54 |
| 01-06a-021 | 325.67 | 0.6777 | 19.32 |
| 01-06a-026 | 327.33 | 0.6798 | 19.39 |
| 01-06A-041 | 338.00 | 0.6590 | 18.76 |
| 01-06A-051 | 347.00 | 0.6615 | 18.83 |
| 02-01a-020 | 361.89 | 0.5558 | 15.63 |
| 02-01a-036 | 366.33 | 0.5831 | 16.46 |
| 02-01-046 | 369.11 | 0.6435 | 18.29 |
| 02-01a-061 | 371.89 | 0.5917 | 16.72 |
| 02-01a-076 | 376.91 | 0.6169 | 17.46 |
| 02-01a-091 | 379.52 | 0.6456 | 18.35 |
| 02-01a-121 | 386.80 | 0.6399 | 18.15 |
| 02-01a-137 | 391.26 | 0.6597 | 18.78 |

| | | | |
|---|---|---|---|
| 02-02a-000 | 395.83 | 0.6997 | 19.99 |
| 02-02a-021 | 400.39 | 0.6761 | 19.27 |
| 02-02a-036 | 403.39 | 0.6905 | 19.70 |
| 02-02a-051 | 404.56 | 0.6812 | 19.43 |
| 02-02A-071 | 406.11 | 0.6622 | 18.85 |
| 02-02a-081 | 406.89 | 0.6835 | 19.50 |
| 02-02a-092 | 407.67 | 0.6759 | 19.27 |
| 02-02a-101 | 408.44 | 0.6796 | 19.38 |
| 02-02a-111 | 409.22 | 0.6783 | 19.34 |
| 02-02a-121 | 410.00 | 0.6834 | 19.50 |
| 02-02a-131 | 413.33 | 0.6733 | 19.19 |
| 02-02a-141 | 415.00 | 0.6734 | 19.17 |
| 02-03a-011 | 422.00 | 0.6605 | 18.80 |
| 02-03a-020 | 423.90 | 0.6699 | 19.09 |
| 02-03a-031 | 424.50 | 0.6617 | 18.84 |
| 02-03a-041 | 425.50 | 0.6684 | 19.04 |
| 02-03a-051 | 426.50 | 0.6497 | 18.48 |
| 02-03a-056 | 427.00 | 0.6967 | 19.90 |
| 02-03a-061 | 428.25 | 0.6913 | 19.74 |
| 02-03a-066 | 429.50 | 0.6724 | 19.17 |
| 02-03a-071 | 430.75 | 0.6869 | 19.60 |
| 02-03a-076 | 432.00 | 0.6590 | 18.76 |
| 02-03a-080 | 433.00 | 0.6253 | 17.74 |
| 02-03a-085 | 434.00 | 0.5955 | 16.83 |
| 02-03a-091 | 435.00 | 0.5871 | 16.58 |
| 02-03a-096 | 436.00 | 0.5755 | 16.23 |
| 02-03a-101 | 437.00 | 0.5830 | 16.46 |
| 02-03a-106 | 438.40 | 0.5850 | 16.51 |
| 02-03a-111 | 439.80 | 0.5749 | 16.21 |
| 02-03a-116 | 441.60 | 0.5838 | 16.48 |
| 02-03a-120 | 443.40 | 0.5658 | 15.93 |
| 02-03a-126 | 445.20 | 0.6090 | 17.24 |
| 02-03a-131 | 447.00 | 0.5762 | 16.25 |
| 02-03a-136 | 452.20 | 0.5936 | 16.77 |
| 02-04a-000 | 457.40 | 0.5263 | 14.74 |
| 02-04a-006 | 462.60 | 0.6058 | 17.14 |
| 02-04a-011 | 467.80 | 0.6196 | 17.56 |
| 02-04a-030 | 475.00 | 0.6458 | 18.36 |
| 02-04a-036 | 486.00 | 0.6733 | 19.19 |
| 02-04a-045 | 494.67 | 0.6271 | 17.79 |
| 02-04a-061 | 509.25 | 0.6506 | 18.50 |
| 02-04a-076 | 531.00 | 0.6263 | 17.77 |
| 02-04a-091 | 534.75 | 0.6243 | 17.71 |
| 02-04a-106 | 569.43 | 0.5946 | 16.81 |
| 02-04a-121 | 579.71 | 0.6145 | 17.41 |
| 02-04a-136 | 590.00 | 0.4428 | 12.20 |
| 02-04a-145 | 596.86 | 0.6266 | 17.78 |
| 06-01w-141 | 1572.16 | 0.6572 | 18.70 |
| 06-01w-148 | 1574.68 | 0.7021 | 20.06 |
| 06-02w-068 | 1599.03 | 0.6814 | 19.44 |
| 06-02w-138 | 1622.92 | 0.7064 | 20.19 |
| 06-03w-025 | 1635.90 | 0.6380 | 18.12 |
| 06-03w-083 | 1655.80 | 0.7405 | 21.23 |
| 06-03w-103 | 1662.73 | 0.7170 | 20.52 |

| | | | |
|---|---|---|---|
| 06-04w-066 | 1694.44 | 0.6970 | 19.91 |
| 06-05w-008 | 1719.00 | 0.7055 | 20.17 |
| 06-05w-053 | 1731.17 | 0.6842 | 19.52 |
| 06-05w-145 | 1755.82 | 0.6397 | 18.17 |
| 06-06w-042 | 1768.30 | 0.5873 | 16.58 |
| 06-06w-135 | 1793.26 | 0.6239 | 17.69 |
| 06-07w-032 | 1805.74 | 0.6351 | 18.03 |
| 07-01w-076 | 1830.79 | 0.6926 | 19.78 |
| 07-01w-123 | 1843.36 | 0.7119 | 20.36 |
| 07-02w-065 | 1868.14 | 0.6516 | 18.53 |
| 07-04w-013 | 1935.55 | 0.6943 | 19.83 |
| 07-04w-137 | 1969.95 | 0.6283 | 17.83 |
| 07-05w-023 | 1982.84 | 0.6517 | 18.53 |
| 07-05w-101 | 2008.10 | 0.6944 | 19.83 |
| 07-05w-139 | 2020.46 | 0.7090 | 20.27 |
| 07-06w-066 | 2045.44 | 0.6753 | 19.25 |
| 7-06w-105 | 2058.07 | 0.6319 | 17.94 |
| 07-07w-032 | 2083.11 | 0.7087 | 20.26 |
| 08-01w-021 | 2095.53 | 0.7200 | 20.61 |
| 08-01w-137 | 2133.19 | 0.7326 | 20.99 |
| 08-02w-069 | 2159.75 | 0.7365 | 21.10 |
| 08-02w-112 | 2173.67 | 0.7685 | 22.07 |
| 08-03w-038 | 2198.39 | 0.6698 | 19.09 |
| 8-03w-072 | 2209.18 | 0.7139 | 20.42 |
| 08-03w-145 | 2232.87 | 0.7466 | 21.41 |
| 08-04w-035 | 2245.77 | 0.6989 | 19.97 |
| 08-04w-114 | 2271.46 | 0.7194 | 20.59 |
| 08-05w-005 | 2284.25 | 0.7356 | 21.08 |
| 08-05w-082 | 2309.34 | 0.7071 | 20.22 |
| 08-05w-119 | 2321.65 | 0.7229 | 20.69 |
| 08-06w-047 | 2347.01 | 0.6570 | 18.70 |
| 08-06w-088 | 2360.07 | 0.6716 | 19.14 |
| 08-07w-016 | 2385.27 | 0.7022 | 20.07 |
| 09-04w-079 | 2422.02 | 0.7363 | 21.10 |
| 09-01w-118 | 2434.49 | 0.7787 | 22.39 |
| 09-02w-045 | 2459.58 | 0.6896 | 19.68 |
| 09-02w-084 | 2472.21 | 0.6137 | 17.39 |
| 09-03w-109 | 2531.63 | 0.7199 | 20.60 |
| 09-03w-131 | 2541.19 | 0.7217 | 20.66 |
| 09-04w-087 | 2563.27 | 0.6981 | 19.94 |
| 09-06w-041 | 2600.55 | 0.7393 | 21.19 |
| 09-06w-125 | 2612.78 | 0.7465 | 21.41 |
| 10-01w-028 | 2650.11 | 0.7132 | 20.40 |
| 10-03w-048 | 2675.08 | 0.7428 | 21.30 |
| 10-03w-131 | 2687.51 | 0.6972 | 19.91 |
| 10-05w-002 | 2712.46 | 0.7261 | 20.79 |
| 10-05w-087 | 2724.98 | 0.7305 | 20.92 |
| 10-06w-107 | 2750.01 | 0.6805 | 19.41 |
| 11-01w-042 | 2762.51 | 0.6314 | 17.92 |
| 11-02w-014 | 2787.85 | 0.7412 | 21.25 |
| 11-02w-101 | 2800.69 | 0.7618 | 21.87 |
| 11-03w-101 | 2825.75 | 0.7446 | 21.35 |
| 11-04w-014 | 2837.95 | 0.7747 | 22.26 |
| 11-05w-020 | 2862.64 | 0.7241 | 20.73 |

| | | | |
|---|---|---|---|
| 11-05w-115 | 2875.12 | 0.7950 | 22.88 |
| 11-07w-005 | 2900.14 | 0.6966 | 19.90 |
| 12-02w-091 | 2937.69 | 0.7225 | 20.68 |
| 12-03w-036 | 2950.14 | 0.7392 | 21.19 |
| 12-04w-075 | 2975.10 | 0.7485 | 21.47 |
| 12-05w-020 | 2987.60 | 0.7158 | 20.48 |
| 12-06w-064 | 3000.00 | 0.7564 | 21.71 |
| 12-07w-013 | 3004.58 | 0.7758 | 22.30 |
| 13-01w-050 | 3008.81 | 0.7022 | 20.07 |
| 13-01w-148 | 3017.28 | 0.7338 | 21.02 |
| 13-02w-097 | 3021.51 | 0.7738 | 22.24 |
| 13-03w-076 | 3025.74 | 0.7424 | 21.28 |
| 13-04w-145 | 3029.97 | 0.7540 | 21.64 |
| 13-05w-000 | 3034.20 | 0.7519 | 21.57 |
| 13-05w-020 | 3035.04 | 0.7403 | 21.22 |
| 13-05w-040 | 3035.89 | 0.7836 | 22.53 |
| 13-05w-060 | 3036.74 | 0.7369 | 21.12 |
| 13-05w-080 | 3037.58 | 0.7215 | 20.65 |
| 13-05w-093 | 3038.43 | 0.7382 | 21.16 |
| 13-05w-100 | 3039.13 | 0.7067 | 20.20 |
| 13-05w-120 | 3039.84 | 0.7375 | 21.14 |
| 13-05w-140 | 3040.54 | 0.7255 | 20.77 |
| 13-06w-000 | 3041.25 | 0.7321 | 20.97 |
| 13-06w-020 | 3041.95 | 0.7135 | 20.41 |
| 13-06w-042 | 3042.66 | 0.7099 | 20.30 |
| 13-06w-080 | 3043.72 | 0.7302 | 20.91 |
| 13-06w-100 | 3044.78 | 0.6911 | 19.73 |
| 13-06w-120 | 3045.83 | 0.7467 | 21.41 |
| 13-06w-140 | 3046.89 | 0.7382 | 21.16 |
| 13-07w-010 | 3048.91 | 0.7392 | 21.19 |
| 13-07w-030 | 3050.93 | 0.7355 | 21.08 |
| 13-07w-050 | 3052.95 | 0.7364 | 21.10 |
| 14-01w-005 | 3055.00 | 0.7570 | 21.73 |
| 14-01w-025 | 3057.42 | 0.7559 | 21.69 |
| 14-01w-065 | 3060.00 | 0.7718 | 22.18 |
| 14-01w-085 | 3062.78 | 0.7319 | 20.97 |
| 14-01w-105 | 3065.56 | 0.7338 | 21.02 |
| 14-01w-125 | 3068.33 | 0.7654 | 21.98 |
| 14-01w-145 | 3071.11 | 0.7498 | 21.51 |
| 14-02w-015 | 3073.89 | 0.7877 | 22.66 |
| 14-02w-035 | 3076.67 | 0.7448 | 21.29 |
| 14-02w-055 | 3079.44 | 0.7528 | 21.60 |
| 14-02w-075 | 3082.22 | 0.7721 | 22.18 |
| 14-02w-095 | 3085.00 | 0.7986 | 22.99 |
| 14-02w-015 | 3088.33 | 0.7877 | 22.66 |
| 14-02w-135 | 3091.67 | 0.7635 | 21.93 |
| 14-03w-005 | 3095.00 | 0.7228 | 20.69 |
| 14-03w-025 | 3098.33 | 0.7401 | 21.22 |
| 14-03w-065 | 3105.00 | 0.7093 | 20.28 |
| 14-03w-085 | 3108.33 | 0.7265 | 20.80 |
| 14-03w-165 | 3111.67 | 0.7035 | 20.11 |
| 14-03w-125 | 3115.00 | 0.6569 | 18.69 |
| 14-03w-165 | 3118.33 | 0.7035 | 20.11 |
| 14-04w-015 | 3121.67 | 0.7270 | 20.82 |

| | | | |
|---|---|---|---|
| 14-04w-035 | 3125.00 | 0.6666 | 18.99 |
| 14-04w-055 | 3128.33 | 0.6705 | 19.10 |
| 14-04w-095 | 3135.00 | 0.6428 | 18.27 |
| 14-04w-115 | 3137.86 | 0.7113 | 20.34 |
| 14-04w-135 | 3143.57 | 0.7383 | 21.16 |
| 14-05w-025 | 3146.43 | 0.7649 | 21.97 |
| 14-05w-045 | 3149.29 | 0.7556 | 21.68 |
| 14-05w-065 | 3152.14 | 0.7728 | 22.20 |
| 14-05w-085 | 3155.00 | 0.7932 | 22.82 |
| 14-05w-103 | 3156.43 | 0.7461 | 21.40 |
| 14-05w-103 | 3157.86 | 0.7461 | 21.40 |
| 14-05w-145 | 3159.29 | 0.7868 | 22.63 |
| 14-06w-015 | 3160.71 | 0.7647 | 21.96 |
| 14-06w-035 | 3162.14 | 0.7424 | 21.29 |
| 14-06w-055 | 3163.57 | 0.7098 | 20.30 |
| 14-06w-075 | 3165.00 | 0.7412 | 21.25 |
| 14-06w-135 | 3169.29 | 0.6924 | 19.77 |
| 14-07w-005 | 3170.71 | 0.7130 | 20.39 |
| 14-07w-025 | 3172.14 | 0.6908 | 19.72 |
| 14-07w-045 | 3173.57 | 0.6947 | 19.84 |
| 15-01w-015 | 3175.00 | 0.6742 | 19.22 |
| 15-01w-035 | 3177.00 | 0.7412 | 21.25 |
| 15-01w-055 | 3179.00 | 0.7530 | 21.61 |
| 15-01w-075 | 3181.00 | 0.7664 | 22.01 |
| 15-01w-096 | 3183.00 | 0.7184 | 20.56 |
| 15-01w-115 | 3185.00 | 0.7429 | 21.30 |
| 15-01w-135 | 3187.00 | 0.7588 | 21.78 |
| 15-03w-005 | 3189.00 | 0.7458 | 21.39 |
| 15-02w-025 | 3191.00 | 0.7138 | 20.42 |
| 15-02w-045 | 3193.00 | 0.7326 | 20.99 |
| 15-02w-065 | 3195.00 | 0.7234 | 20.71 |
| 15-02w-085 | 3197.00 | 0.7013 | 20.04 |
| 15-02w-105 | 3199.00 | 0.6923 | 19.77 |
| 15-02w-125 | 3201.00 | 0.7272 | 20.82 |
| 15-02w-145 | 3203.00 | 0.6895 | 19.68 |
| 15-03w-015 | 3205.00 | 0.7260 | 20.79 |
| 15-03w-035 | 3207.00 | 0.7345 | 21.04 |
| 15-03w-055 | 3209.00 | 0.7140 | 20.43 |
| 15-03w-075 | 3211.00 | 0.7321 | 20.97 |
| 16-03w-095 | 3213.00 | 0.7237 | 20.72 |
| 15-03w-115 | 3215.00 | 0.7405 | 21.23 |
| 15-03w-135 | 3217.00 | 0.7113 | 20.34 |
| 15-04w-005 | 3219.00 | 0.7282 | 20.86 |
| 15-04w-045 | 3223.00 | 0.7459 | 21.39 |
| 15-04w-065 | 3225.00 | 0.7246 | 20.75 |
| 15-04w-085 | 3227.00 | 0.7032 | 20.10 |
| 15-04w-105 | 3229.00 | 0.7424 | 21.28 |
| 15-04w-125 | 3231.00 | 0.7895 | 22.71 |
| 15-04w-145 | 3233.00 | 0.7362 | 21.10 |
| 15-05w-015 | 3235.00 | 0.7095 | 20.29 |
| 15-05w-035 | 3237.00 | 0.7377 | 21.14 |
| 15-05w-055 | 3239.00 | 0.7137 | 20.42 |
| 15-05w-075 | 3241.00 | 0.6671 | 19.00 |
| 15-05w-095 | 3243.00 | 0.7581 | 21.76 |

| | | | |
|---|---|---|---|
| 15-05w-115 | 3245.00 | 0.7453 | 21.37 |
| 15-05w-135 | 3250.56 | 0.7513 | 21.55 |
| 15-06w-005 | 3256.11 | 0.7410 | 21.24 |
| 15-06w-025 | 3261.67 | 0.6974 | 19.92 |
| 15-06w-045 | 3267.22 | 0.6768 | 19.30 |
| 15-06w-065 | 3272.78 | 0.6697 | 19.08 |
| 15-06w-085 | 3278.33 | 0.6624 | 18.86 |
| 15-06w-106 | 3283.89 | 0.6412 | 18.22 |
| 15-06w-145 | 3295.00 | 0.6775 | 19.32 |
| 15-07w-015 | 3304.00 | 0.6639 | 18.91 |
| 15-07w-035 | 3313.00 | 0.6432 | 18.28 |
| 15-07w-055 | 3322.00 | 0.6657 | 18.96 |
| 16-01w-025 | 3331.00 | 0.7351 | 21.06 |
| 16-01w-045 | 3340.00 | 0.7000 | 20.00 |
| 16-01w-065 | 3343.33 | 0.7007 | 20.02 |
| 16-01w-085 | 3346.67 | 0.7102 | 20.31 |
| 16-01w-105 | 3350.00 | 0.7299 | 20.91 |
| 16-01w-125 | 3353.33 | 0.7506 | 21.53 |
| 16-01w-145 | 3356.67 | 0.7285 | 20.86 |
| 16-02w-015 | 3360.00 | 0.7297 | 20.90 |
| 16-02w-035 | 3363.33 | 0.7713 | 22.16 |
| 16-02w-055 | 3366.67 | 0.6939 | 19.81 |
| 16-02w-075 | 3370.00 | 0.7189 | 20.57 |
| 16-04w-095 | 3376.67 | 0.7371 | 21.12 |
| 16-02w-115 | 3380.00 | 0.6875 | 19.62 |
| 16-02w-135 | 3383.86 | 0.7418 | 21.27 |
| 16-03w-005 | 3387.73 | 0.7498 | 21.51 |
| 16-03w-025 | 3391.59 | 0.7590 | 21.79 |
| 16-03w-045 | 3395.45 | 0.7458 | 21.39 |
| 16-03w-065 | 3399.32 | 0.7609 | 21.85 |
| 16-03w-085 | 3403.18 | 0.7628 | 21.90 |
| 16-03w-105 | 3407.05 | 0.7571 | 21.73 |
| 16-03w-125 | 3410.91 | 0.7358 | 21.09 |
| 16-03w-145 | 3414.77 | 0.7235 | 20.71 |
| 16-04w-019 | 3418.64 | 0.6580 | 18.73 |
| 16-04w-035 | 3422.50 | 0.6992 | 19.98 |
| 16-04w-055 | 3426.36 | 0.6928 | 19.78 |
| 16-04w-075 | 3430.23 | 0.7560 | 21.70 |
| 16-04w-115 | 3434.09 | 0.6838 | 19.51 |
| 16-04w-135 | 3437.95 | 0.7385 | 21.17 |
| 16-05w-025 | 3445.68 | 0.7145 | 20.44 |
| 16-05w-045 | 3449.55 | 0.6990 | 19.97 |
| 16-05w-065 | 3453.41 | 0.7175 | 20.53 |
| 16-05w-085 | 3457.27 | 0.7188 | 20.57 |
| 16-05w-125 | 3465.00 | 0.6871 | 19.61 |
| 16-05w-145 | 3467.50 | 0.7502 | 21.52 |
| 16-06w-015 | 3470.00 | 0.7597 | 21.81 |
| 16-06w-035 | 3472.50 | 0.7747 | 22.26 |
| 16-06w-055 | 3475.00 | 0.7724 | 22.19 |
| 16-06w-076 | 3477.50 | 0.7589 | 21.79 |
| 16-06w-095 | 3480.00 | 0.7959 | 22.91 |
| 16-06w-115 | 3481.25 | 0.7777 | 22.36 |
| 16-06w-135 | 3482.50 | 0.8312 | 23.98 |
| 16-07w-005 | 3483.75 | 0.7683 | 22.07 |

| 16-07w-025 | 3485.00 | 0.7827 | 22.51 |

A2: U$^K_{37}$' temperatures from ODP 1087C. Nomenclature is as follows Core- section - depth from top of section

| Name | Age (ka) | U$^K_{37}$' | Temperature (ºC) |
|---|---|---|---|
| C2-04-055 | 309 | 0.602398 | 17.04 |
| C2-04-060 | 312.1429 | 0.685801 | 19.57 |
| C2-04-065 | 315.2857 | 0.647767 | 18.42 |
| C2-04-070 | 318.4286 | 0.632091 | 17.94 |
| C2-04-075 | 321.5714 | 0.626989 | 17.79 |
| C2-04-080 | 324.7143 | 0.677285 | 19.31 |
| C2-04-085 | 327.8571 | 0.663849 | 18.90 |
| C2-04-090 | 331 | 0.718639 | 20.56 |
| C2-04-095 | 332.4583 | 0.678016 | 19.33 |
| C2-04-100 | 333.9801 | 0.630441 | 17.89 |
| C2-04-105 | 335.5018 | 0.671182 | 19.13 |
| C2-04-110 | 337.0236 | 0.653756 | 18.60 |
| C2-04-115 | 338.5453 | 0.568828 | 16.03 |
| C2-04-120 | 340.067 | 0.459428 | 12.71 |
| C2-04-130 | 343.1105 | 0.417487 | 11.44 |
| C2-04-135 | 344.6322 | 0.497867 | 13.87 |
| C2-04-140 | 346.154 | 0.406695 | 11.11 |
| C2-04-145 | 347.6757 | 0.530108 | 14.85 |
| C2-05-005 | 349.1975 | 0.436483 | 12.01 |
| C2-05-010 | 350.7192 | 0.446523 | 12.32 |
| C2-05-015 | 352.2409 | 0.445776 | 12.30 |
| C2-05-020 | 353.7627 | 0.438181 | 12.07 |
| C2-05-025 | 355.2844 | 0.458185 | 12.67 |
| C2-05-030 | 356.8062 | 0.40732 | 11.13 |
| C2-05-035 | 358.3279 | 0.491997 | 13.70 |
| C2-05-040 | 359.8496 | 0.465795 | 12.90 |
| C2-05-045 | 361.3714 | 0.404117 | 11.03 |
| C2-05-050 | 362.8931 | 0.463323 | 12.83 |
| C2-05-055 | 364.4149 | 0.507595 | 14.17 |
| C2-05-060 | 366 | 0.546289 | 15.34 |
| C2-05-065 | 369.75 | 0.45846 | 12.68 |
| C2-05-070 | 373.5 | 0.502097 | 14.00 |
| C2-05-075 | 377.25 | 0.460689 | 12.75 |
| C2-05-080 | 381 | 0.603044 | 17.06 |

A3: Chlorin values for ODP 1087A

| Name | Age (ka) | 410 nm abs g$^{-1}$ |
|---|---|---|
| 01-01-015 | 3.17 | 0.21 |
| 01-01-020 | 4.00 | 0.02 |
| 01-01-030 | 6.00 | 0.14 |
| 01-01-045 | 10.00 | 0.12 |
| 01-01-055 | 12.04 | 0.22 |
| 01-01-060 | 14.00 | 0.16 |
| 01-01-070 | 17.26 | 0.14 |
| 01-01-080 | 24.50 | 0.14 |
| 01-01-085 | 30.00 | 0.18 |
| 01-01-090 | 35.50 | 0.15 |
| 01-01-095 | 41.00 | 0.18 |
| 01-01-100 | 46.50 | 0.13 |
| 01-01-105 | 52.00 | 0.16 |
| 01-01-110 | 54.00 | 0.10 |
| 01-01-115 | 56.00 | 0.14 |
| 01-01-125 | 60.00 | 0.11 |
| 01-01-130 | 62.00 | 0.12 |
| 01-01-135 | 64.00 | 0.12 |
| 01-02-000 | 70.00 | 0.15 |
| 01-02-005 | 72.00 | 0.07 |
| 01-02-010 | 74.00 | 0.09 |
| 01-02-015 | 76.00 | 0.12 |
| 01-02-020 | 78.00 | 0.13 |
| 01-02-025 | 80.00 | 0.14 |
| 01-02-035 | 82.71 | 0.20 |
| 01-02-045 | 85.00 | 0.13 |
| 01-02-055 | 88.14 | 0.19 |
| 01-02-065 | 90.86 | 0.16 |
| 01-02-085 | 96.29 | 0.12 |
| 01-02-095 | 99.00 | 0.16 |
| 01-02-110 | 107.00 | 0.17 |
| 01-02-120 | 111.00 | 0.29 |
| 01-02-130 | 112.42 | 0.12 |
| 01-02-140 | 116.00 | 0.12 |
| 01-03-000 | 120.08 | 0.08 |
| 01-03-010 | 124.08 | 0.13 |
| 01-03-015 | 126.00 | 0.10 |
| 01-03-020 | 128.00 | 0.07 |
| 01-03-030 | 130.00 | 0.10 |
| 01-03-040 | 133.00 | 0.10 |
| 01-03-050 | 135.00 | 0.08 |
| 01-03-055 | 138.00 | 0.10 |
| 01-03-060 | 141.40 | 0.06 |
| 01-03-065 | 145.00 | 0.09 |
| 01-03-070 | 148.00 | 0.13 |
| 01-03-075 | 151.00 | 0.09 |
| 01-03-080 | 154.00 | 0.10 |
| 01-03-085 | 156.00 | 0.21 |
| 01-03-090 | 159.00 | 0.13 |
| 01-03-100 | 164.00 | 0.13 |
| 01-03-106 | 166.00 | 0.09 |

| | | |
|---|---|---|
| 01-03-110 | 168.50 | 0.14 |
| 01-03-115 | 171.00 | 0.12 |
| 01-03-120 | 177.00 | 0.29 |
| 01-03-130 | 213.56 | 0.16 |
| 01-04-000 | 214.95 | 0.07 |
| 01-04-020 | 218.75 | 0.07 |
| 01-04-030 | 224.25 | 0.16 |
| 01-04-035 | 227.00 | 0.15 |
| 01-04-040 | 229.75 | 0.13 |
| 01-04-047 | 233.60 | 0.16 |
| 01-04-055 | 238.00 | 0.08 |
| 01-04-070 | 240.40 | 0.16 |
| 01-04-085 | 243.28 | 0.11 |
| 01-04-095 | 245.84 | 0.17 |
| 01-04-105 | 248.39 | 0.16 |
| 01-04-115 | 251.00 | 0.14 |
| 01-04-126 | 254.00 | 0.21 |
| 01-04-135 | 256.00 | 0.18 |
| 01-04-145 | 258.62 | 0.06 |
| 01-05-005 | 261.00 | 0.15 |
| 01-05-006 | 261.00 | 0.15 |
| 01-05-015 | 264.00 | 0.09 |
| 01-05-026 | 266.00 | 0.09 |
| 01-05-035 | 269.00 | 0.15 |
| 01-05-056 | 274.00 | 0.12 |
| 01-05-056 | 274.00 | 0.13 |
| 01-05-066 | 277.00 | 0.19 |
| 01-05-076 | 279.00 | 0.21 |
| 01-05-086 | 282.00 | 0.19 |
| 01-05-096 | 284.00 | 0.19 |
| 01-05-106 | 287.00 | 0.14 |
| 01-05-111 | 290.00 | 0.20 |
| 01-05-116 | 293.00 | 0.20 |
| 01-05-121 | 296.00 | 0.14 |
| 01-05-126 | 300.00 | 0.19 |
| 01-05-131 | 303.00 | 0.32 |
| 01-05-136 | 306.00 | 0.24 |
| 01-05-141 | 309.00 | 0.25 |
| 01-05-146 | 312.00 | 0.21 |
| 01-06-001 | 315.00 | 0.14 |
| 01-06-006 | 319.00 | 0.15 |
| 01-06-012 | 322.00 | 0.10 |
| 01-06-016 | 325.00 | 0.15 |
| 01-06-021 | 328.41 | 0.08 |
| 01-06-041 | 334.00 | 0.16 |
| 01-06-051 | 336.00 | 0.20 |
| 02-01-031 | 368.33 | 0.32 |
| 02-01-061 | 373.58 | 0.27 |
| 02-01-076 | 376.21 | 0.36 |
| 02-01-091 | 378.84 | 0.33 |
| 02-01-106 | 381.47 | 0.43 |
| 02-01-121 | 384.10 | 0.28 |
| 02-02-021 | 392.86 | 0.10 |
| 02-02-051 | 398.12 | 0.12 |

| | | |
|---|---|---|
| 02-02-071 | 401.62 | 0.09 |
| 02-02-081 | 403.37 | 0.10 |
| 02-02-092 | 405.30 | 0.10 |
| 02-02-101 | 406.88 | 0.10 |
| 02-02-111 | 408.63 | 0.06 |
| 02-02-121 | 410.38 | 0.09 |
| 02-02-131 | 412.14 | 0.00 |
| 02-02-141 | 413.89 | 0.06 |
| 02-03-002 | 415.64 | 0.23 |
| 02-03-011 | 417.39 | 0.12 |
| 02-03-031 | 420.90 | 0.10 |
| 02-03-041 | 422.65 | 0.11 |
| 02-03-051 | 427.89 | 0.14 |
| 02-03-056 | 430.94 | 0.09 |
| 02-03-061 | 434.00 | 0.10 |
| 02-03-066 | 437.06 | 0.11 |
| 02-03-072 | 440.11 | 0.09 |
| 02-03-076 | 443.17 | 0.11 |
| 02-03-080 | 445.61 | 0.07 |
| 02-03-085 | 449.28 | 0.12 |
| 02-03-091 | 452.33 | 0.07 |
| 02-03-096 | 455.39 | 0.06 |
| 02-03-101 | 458.44 | 0.07 |
| 02-03-111 | 461.50 | 0.14 |
| 02-03-116 | 467.61 | 0.10 |
| 02-03-126 | 473.72 | 0.10 |
| 02-03-131 | 476.78 | 0.20 |
| 02-04-001 | 484.30 | 0.16 |
| 02-04-006 | 486.52 | 0.20 |
| 02-04-011 | 488.37 | 0.22 |
| 02-04-030 | 495.41 | 0.26 |
| 02-04-036 | 497.63 | 0.17 |
| 02-04-045 | 500.96 | 0.09 |
| 02-04-061 | 506.89 | 0.18 |
| 02-04-076 | 512.44 | 0.14 |
| 02-04-106 | 523.56 | 0.05 |
| 02-04-121 | 530.75 | 0.07 |
| 02-04-136 | 544.48 | 0.18 |
| 02-04-145 | 552.73 | 0.10 |
| 06-01-141 | 1572.16 | 0.31 |
| 06-01-148 | 1574.68 | 0.31 |
| 06-04-019 | 1682.05 | 0.28 |
| 06-05-053 | 1731.17 | 0.34 |
| 06-05-145 | 1755.82 | 0.64 |
| 06-06-042 | 1768.30 | 0.35 |
| 06-06-135 | 1793.26 | 0.56 |
| 07-01-076 | 1830.79 | 0.28 |
| 07-01-123 | 1843.36 | 0.24 |
| 07-04-013 | 1935.55 | 0.19 |
| 07-04-133 | 1969.95 | 0.41 |
| 07-05-023 | 1982.84 | 0.40 |
| 07-05-139 | 2020.46 | 0.17 |
| 07-06-066 | 2045.44 | 0.29 |
| 08-01-021 | 2095.53 | 0.12 |

| | | |
|---|---|---|
| 08-01-137 | 2133.19 | 0.17 |
| 08-04-035 | 2245.77 | 0.14 |
| 08-04-114 | 2271.46 | 0.46 |
| 08-05-005 | 2284.25 | 0.11 |
| 08-05-082 | 2309.34 | 0.22 |
| 08-05-119 | 2321.65 | 0.18 |
| 08-06-047 | 2347.01 | 0.26 |
| 08-07-016 | 2385.27 | 0.32 |
| 09-06-041 | 2600.55 | 0.04 |
| 09-06-125 | 2612.78 | 0.13 |
| 10-03-048 | 2675.08 | 0.04 |
| 10-05-087 | 2724.98 | 0.16 |
| 10-06-107 | 2750.01 | 0.28 |
| 11-01-042 | 2762.51 | 0.63 |
| 11-02-014 | 2787.85 | 0.15 |
| 11-03-101 | 2825.75 | 0.12 |
| 11-05-115 | 2875.12 | 0.11 |
| 12-02-091 | 2937.69 | 0.14 |
| 12-05-020 | 2987.60 | 0.24 |
| 12-06-064 | 3004.58 | 0.15 |
| 13-01-050 | 3008.81 | 0.11 |
| 13-01-148 | 3017.28 | 0.20 |
| 13-05-060 | 3036.74 | 0.21 |
| 13-05-093 | 3038.43 | 0.23 |
| 13-05-100 | 3039.13 | 0.17 |
| 13-06-020 | 3041.95 | 0.44 |
| 13-06-100 | 3044.78 | 0.26 |
| 13-07-050 | 3052.95 | 0.38 |
| 14-01-005 | 3055.00 | 0.25 |
| 14-01-025 | 3057.42 | 0.35 |
| 14-01-065 | 3060.00 | 0.13 |
| 14-01-085 | 3062.78 | 0.18 |
| 14-01-105 | 3065.56 | 0.16 |
| 14-01-145 | 3071.11 | 0.22 |
| 14-02-035 | 3076.67 | 0.20 |
| 14-02-055 | 3079.44 | 0.18 |
| 14-02-075 | 3082.22 | 0.26 |
| 14-02-095 | 3085.00 | 0.09 |
| 14-02-015 | 3088.33 | 0.31 |
| 14-02-135 | 3091.67 | 0.34 |
| 14-03-005 | 3095.00 | 0.22 |
| 14-03-025 | 3098.33 | 0.41 |
| 14-03-045 | 3101.67 | 0.32 |
| 14-03-085 | 3108.33 | 0.57 |
| 14-03-105 | 3111.67 | 0.64 |
| 14-03-125 | 3115.00 | 0.56 |
| 14-04-015 | 3121.67 | 0.44 |
| 14-04-055 | 3128.33 | 0.22 |
| 14-04-075 | 3131.67 | 0.26 |
| 14-04-095 | 3135.00 | 0.30 |
| 14-04-115 | 3137.86 | 0.40 |
| 14-05-045 | 3149.29 | 0.29 |
| 14-05-065 | 3152.14 | 0.17 |
| 14-05-085 | 3155.00 | 0.15 |

| | | |
|---|---|---|
| 14-05-125 | 3157.86 | 0.27 |
| 14-05-145 | 3159.29 | 0.28 |
| 14-06-015 | 3160.71 | 0.29 |
| 14-06-035 | 3162.14 | 0.19 |
| 14-06-055 | 3163.57 | 0.26 |
| 14-06-075 | 3165.00 | 0.33 |
| 14-06-95 | 3166.43 | 0.25 |
| 14-06-135 | 3169.29 | 0.36 |
| 14-07-005 | 3170.71 | 0.39 |
| 14-07-025 | 3172.14 | 0.59 |
| 14-07-045 | 3173.57 | 0.47 |
| 15-01-015 | 3175.00 | 0.29 |
| 15-01-035 | 3177.00 | 0.52 |
| 15-01-075 | 3181.00 | 0.38 |
| 15-01-090 | 3183.00 | 0.38 |
| 15-01-115 | 3185.00 | 0.43 |
| 15-1W-135 | 3187.00 | 0.36 |
| 15-02-005 | 3189.00 | 0.34 |
| 15-02-025 | 3191.00 | 0.41 |
| 15-02-045 | 3193.00 | 0.22 |
| 15-02-065 | 3195.00 | 0.40 |
| 15-02-105 | 3199.00 | 0.26 |
| 15-02-125 | 3201.00 | 0.37 |
| 15-03-015 | 3205.00 | 0.23 |
| 15-03-035 | 3207.00 | 0.46 |
| 15-03-056 | 3209.00 | 0.24 |
| 15-03-075 | 3211.00 | 0.16 |
| 15-03-115 | 3215.00 | 0.33 |
| 15-03-135 | 3217.00 | 0.27 |
| 15-04-005 | 3219.00 | 0.26 |
| 15-04-025 | 3221.00 | 0.27 |
| 15-04-045 | 3223.00 | 0.16 |
| 15-04-065 | 3225.00 | 0.47 |
| 15-04-085 | 3227.00 | 0.28 |
| 15-04-105 | 3229.00 | 0.21 |
| 15-04-145 | 3233.00 | 0.25 |
| 15-05-015 | 3235.00 | 0.17 |
| 15-05-055 | 3239.00 | 0.21 |
| 15-05-075 | 3241.00 | 0.16 |
| 15-05-095 | 3243.00 | 0.17 |
| 15-05-115 | 3245.00 | 0.21 |
| 16-05-145 | 3250.56 | 0.24 |
| 15-06-025 | 3261.67 | 0.24 |
| 15-06-045 | 3267.22 | |
| 15-06-065 | 3272.78 | 0.29 |
| 15-06-085 | 3278.33 | 0.31 |
| 15-06-105 | 3283.89 | 0.28 |
| 15-06-125 | 3289.44 | 0.39 |
| 15-07-035 | 3313.00 | 0.73 |
| 16-01W-025 | 3331.00 | 0.20 |
| 16-01W-085 | 3346.67 | 0.32 |
| 16-01-105 | 3350.00 | 0.39 |
| 16-01-125 | 3353.33 | 0.47 |
| 16-01W-145 | 3356.67 | 0.32 |

| | | |
|---|---|---|
| 16-02W-055 | 3366.67 | 0.22 |
| 16-02-075 | 3370.00 | 0.49 |
| 16-02-095 | 3376.67 | 0.52 |
| 16-02W-115 | 3380.00 | 0.31 |
| 16-02w-135 | 3383.86 | 0.39 |
| 16-03-045 | 3395.45 | 0.30 |
| 16-03-065 | 3399.32 | 0.26 |
| 16-03-085 | 3403.18 | 0.14 |
| 16-03-105 | 3407.05 | 0.24 |
| 16-03-125 | 3410.91 | 0.22 |
| 16-03-145 | 3414.77 | 0.34 |
| 16-04-015 | 3418.64 | 0.43 |
| 16-04-035 | 3422.50 | 0.37 |
| 16-04-055 | 3426.36 | 0.54 |
| 16-04-075 | 3430.23 | 0.30 |
| 16-04-115 | 3434.09 | 0.37 |
| 16-05-005 | 3441.82 | 0.49 |
| 16-05-045 | 3449.55 | 0.61 |
| 16-05-065 | 3453.41 | 0.32 |
| 16-05-85 | 3457.27 | 0.26 |
| 16-05-105 | 3461.14 | 0.48 |
| 16-05-125 | 3465.00 | 0.34 |
| 16-06-015 | 3467.50 | 0.15 |
| 16-06-015 | 3470.00 | 0.20 |
| 16-06-035 | 3472.50 | 0.21 |
| 16-06-055 | 3475.00 | 0.25 |
| 16-06-095 | 3480.00 | 0.13 |
| 16-07-005 | 3483.75 | 0.23 |
| 16-07-025 | 3485.00 | 0.25 |

A4: Chlorin values for ODP 1087C

| Name | Age (ka) | 410 nm abs g$^{-1}$ |
|---|---|---|
| C2-04-055 | 309.00 | 2.20 |
| C2-04-060 | 312.14 | 1.59 |
| C2-04-065 | 315.29 | 2.06 |
| C2-04-070 | 318.43 | 1.82 |
| C2-04-075 | 321.57 | 1.21 |
| C2-04-080 | 324.71 | 1.03 |
| C2-04-085 | 327.86 | 0.71 |
| C2-04-090 | 331.00 | 0.60 |
| C2-04-095 | 332.46 | 0.77 |
| C2-04-100 | 333.98 | 0.80 |
| C2-04-105 | 335.50 | 0.98 |
| C2-04-110 | 337.02 | 0.88 |
| C2-04-115 | 338.55 | 1.82 |
| C2-04-120 | 340.07 | 3.02 |
| C2-04-125 | 341.59 | 2.05 |
| C2-04-130 | 343.11 | 3.17 |
| C2-04-135 | 344.63 | 2.44 |
| C2-04-140 | 346.15 | 2.31 |
| C2-05-145 | 347.68 | 1.97 |
| C2-05-005 | 349.20 | 2.96 |
| C2-05-010 | 350.72 | 2.69 |
| C2-05-015 | 352.24 | 4.37 |
| C2-05-020 | 353.76 | 4.66 |
| C2-05-025 | 355.28 | 4.94 |
| C2-05-030 | 356.81 | 5.99 |
| c2-05-035 | 358.33 | 5.04 |
| C2-05-040 | 359.85 | 5.21 |
| C2-05-045 | 361.37 | 3.69 |
| C2-05-050 | 362.89 | 3.96 |
| C2-05-055 | 364.41 | 3.75 |
| C2-05-060 | 366.00 | 5.03 |
| C2-05-065 | 369.75 | 3.79 |
| c2-05-070 | 373.50 | 5.28 |
| C2-05-075 | 377.25 | 4.99 |
| C2-05-080 | 381.00 | 7.50 |

A5: TEX$_{86}$ SST values from ODP 1087

| name | Age (ka) | TEX$_{86}$ SST (Kim *et al.* 2008) | SST TEX$^H_{86}$ | BIT |
|---|---|---|---|---|
| 01-01-055 | 12.00 | 18.22 | 18.95 | 0.05 |
| 01-01-085 | 26.46 | 17.16 | 17.84 | 0.04 |
| 01-01-116 | 45.85 | 16.12 | 16.71 | 0.06 |
| 01-02-015 | 74.00 | 15.20 | 15.68 | 0.04 |
| 01-02-045 | 86.20 | 15.04 | 15.50 | 0.06 |
| 01-02-075 | 94.50 | 18.89 | 19.63 | 0.05 |
| 01-02-120 | 111.25 | 18.50 | 19.23 | 0.07 |
| 01-03-020 | 135.00 | 20.90 | 21.57 | 0.06 |
| 01-03-125 | 184.80 | 16.74 | 17.39 | 0.09 |
| 1087C-2-04-090 | 331.00 | 22.78 | 23.28 | 0.07 |
| 1087C-2-05-025 | 355.28 | 14.80 | 15.22 | 0.06 |
| 02-01-076 | 376.00 | 16.75 | 17.41 | 0.05 |
| 02-01-091 | 379.52 | 18.19 | 18.92 | 0.06 |
| 02-02-101 | 408.44 | 18.14 | 18.87 | 0.09 |
| 02-02-121 | 410.00 | 19.39 | 20.12 | 0.05 |
| 02-03-031 | 424.50 | 18.62 | 19.35 | 0.06 |
| 02-03-071 | 430.75 | 20.64 | 21.32 | 0.05 |
| 02-03-091 | 435.00 | 19.87 | 20.59 | 0.05 |
| 06-06-135 | 1793.26 | 14.36 | 14.70 | 0.10 |
| 11-05-115 | 2875.12 | 14.32 | 14.65 | 0.10 |
| 12-06-064 | 3000.00 | 15.77 | 16.33 | 0.13 |
| 13-05-080 | 3037.50 | 13.77 | 14.00 | 0.16 |
| 14-01-065 | 3060.00 | 15.82 | 16.37 | 0.18 |
| 14-02-035 | 3076.67 | 16.74 | 17.39 | 0.17 |
| 14-02-095 | 3085.00 | 16.93 | 17.60 | 0.12 |
| 14-03-045 | 3101.67 | 14.17 | 14.47 | 0.18 |
| 14-04-095 | 3135.00 | 14.73 | 15.13 | 0.12 |
| 14-04-115 | 3137.86 | 13.76 | 13.98 | 0.15 |
| 14-05-065 | 3152.14 | 16.24 | 16.84 | 0.15 |
| 14-07-025 | 3173.57 | 15.21 | 15.70 | 0.15 |
| 15-01-035 | 3179.62 | 15.96 | 16.53 | 0.13 |
| 15-04-005 | 3221.15 | 16.15 | 16.74 | 0.10 |
| 15-05-115 | 3245.00 | 16.28 | 16.89 | 0.19 |
| 15-06-025 | 3261.67 | 14.63 | 15.02 | 0.12 |
| 15-07-035 | 3313.00 | 12.74 | 12.72 | 0.10 |
| 16-01-025 | 3331.00 | 14.49 | 14.86 | 0.11 |
| 16-03-085 | 3403.18 | 16.99 | 17.66 | 0.11 |
| 16-04-055 | 3426.36 | 12.57 | 12.50 | 0.12 |
| 16-05-145 | 3467.50 | 16.56 | 17.20 | 0.09 |
| 16-07-025 | 3485.00 | 15.94 | 16.52 | 0.13 |

A6 *n*-alkane values from ODP 1087

| Name | Age (ka) | *n*-alkane m² g⁻¹ |
|---|---|---|
| 01-01-055 | 12.00 | 0.21 |
| 01-01-085 | 26.46 | 0.16 |
| 01-01-116 | 45.85 | 1.83 |
| 01-02-045 | 86.20 | 0.23 |
| 01-02-075 | 94.50 | 0.69 |
| 01-02-120 | 111.25 | 0.30 |
| 01-03-020 | 135.00 | 1.72 |
| C2-04-090 | 331.00 | 0.33 |
| C2-05-025 | 355.28 | 0.50 |
| 02-01-076 | 376.00 | 0.49 |
| 02-01-091 | 379.52 | 0.27 |
| 02-02-121 | 410.00 | 0.25 |
| 02-03-031 | 424.50 | 0.30 |
| 02-03-091 | 435.00 | 0.19 |
| 06-06-135 | 1793.26 | 1.02 |
| 11-05-115 | 2875.12 | 1.57 |
| 13-05-080 | 3037.50 | 1.32 |
| 14-01-065 | 3060.00 | 1.20 |
| 14-02-095 | 3085.00 | 1.20 |
| 14-03-045 | 3101.67 | 1.07 |
| 14-0-095 | 3135.00 | 0.93 |
| 14-05-065 | 3152.14 | 1.13 |
| 15-01-035 | 3179.62 | 0.77 |
| 15-04-005 | 3221.15 | 0.76 |
| 15-07-035 | 3313.00 | 0.48 |
| 16-01a-025 | 3331.00 | 0.61 |
| 16-03a-085 | 3403.18 | 0.74 |
| 16-04a-055 | 3426.36 | 0.45 |
| 16-05a-145 | 3467.50 | 0.77 |
| 16-07-025 | 3485.00 | 0.67 |

A7: $\delta^{18}O_{FF}$ values from ODP 1087

| Name | Age (ka) | $\delta^{13}C$ | $\delta^{18}O$ |
|---|---|---|---|
| 14-01-005 | 3057.417 | +0.18 | +0.76 |
| 14-01-025 | 3059.833 | +0.19 | +0.72 |
| 14-01-065 | 3062.778 | +0.36 | +0.91 |
| 14-01-085 | 3065.556 | +0.58 | +1.10 |
| 14-01-125 | 3071.111 | +0.19 | +0.78 |
| 14-01-145 | 3073.889 | -0.10 | +0.63 |
| 14-02-035 | 3079.444 | +0.05 | +0.91 |
| 14-02-095 | 3088.333 | +0.20 | +1.00 |
| 14-02-015 | 3091.667 | +0.26 | +1.00 |
| 14-03-005 | 3098.333 | +0.32 | +0.95 |
| 14-03-025 | 3101.667 | +0.35 | +1.03 |
| 14-03-065 | 3108.333 | +0.44 | +1.34 |
| 14-03-085 | 3111.667 | +0.36 | +1.32 |
| 14-03-165 | 3121.667 | +0.20 | +1.08 |
| 14-04-035 | 3128.333 | +0.73 | +1.49 |
| 14-04-055 | 3131.667 | +0.61 | +1.66 |
| 14-04-095 | 3137.857 | +0.02 | +1.13 |
| 14-04-115 | 3140.714 | -0.04 | +0.66 |
| 14-04-135 | 3146.429 | +0.28 | +0.78 |
| 14-05-025 | 3149.286 | +0.10 | +0.81 |
| 14-05-065 | 3155 | +0.17 | +0.70 |
| 14-05-085 | 3156.429 | +0.23 | +0.75 |
| 14-05-103 | 3159.286 | +0.37 | +0.95 |
| 14-05-145 | 3160.714 | +0.23 | +0.93 |
| 14-06-035 | 3163.571 | +0.15 | +0.81 |
| 14-06-055 | 3165 | +0.19 | +0.91 |
| 14-05-115 | 3169.286 | +0.23 | +0.85 |
| 14-07-005 | 3172.143 | +0.31 | +1.02 |
| 14-07-025 | 3173.571 | +0.36 | +0.98 |
| 15-01-015 | 3177 | -0.00 | +0.59 |
| 15-01-035 | 3179 | +0.11 | +0.62 |
| 15-01-075 | 3183 | +0.44 | +0.84 |
| 15-01-096 | 3185 | +0.34 | +0.81 |
| 15-01-135 | 3189 | +0.07 | +0.79 |
| 15-03-005 | 3191 | -0.11 | +0.72 |
| 15-02-045 | 3195 | -0.05 | +0.82 |
| 15-02-065 | 3197 | -0.02 | +0.84 |
| 15-02-105 | 3201 | +0.22 | +0.92 |
| 15-02-125 | 3203 | +0.04 | +0.86 |
| 15-03-015 | 3207 | -0.13 | +0.80 |
| 15-03-075 | 3213 | -0.19 | +0.64 |
| 16-03-095 | 3215 | -0.01 | +0.94 |
| 15-03-135 | 3219 | +0.01 | +0.96 |
| 15-04-005 | 3221 | -0.08 | +0.76 |
| 15-04-045 | 3225 | -0.33 | +0.75 |
| 15-04-065 | 3227 | -0.07 | +0.73 |
| 15-04-105 | 3231 | -0.15 | +0.83 |
| 15-04-125 | 3233 | -0.12 | +0.75 |
| 15-05-035 | 3237 | -0.17 | +0.65 |
| 15-05-055 | 3239 | +0.04 | +0.74 |

| | | | |
|---|---|---|---|
| 15-05-095 | 3243 | +0.04 | +0.75 |
| 15-05-115 | 3245 | +0.02 | +0.76 |
| 15-06-005 | 3256.111 | -0.15 | +0.80 |
| 15-06-025 | 3261.667 | -0.19 | +0.90 |
| 15-06-085 | 3278.333 | -0.14 | +1.26 |
| 15-06-125 | 3289.444 | -0.05 | +1.42 |
| 15-06-145 | 3295 | +0.04 | +1.38 |
| 15-07-035 | 3313 | -0.14 | +1.03 |
| 15-07-055 | 3322 | -0.16 | +1.12 |
| 16-01-045 | 3340 | +0.03 | +0.76 |
| 16-01-065 | 3343.333 | +0.18 | +0.97 |
| 16-01-105 | 3350 | -0.00 | +0.88 |
| 16-01-125r | 3353.333 | +0.01 | +0.68 |
| 16-02-015 | 3360 | +0.18 | +0.93 |
| 16-02-035 | 3363.333 | +0.30 | +1.10 |
| 16-02-075 | 3370 | +0.12 | +0.90 |
| 16-02-095 | 3373.333 | +0.05 | +0.86 |
| 16-02-135 | 3383.864 | -0.06 | +0.64 |
| 16-03-005 | 3387.727 | +0.00 | +0.48 |
| 16-03-045 | 3395.455 | +0.24 | +0.65 |
| 16-03-065 | 3399.318 | +0.26 | +0.59 |
| 16-03-105 | 3407.045 | +0.25 | +0.92 |
| 16-03-125 | 3410.909 | +0.24 | +0.81 |
| 16-04-019 | 3418.636 | +0.52 | +1.10 |
| 16-04-035 | 3422.5 | +0.59 | +0.98 |
| 16-04-075 | 3430.227 | +0.55 | +0.92 |
| 16-04-135r | 3437.955 | +0.49 | +0.95 |
| 16-05-005 | 3441.818 | -0.12 | +0.70 |
| 16-05-045 | 3449.545 | +0.18 | +0.95 |
| 16-05-065-1/2 | 3453.409 | +0.45 | +1.18 |
| 16-05-105 | 3461.136 | +0.35 | +1.21 |
| 16-05-125 | 3465 | +0.37 | +1.09 |
| 16-06-035 | 3472.5 | +0.46 | +1.11 |
| 16-06-055 | 3475 | +0.47 | +1.00 |
| 16-06-076 | 3477.5 | +0.70 | +0.98 |
| 16-06-095 | 3480 | +0.84 | +1.05 |
| 16-06-115 | 3481.25 | +0.93 | +0.93 |
| 16-06-135 | 3482.5 | +0.78 | +1.07 |
| 16-07-005 | 3483.75 | +0.57 | +0.81 |
| 16-07-025 | 3485 | +0.56 | +0.99 |

A8: *C. wuellerstorfi* benthic Isotopes.

| Name | Time (ka) | δ¹³C | δ¹⁸O |
|------|-----------|------|------|
| 14-01-025 | 3057.42 | 0.15 | 2.63 |
| 14-03-025 | 3098.33 | 0.23 | 2.67 |
| 14-03-105 | 3111.67 | 0.37 | 2.27 |
| 14-04-015 | 3121.67 | 0.20 | 3.05 |
| 14-04-055 | 3128.33 | 0.18 | 3.15 |
| 14-04-075 | 3131.67 | 0.14 | 3.16 |
| 14-04-095 | 3135.00 | -0.08 | 3.37 |
| 14-04-115 | 3137.86 | -0.08 | 3.17 |
| 14-04-135 | 3140.71 | 0.00 | 2.80 |
| 14-05-045 | 3149.29 | 0.27 | 2.54 |
| 14-05-065 | 3152.14 | -0.03 | 2.35 |
| 14-05-105 | 3156.43 | 0.33 | 2.57 |
| 14-04-125 | 3157.86 | 0.30 | 2.55 |
| 14-06-015 | 3160.71 | 0.34 | 2.82 |
| 14-06-035 | 3162.14 | 0.28 | 2.69 |
| 14-06-095 | 3166.43 | 0.30 | 2.77 |
| 14-06-135 | 3169.29 | -0.23 | 2.69 |
| 14-07-025 | 3172.14 | 0.31 | 2.76 |
| 15-01-015 | 3175.00 | 0.42 | 2.63 |
| 15-01-035 | 3177.00 | 0.41 | 2.59 |
| 15-01-055 | 3179.00 | 0.42 | 2.68 |
| 15-01-115 | 3185.00 | 0.44 | 2.72 |
| 15-02-025 | 3191.00 | 0.50 | 2.61 |
| 15-03-135 | 3217.00 | 0.38 | 2.65 |
| 15-04-085 | 3227.00 | 0.25 | 2.50 |
| 15-04-105 | 3229.00 | -0.24 | 2.97 |
| 15-05-015 | 3235.00 | 0.13 | 2.74 |
| 16-01-105 | 3350.00 | -0.06 | 2.33 |
| 16-01-125 | 3353.33 | 0.07 | 2.69 |
| 16-02-035 | 3363.33 | 0.31 | 2.72 |
| 16-02-055 | 3366.67 | 0.92 | 4.43 |
| 16-02-095 | 3376.67 | 0.19 | 2.50 |
| 16-03-005 | 3383.86 | 0.35 | 2.66 |
| 16-03-065 | 3399.32 | 0.49 | 2.34 |
| 16-03-085 | 3403.18 | 0.36 | 2.66 |
| 16-03-125 | 3410.91 | 0.23 | 2.61 |
| 16-03-145 | 3414.77 | 0.10 | 2.40 |
| 16-04-035 | 3422.50 | 0.14 | 2.58 |
| 16-04-115 | 3434.09 | 0.12 | 2.52 |
| 16-05-005 | 3441.82 | -0.03 | 2.50 |
| 16-05-065 | 3453.41 | 0.06 | 2.98 |
| 16-05-085 | 3457.27 | -0.33 | 3.23 |
| 16-06-035 | 3472.50 | 0.23 | 2.58 |
| 16-06-055 | 3475.00 | 0.14 | 2.72 |
| 16-07-005 | 3485.00 | 0.09 | 2.67 |

# References

Alley, R.B. (2000) 'The Younger Dryas cold interval as viewed from central Greenland', *Quaternary Science Reviews*, 19(1-5), pp. 213-226.

Andrews, W.R.H. and Cram, D.L. (1969) 'Combined Aerial and Shipboard Upwelling Study in the Benguela Current', *Nature*, 224(5222), pp. 902-904.

Andrews, W.R.H. and Hutchings, L. (1980) 'Upwelling in the Southern Benguela Current', *Progress In Oceanography*, 9(1), pp. 1-8, IN1-IN2, 9-76, IN3-IN4, 77-81.

Ba, A.W.H. and Duplessy, J.-C. (1976) 'Subtropical Convergence Fluctuations and Quaternary Climates in the Middle Latitudes of the Indian Ocean', *Science*, 194(4263), pp. 419-422.

Barale, V. (1987) 'Remote observations of the marine environment: Spatial heterogeneity of the mesoscale ocean color field in CZCS imagery of California near-coastal waters', *Remote Sensing of Environment*, 22(2), pp. 173-186.

Bard, E. (2001) 'Comparison of alkenone estimates with other paleotemperature proxies', *Geochemistry Geophysics Geosystems*, 2(1).

Bard, E. and Rickaby, R.E.M. (2009) 'Migration of the subtropical front as a modulator of glacial climate', *Nature*, 460(7253), pp. 380-U93.

Barker, S., Diz, P., Vautravers, M.J., Pike, J., Knorr, G., Hall, I.R. and Broecker, W.S. (2009) 'Interhemispheric Atlantic seesaw response during the last deglaciation', *Nature*, 457(7233), pp. 1097-U50.

Barker, S., Knorr, G., Edwards, R.L., Parrenin, F.d.r., Putnam, A.E., Skinner, L.C., Wolff, E. and Ziegler, M. (2011) '800,000 Years of Abrupt Climate Variability', *Science*, 334(6054), pp. 347-351.

Barnes, P.W., Tieszen, L.L. and Ode, D.J. (1983) 'Distribution, production, and diversity of C3 dominated and C4 dominated communities in a mixed prairie ', *Canadian Journal of Botany-Revue Canadienne De Botanique*, 61(3), pp. 741-751.

Barron, J.A. (1996) 'Diatom constraints on the position of the Antarctic Polar Front in the middle part of the Pliocene', *Marine Micropaleontology*, 27(1-4), pp. 195-&.

Bartoli, G., Honisch, B. and Zeebe, R.E. (2011) 'Atmospheric CO2 decline during the Pliocene intensification of Northern Hemisphere glaciations', *Paleoceanography*, 26, p. 14.

Bartoli, G., Sarnthein, M. and Weinelt, M. (2006) 'Late Pliocene millennial-scale climate variability in the northern North Atlantic prior to and after the onset of Northern Hemisphere glaciation', *Paleoceanography*, 21(4), p. 15.

Bartoli, G., Sarnthein, M., Weinelt, M., Erlenkeuser, H., Garbe-Schönberg, D. and Lea, D.W. (2005) 'Final closure of Panama and the onset of northern hemisphere glaciation', *Earth and Planetary Science Letters*, 237(1-2), pp. 33-44.

Bé, A.W.H. (1977) 'An ecological, Zoogeographie and taxonomic review of Recent planktonic foraminifera', in Ramsay, A.T.S. (ed.) *Oceanic Micropaleontology*. San Diego, Calif: Academic, pp. 1-100.

Be, A.W.H. and Hutson, W.H. (1977) 'Ecology of Planktonic Foraminifera and Biogeographic Patterns of Life and Fossil Assemblages in the Indian Ocean', *Micropaleontology*, 23(4), pp. 369-414.

Becquey, S. and Gersonde, R. (2002) 'Past hydrographic and climatic changes in the Subantarctic Zone of the South Atlantic - The Pleistocene record from ODP Site 1090', *Palaeogeography Palaeoclimatology Palaeoecology*, 182(3-4), pp. 221-239.

Belanger, P.E., Curry, W.B. and Matthews, R.K. (1981) 'Core-top evaluation of benthic foraminiferal isotopic ratios for paleo-oceanographic interpretations', *Palaeogeography, Palaeoclimatology, Palaeoecology*, 33(1-3), pp. 205-220.

Belt, S.T., Brown, T.A., Rodriguez, A.N., Sanz, P.C., Tonkin, A. and Ingle, R. (2012) 'A reproducible method for the extraction, identification and quantification of the Arctic sea ice proxy IP25 from marine sediments', *Analytical Methods*, 4(3), pp. 705-713.

Bendle, J. and Rosell-Mele, A. (2004) 'Distributions of U-37(K) and U-37 '(K) in the surface waters and sediments of the Nordic Seas: Implications for paleoceanography', *Geochemistry Geophysics Geosystems*, 5, p. 19.

Bentaleb, I., Fontugne, M. and Beaufort, L. (2002) 'Long-chain alkenones and U-37(k ') variability along a south-north transect in the Western Pacific Ocean', *Global and Planetary Change*, 34(3-4), pp. 173-183.

Bentaleb, I., Grimalt, J.O., Vidussi, F., Marty, J.C., Martin, V., Denis, M., Hatte, C. and Fontugne, M. (1999) 'The C-37 alkenone record of seawater temperature during seasonal thermocline stratification', *Marine Chemistry*, 64(4), pp. 301-313.

Berger, A. and Loutre, M.F. (2002) 'CLIMATE: An Exceptionally Long Interglacial Ahead?', *Science*, 297(5585), pp. 1287-1288.

Berger, W.H. (1970) 'Planktonic Foraminifera: Selective solution and the lysocline', *Marine Geology*, 8(2), pp. 111-138.

Berger, W.H. (1971) 'Sedimentation of planktonic foraminifera', *Marine Geology*, 11(5), pp. 325-358.

Berger, W.H., Lange, C.B. and Perez, M.E. (2002) 'The early Matuyama Diatom Maximum off SW Africa: a conceptual model', *Marine Geology*, 180(1-4), pp. 105-116.

Biastoch, A., Boning, C.W., Getzlaff, J., Molines, J.M. and Madec, G. (2008a) 'Causes of Interannual-Decadal Variability in the Meridional Overturning Circulation of the Midlatitude North Atlantic Ocean', *Journal of Climate*, 21(24), pp. 6599-6615.

Biastoch, A., Boning, C.W. and Lutjeharms, J.R.E. (2008b) 'Agulhas Leakage dynamics affects decadal variability in Atlantic overturning circulation', *Nature*, 456(7221), pp. 489-492.

Biastoch, A., Boning, C.W., Schwarzkopf, F.U. and Lutjeharms, J.R.E. (2009) 'Increase in Agulhas Leakage due to poleward shift of Southern Hemisphere westerlies', *Nature*, 462(7272), pp. 495-498.

Biastoch, A., Lutjeharms, J.R.E., Böning, C.W. and Scheinert, M. (2008c) 'Mesoscale perturbations control inter-ocean exchange south of Africa', *Geophys. Res. Lett.*, 35.

Billups, K., Ravelo, A.C. and Zachos, J.C. (1998) 'Early Pliocene deep water circulation in the western equatorial Atlantic: Implications for high-latitude climate change', *Paleoceanography*, 13(1), pp. 84-95.

Blanke, B., Penven, P., Roy, C., Chang, N. and Kokoszka, F. (2009) 'Ocean variability over the Agulhas Bank and its dynamical connection with the southern Benguela upwelling system', *J. Geophys. Res.*, 114(C12), p. C12028.

Bockelmann, F.D., Zonneveld, K.A.F. and Schmidt, M. (2007) 'Assessing environmental control on dinoflagellate cyst distribution in surface sediments of the Benguela upwelling region (eastern South Atlantic)', *Limnology and Oceanography*, 52(6), pp. 2582-2594.

Boebel, O., Davis, R.E., Ollitrault, M., Peterson, R.G., Richardson, P.L., Schmid, C. and Zenk, W. (1999) 'The intermediate depth circulation of the western South Atlantic', *Geophys. Res. Lett.*, 26(21), pp. 3329-3332.

Boebel, O., Lutjeharms, J., Schmid, C., Zenk, W., Rossby, T. and Barron, C. (2003) 'The Cape Cauldron: a regime of turbulent inter-ocean exchange', *Deep-Sea Research Part Ii-Topical Studies in Oceanography*, 50(1), pp. 57-86.

Boltovskoy, E. (1983) 'Late Cenozoic deep-sea benthic Foraminifera off the coast of northwest Africa (DSDP Site 369)', *Journal of African Earth Sciences (1983)*, 1(2), pp. 83-102.

Bonham, S.G., Haywood, A.M., Lunt, D.J., Collins, M. and Salzmann, U. (2009) 'El Nino Southern Oscillation, Pliocene climate and equifinality', *Philosophical Transactions of the Royal Society A: Mathematical, Physical and Engineering Sciences*, 367(1886), pp. 127-156.

Boudra, D.B. and De Ruijter, W.P.M. (1986) 'The wind-driven circulation of the South Atlantic-Indian ocean -- II. Experiments using a multi-layer numerical model', *Deep Sea Research Part A. Oceanographic Research Papers*, 33(4), pp. 447-482.

Boyle, E.A. (1988) 'Cadmium: Chemical tracer of deepwater paleoceanography', *Paleoceanography*, 3(4), pp. 471-489.

Bradley, R.S. (1999) *Paleoclimatology: reconstructing climates of the Quaternary*. Amsterdam: Elsevier.

Brassell, S.C., Eglinton, G., Marlowe, I.T., Pflaumann, U. and Sarnthein, M. (1986) 'Molecular stratigraphy: a new tool for climatic assessment', *Nature*, 320(6058), pp. 129-133.

Brierley, C.M. and Fedorov, A.V. (2010) 'Relative importance of meridional and zonal sea surface temperature gradients for the onset of the ice ages and Pliocene-Pleistocene climate evolution', *Paleoceanography*, 25(2), p. PA2214.

Brierley, C.M., Fedorov, A.V., Liu, Z., Herbert, T.D., Lawrence, K.T. and LaRiviere, J.P. (2009a) 'Greatly Expanded Tropical Warm Pool and Weakened Hadley Circulation in the Early Pliocene', *Science*, 323(5922), pp. 1714-1718.

Brierley, C.M., Fedorov, A.V., Liu, Z.H., Herbert, T.D., Lawrence, K.T. and LaRiviere, J.P. (2009b) 'Greatly Expanded Tropical Warm Pool and Weakened Hadley Circulation in the Early Pliocene', *Science*, 323(5922), pp. 1714-1718.

Broecker, W.S. (1998) 'Paleocean Circulation during the Last Deglaciation: A Bipolar Seesaw?', *Paleoceanography*, 13(2), pp. 119-121.

Broecker, W.S., Takahashi, T. and Takahashi, T. (1985) 'Sources and Flow Patterns of Deep-Ocean Waters as Deduced From Potential Temperature, Salinity, and Initial Phosphate Concentration', *J. Geophys. Res.*, 90(C4), pp. 6925-6939.

Burls, N. and Reason, C.J.C. (2008) 'Modelling the sensitivity of coastal winds over the Southern Benguela upwelling system to different SST forcing', *Journal of Marine Systems*, 74(1-2), pp. 561-584.

Burton, K.W., Ling, H.F. and Onions, R.K. (1997) 'Closure of the Central American Isthmus and its effect on deep-water formation in the North Atlantic', *Nature*, 386(6623), pp. 382-385.

Caley, T., Giraudeau, J., Malaize, B., Rossignol, L. and Pierre, C. (2012) 'Agulhas Leakage as a key process in the modes of Quaternary climate changes', *Proceedings of the National Academy of Sciences*, 109(18), pp. 6835-6839.

Caley, T., Kim, J.H., Malaize, B., Giraudeau, J., Laepple, T., Caillon, N., Charlier, K., Rebaubier, H., Rossignol, L., Castaneda, I.S., Schouten, S. and Damste, J.S.S. (2011) 'High-latitude obliquity as a dominant forcing in the Agulhas current system', *Climate of the Past*, 7(4), pp. 1285-1296.

Candy, I., Coope, G.R., Lee, J.R., Parfitt, S.A., Preece, R.C., Rose, J. and Schreve, D.C. (2010) 'Pronounced warmth during early Middle Pleistocene interglacials: Investigating the Mid-Brunhes Event in the British terrestrial sequence', *Earth-Science Reviews*, 103(3-4), pp. 183-196.

Candy, I. and McClymont, E.L. (2013) 'Interglacial intensity in the North Atlantic over the last 800,000 years: investigating the complexity of the mid-Brunhes Event (MBE).', *Journal of Quaternary Science*, In reveiw.

Cane, M.A. and Molnar, P. (2001) 'Closing of the Indonesian seaway as a precursor to east African aridircation around 3-4 million years ago', *Nature*, 411(6834), pp. 157-162.

Carlson, A.E., Oppo, D.W., Came, R.E., LeGrande, A.N., Keigwin, L.D. and Curry, W.B. (2008) 'Subtropical Atlantic salinity variability and Atlantic meridional circulation during the last deglaciation', *Geology*, 36(12), pp. 991-994.

Chiang, J.C.H. (2009) 'The Tropics in Paleoclimate', *Annual Review of Earth and Planetary Sciences*, 37, pp. 263-297.

Chiessi, C.M., Mulitza, S., Paul, A., Patzold, J., Groeneveld, J. and Wefer, G. (2008) 'South Atlantic interocean exchange as the trigger for the Bolling warm event', *Geology*, 36(12), pp. 919-922.

Clark, P.U. (2012) 'Ice Sheets in Transition', *Science*, 337(6095), pp. 656-658.

Clark, P.U., Archer, D., Pollard, D., Blum, J.D., Rial, J.A., Brovkin, V., Mix, A.C., Pisias, N.G. and Roy, M. (2006) 'The middle Pleistocene transition: characteristics.

mechanisms, and implications for long-term changes in atmospheric PCO2', *Quaternary Science Reviews*, 25(23-24), pp. 3150-3184.

Clark, P.U., Pisias, N.G., Stocker, T.F. and Weaver, A.J. (2002) 'The role of the thermohaline circulation in abrupt climate change', *Nature*, 415(6874), pp. 863-869.

Clark, P.U. and Pollard, D. (1998) 'Origin of the middle Pleistocene transition by ice sheet erosion of regolith', *Paleoceanography*, 13(1), pp. 1-9.

Clarkson, M. (2010) *Using UK'37 and TEX86 to reconstuct the plopleistocene oceanography of the bengula reigon*. MS thesis. Royal Holloway, University of London (Accessed: ).

CLIMAP Project, Ruddiman, W.F., Cline, R.M.L., Hays, J.D., Prell, W.L., Moore, T.C., Kipp, N.G., Molfino, B.E., Denton, G.H., Hughes, T.J., Balsam, W.L., Brunner, C.A., Duplessy, J.-C., Fastook, J.L., Imbrie, J., Keigwin, L.D., Kellogg, T.B., McIntyre, A., Matthews, R.K., Mix, A.C., Morley, J.J., Shackleton, N.J., Streeter, S.S. and Thompson, P.R. (1984) 'The last interglacial ocean', *Quaternary Research*, 21(2), pp. 123-224.

Coates, A.G., Jackson, J.B.C., Collins, L.S., Cronin, T.M., Dowsett, H.J., Bybell, L.M., Jung, P. and Obando, J.A. (1992) 'Closure of the Isthmus of Panama: The near-shore marine record of Costa Rica and western Panama', *Geological Society of America Bulletin*, 104(7), pp. 814-828.

Conte, M.H., Eglinton, G. and Madureira, L.A.S. (1992) 'Long-chain alkenones and alkyl alkenoates as palaeotemperature indicators: their production, flux and early sedimentary diagenesis in the Eastern North Atlantic', *Organic Geochemistry*, 19(1-3), pp. 287-298.

Conte, M.H., Sicre, M.-A., Rühlemann, C., Weber, J.C., Schulte, S., Schulz-Bull, D. and Blanz, T. (2006) 'Global temperature calibration of the alkenone unsaturation index (U(37)(K)) in surface waters and comparison with surface sediments', *Geochemistry Geophysics Geosystems*, 7(2), p. Q02005.

Conte, M.H., Thompson, A. and Eglinton, G. (1994) 'Primary production of lipid biomarker compounds by emiliania-Huxleyi - results from an experimental mesocosm study in fjords of southwest norway', *Sarsia*, 79(4), pp. 319-331.

Coolen, M.J.L. and Overmann, J. (2007) '217 000-year-old DNA sequences of green sulfur bacteria in Mediterranean sapropels and their implications for the reconstruction of the paleoenvironment', *Environmental Microbiology*, 9(1), pp. 238-249.

Corliss, B.H. (1983) 'Distribution of Holocene deep-sea benthonic foraminifera in the southwest Indian Ocean', *Deep Sea Research Part A. Oceanographic Research Papers*, 30(2), pp. 95-117.

Corliss, B.H. (1985) 'Microhabitats of benthic foraminifera within deep-sea sediments', *Nature*, 314(6010), pp. 435-438.

Cortese, G. and Abelmann, A. (2002) 'Radiolarian-based paleotemperatures during the last 160 kyr at ODP Site 1089 (Southern Ocean, Atlantic Sector)', *Palaeogeography Palaeoclimatology Palaeoecology*, 182(3-4), pp. 259-286.

Cortese, G., Abelmann, A. and Gersonde, R. (2004) 'A glacial warm water anomaly in the subantarctic Atlantic Ocean, near the Agulhas Retroflection', *Earth and Planetary Science Letters*, 222(3-4), pp. 767-778.

Cortese, G., Abelmann, A. and Gersonde, R. (2007) 'The last five glacial-interglacial transitions: A high-resolution 450,000-year record from the subantarctic Atlantic', *Paleoceanography*, 22(4), p. PA4203.

Cronblad, H.G. and Malmgren, B.A. (1981) 'Climatically controlled variation of Sr and Mg in Quaternary planktonic foraminifera', *Nature*, 291(5810), pp. 61-64.

Crowley, T.J. (1996) 'Pliocene climates: the nature of the problem', *Marine Micropaleontology*, 27(1â€"4), pp. 3-12.

Crowley, T.J. and Hyde, W.T. (2008) 'Transient nature of late Pleistocene climate variability', *Nature*, 456(7219), pp. 226-230.

Curry, W.B. and Crowley, T.J. (1987) 'The δ13C of equatorial Atlantic surface waters: Implications for Ice Age pCO2 levels', *Paleoceanography*, 2(5), pp. 489-517.

Curry, W.B., Duplessy, J.C., Labeyrie, L.D. and Shackleton, N.J. (1988) 'Changes in the distribution of δ13C of deep water ΣCO2 between the Last Glaciation and the Holocene', *Paleoceanography*, 3(3), pp. 317-341.

Curry, W.B. and Lohmann, G.P. (1983) 'Reduced advection into Atlantic Ocean deep eastern basins during last glaciation maximum', *Nature*, 306(5943), pp. 577-580.

Darwin, C. (1846) 'An account of the Fine Dust which often falls on Vessels in the Atlantic Ocean', *Quarterly Journal of the Geological Society*, 2(1-2), pp. 26-30.

de Abreu, C., Abrantes, F.F., Shackleton, N.J., Tzedakis, P.C., McManus, J.F., Oppo, D.W. and Hall, M.A. (2005) 'Ocean climate variability in the eastern North Atlantic during interglacial marine isotope stage 11: A partial analogue to the Holocene?', *Paleoceanography*, 20(3), p. 16.

de Leeuw, J.W., v.d. Meer, F.W., Rijpstra, W.I.C. and Schenck, P.A. (1980) 'On the occurrence and structural identification of long chain unsaturated ketones and hydrocarbons in sediments', *Physics and Chemistry of The Earth*, 12, pp. 211-217.

De Ruijter, W. (1982) 'Asymptotic Analysis of the Agulhas and Brazil Current Systems', *Journal of Physical Oceanography*, 12(4), pp. 361-373.

de Ruijter, W.P.M., Biastoch, A., Drijfhout, S.S., Lutjeharms, J.R.E., Matano, R.P., Pichevin, T., van Leeuwen, P.J. and Weijer, W. (1999) 'Indian-Atlantic interocean exchange: Dynamics, estimation and impact', *J. Geophys. Res.*, 104(C9), pp. 20885-20910.

de Ruijter, W.P.M. and Boudra, D.B. (1985) 'The wind-driven circulation in the South Atlantic-Indian Ocean--I. Numerical experiments in a one-layer model', *Deep Sea Research Part A. Oceanographic Research Papers*, 32(5), pp. 557-574.

De Schepper, S. and Head, M.J. (2008) 'Age calibration of dinoflagellate cyst and acritarch events in the Pliocene-Pleistocene of the eastern North Atlantic (DSDP Hole 610A)', *Stratigraphy*, 5(2), pp. 137-161.

De Schepper, S., Head, M.J. and Groeneveld, J. (2009) 'North Atlantic Current variability through marine isotope stage M2 (circa 3.3 Ma) during the mid-Pliocene', *Paleoceanography*, 24(4), p. PA4206.

de Vernal, A., Eynaud, F., Henry, M., Hillaire-Marcel, C., Londeix, L., Mangin, S., Matthiessen, J., Marret, F., Radi, T., Rochon, A., Solignac, S. and Turon, J.L. (2005) 'Reconstruction of sea-surface conditions at middle to high latitudes of the Northern Hemisphere during the Last Glacial Maximum (LGM) based on dinoflagellate cyst assemblages', *Quaternary Science Reviews*, 24(7–9), pp. 897-924.

de Vernal, A., Henry, M., Matthiessen, J., Mudie, P.J., Rochon, A., Boessenkool, K.P., Eynaud, F., Grosfjeld, K., Guiot, J., Hamel, D., Harland, R., Head, M.J., Kunz-Pirrung, M., Levac, E., Loucheur, V., Peyron, O., Pospelova, V., Radi, T., Turon, J.L. and Voronina, E. (2001) 'Dinoflagellate cyst assemblages as tracers of sea-surface conditions in the northern North Atlantic, Arctic and sub-Arctic seas: the new 'n=677' data base and its application for quantitative palaeoceanographic reconstruction', *Journal of Quaternary Science*, 16(7), pp. 681-698.

de Vernal, A. and Hillaire-Marcel, C. (2000) 'Sea-ice cover, sea-surface salinity and halo-thermocline structure of the northwest North Atlantic: modern versus full glacial conditions', *Quaternary Science Reviews*, 19(1-5), pp. 65-85.

de Vernal, A. and Hillaire-Marcel, C. (2008) 'Natural Variability of Greenland Climate, Vegetation, and Ice Volume During the Past Million Years', *Science*, 320(5883), pp. 1622-1625.

De Vernal, A., Rochon, A., Turon, J.-L. and Matthiessen, J. (1997) 'Organic-walled dinoflagellate cysts: Palynological tracers of sea-surface conditions in middle to high latitude marine environments', *Geobios*, 30(7), pp. 905-920.

DeConto, R., Pollard, D. and Harwood, D. (2007) 'Sea ice feedback and Cenozoic evolution of Antarctic climate and ice sheets', *Paleoceanography*, 22(3), p. 18.

Dekens, P.S., Lea, D.W., Pak, D.K. and Spero, H.J. (2002) 'Core top calibration of Mg/Ca in tropical foraminifera: Refining paleotemperature estimation', *Geochemistry Geophysics Geosystems*, 3, p. 29.

Dekens, P.S., Ravelo, A.C. and McCarthy, M.D. (2007a) 'Warm upwelling regions in the Pliocene warm period', *Paleoceanography*, 22(3), p. PA3211.

Dekens, P.S., Ravelo, A.C. and McCarthy, M.D. (2007b) 'Warm upwelling regions in the Pliocene warm period', *Paleoceanography*, 22(3), p. 12.

Dekens, P.S., Ravelo, A.C., McCarthy, M.D. and Edwards, C.A. (2008) 'A 5 million year comparison of Mg/Ca and alkenone paleothermometers', *Geochemistry Geophysics Geosystems*, 9, p. 18.

Delaney, M.L., W.H.Bé, A. and Boyle, E.A. (1985) 'Li, Sr, Mg, and Na in foraminiferal calcite shells from laboratory culture, sediment traps, and sediment cores', *Geochimica et Cosmochimica Acta*, 49(6), pp. 1327-1341.

deMenocal, P.B. (1995) 'Plio-Pleistocene African Climate', *Science*, 270(5233), pp. 53-59.

deMenocal, P.B. (2004) 'African climate change and faunal evolution during the Pliocene-Pleistocene', *Earth and Planetary Science Letters*, 220(1-2), pp. 3-24.

deMenocal, P.B. (2011) 'Climate and Human Evolution', *Science*, 331(6017), pp. 540-542.

Deuser, W.G. and Ross, E.H. (1989) 'Seasonally abundant planktonic foraminifera of the Sargasso Sea; succession, deep-water fluxes, isotopic compositions, and paleoceanographic implications', *The Journal of Foraminiferal Research*, 19(4), pp. 268-293.

Dickson, A.J., Beer, C.J., Dempsey, C., Maslin, M.A., Bendle, J.A., McClymont, E.L. and Pancost, R.D. (2009) 'Oceanic forcing of the Marine Isotope Stage 11 interglacial', *Nature Geoscience*, 2(6), pp. 427-432.

Dickson, A.J., Leng, M.J., Maslin, M.A. and Röhl, U. (2010a) 'Oceanic, atmospheric and ice-sheet forcing of South East Atlantic Ocean productivity and South African monsoon intensity during MIS-12 to 10', *Quaternary Science Reviews*, 29(27-28), pp. 3936-3947.

Dickson, A.J., Leng, M.J., Maslin, M.A., Sloane, H.J., Green, J., Bendle, J.A., McClymont, E.L. and Pancost, R.D. (2010b) 'Atlantic overturning circulation and Agulhas Leakage influences on southeast Atlantic upper ocean hydrography during marine isotope stage 11', *Paleoceanography*, 25, p. 14.

Diekmann, B., Falker, M. and Kuhn, G. (2003) 'Environmental history of the south-eastern South Atlantic since the Middle Miocene: evidence from the sedimentological records of ODP Sites 1088 and 1092', *Sedimentology*, 50(3), pp. 511-529.

Diekmann, B. and Kuhn, G. (2002) 'Sedimentary record of the mid-Pleistocene climate transition in the southeastern South Atlantic (ODP Site 1090)', *Palaeogeography Palaeoclimatology Palaeoecology*, 182(3-4), pp. 241-258.

Dodge, J.G. (1985) *Atlas of dinoflagellates: A scanning electron microscpe survey*. London: Farrand Press.

Dodson, J.R. and Macphail, M.K. (2004) 'Palynological evidence for aridity events and vegetation change during the Middle Pliocene, a warm period in Southwestern Australia', *Global and Planetary Change*, 41(3-4), pp. 285-307.

Donders, T.H., Weijers, J.W.H., Munsterman, D.K., Hoeve, M., Buckles, L.K., Pancost, R.D., Schouten, S., Damste, J.S.S. and Brinkhuis, H. (2009) 'Strong climate coupling of terrestrial and marine environments in the Miocene of northwest Europe', *Earth and Planetary Science Letters*, 281(3-4), pp. 215-225.

dos Santos, R.A.L., Prange, M., Castaneda, I.S., Schefuss, E., Mulitza, S., Schulz, M., Niedermeyer, E.M., Damste, J.S.S. and Schouten, S. (2010) 'Glacial-interglacial variability in Atlantic meridional overturning circulation and thermocline adjustments in the tropical North Atlantic', *Earth and Planetary Science Letters*, 300(3-4), pp. 407-414.

Dowsett, H., Barron, J. and Poore, R. (1996) 'Middle Pliocene sea surface temperatures: A global reconstruction', *Marine Micropaleontology*, 27(1-4), pp. 13-25.

Dowsett, H.J., Chandler, M.A., Cronin, T.M. and Dwyer, G.S. (2005) 'Middle Pliocene sea surface temperature variability', *Paleoceanography*, 20(2), p. 9.

Dowsett, H.J., Chandler, M.A. and Robinson, M.M. (2009a) 'Surface temperatures of the Mid-Pliocene North Atlantic Ocean: implications for future climate', *Philosophical Transactions of the Royal Society a-Mathematical Physical and Engineering Sciences*, 367(1886), pp. 69-84.

Dowsett, H.J. and Cronin, T.M. (1991) 'Preface', *Quaternary Science Reviews*, 10(2-3), pp. v-vi.

Dowsett, H.J., Haywood, A.M., Valdes, P.J., Robinson, M.M., Lunt, D.J., Hill, D.J., Stoll, D.K. and Foley, K.M. (2011) 'Sea surface temperatures of the mid-Piacenzian Warm Period: A comparison of PRISM3 and HadCM3', *Palaeogeography, Palaeoclimatology, Palaeoecology*, 309(1-2), pp. 83-91.

Dowsett, H.J. and Robinson, M.M. (2009) 'Mid-Pliocene equatorial Pacific sea surface temperature reconstruction: a multi-proxy perspective', *Philosophical Transactions of the Royal Society a-Mathematical Physical and Engineering Sciences*, 367(1886), pp. 109-125.

Dowsett, H.J., Robinson, M.M. and Foley, K.M. (2009b) 'Pliocene three-dimensional global ocean temperature reconstruction', *Clim. Past*, 5(4), pp. 769-783.

Dowsett, H.J., Robinson, M.M., Haywood, A.M., Hill, D.J., Dolan, A.M., Stoll, D.K., Chan, W.-L., Abe-Ouchi, A., Chandler, M.A., Rosenbloom, N.A., Otto-Bliesner, B.L., Bragg, F.J., Lunt, D.J., Foley, K.M. and Riesselman, C.R. (2012) 'Assessing confidence in Pliocene sea surface temperatures to evaluate predictive models', *Nature Clim. Change*, 2(5), pp. 365-371.

Draut, A.E., Raymo, M.E., McManus, J.F. and Oppo, D.W. (2003) 'Climate stability during the Pliocene warm period', *Paleoceanography*, 18(4), p. 12.

Dupont, L.M., Donner, B., Vidal, L., Perez, E.M. and Wefer, G. (2005) 'Linking desert evolution and coastal upwelling: Pliocene climate change in Namibia', *Geology*, 33(6), pp. 461-464.

Dwyer, G.S. and Chandler, M.A. (2009) 'Mid-Pliocene sea level and continental ice volume based on coupled benthic Mg/Ca palaeotemperatures and oxygen isotopes', *Philosophical Transactions of the Royal Society A: Mathematical, Physical and Engineering Sciences*, 367(1886), pp. 157-168.

Eckardt, C.B., Keely, B.J., Waring, J.R., Chicarelli, M.I., Maxwell, J.R., Leeuw, J.W.D., Boon, J.J., Runnegar, B., Macko, S. and Hudson, J.D. (1991) 'Preservation of Chlorophyll-Derived Pigments in Sedimentary Organic Matter [and Discussion]', *Philosophical Transactions of the Royal Society of London. Series B: Biological Sciences*, 333(1268), pp. 339-348.

Eglinton, G., Bradshaw, S., Resell, A., Sarnthein, M., Pflaumann, U. and Tiedemann, R. (1992) 'Molecular record of secular sea surface temperature changes on 100-year timescales for glacial terminations I, II and IV', *Nature*, 356(6368), pp. 423-426.

Eglinton, G., Gonzalez, A.G., Hamilton, R.J. and Raphael, R.A. (1962) 'Hydrocarbon constituents of the wax coatings of plant leaves: A taxonomic survey', *Phytochemistry*, 1(2), pp. 89-102.

Eglinton, G. and Hamilton, R.J. (eds.) (1963) *The distribution of n-alkanes*. Academic Press.

Eglinton, G. and Hamilton, R.J. (1967) 'Leaf epicuticular waxes', *Science (New York, N.Y.)*, 156(3780), pp. 1322-35.

Eglinton, T.I. and Eglinton, G. (2008) 'Molecular proxies for paleoclimatology', *Earth and Planetary Science Letters*, 275(1-2), pp. 1-16.

Ehleringer, J.R., Cerling, T.E. and Helliker, B.R. (1997) 'C-4 photosynthesis, atmospheric CO2 and climate', *Oecologia*, 112(3), pp. 285-299.

Elderfield, H., Ferretti, P., Greaves, M., Crowhurst, S., McCave, I.N., Hodell, D. and Piotrowski, A.M. (2012) 'Evolution of Ocean Temperature and Ice Volume Through the Mid-Pleistocene Climate Transition', *Science*, 337(6095), pp. 704-709.

Elderfield, H. and Ganssen, G. (2000) 'Past temperature and [delta]18O of surface ocean waters inferred from foraminiferal Mg/Ca ratios', *Nature*, 405(6785), pp. 442-445.

Emiliani, C. (1955) 'Pleistocene Temperatures', *The Journal of Geology*, 63(6), pp. 538-578.

Emiliani, C. (1966) 'Paleotemperature Analysis of Caribbean Cores P6304-8 and P6304-9 and a Generalized Temperature Curve for the past 425,000 Years', *The Journal of Geology*, 74(2), pp. 109-124.

EPICA (2004) 'Eight glacial cycles from an Antarctic ice core', *Nature*, 429(6992), pp. 623-628.

Epstein, S. and Mayeda, T. (1953) 'Variation of O18 content of waters from natural sources', *Geochimica et Cosmochimica Acta*, 4(5), pp. 213-224.

Etourneau, J., Ehlert, C., Frank, M., Martinez, P. and Schneider, R. (2012) 'Contribution of changes in opal productivity and nutrient distribution in the coastal upwelling systems to Late Pliocene/Early Pleistocene climate cooling', *Clim. Past*, 8(5), pp. 1435-1445.

Etourneau, J., Martinez, P., Blanz, T. and Schneider, R. (2009) 'Pliocene-Pleistocene variability of upwelling activity, productivity, and nutrient cycling in the Benguela region', *Geology*, 37(10), pp. 871-874.

Etourneau, J., Schneider, R., Blanz, T. and Martinez, P. (2010) 'Intensification of the Walker and Hadley atmospheric circulations during the Pliocene-Pleistocene climate transition', *Earth and Planetary Science Letters*, 297(1-2), pp. 103-110.

Evitt, W.R. (1963) 'A discussion and proposals concerning fossil dinoflagellates, hystrichospheres, and acritarchs, I', *Proceedings of the National Academy of Sciences*, 49(2), pp. 158-164.

Fairbanks, R.G., Wiebe, P.H. and Ba, A.W.H. (1980) 'Vertical Distribution and Isotopic Composition of Living Planktonic Foraminifera in the Western North Atlantic', *Science*, 207(4426), pp. 61-63.

Farmer, E.C., deMenocal, P.B. and Marchitto, T.M. (2005) 'Holocene and deglacial ocean temperature variability in the Benguela upwelling region: Implications for low-latitude atmospheric circulation', *Paleoceanography*, 20(2), p. PA2018.

Fedorov, A., Barreiro, M., Boccaletti, G., Pacanowski, R. and Philander, S.G. (2007) 'The Freshening of Surface Waters in High Latitudes: Effects on the Thermohaline and Wind-Driven Circulations', *Journal of Physical Oceanography*, 37(4), pp. 896-907.

Fedorov, A.V., Brierley, C.M. and Emanuel, K. (2010) 'Tropical cyclones and permanent El Nino in the early Pliocene epoch', *Nature*, 463(7284), pp. 1066-1070.

Fedorov, A.V., Dekens, P.S., McCarthy, M., Ravelo, A.C., deMenocal, P.B., Barreiro, M., Pacanowski, R.C. and Philander, S.G. (2006) 'The Pliocene paradox (mechanisms for a permanent El Nino)', *Science*, 312(5779), pp. 1485-1489.

Ferretti, P., Shackleton, N.J., Rio, D. and Hall, M.A. (2005) 'Early-Middle Pleistocene deep circulation in the western subtropical Atlantic: southern hemisphere modulation of the North Atlantic Ocean', *Geological Society, London, Special Publications*, 247(1), pp. 131-145.

Filippelli, G.M. and Flores, J.A. (2009) 'From the warm Pliocene to the cold Pleistocene: A tale of two oceans', *Geology*, 37(10), pp. 959-960.

Fine, R.A., Warner, M.J. and Weiss, R.F. (1988) 'Water mass modification at the Agulhas retroflection: chlorofluoromethane studies', *Deep Sea Research Part A. Oceanographic Research Papers*, 35(3), pp. 311-332.

Flesche Kleiven, H., Jansen, E., Fronval, T. and Smith, T.M. (2002) 'Intensification of Northern Hemisphere glaciations in the circum Atlantic region (3.5–2.4 Ma) – ice-rafted detritus evidence', *Palaeogeography, Palaeoclimatology, Palaeoecology*, 184(3–4), pp. 213-223.

Flores, J.-A., Gersonde, R. and Sierro, F.J. (1999) 'Pleistocene fluctuations in the Agulhas Current Retroflection based on the calcareous plankton record', *Marine Micropaleontology*, 37(1), pp. 1-22.

Flores, J.-A. and Sierro, F.J. (2007) 'Pronounced mid-Pleistocene southward shift of the Polar Front in the Atlantic sector of the Southern Ocean', *Deep Sea Research Part II: Topical Studies in Oceanography*, 54(21-22), pp. 2432-2442.

Flower, B.P., Oppo, D.W., McManus, J.F., Venz, K.A., Hodell, D.A. and Cullen, J.L. (2000) 'North Atlantic intermediate to deep water circulation and chemical stratification during the past 1 Myr', *Paleoceanography*, 15(4), pp. 388-403.

Franzese, A.M., Hemming, S.R. and Goldstein, S.L. (2009) 'Use of strontium isotopes in detrital sediments to constrain the glacial position of the Agulhas Retroflection', *Paleoceanography*, 24, p. 12.

Franzese, A.M., Hemming, S.R., Goldstein, S.L. and Anderson, R.F. (2006) 'Reduced Agulhas Leakage during the Last Glacial Maximum inferred from an integrated provenance and flux study', *Earth and Planetary Science Letters*, 250(1-2), pp. 72-88.

Friedman, I., Schoen, B. and Harris, J. (1961) 'The deuterium concentration in Arctic sea ice', *Journal of Geophysical Research*, 66(6), pp. 1861-1864.

Garzoli, S.L. and Giulivi, C. (1994) 'What forces the variability of the southwestern Atlantic boundary currents?', *Deep Sea Research Part I: Oceanographic Research Papers*, 41(10), pp. 1527-1550.

Giraudeau, J., Meyers, P.A. and Christensen, B.A. (2002) 'Accumulation of organic and inorganic carbon in Pliocene-Pleistocene sediments along the SW African margin', *Marine Geology*, 180(1-4), pp. 49-69.

Giraudeau, J., Pierre, C. and Herve, L. (2001) *A Late Quarternary,* High-Resolution Record of Planktonic Foraminiferal Species Distribution in the Southern Benguela Region: Site 1087. *Proceedings of the Ocean Drilling Program, Scientific Results*

Gong, C. and Hollander, D.J. (1999) 'Evidence for differential degradation of alkenones under contrasting bottom water oxygen conditions: Implication for paleotemperature reconstruction', *Geochimica et Cosmochimica Acta*, 63(3-4), pp. 405-411.

Gooday, A.J., Editors-in-Chief:Â Â John, H.S., Karl, K.T. and Steve, A.T. (2001) 'Benthic Foraminifera', in *Encyclopedia of Ocean Sciences (Second Edition)*. Oxford: Academic Press, pp. 336-347.

Gooday, A.J. and Jorissen, F.J. (2012) 'Benthic Foraminiferal Biogeography: Controls on Global Distribution Patterns in Deep-Water Settings', in Carlson, C.A. and Giovannoni, S.J. (eds.) *Annual Review of Marine Science, Vol 4*. Palo Alto: Annual Reviews, pp. 237-262.

Gordon, A.L. (1985) 'Indian-Atlantic Transfer of Thermocline Water at the Agulhas Retroflection', *Science*, 227(4690), pp. 1030-1033.

Gordon, A.L. and Haxby, W.F. (1990) 'Agulhas Eddies Invade the South Atlantic: Evidence From Geosat Altimeter and Shipboard Conductivity-Temperature-Depth Survey', *J. Geophys. Res.*, 95(C3), pp. 3117-3125.

Gordon, A.L., Lutjeharms, J.R.E. and Gründlingh, M.L. (1987) 'Stratification and circulation at the Agulhas Retroflection', *Deep Sea Research Part A. Oceanographic Research Papers*, 34(4), pp. 565-599.

Gordon, A.L., Weiss, R.F., Smethie, W.M., Jr. and Warner, M.J. (1992) 'Thermocline and Intermediate Water Communication Between the South Atlantic and Indian Oceans', *J. Geophys. Res.*, 97(C5), pp. 7223-7240.

Gordon, H.R., Clark, D.K., Mueller, J.L. and Hovis, W.A. (1980) 'Phytoplankton Pigments from the Nimbus-7 Coastal Zone Color Scanner: Comparisons with Surface Measurements', *Science*, 210(4465), pp. 63-66.

Grimalt, J.O., Rullkötter, J., Sicre, M.-A., Summons, R., Farrington, J., Harvey, H.R., Goñi, M. and Sawada, K. (2000) 'Modifications of the C37 alkenone and alkenoate composition in the water column and sediment: Possible implications for sea surface temperature estimates in paleoceanography', *Geochemistry Geophysics Geosystems*, 1(11).

Groeneveld, J. and Chiessi, C.M. (2011) 'Mg/Ca of Globorotalia inflata as a recorder of permanent thermocline temperatures in the South Atlantic', *Paleoceanography*, 26(2), p. PA2203.

Gründlingh, M.L. (1980) 'On the volume transport of the Agulhas Current', *Deep Sea Research Part A. Oceanographic Research Papers*, 27(7), pp. 557-563.

Guiot, J. and de Vernal, A. (2007) *Transfer functions: methods for quantitative paleoceanography based on microfossils*. Elsevier.

Hargreaves, J.C., Paul, A., Ohgaito, R., Abe-Ouchi, A. and Annan, J.D. (2012) 'Are paleoclimate model ensembles consistent with the MARGO data synthesis?', *Climate of the Past*, 7(3), pp. 917-933.

Harris, P.G., Zhao, M., Rosell-Mele, A., Tiedemann, R., Sarnthein, M. and Maxwell, J.R. (1996) 'Chlorin accumulation rate as a proxy for Quaternary marine primary productivity', *Nature*, 383(6595), pp. 63-65.

Harris, T.F.W. and van Foreest, D. (1978) 'The Agulhas Current in March 1969', *Deep Sea Research*, 25(6), pp. 549-550, IN7-IN8, 551-561.

Haug, G.H., Ganopolski, A., Sigman, D.M., Rosell-Mele, A., Swann, G.E.A., Tiedemann, R., Jaccard, S.L., Bollmann, J., Maslin, M.A., Leng, M.J. and Eglinton, G. (2005) 'North Pacific seasonality and the glaciation of North America 2.7 million years ago', *Nature*, 433(7028), pp. 821-825.

Haug, G.H., Sigman, D.M., Tiedemann, R., Pedersen, T.F. and Sarnthein, M. (1999) 'Onset of permanent stratification in the subarctic Pacific Ocean', *Nature*, 401(6755), pp. 779-782.

Haug, G.H., Tiedemann, R., Zahn, R. and Ravelo, A.C. (2001) 'Role of Panama uplift on oceanic freshwater balance', *Geology*, 29(3), pp. 207-210.

Hays, J.D., Imbrie, J. and Shackleton, N.J. (1976) 'Variations in the Earth's Orbit: Pacemaker of the Ice Ages', *Science*, 194(4270), pp. 1121-1132.

Haywood, A.M., Chandler, M.A., Valdes, P.J., Salzmann, U., Lunt, D.J. and Dowsett, H.J. (2009a) 'Comparison of mid-Pliocene climate predictions produced by the HadAM3 and GCMAM3 General Circulation Models', *Global and Planetary Change*, 66(3-4), pp. 208-224.

Haywood, A.M., Dowsett, H.J., Valdes, P.J., Lunt, D.J., Francis, J.E. and Sellwood, B.W. (2009b) 'Introduction. Pliocene climate, processes and problems', *Philosophical Transactions of the Royal Society a-Mathematical Physical and Engineering Sciences*, 367(1886), pp. 3-17.

Haywood, A.M., Hill, D.J., Dolan, A.M., Otto-Bliesner, B.L., Bragg, F., Chan, W.L., Chandler, M.A., Contoux, C., Dowsett, H.J., Jost, A., Kamae, Y., Lohmann, G., Lunt, D.J., Abe-Ouchi, A., Pickering, S.J., Ramstein, G., Rosenbloom, N.A., Salzmann, U., Sohl, L., Stepanek, C., Ueda, H., Yan, Q. and Zhang, Z. (2013) 'Large-scale features of Pliocene climate: results from the Pliocene Model Intercomparison Project', *Clim. Past*, 9(1), pp. 191-209.

Haywood, A.M. and Valdes, P.J. (2004) 'Modelling Pliocene warmth: contribution of atmosphere, oceans and cryosphere', *Earth and Planetary Science Letters*, 218(3-4), pp. 363-377.

Haywood, A.M., Valdes, P.J. and Sellwood, B.W. (2000) 'Global scale palaeoclimate reconstruction of the middle Pliocene climate using the UKMO GCM: initial results', *Global and Planetary Change*, 25(3-4), pp. 239-256.

Heinrich, S., Zonneveld, K.A.F., Bickert, T. and Willems, H. (2011) 'The Benguela upwelling related to the Miocene cooling events and the development of the Antarctic Circumpolar Current: Evidence from calcareous dinoflagellate cysts', *Paleoceanography*, 26(3), p. PA3209.

Henderiks, J. and Pagani, M. (2007) 'Refining ancient carbon dioxide estimates: Significance of coccolithophore cell size for alkenone-based pCO2 records', *Paleoceanography*, 22(3), p. PA3202.

Herbert, T.D., Peterson, L.C., Lawrence, K.T. and Liu, Z. (2010) 'Tropical Ocean Temperatures Over the Past 3.5 Million Years', *Science*, 328(5985), pp. 1530-1534.

Ho, S.L., Mollenhauer, G., Lamy, F., Martínez-Garcia, A., Mohtadi, M., Gersonde, R., Hebbeln, D., Nunez-Ricardo, S., Rosell-Melé, A. and Tiedemann, R. (2012) 'Sea surface temperature variability in the Pacific sector of the Southern Ocean over the past 700 kyr', *Paleoceanography*, 27(4), pp. n/a-n/a.

Hodell, D.A., Charles, C.D. and Ninnemann, U.S. (2000) 'Comparison of interglacial stages in the South Atlantic sector of the southern ocean for the past 450 kyr: implifications for Marine Isotope Stage (MIS) 11', *Global and Planetary Change*, 24(1), pp. 7-26.

Hodell, D.A., Venz, K.A., Charles, C.D. and Ninnemann, U.S. (2003) 'Pleistocene vertical carbon isotope and carbonate gradients in the South Atlantic sector of the Southern Ocean', *Geochemistry Geophysics Geosystems*, 4, p. 19.

Hodell, D.A., Williams, D.F. and Kennett, J.P. (1985) 'Late Pliocene reorganization of deep vertical water-mass structure in the western South Atlantic: Faunal and isotopic evidence', *Geological Society of America Bulletin*, 96(4), pp. 495-503.

Holden, P.B., Edwards, N.R., Wolff, E.W., Valdes, P.J. and Singarayer, J.S. (2011) 'The Mid-Brunhes Event and West Antarctic ice sheet stability', *Journal of Quaternary Science*, 26(5), pp. 474-477.

Holliday, N.P. and Read, J.F. (1998) 'Surface oceanic fronts between Africa and Antarctica', *Deep Sea Research Part I: Oceanographic Research Papers*, 45(2-3), pp. 217-238.

Hollis, C.J., Taylor, K.W.R., Handley, L., Pancost, R.D., Huber, M., Creech, J.B., Hines, B.R., Crouch, E.M., Morgans, H.E.G., Crampton, J.S., Gibbs, S., Pearson, P.N. and Zachos, J.C. (2012) 'Early Paleogene temperature history of the Southwest Pacific Ocean: Reconciling proxies and models', *Earth and Planetary Science Letters*, 349, pp. 53-66.

Holzwarth, U., Esper, O. and Zonneveld, K. (2007) 'Distribution of organic-walled dinoflagellate cysts in shelf surface sediments of the Benguela upwelling system in relationship to environmental conditions', *Marine Micropaleontology*, 64(1-2), pp. 91-119.

Honisch, B., Hemming, N.G., Archer, D., Siddall, M. and McManus, J.F. (2009) 'Atmospheric Carbon Dioxide Concentration Across the Mid-Pleistocene Transition', *Science*, 324(5934), pp. 1551-1554.

Hoogakker, B.A.A., Rohling, E.J., Palmer, M.R., Tyrrell, T. and Rothwell, R.G. (2006) 'Underlying causes for long-term global ocean $\delta^{13}C$ fluctuations over the last 1.20 Myr', *Earth and Planetary Science Letters*, 248(1-2), pp. 15-29.

Huang, Y., Dupont, L., Sarnthein, M., Hayes, J.M. and Eglinton, G. (2000) 'Mapping of C4 plant input from North West Africa into North East Atlantic sediments', *Geochimica et Cosmochimica Acta*, 64(20), pp. 3505-3513.

Huguet, C., Kim, J.H., de Lange, G.J., Damste, J.S.S. and Schouten, S. (2009) 'Effects of long term oxic degradation on the U-37(K '), TEX86 and BIT organic proxies', *Organic Geochemistry*, 40(12), pp. 1188-1194.

Huguet, C., Schimmelmann, A., Thunell, R., Lourens, L.J., Damste, J.S.S. and Schouten, S. (2007) 'A study of the TEX(86) paleothermometer in the water column and sediments of the Santa Barbara Basin, California', *Paleoceanography*, 22(3), p. 9.

Hutchings, L., van der Lingen, C.D., Shannon, L.J., Crawford, R.J.M., Verheye, H.M.S., Bartholomae, C.H., van der Plas, A.K., Louw, D., Kreiner, A., Ostrowski, M., Fidel, Q., Barlow, R.G., Lamont, T., Coetzee, J., Shillington, F., Veitch, J., Currie, J.C. and Monteiro, P.M.S. (2009) 'The Benguela Current: An ecosystem of four components', *Progress In Oceanography*, 83(1-4), pp. 15-32.

Hutson, W.H. (1980) 'The Agulhas Current During the Late Pleistocene: Analysis of Modern Faunal Analogs', *Science*, 207(4426), pp. 64-66.

Huybers, P. (2009) 'Pleistocene glacial variability as a chaotic response to obliquity forcing', *Climate of the Past*, 5(3), pp. 481-488.

Imbrie, J., Mix, A.C. and Martinson, D.G. (1993) 'Milankovitch theory viewed from Devils Hole', *Nature*, 363(6429), pp. 531-533.

IPCC (2007) 'Climate Change 2007: Synthesis Report ', in Pachauri, R.K.a.R., A. (ed.) *Contribution of Working Groups I, II and III to the Fourth Assessment Report of the Intergovernmental Panel on Climate Change*. Geneva, Switzerland: IGPCC, p. pp. 104.

Jansen, E., Fronval, T., Rack, F. and Channell, J.E.T. (2000) 'Pliocene-Pleistocene Ice Rafting History and Cyclicity in the Nordic Seas During the Last 3.5 Myr', *Paleoceanography*, 15(6), pp. 709-721.

Jansen, E. and Sjoholm, J. (1991) 'Reconstruction of glaciation over the past 6 Myr from ice-borne deposits in the Norwegian Sea', *Nature*, 349(6310), pp. 600-603.

Jochum, M., Fox-Kemper, B., Molnar, P.H. and Shields, C. (2009) 'Differences in the Indonesian seaway in a coupled climate model and their relevance to Pliocene climate and El Nino', *Paleoceanography*, 24, p. 13.

Johnstone, H.J.H., Yu, J., Elderfield, H. and Schulz, M. (2011) 'Improving temperature estimates derived from Mg/Ca of planktonic foraminifera using X-ray computed tomography–based dissolution index, XDX', *Paleoceanography*, 26(1), p. PA1215.

Jones, J.I. (1967) 'Significance of Distribution of Planktonic Foraminifera in the Equatorial Atlantic Undercurrent', *Micropaleontology*, 13(4), pp. 489-501.

Kandiano, E.S. and Bauch, H.A. (2007) 'Phase relationship and surface water mass change in the northeast Atlantic during marine isotope stage 11 (MIS 11)', *Quaternary Research*, 68(3), pp. 445-455.

Karas, C., Nurnberg, D., Gupta, A.K., Tiedemann, R., Mohan, K. and Bickert, T. (2009) 'Mid-Pliocene climate change amplified by a switch in Indonesian subsurface throughflow', *Nature Geoscience*, 2(6), pp. 433-437.

Karas, C., Nurnberg, D. and Tiedemann, R. (2012) 'The Southwest Pacific during the Pliocene: A reply to Dickens and Backman, 2011', *Earth and Planetary Science Letters*, 331â€"332(0), pp. 360-363.

Karas, C., Nurnberg, D., Tiedemann, R. and Garbe-Schonberg, D. (2011a) 'Pliocene climate change of the Southwest Pacific and the impact of ocean gateways', *Earth and Planetary Science Letters*, 301(1-2), pp. 117-124.

Karas, C., Nürnberg, D., Tiedemann, R. and Garbe-Schönberg, D. (2011b) 'Pliocene Indonesian Throughflow and Leeuwin Current dynamics: Implications for Indian Ocean polar heat flux', *Paleoceanography*, 26(2), p. PA2217.

Keany, J. and Kennett, J.P. (1972) 'Pliocene-early Pleistocene paleoclimatic history recorded in Antarctic-Subantarctic deep-sea cores', *Deep Sea Research and Oceanographic Abstracts*, 19(8), pp. 529-548.

Kemp, A.E.S., Grigorov, I., Pearce, R.B. and Naveira Garabato, A.C. (2010) 'Migration of the Antarctic Polar Front through the mid-Pleistocene transition: evidence and climatic implications', *Quaternary Science Reviews*, 29(17-18), pp. 1993-2009.

Killops, S. and Killops, V. (2005) *Introduction to Organic Geochemistry*. 2nd edn. Malden ME: Blackwell Publishing.

Kim, J.-H., Schouten, S., Hopmans, E.C., Donner, B. and Sinninghe Damsté, J.S. (2008) 'Global sediment core-top calibration of the TEX86 paleothermometer in the ocean', *Geochimica Et Cosmochimica Acta*, 72(4), pp. 1154-1173.

Kim, J.-H., van der Meer, J., Schouten, S., Helmke, P., Willmott, V., Sangiorgi, F., KoÃ§, N.n., Hopmans, E.C. and DamstÃ©, J.S.S. (2010) 'New indices and calibrations derived from the distribution of crenarchaeal isoprenoid tetraether lipids: Implications for past sea surface temperature reconstructions', *Geochimica et Cosmochimica Acta*, 74(16), pp. 4639-4654.

Kim, J.-H., Zell, C., Moreira-Turcq, P., Pérez, M.A.P., Abril, G., Mortillaro, J.-M., Weijers, J.W.H., Meziane, T. and Sinninghe Damsté, J.S. (2012) 'Tracing soil organic carbon in the lower Amazon River and its tributaries using GDGT distributions and bulk organic matter properties', *Geochimica et Cosmochimica Acta*, 90(0), pp. 163-180.

Kim, J.H., Huguet, C., Zonneveld, K.A.F., Versteegh, G.J.M., Roeder, W., Damste, J.S.S. and Schouten, S. (2009) 'An experimental field study to test the stability of lipids used for the TEX86 and U-37(K ') palaeothermometers', *Geochimica et Cosmochimica Acta*, 73(10), pp. 2888-2898.

Kitamura, A. and Kawagoe, T. (2006) 'Eustatic sea-level change at the Mid-Pleistocene climate transition: new evidence from the shallow-marine sediment record of Japan', *Quaternary Science Reviews*, 25(3-4), pp. 323-335.

Kleiven, H.F., Jansen, E., Fronval, T. and Smith, T.M. (2002) 'Intensification of Northern Hemisphere glaciations in the circum Atlantic region (3.5-2.4 Ma)  ice-rafted detritus evidence', *Palaeogeography, Palaeoclimatology, Palaeoecology*, 184(3-4), pp. 213-223.

Knorr, G. and Lohmann, G. (2003) 'Southern Ocean origin for the resumption of Atlantic thermohaline circulation during deglaciation', *Nature*, 424(6948), pp. 532-536.

Knorr, G. and Lohmann, G. (2007) 'Rapid transitions in the Atlantic thermohaline circulation triggered by global warming and meltwater during the last deglaciation', *Geochemistry Geophysics Geosystems*, 8, p. 22.

Kornilova, O. and Rosell-Mele, A. (2003) 'Application of microwave-assisted extraction to the analysis of biomarker climate proxies in marine sediments', *Organic Geochemistry*, 34(11), pp. 1517-1523.

Kroon, D. and Ganssen, G. (1989) 'Northern Indian Ocean upwelling cells and the stable isotope composition of living planktonic foraminifers', *Deep Sea Research Part A. Oceanographic Research Papers*, 36(8), pp. 1219-1236.

Krueger, S., Leuschner, D.C., Ehrmann, W., Schmiedl, G., Mackensen, A. and Diekmann, B. (2008) 'Ocean circulation patterns and dust supply into the South Atlantic during the last glacial cycle revealed by statistical analysis of kaolinite/chlorite ratios', *Marine Geology*, 253(3-4), pp. 82-91.

Kucera, M., Rosell-Mele, A., Schneider, R., Waelbroeck, C. and Weinelt, M. (2005) 'Multiproxy approach for the reconstruction of the glacial ocean surface (MARGO)', *Quaternary Science Reviews*, 24(7-9), pp. 813-819.

Labeyrie, L., Labracherie, M., Gorfti, N., Pichon, J.J., Vautravers, M., Arnold, M., Duplessy, J.-C., Paterne, M., Michel, E., Duprat, J., Caralp, M. and Turon, J.-L. (1996) 'Hydrographic Changes of the Southern Ocean (Southeast Indian Sector) Over the Last 230 kyr', *Paleoceanography*, 11(1), pp. 57-76.

Lang, N. and Wolff, E.W. (2011) 'Interglacial and glacial variability from the last 800 ka in marine, ice and terrestrial archives', *Climate of the Past*, 7(2), pp. 361-380.

Lange, C.B., Berger, W.H., Lin, H.L. and Wefer, G. (1999) 'The early Matuyama Diatom Maximum off SW Africa, Benguela Current System (ODP Leg 175)', *Marine Geology*, 161(2-4), pp. 93-114.

Larsen, H.C., Saunders, A.D., Clift, P.D., Beget, J., Wei, W., Spezzaferri, S. and Party, O.D.P.L.S. (1994) 'Seven Million Years of Glaciation in Greenland', *Science*, 264(5161), pp. 952-955.

Laurian, A. and Drijfhout, S.S. (2011) 'Response of the South Atlantic circulation to an abrupt collapse of the Atlantic meridional overturning circulation', *Climate Dynamics*, 37(3-4), pp. 521-530.

Lawrence, K.T., Herbert, T.D., Brown, C.M., Raymo, M.E. and Haywood, A.M. (2009) 'High-amplitude variations in North Atlantic sea surface temperature during the early Pliocene warm period', *Paleoceanography*, 24, p. 15.

Lawrence, K.T., Sosdian, S., White, H.E. and Rosenthal, Y. (2010) 'North Atlantic climate evolution through the Plio-Pleistocene climate transitions', *Earth and Planetary Science Letters*, 300(3-4), pp. 329-342.

Lea, D.W., Mashiotta, T.A. and Spero, H.J. (1999) 'Controls on magnesium and strontium uptake in planktonic foraminifera determined by live culturing', *Geochimica et Cosmochimica Acta*, 63(16), pp. 2369-2379.

Lee, K.E., Kim, J.-H., Wilke, I., Helmke, P. and Schouten, S. (2008) 'A study of the alkenone, TEX86, and planktonic foraminifera in the Benguela Upwelling System: Implications for past sea surface temperature estimates', *Geochemistry Geophysics Geosystems*, 9(10), p. Q10019.

Linke, P. and Lutze, G.F. (1993) 'Microhabitat preferences of benthic foraminifera a static concept or a dynamic adaptation to optimize food acquisition?', *Marine Micropaleontology*, 20(3-4), pp. 215-234.

Lisiecki, L.E. and Raymo, M.E. (2005) 'A Pliocene-Pleistocene stack of 57 globally distributed benthic delta O-18 records', *Paleoceanography*, 20(1), p. 17.

Lisiecki, L.E. and Raymo, M.E. (2007) 'Plio-Pleistocene climate evolution: trends and transitions in glacial cycle dynamics', *Quaternary Science Reviews*, 26(1-2), pp. 56-69.

Little, M.G., Schneider, R.R., Kroon, D., Price, B., Summerhayes, C.P. and Segl, M. (1997) 'Trade Wind Forcing of Upwelling, Seasonally, and Heinrich Events as a Response to Sub-Milankovitch Climate Variability', *Paleoceanography*, 12(4), pp. 568-576.

Liu, Z.H., Cleaveland, L.C. and Herbert, T.D. (2008) 'Early onset and origin of 100-kyr cycles in Pleistocene tropical SST records', *Earth and Planetary Science Letters*, 265(3-4), pp. 703-715.

Lohmann, G.P. (1992) 'Increasing seasonal upwelling in the subtropical South Atlantic over the past 700,000 yrs: Evidence from deep-living planktonic foraminifera', *Marine Micropaleontology*, 19(1â€"2), pp. 1-12.

Loutre, M.F. and Berger, A. (2003) 'Marine Isotope Stage 11 as an analogue for the present interglacial', *Global and Planetary Change*, 36(3), pp. 209-217.

Lunt, D.J., Haywood, A.M., Foster, G.L. and Stone, E.J. (2009) 'The Arctic cryosphere in the Mid-Pliocene and the future', *Philosophical Transactions of the Royal Society A: Mathematical, Physical and Engineering Sciences*, 367(1886), pp. 49-67.

Luthi, D., Le Floch, M., Bereiter, B., Blunier, T., Barnola, J.-M., Siegenthaler, U., Raynaud, D., Jouzel, J., Fischer, H., Kawamura, K. and Stocker, T.F. (2008) 'High-resolution carbon dioxide concentration record 650,000-800,000 years before present', *Nature*, 453(7193), pp. 379-382.

Lutjeharms, J.R.E. (1981) 'Spatial scales and intensities of circulation in the ocean areas adjacent to South Africa', *Deep Sea Research Part A. Oceanographic Research Papers*, 28(11), pp. 1289-1302.

Lutjeharms, J.R.E. (1985) 'Location of frontal systems between Africa and Antarctica: some preliminary results', *Deep Sea Research Part A. Oceanographic Research Papers*, 32(12), pp. 1499-1509.

Lutjeharms, J.R.E. (1994) *Symposium on the South Atlantic - Present and Past Circulation*. Bremen, Germany, Aug 15-18. Springer-Verlag Berlin(Accessed: <Go to ISI>://A1996BH55D00008).

Lutjeharms, J.R.E. (2007) 'Three decades of research on the greater Agulhas Current', *Ocean Science*, 3(1), pp. 129-147.

Lutjeharms, J.R.E. and Gordon, A.L. (1987) 'Shedding of an Agulhas ring observed at sea', *Nature*, 325(6100), pp. 138-140.

Lutjeharms, J.R.E., John, H.S., Karl, K.T. and Steve, A.T. (2001) 'Agulhas Current', in *Encyclopedia of Ocean Sciences*. Oxford: Academic Press,  pp. 128-137.

Mackensen, A. (2004) 'Changing Southern Ocean palaeocirculation and effects on global climate', *Antarctic Science*, 16(4), pp. 369-386.

Maiorano, P., Marino, M. and Flores, J.-A. (2009) 'The warm interglacial Marine Isotope Stage 31: Evidences from the calcareous nannofossil assemblages at Site 1090 (Southern Ocean)', *Marine Micropaleontology*, 71(3-4), pp. 166-175.

MARGO (2009) 'Constraints on the magnitude and patterns of ocean cooling at the Last Glacial Maximum', *Nature Geosci*, 2(2), pp. 127-132.

Marino, M., Maiorano, P., Lirer, F. and Pelosi, N. (2009) 'Response of calcareous nannofossil assemblages to paleoenvironmental changes through the mid-Pleistocene revolution at Site 1090 (Southern Ocean)', *Palaeogeography, Palaeoclimatology, Palaeoecology*, 280(3-4), pp. 333-349.

Marlow, J.R., Lange, C.B., Wefer, G. and Rosell-Mele, A. (2000) 'Upwelling intensification as part of the Pliocene-Pleistocene climate transition', *Science*, 290(5500), pp. 2288-+.

Marlowe, I.T., Brassell, S.C., Eglinton, G. and Green, J.C. (1984a) 'Long chain unsaturated ketones and esters in living algae and marine sediments', *Organic Geochemistry*, 6, pp. 135-141.

Marlowe, I.T., Green, J.C., Neal, A.C., Brassell, S.C., Eglinton, G. and Course, P.A. (1984b) 'Long-chain (n-C37-C39) alkenones in the prymnisiophyceae – distribution of alkenones and other lipids and their taxonomic significance', *British Phycological Journal*, 19(3), pp. 203-216.

Marret, F., Maley, J. and Scourse, J. (2006) 'Climatic instability in west equatorial Africa during the Mid- and Late Holocene', *Quaternary International*, 150(1), pp. 71-81.

Marret, F., Scourse, J., Kennedy, H., Ufkes, E. and Jansen, J.H.F. (2008) 'Marine production in the Congo-influenced SE Atlantic over the past 30,000 years: A novel dinoflagellate-cyst based transfer function approach', *Marine Micropaleontology*, 68(1-2), pp. 198-222.

Marret, F. and Zonneveld, K.A.F. (2003) 'Atlas of modern organic-walled dinoflagellate cyst distribution', *Review of Palaeobotany and Palynology*, 125(1-2), pp. 1-200.

Martinez-Garcia, A., Rosell-Mele, A., Jaccard, S.L., Geibert, W., Sigman, D.M. and Haug, G.H. (2011) 'Southern Ocean dust-climate coupling over the past four million years', *Nature*, 476(7360), pp. 312-315.

Martinez-Garcia, A., Rosell-Mele, A., McClymont, E.L., Gersonde, R. and Haug, G.H. (2010) 'Subpolar Link to the Emergence of the Modern Equatorial Pacific Cold Tongue', *Science*, 328(5985), pp. 1550-1553.

Martínez-Méndez, G., Zahn, R., Hall, I.R., Peeters, F.J.C., Pena, L.D., Cacho, I. and Negre, C. (2010) 'Contrasting multiproxy reconstructions of surface ocean hydrography in the Agulhas Corridor and implications for the Agulhas Leakage during the last 345,000 years', *Paleoceanography*, 25(4), p. PA4227.

Martínez-Méndez, G., Zahn, R., Hall, I.R., Pena, L.D. and Cacho, I. (2008) '345,000-year-long multi-proxy records off South Africa document variable contributions of Northern versus Southern Component Water to the Deep South Atlantic', *Earth and Planetary Science Letters*, 267(1-2), pp. 309-321.

März, C., Schnetger, B. and Brumsack, H.J. (2013) 'Nutrient leakage from the North Pacific to the Bering Sea (IODP Site U1341) following the onset of Northern Hemispheric Glaciation?', *Paleoceanography*.

Masson-Delmotte, V., Stenni, B., Pol, K., Braconnot, P., Cattani, O., Falourd, S., Kageyama, M., Jouzel, J., Landais, A., Minster, B., Barnola, J.M., Chappellaz, J.,

Krinner, G., Johnsen, S., Röthlisberger, R., Hansen, J., Mikolajewicz, U. and Otto-Bliesner, B. (2010) 'EPICA Dome C record of glacial and interglacial intensities', *Quaternary Science Reviews*, 29(1-2), pp. 113-128.

McClain, C.R. (2009) 'A Decade of Satellite Ocean Color Observations', *Annual Review of Marine Science*, 1(1), pp. 19-42.

McClymont, E.L., Ganeshram, R.S., Pichevin, L.E., Talbot, H.M., van Dongen, B.E., Thunell, R.C., Haywood, A.M., Singarayer, J.S. and Valdes, P.J. (2012) 'Sea-surface temperature records of Termination 1 in the Gulf of California: Challenges for seasonal and interannual analogues of tropical Pacific climate change', *Paleoceanography*, 27(2), p. PA2202.

McClymont, E.L., Martinez-Garcia, A. and Rosell-Mele, A. (2007) 'Benefits of freeze-drying sediments for the analysis of total chlorins and alkenone concentrations in marine sediments', *Organic Geochemistry*, 38(6), pp. 1002-1007.

McClymont, E.L. and Rosell-Mele, A. (2005) 'Links between the onset of modern Walker circulation and the mid-Pleistocene climate transition', *Geology*, 33(5), pp. 389-392.

McClymont, E.L., Rosell-Mele, A., Giraudeau, J., Pierre, C. and Lloyd, J.M. (2005) 'Alkenone and coccolith records of the mid-Pleistocene in the south-east Atlantic: Implications for the U-37(K) index and South African climate', *Quaternary Science Reviews*, 24(14-15), pp. 1559-1572.

McClymont, E.L., Sosdianb, S.M., Rosell-Melé, A. and Rosenthalb, Y. (2013) 'Pleistocene sea-surface temperature evolution: early cooling, delayed glacial intensification, and implications for the mid-Pleistocene climate transition', *Earth Science Reveiw*.

McCrea, J.M. (1950) 'On the Isotopic Chemistry of Carbonates and a Paleotemperature Scale', *The Journal of Chemical Physics*, 18(6), pp. 849-857.

McKay, R., Naish, T., Carter, L., Riesselman, C., Dunbar, R., Sjunneskog, C., Winter, D., Sangiorgi, F., Warren, C., Pagani, M., Schouten, S., Willmott, V., Levy, R., DeConto, R. and Powell, R.D. (2012) 'Antarctic and Southern Ocean influences on Late Pliocene global cooling', *Proceedings of the National Academy of Sciences*, 109(17), pp. 6423-6428.

McKinney, C.R., McCrea, J.M., Epstein, S., Allen, H.A. and Urey, H.C. (1950) 'Improvements in Mass Spectrometers for the Measurement of Small Differences in Isotope Abundance Ratios', *Review of Scientific Instruments*, 21(8), pp. 724-730.

Mertens, K.N., Rengefors, K., Moestrup, O. and Ellegaard, M. (2012) 'A review of recent freshwater dinoflagellate cysts: taxonomy, phylogeny, ecology and palaeocology', *Phycologia*, 51(6), pp. 612-619.

Mertens, K.N., Verhoeven, K., Verleye, T., Louwye, S., Amorim, A., Ribeiro, S., Deaf, A.S., Harding, I.C., De Schepper, S., GonzÃ¡lez, C., Kodrans-Nsiah, M., De Vernal, A., Henry, M., Radi, T., Dybkjaer, K., Poulsen, N.E., Feist-Burkhardt, S., Chitolie, J., Heilmann-Clausen, C., Londeix, L., Turon, J.-L., Marret, F., Matthiessen, J., McCarthy, F.M.G., Prasad, V., Pospelova, V., Kyffin Hughes, J.E., Riding, J.B., Rochon, A., Sangiorgi, F., Welters, N., Sinclair, N., Thun, C., Soliman, A., Van Nieuwenhove, N., Vink, A. and Young, M. (2009) 'Determining the absolute abundance of dinoflagellate cysts in recent marine sediments: The Lycopodium marker-grain method put to the test', *Review of Palaeobotany and Palynology*, 157(3-4), pp. 238-252.

Meyers, S.R. and Hinnov, L.A. (2010) 'Northern Hemisphere glaciation and the evolution of Plio-Pleistocene climate noise', *Paleoceanography*, 25, p. 11.

Moldowan, J.M., Dahl, J., Jacobson, S.R., Huizinga, B.J., Fago, F.J., Shetty, R., Watt, D.S. and Peters, K.E. (1996) 'Chemostratigraphic reconstruction of biofacies: Molecular evidence linking cyst-forming dinoflagellates with pre-Triassic ancestors', *Geology*, 24(2), pp. 159-162.

Molnar, P. (2008) 'Closing of the Central American Seaway and the ice age: A critical review', *Paleoceanography*, 23(1), p. 15.

Molyneux, E.G., Hall, I.R., Zahn, R. and Diz, P. (2007) 'Deep water variability on the southern Agulhas Plateau: Interhemispheric links over the past 170 ka', *Paleoceanography*, 22(4), p. 14.

Mudelsee, M. and Raymo, M.E. (2005) 'Slow dynamics of the Northern Hemisphere glaciation', *Paleoceanography*, 20(4), p. PA4022.

Mudelsee, M. and Schulz, M. (1997) 'The Mid-Pleistocene climate transition: onset of 100 ka cycle lags ice volume build-up by 280 ka', *Earth and Planetary Science Letters*, 151(1-2), pp. 117-123.

Mulitza, S., DÃ¼rkoop, A., Hale, W., Wefer, G. and Stefan Niebler, H. (1997) 'Planktonic foraminifera as recorders of past surface-water stratification', *Geology*, 25(4), pp. 335-338.

Müller, P.J., Cepek, M., Ruhland, G. and Schneider, R.R. (1997) 'Alkenone and coccolithophorid species changes in late Quaternary sediments from the Walvis Ridge: Implications for the alkenone paleotemperature method', *Palaeogeography Palaeoclimatology Palaeoecology*, 135(1-4), pp. 71-96.

Müller , P.J., Cepek, M., Ruhland, G. and Schneider, R.R. (1997) 'Alkenone and coccolithophorid species changes in late Quaternary sediments from the Walvis Ridge: Implications for the alkenone paleotemperature method', *Palaeogeography Palaeoclimatology Palaeoecology*, 135(1-4), pp. 71-96.

Müller, P.J., Kirst, G., Ruhland, G., von Storch, I. and Rosell-Mele, A. (1998) 'Calibration of the alkenone paleotemperature index U-37(K ') based on core-tops from the eastern South Atlantic and the global ocean (60 degrees N-60 degrees S)', *Geochimica et Cosmochimica Acta*, 62(10), pp. 1757-1772.

Murray, J.W. (2001) 'The niche of benthic foraminifera, critical thresholds and proxies', *Marine Micropaleontology*, 41(1-2), pp. 1-7.

Naish, T., Powell, R., Levy, R., Wilson, G., Scherer, R., Talarico, F., Krissek, L., Niessen, F., Pompilio, M., Wilson, T., Carter, L., DeConto, R., Huybers, P., McKay, R., Pollard, D., Ross, J., Winter, D., Barrett, P., Browne, G., Cody, R., Cowan, E., Crampton, J., Dunbar, G., Dunbar, N., Florindo, F., Gebhardt, C., Graham, I., Hannah, M., Hansaraj, D., Harwood, D., Helling, D., Henrys, S., Hinnov, L., Kuhn, G., Kyle, P., Laufer, A., Maffioli, P., Magens, D., Mandernack, K., McIntosh, W., Millan, C., Morin, R., Ohneiser, C., Paulsen, T., Persico, D., Raine, I., Reed, J., Riesselman, C., Sagnotti, L., Schmitt, D., Sjunneskog, C., Strong, P., Taviani, M., Vogel, S., Wilch, T. and Williams, T. (2009) 'Obliquity-paced Pliocene West Antarctic ice sheet oscillations', *Nature*, 458(7236), pp. 322-U84.

Nie, J.S., King, J., Liu, Z.Y., Clemens, S., Prell, W. and Fang, X.M. (2008) 'Surface-water freshening: A cause for the onset of North Pacific stratification from 2.75 Ma onward?', *Global and Planetary Change*, 64(1-2), pp. 49-52.

Nürnberg, D., Bijma, J. and Hemleben, C. (1996) 'Assessing the reliability of magnesium in foraminiferal calcite as a proxy for water mass temperatures', *Geochimica et Cosmochimica Acta*, 60(5), pp. 803-814.

Olson, D.B. and Evans, R.H. (1986) 'Rings of the Agulhas current', *Deep Sea Research Part A. Oceanographic Research Papers*, 33(1), pp. 27-42.

Oppo, D.W. and Fairbanks, R.G. (1989) 'Carbon Isotope Composition of Tropical Surface Water during the Past 22,000 Years', *Paleoceanography*, 4(4), pp. 333-351.

Oppo, D.W. and Fairbanks, R.G. (1990) 'Atlantic Ocean thermohaline circulation of the last 150,000 years: Relationship to climate and atmospheric CO2', *Paleoceanography*, 5(3), pp. 277-288.

Oppo, D.W., Raymo, M.E., Lohmann, G.P., Mix, A.C., Wright, J.D. and Prell, W.L. (1995) 'A δ13C record of Upper North Atlantic Deep Water during the past 2.6 million years', *Paleoceanography*, 10(3), pp. 373-394.

Orsi, A.H., Whitworth Iii, T. and Nowlin Jr, W.D. (1995) 'On the meridional extent and fronts of the Antarctic Circumpolar Current', *Deep Sea Research Part I: Oceanographic Research Papers*, 42(5), pp. 641-673.

Pagani, M., Liu, Z.H., LaRiviere, J. and Ravelo, A.C. (2010) 'High Earth-system climate sensitivity determined from Pliocene carbon dioxide concentrations', *Nature Geoscience*, 3(1), pp. 27-30.

Pancost, R.D. and Boot, C.S. (2004) 'The palaeoclimatic utility of terrestrial biomarkers in marine sediments', *Marine Chemistry*, 92(1-4), pp. 239-261.

Passchier, S. (2011) 'Linkages between East Antarctic Ice Sheet extent and Southern Ocean temperatures based on a Pliocene high-resolution record of ice-rafted debris off Prydz Bay, East Antarctica', *Paleoceanography*, 26(4), p. PA4204.

Pearson, E.J., Juggins, S., Talbot, H.M., Weckstrom, J., Rosen, P., Ryves, D.B., Roberts, S.J. and Schmidt, R. (2011) 'A lacustrine GDGT-temperature calibration from the Scandinavian Arctic to Antarctic: Renewed potential for the application of GDGT-paleothermometry in lakes', *Geochimica et Cosmochimica Acta*, 75(20), pp. 6225-6238.

Pearson, P.N., van Dongen, B.E., Nicholas, C.J., Pancost, R.D., Schouten, S., Singano, J.M. and Wade, B.S. (2007) 'Stable warm tropical climate through the Eocene Epoch', *Geology*, 35(3), pp. 211-214.

Peeters, F.J.C., Acheson, R., Brummer, G.-J.A., de Ruijter, W.P.M., Schneider, R.R., Ganssen, G.M., Ufkes, E. and Kroon, D. (2004) 'Vigorous exchange between the Indian and Atlantic oceans at the end of the past five glacial periods', *Nature*, 430(7000), pp. 661-665.

Pena, L.D., Calvo, E., Cacho, I., Eggins, S. and Pelejero, C. (2005) 'Identification and removal of Mn-Mg-rich contaminant phases on foraminiferal tests: Implications for Mg/Ca past temperature reconstructions', *Geochemistry, Geophysics, Geosystems*, 6(9), p. Q09P02.

Peterson, R.G. and Stramma, L. (1991) 'Upper-level circulation in the South Atlantic Ocean', *Progress In Oceanography*, 26(1), pp. 1-73.

Peyron, O. and Vernal, A.d. (2001) 'Application of artificial neural networks (ANN) to high-latitude dinocyst assemblages for the reconstruction of past sea-surface conditions in Arctic and sub-Arctic seas', *Journal of Quaternary Science*, 16(7), pp. 699-709.

Pflaumann, U., Duprat, J., Pujol, C. and Labeyrie, L.D. (1996) 'SIMMAX: A modern analog technique to deduce Atlantic sea surface temperatures from planktonic foraminifera in deep-sea sediments', *Paleoceanography*, 11(1), pp. 15-35.

Pierre, C., Saliege, J.F., Urrutiaguer, M.J. and Giraudeau, J. (eds.) (2001) *Stable isotope record of the last 500 k.y. at Site 1087 (Southern Cape Basin)*. College Station, TX: Ocean Drilling Program.

Pollard, D. and DeConto, R.M. (2009a) 'Modelling West Antarctic ice sheet growth and collapse through the past five million years', *Nature*, 458(7236), pp. 329-U89.

Pollard, D. and DeConto, R.M. (2009b) 'Modelling West Antarctic ice sheet growth and collapse through the past five million years', *Nature*, 458(7236), pp. 329-332.

Powers, L.A., Johnson, T.C., Werne, J.P., Castanada, I.S., Hopmans, E.C., Damste, J.S.S. and Schouten, S. (2005a) 'Large temperature variability in the southern African tropics since the Last Glacial Maximum', *Geophysical Research Letters*, 32(8).

Powers, L.A., Werne, J.P., Johnson, T.C., Hopmans, E.C., Damste, J.S.S. and Schouten, S. (2004) 'Crenarchaeotal membrane lipids in lake sediments: A new paleotemperature proxy for continental paleoclimate reconstruction?', *Geology*, 32(7), pp. 613-616.

Powers, L.A., Werne, J.P., Johnson, T.C., Hopmans, E.C., Damste, J.S.S. and Schouten, S. (2005b) 'The development of TEX86 for continental paleotemperature reconstruction: Problems and promise', *Geochimica Et Cosmochimica Acta*, 69(10), pp. A78-A78.

Prahl, F.G., Cowie, G.L., De Lange, G.J. and Sparrow, M.A. (2003) 'Selective organic matter preservation in "burn-down" turbidites on the Madeira Abyssal Plain', *Paleoceanography*, 18(2), p. 13.

Prahl, F.G., de Lange, G.J., Lyle, M. and Sparrow, M.A. (1989) 'Post-depositional stability of long-chain alkenones under contrasting redox conditions', *Nature*, 341(6241), pp. 434-437.

Prahl, F.G., Muehlhausen, L.A. and Zahnle, D.L. (1988) 'Further evaluation of long-chain alkenones as indicators of paleoceanographic conditions', *Geochimica et Cosmochimica Acta*, 52(9), pp. 2303-2310.

Prahl, F.G., Rontani, J.F., Zabeti, N., Walinsky, S.E. and Sparrow, M.A. (2010) 'Systematic pattern in - Temperature residuals for surface sediments from high latitude and other oceanographic settings', *Geochimica et Cosmochimica Acta*, 74(1), pp. 131-143.

Prahl, F.G. and Wakeham, S.G. (1987) 'Calibration of unsaturation patterns in long-chain ketone compositions for palaeotemperature assessment', *Nature*, 330(6146), pp. 367-369.

Prell, W.L. (1984) 'Covariance Patterns of Foraminiferal δ18O: An Evaluation of Pliocene Ice Volume Changes Near 3.2 Million Years Ago', *Science*, 226(4675), pp. 692-694.

Rae, J.W.B., Foster, G.L., Schmidt, D.N. and Elliott, T. (2011) 'Boron isotopes and B/Ca in benthic foraminifera: Proxies for the deep ocean carbonate system', *Earth and Planetary Science Letters*, 302(3-4), pp. 403-413.

Rau, A.J., Rogers, J., Lutjeharms, J.R.E., Giraudeau, J., Lee-Thorp, J.A., Chen, M.T. and Waelbroeck, C. (2002) 'A 450-kyr record of hydrological conditions on the western Agulhas Bank Slope, south of Africa', *Marine Geology*, 180(1-4), pp. 183-201.

Ravelo, A.C., Andreasen, D.H., Lyle, M., Lyle, A.O. and Wara, M.W. (2004) 'Regional climate shifts caused by gradual global cooling in the Pliocene epoch', *Nature*, 429(6989), pp. 263-267.

Ravelo, A.C., Fairbanks, R.G. and Philander, S.G.H. (1990) 'Reconstructing tropical Atlantic hydrography using planktontic foraminifera and an ocean model', *Paleoceanography*, 5(3), pp. 409-431.

Raymo, M.E. (1994) 'The initiation of northern hemisphere glaciation', *Annual Review of Earth and Planetary Sciences*, 22, pp. 353-383.

Raymo, M.E., Grant, B., Horowitz, M. and Rau, G.H. (1996) 'Mid-Pliocene warmth: Stronger greenhouse and stronger conveyor', *Marine Micropaleontology*, 27(1-4), pp. 313-326.

Raymo, M.E., Lisiecki, L.E. and Nisancioglu, K.H. (2006) 'Plio-pleistocene ice volume, Antarctic climate, and the global delta O-18 record', *Science*, 313(5786), pp. 492-495.

Raymo, M.E., Oppo, D.W. and Curry, W. (1997) 'The Mid-Pleistocene Climate Transition: A Deep Sea Carbon Isotopic Perspective', *Paleoceanography*, 12(4), pp. 546-559.

Raymo, M.E., Oppo, D.W., Flower, B.P., Hodell, D.A., McManus, J.F., Venz, K.A., Kleiven, K.F. and McIntyre, K. (2004) 'Stability of North Atlantic water masses in face of pronounced climate variability during the Pleistocene', *Paleoceanography*, 19(2), p. PA2008.

Raymo, M.E., Ruddiman, W.F., Shackleton, N.J. and Oppo, D.W. (1990) 'Evolution of Atlantic-Pacific $\delta^{13}$C gradients over the last 2.5 m.y', *Earth and Planetary Science Letters*, 97(3-4), pp. 353-368.

Reason, C.J.C., Lutjeharms, J.R.E., Hermes, J., Biastoch, A. and Roman, R.E. (2003) 'Inter-ocean fluxes south of Africa in an eddy-permitting model', *Deep-Sea Research Part Ii-Topical Studies in Oceanography*, 50(1), pp. 281-298.

Regenberg, M., Steph, S., Nürnberg, D., Tiedemann, R. and Garbe-Schönberg, D. (2009) 'Calibrating Mg/Ca ratios of multiple planktonic foraminiferal species with δ18O-calcification temperatures: Paleothermometry for the upper water column', *Earth and Planetary Science Letters*, 278(3–4), pp. 324-336.

Reid, J.L. (1989) 'On the total geostrophic circulation of the South Atlantic Ocean: Flow patterns, tracers, and transports', *Progress In Oceanography*, 23(3), pp. 149-244.

Rickaby, R.E.M. and Halloran, P. (2005) 'Cool La Nina during the warmth of the Pliocene?', *Science*, 307(5717), pp. 1948-1952.

Rintoul, S.R. (1991) 'South Atlantic Interbasin Exchange', *J. Geophys. Res.*, 96(C2), pp. 2675-2692.

Robinson, M.M. (2009) 'New quantitative evidence of extreme warmth in the Pliocene Arctic', *Stratigraphy*, 6(4), pp. 265-275.

Robinson, R.S. and Meyers, P.A. (2002) 'Biogeochemical changes within the Benguela Current upwelling system during the Matuyama Diatom Maximum: Nitrogen isotope evidence from Ocean Drilling Program Sites 1082 and 1084', *Paleoceanography*, 17(4), p. 1064.

Rodriguez-Sanz, L., Graham Mortyn, P., Martanez-Garcia, A., Rosell-Mele, A. and Hall, I.R. (2012) 'Glacial Southern Ocean freshening at the onset of the Middle Pleistocene Climate Transition', *Earth and Planetary Science Letters*, 345-348(0), pp. 194-202.

Rohling, E.J. (1994) 'Glacial conditions in the Red Sea', *Paleoceanography*, 9(5), pp. 653-660.

Rohling, E.J. (2007) 'Progress in paleosalinity: Overview and presentation of a new approach', *Paleoceanography*, 22(3), p. PA3215.

Rohling, E.J. and Bigg, G.R. (1998) 'Paleosalinity and δ18O: A critical assessment', *Journal of Geophysical Research: Oceans*, 103(C1), pp. 1307-1318.

Rohling, E.J., Sprovieri, M., Cane, T., Casford, J.S.L., Cooke, S., Bouloubassi, I., Emeis, K.C., Schiebel, R., Rogerson, M., Hayes, A., Jorissen, F.J. and Kroon, D. (2004) 'Reconstructing past planktic foraminiferal habitats using stable isotope data: a case history for Mediterranean sapropel S5', *Marine Micropaleontology*, 50(1-2), pp. 89-123.

Roman, R.E. and Lutjeharms, J.R.E. (2009) 'Red Sea Intermediate Water in the source regions of the Agulhas Current', *Deep-Sea Research Part I-Oceanographic Research Papers*, 56(6), pp. 939-962.

Rommerskirchen, F., Condon, T., Mollenhauer, G., Dupont, L. and Schefuss, E. (2011) 'Miocene to Pliocene development of surface and subsurface temperatures in the Benguela Current system', *Paleoceanography*, 26, p. 15.

Rontani, J.F., Harji, R., Guasco, S., Prahl, F.G., Volkman, J.K., Bhosle, N.B. and Bonin, P. (2008) 'Degradation of alkenones by aerobic heterotrophic bacteria: Selective or not?', *Organic Geochemistry*, 39(1), pp. 34-51.

Rontani, J.F., Volkman, J.K., Prahl, F.G. and Wakeham, S.G. (2013) 'Biotic and abiotic degradation of alkenones and implications for paleoproxy applications: A review', *Organic Geochemistry*, 59(0), pp. 95-113.

Rosell-Melé, A., Maslin, M.A., Maxwell, J.R. and Schaeffer, P. (1997) 'Biomarker evidence for "Heinrich" events', *Geochimica et Cosmochimica Acta*, 61(8), pp. 1671-1678.

Rosell-Melé, A. and Maxwell, J.R. (1996) 'Rapid Characterization of Metallo Porphyrin Classes in Natural Extracts by Gel Permeation Chromatography/Atmospheric Pressure Chemical Ionization/Mass Spectrometry', *Rapid Communications in Mass Spectrometry*, 10(2), pp. 209-213.

Rosell-Mele, A. and McClymont, E. (2008) 'Biomarkers as Paleoceanographic Proxies', in C., H.-M. and A., d.V. (eds.) *Proxies in Late Cenozoic Paleoceanography*. Amsterdam Oxford: Elsevier, pp. 441-490.

Ruddiman, W.F. (2003) 'Orbital insolation, ice volume, and greenhouse gases', *Quaternary Science Reviews*, 22(15-17), pp. 1597-1629.

Ruddiman, W.F. (2005) 'Cold climate during the closest Stage 11 analog to recent Millennia', *Quaternary Science Reviews*, 24(10-11), pp. 1111-1121.

Ruddiman, W.F., Raymo, M.E., Martinson, D.G., Clement, B.M. and Backman, J. (1989) 'Pleistocene evolution: Northern hemisphere ice sheets and North Atlantic Ocean', *Paleoceanography*, 4(4), pp. 353-412.

Ruddiman, W.F., Vavrus, S.J. and Kutzbach, J.E. (2005) 'A test of the overdue-glaciation hypothesis', *Quaternary Science Reviews*, 24(1-2), pp. 1-10.

Ruhlemann, C., Mulitza, S., Muller, P.J., Wefer, G. and Zahn, R. (1999) 'Warming of the tropical Atlantic Ocean and slowdown of thermohaline circulation during the last deglaciation', *Nature*, 402(6761), pp. 511-514.

Sachs, J.P. and Anderson, R.F. (2003) 'Fidelity of alkenone paleotemperatures in southern Cape Basin sediment drifts', *Paleoceanography*, 18(4), p. 1082.

Saher, M.H., Rostek, F., Jung, S.J.A., Bard, E., Schneider, R.R., Greaves, M., Ganssen, G.M., Elderfield, H. and Kroon, D. (2009) 'Western Arabian Sea SST during the penultimate interglacial: A comparison of U-37(K ') and Mg/Ca paleothermometry', *Paleoceanography*, 24, p. 12.

Salzmann, U., Haywood, A.M. and Lunt, D.J. (2009) 'The past is a guide to the future? Comparing Middle Pliocene vegetation with predicted biome distributions for the twenty-first century', *Philosophical Transactions of the Royal Society a-Mathematical Physical and Engineering Sciences*, 367(1886), pp. 189-204.

Salzmann, U., Williams, M., Haywood, A.M., Johnson, A.L.A., Kender, S. and Zalasiewicz, J. (2011) 'Climate and environment of a Pliocene warm world', *Palaeogeography, Palaeoclimatology, Palaeoecology*, 309(1-2), pp. 1-8.

Schefuss, E., Ratmeyer, V., Stuut, J.B.W., Jansen, J.H.F. and Damste, J.S.S. (2003a) 'Carbon isotope analyses of n-alkanes in dust from the lower atmosphere over the central eastern Atlantic', *Geochimica et Cosmochimica Acta*, 67(10), pp. 1757-1767.

Schefuss, E., Schouten, S., Jansen, J.H.F. and Damste, J.S.S. (2003b) 'African vegetation controlled by tropical sea surface temperatures in the mid-Pleistocene period', *Nature*, 422(6930), pp. 418-421.

Scherer, R.P., Bohaty, S.M., Dunbar, R.B., Esper, O., Flores, J.A., Gersonde, R., Harwood, D.M., Roberts, A.P. and Taviani, M. (2008) 'Antarctic records of precession-paced insolation-driven warming during early Pleistocene Marine Isotope Stage 31', *Geophysical Research Letters*, 35(3), p. 5.

Schmidt, M.W., Spero, H.J. and Lea, D.W. (2004) 'Links between salinity variation in the Caribbean and North Atlantic thermohaline circulation', *Nature*, 428(6979), pp. 160-163.

Schmieder, F., von Dobeneck, T. and Bleil, U. (2000) 'The Mid-Pleistocene climate transition as documented in the deep South Atlantic Ocean: initiation, interim state and terminal event', *Earth and Planetary Science Letters*, 179(3-4), pp. 539-549.

Schouten, S., Forster, A., Panoto, F.E. and Sinninghe Damsté, J.S. (2007) 'Towards calibration of the TEX86 palaeothermometer for tropical sea surface temperatures in ancient greenhouse worlds', *Organic Geochemistry*, 38(9), pp. 1537-1546.

Schouten, S., Hopmans, E.C., Schefuss, E. and Damste, J.S.S. (2002) 'Distributional variations in marine crenarchaeotal membrane lipids: a new tool for reconstructing ancient sea water temperatures?', *Earth and Planetary Science Letters*, 204(1-2), pp. 265-274.

Schouten, S., Hopmans, E.C., Schefuss, E. and Damste, J.S.S. (2003) 'Distributional variations in marine crenarchaeotal membrane lipids: a new tool for reconstructing ancient sea water temperatures? (vol 204, pg 265, 2002)', *Earth and Planetary Science Letters*, 211(1-2), pp. 205-206.

Seidov, D. and Maslin, M. (2001) 'Atlantic ocean heat piracy and the bipolar climate see-saw during Heinrich and Dansgaard–Oeschger events', *Journal of Quaternary Science*, 16(4), pp. 321-328.

Seki, O., Foster, G.L., Schmidt, D.N., Mackensen, A., Kawamura, K. and Pancost, R.D. (2010) 'Alkenone and boron-based Pliocene pCO2 records', *Earth and Planetary Science Letters*, 292(1-2), pp. 201-211.

Seki, O., Schmidt, D.N., Schouten, S., Hopmans, E.C., Damste, J.S.S. and Pancost, R.D. (2012) 'Paleoceanographic changes in the Eastern Equatorial Pacific over the last 10 Myr', *Paleoceanography*, 27, p. 14.

Sepulcre, S., Vidal, L., Tachikawa, K., Rostek, F. and Bard, E. (2011) 'Sea-surface salinity variations in the northern Caribbean Sea across the Mid-Pleistocene Transition', *Climate of the Past*, 7(1), pp. 75-90.

Sexton, P.F. and Norris, R.D. (2011) 'High latitude regulation of low latitude thermocline ventilation and planktic foraminifer populations across glacial-interglacial cycles', *Earth and Planetary Science Letters*, 311(1-2), pp. 69-81.

Shackleton, N. (1967) 'Oxygen Isotope Analyses and Pleistocene Temperatures Re-assessed', *Nature*, 215(5096), pp. 15-17.

Shackleton, N.J. (2000) 'The 100,000-Year Ice-Age Cycle Identified and Found to Lag Temperature, Carbon Dioxide, and Orbital Eccentricity', *Science*, 289(5486), pp. 1897-1902.

Shackleton, N.J. and Opdyke, N.D. (1973) 'Oxygen isotope and palaeomagnetic stratigraphy of Equatorial Pacific core V28-238: Oxygen isotope temperatures and ice volumes on a 105 year and 106 year scale', *Quaternary Research*, 3(1), pp. 39-55.

Shannon, L.V. and Hunter, D. (1988) 'Notes on Antarctic intermediate water around southern Africa', *South African Journal of Marine Science*, 6(1), pp. 107-117.

Sharp, Z. (2007) *Stable Isotope Geochemistry*. Upper Saddle River, NJ: Person Education, Inc.

Shipboard Scientific Party (1998) 'Site 1087', in Wefer, G., Berger, W.H., Richter, C. and al., e. (eds.) *Proc. ODP, Init. Repts*. College Station, TX (Ocean Drilling Program), pp. 457–484.

Shukla, S.P., Chandler, M.A., Jonas, J., Sohl, L.E., Mankoff, K. and Dowsett, H. (2009) 'Impact of a permanent El Nino (El Padre) and Indian Ocean Dipole in warm Pliocene climates', *Paleoceanography*, 24, p. 12.

Sigman, D.M. and Boyle, E.A. (2000) 'Glacial/interglacial variations in atmospheric carbon dioxide', *Nature*, 407(6806), pp. 859-869.

Sigman, D.M., Jaccard, S.L. and Haug, G.H. (2004) 'Polar ocean stratification in a cold climate', *Nature*, 428(6978), pp. 59-63.

Sikes, E.L. and Volkman, J.K. (1993) 'Calibration of alkenone unsaturation ratios (Uk'37) for paleotemperature estimation in cold polar waters', *Geochimica et Cosmochimica Acta*, 57(8), pp. 1883-1889.

Sikes, E.L., Volkman, J.K., Robertson, L.G. and Pichon, J.J. (1997) 'Alkenones and alkenes in surface waters and sediments of the Southern Ocean: Implications for paleotemperature estimation in polar regions', *Geochimica et Cosmochimica Acta*, 61(7), pp. 1495-1505.

Simoneit, B.R.T., Cardoso, J.N. and Robinson, N. (1991) 'An assessment of terrestrial higher molecular weight lipid compounds in aerosol particulate matter over the south atlantic from about 30-70 °S', *Chemosphere*, 23(4), pp. 447-465.

Sinha, D.K. and Singh, A.K. (2007) 'Surface circulation in the eastern Indian Ocean during last 5 million years: Planktic foraminiferal evidences', *Indian Journal of Marine Sciences*, 36(4), pp. 342-350.

Sosdian, S. and Rosenthal, Y. (2009) 'Deep-Sea Temperature and Ice Volume Changes Across the Pliocene-Pleistocene Climate Transitions', *Science*, 325(5938), pp. 306-310.

Sosdian, S. and Rosenthal, Y. (2010) 'Response to Comment on "Deep-Sea Temperature and Ice Volume Changes Across the Pliocene-Pleistocene Climate Transitions"', *Science*, 328(5985), p. 1480.

Still, C.J., Berry, J.A., Collatz, G.J. and DeFries, R.S. (2003) 'Global distribution of C-3 and C-4 vegetation: Carbon cycle implications', *Global Biogeochemical Cycles*, 17(1), p. 14.

Szymczak-Zyla, M., Kowalewska, G. and Louda, J.W. (2011) 'Chlorophyll-a and derivatives in recent sediments as indicators of productivity and depositional conditions', *Marine Chemistry*, 125(1–4), pp. 39-48.

Thunell, R.C. and Reynolds, L.A. (1984) 'Sedimentation of Planktonic Foraminifera: Seasonal Changes in Species Flux in the Panama Basin', *Micropaleontology*, 30(3), pp. 243-262.

Toggweiler, J.R. and Russell, J. (2008) 'Ocean circulation in a warming climate', *Nature*, 451(7176), pp. 286-288.

Trauth, M.H., Larrasoana, J.C. and Mudelsee, M. (2009) 'Trends, rhythms and events in Plio-Pleistocene African climate', *Quaternary Science Reviews*, 28(5-6), pp. 399-411.

Trommer, G., Siccha, M., Rohling, E.J., Grant, K., van der Meer, M.T.J., Schouten, S., Baranowski, U. and Kucera, M. (2012) 'Sensitivity of Red Sea circulation to sea level and insolation forcing during the last interglacial', *Climate of the Past*, 7(3), pp. 941-955.

Turney, C. and Jones, R. (2011) 'Response to Comments on 'Does the Agulhas Current amplify global temperatures during super-interglacials?'', *Journal of Quaternary Science*, 26(8), pp. 870-871.

Turney, C.S. and Jones, R.T. (2010) 'Does the Agulhas Current amplify global temperatures during super-interglacials?', *Journal of Quaternary Science*, 25(6), pp. 839-843.

Ufkes, E., Jansen, J.H.F. and Schneider, R.R. (2000) 'Anomalous occurrences of Neogloboquadrina pachyderma (left) in a 420-ky upwelling record from Walvis Ridge (SE Atlantic)', *Marine Micropaleontology*, 40(1-2), pp. 23-42.

Ufkes, E. and Kroon, D. (2012) 'Sensitivity of south-east Atlantic planktonic foraminifera to mid-Pleistocene climate change', *Palaeontology*, 55, pp. 183-204.

Urey, H.C. (1948) 'Oxygen Isotopes in Nature and in the Laboratory', *Science*, 108(2810), pp. 489-496.

van Sebille, E., Biastoch, A., van Leeuwen, P.J. and de Ruijter, W.P.M. (2009) 'A weaker Agulhas Current leads to more Agulhas Leakage', *Geophys. Res. Lett.*, 36.

van Sebille, E. and van Leeuwen, P.J. (2007) 'Fast northward energy transfer in the Atlantic due to Agulhas rings', *Journal of Physical Oceanography*, 37(9), pp. 2305-2315.

Versteegh, G.J.M. and Zonneveld, K.A.F. (2002) 'Use of selective degradation to separate preservation from productivity', *Geology*, 30(7), pp. 615-618.

Voelker, A.H.L., Rodrigues, T., Billups, K., Oppo, D., McManus, J., Stein, R., Hefter, J. and Grimalt, J.O. (2010) 'Variations in mid-latitude North Atlantic surface water properties during the mid-Brunhes (MIS 9-14) and their implications for the thermohaline circulation', *Climate of the Past*, 6(4), pp. 531-552.

Volkman, J.K. (2000) 'Ecological and environmental factors affecting alkenone distributions in seawater and sediments', *Geochemistry Geophysics Geosystems*, 1(9).

Volkman, J.K., Eglinton, G., Corner, E.D.S. and Forsberg, T.E.V. (1980a) 'Long-chain alkenes and alkenones in the marine coccolithophorid Emiliania huxleyi', *Phytochemistry*, 19(12), pp. 2619-2622.

Volkman, J.K., Eglinton, G., Corner, E.D.S. and Sargent, J.R. (1980b) 'Novel unsaturated straight-chain C37---C39 methyl and ethyl ketones in marine sediments and a coccolithophore Emiliania huxleyi', *Physics and Chemistry of The Earth*, 12, pp. 219-227.

Weijer, W., de Ruijter, W.P.M., Dijkstra, H.A. and van Leeuwen, P.J. (1999) 'Impact of Interbasin Exchange on the Atlantic Overturning Circulation', *Journal of Physical Oceanography*, 29(9), pp. 2266-2284.

Wollenburg, J.E. and Mackensen, A. (1998) 'Living benthic foraminifers from the central Arctic Ocean: faunal composition, standing stock and diversity', *Marine Micropaleontology*, 34(3â€"4), pp. 153-185.

Wright, S.W. and Jeffrey, S.W. (2006) 'Pigment Markers for Phytoplankton Production', *Hdb Env Chem* Vol. 2, (Part N).

Wuchter, C., Schouten, S., Coolen, M.J.L. and Damste, J.S.S. (2004) 'Temperature-dependent variation in the distribution of tetraether membrane lipids of marine Crenarchaeota: Implications for TEX86 paleothermometry', *Paleoceanography*, 19(4).

Wuchter, C., Schouten, S., Wakeham, S.G. and Damste, J.S.S. (2005) 'Temporal and spatial variation in tetraether membrane lipids of marine Crenarchaeota in particulate organic matter: Implications for TEX86 paleothermometry', *Paleoceanography*, 20(3).

Wunsch, C. (2009) 'A Perpetually Running ENSO in the Pliocene?', *Journal of Climate*, 22(12), pp. 3506-3510.

Zachos, J., Pagani, M., Sloan, L., Thomas, E. and Billups, K. (2001) 'Trends, Rhythms, and Aberrations in Global Climate 65 Ma to Present', *Science*, 292(5517), pp. 686-693.

Zachos, J.C., Schouten, S., Bohaty, S., Quattlebaum, T., Sluijs, A., Brinkhuis, H., Gibbs, S.J. and Bralower, T.J. (2006) 'Extreme warming of mid-latitude coastal ocean during the Paleocene-Eocene Thermal Maximum: Inferences from TEX86 and isotope data', *Geology*, 34(9), pp. 737-740.

Zahn, R. (2009) 'Beyond the CO2 connection', *Nature*, 460(7253), pp. 335-336.

Zegarra, M. and Helenes, J. (2011) 'Changes in Miocene through Pleistocene dinoflagellates from the Eastern Equatorial Pacific (ODP Site 1039), in relation to primary productivity', *Marine Micropaleontology*, 81(3-4), pp. 107-121.

Zhang, Y.G., Ji, J.F., Balsam, W., Liu, L.W. and Chen, J. (2009) 'Mid-Pliocene Asian monsoon intensification and the onset of Northern Hemisphere glaciation', *Geology*, 37(7), pp. 599-602.

Zharkov, V. and Nof, D. (2008) 'Agulhas ring injection into the South Atlantic during glacials and interglacials', *Ocean Science*, 4(3), pp. 223-237.

Zonneveld, K.A.F., Hoek, R.P., Brinkhuis, H. and Willems, H. (2001) 'Geographical distributions of organic-walled dinoflagellate cysts in surficial sediments of the Benguela upwelling region and their relationship to upper ocean conditions', *Progress In Oceanography*, 48(1), pp. 25-72.

Zonneveld, K.A.F., Versteegh, G.J.M., Kasten, S., Eglinton, T.I., Emeis, K.C., Huguet, C., Koch, B.P., de Lange, G.J., de Leeuw, J.W., Middelburg, J.J., Mollenhauer, G., Prahl, F.G., Rethemeyer, J. and Wakeham, S.G. (2010) 'Selective preservation of organic matter in marine environments; processes and impact on the sedimentary record', *Biogeosciences*, 7(2), pp. 483-511.

Marry, sir, they have committed false report;

moreover, they have spoken untruths; secondarily,

they are slanders; sixth and lastly, they have

belied a lady; thirdly, they have verified unjust

things; and, to conclude, they are lying knaves.


W. Shakespeare